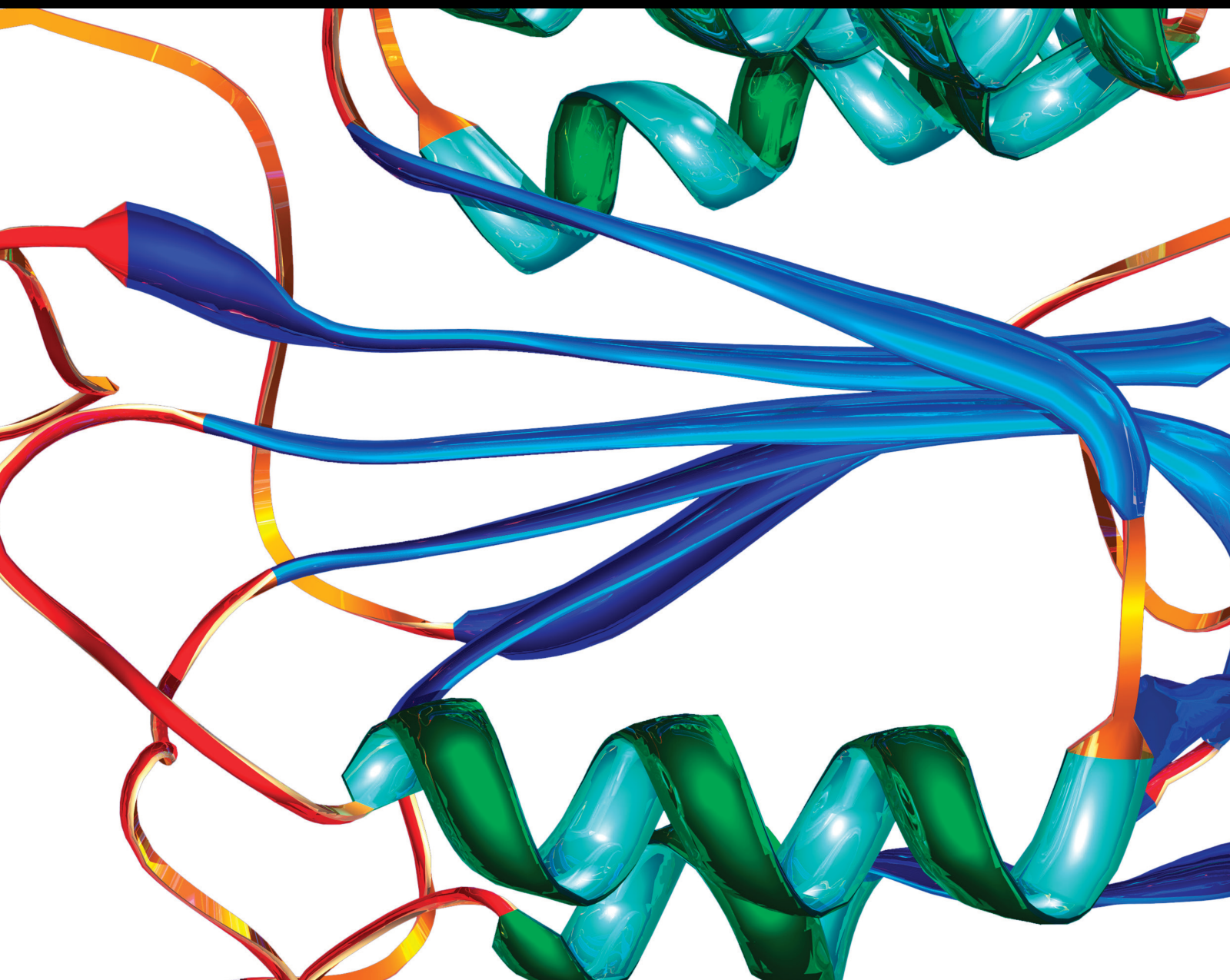


Promising Biomarkers for Risk Stratification and Prognostication of Heart Failure in Diabetics

Lead Guest Editor: Alexander Berezin

Guest Editors: Michael Lichtenauer and Peter Jirak





**Promising Biomarkers for Risk Stratification
and Prognostication of Heart Failure in
Diabetics**

Disease Markers

**Promising Biomarkers for Risk
Stratification and Prognostication of
Heart Failure in Diabetics**

Lead Guest Editor: Alexander Berezin

Guest Editors: Michael Lichtenauer and Peter Jirak



Copyright © 2021 Hindawi Limited. All rights reserved.

This is a special issue published in "Disease Markers." All articles are open access articles distributed under the Creative Commons Attribution License, which permits unrestricted use, distribution, and reproduction in any medium, provided the original work is properly cited.

Chief Editor

Paola Gazzaniga, Italy


Associate Editors

Donald H. Chace , USA
Mariann Harangi, Hungary
Hubertus Himmerich , United Kingdom
Yi-Chia Huang , Taiwan
Giuseppe Murdaca , Italy
Irene Rebelo , Portugal

Academic Editors

Muhammad Abdel Ghafar, Egypt
George Agrogiannis, Greece
Mojgan Alaeddini, Iran
Atif Ali Hashmi , Pakistan
Cornelia Amalinei , Romania
Pasquale Ambrosino , Italy
Paul Ashwood, USA
Faryal Mehwish Awan , Pakistan
Atif Baig , Malaysia
Valeria Barresi , Italy
Lalit Batra , USA
Francesca Belardinilli, Italy
Elisa Belluzzi , Italy
Laura Bergantini , Italy
Sourav Bhattacharya, USA
Anna Birková , Slovakia
Giulia Bivona , Italy
Luisella Bocchio-Chiavetto , Italy
Francesco Paolo Busardó , Italy
Andrea Cabrera-Pastor , Spain
Paolo Cameli , Italy
Chiara Caselli , Italy
Jin Chai, China
Qixing Chen, China
Shaoqiu Chen, USA
Xiangmei Chen, China
Carlo Chiarla , Italy
Marcello Ciaccio , Italy
Luciano Colangelo , Italy
Alexandru Corlateanu, Moldova
Miriana D'Alessandro , Saint Vincent and the Grenadines
Waaqo B. Daddacha, USA
Xi-jian Dai , China
Maria Dalamaga , Greece



Serena Del Turco , Italy
Jiang Du, USA
Xing Du , China
Benoit Dugue , France
Paulina Dumnicka , Poland
Nashwa El-Khazragy , Egypt
Zhe Fan , China
Rudy Foddis, Italy
Serena Fragiotta , Italy
Helge Frieling , Germany
Alain J. Gelibter, Italy
Matteo Giulietti , Italy
Damjan Glavač , Slovenia
Alvaro González , Spain
Rohit Gundamaraju, USA
Emilia Hadziyannis , Greece
Michael Hawkes, Canada
Shih-Ping Hsu , Taiwan
Menghao Huang , USA
Shu-Hong Huang , China
Xuan Huang , China
Ding-Sheng Jiang , China
Esteban Jorge Galarza , Mexico
Mohamed Gomaa Kamel, Japan
Michalis V. Karamouzis, Greece
Muhammad Babar Khawar, Pakistan
Young-Kug Kim , Republic of Korea
Mallikarjuna Korivi , China
Arun Kumar , India
Jinan Li , USA
Peng-fei Li , China
Yiping Li , China
Michael Lichtenauer , Austria
Daniela Ligi, Italy
Hui Liu, China
Jin-Hui Liu, China
Ying Liu , USA
Zhengwen Liu , China
César López-Camarillo, Mexico
Xin Luo , USA
Zhiwen Luo, China
Valentina Magri, Italy
Michele Malaguarnera , Italy
Erminia Manfrin , Italy
Utpender Manne, USA

Alexander G. Mathioudakis, United Kingdom
Andrea Maugeri , Italy
Prasenjit Mitra , India
Ekansh Mittal , USA
Hiroshi Miyamoto , USA
Naoshad Muhammad , USA
Chiara Nicolazzo , Italy
Xing Niu , China
Dong Pan , USA
Dr.Krupakar Parthasarathy, India
Robert Pichler , Austria
Dimitri Poddighe , Kazakhstan
Roberta Rizzo , Italy
Maddalena Ruggieri, Italy
Tamal Sadhukhan, USA
Pier P. Sainaghi , Italy
Cristian Scheau, Romania
Jens-Christian Schewe, Germany
Alexandra Scholze , Denmark
Shabana , Pakistan
Anja Hviid Simonsen , Denmark
Eric A. Singer , USA
Daniele Sola , Italy
Timo Sorsa , Finland
Yaying Sun , China
Mohammad Tarique , USA
Jayaraman Tharmalingam, USA
Sowjanya Thatikonda , USA
Stamatios E. Theocharis , Greece
Tilman Todenhöfer , Germany
Anil Tomar, India
Alok Tripathi, India
Drenka Trivanović , Germany
Natacha Turck , Switzerland
Azizah Ugusman , Malaysia
Shailendra K. Verma, USA
Aristidis S. Veskoukis, Greece
Arianna Vignini, Italy
Jincheng Wang, Japan
Zhongqiu Xie, USA
Yuzhen Xu, China
Zhijie Xu , China
Guan-Jun Yang , China
Yan Yang , USA





Chengwu Zeng , China
Jun Zhang Zhang , USA
Qun Zhang, China
Changli Zhou , USA
Heng Zhou , China
Jian-Guo Zhou, China

Contents




HDL-C/apoA-I Ratio Is Associated with the Severity of Coronary Artery Stenosis in Diabetic Patients with Acute Coronary Syndrome

Lizhe Sun, Manyun Guo, Chenbo Xu, Xiangrui Qiao, Yiming Hua, Gulinigaer Tuerhongjiang, Bowen Lou, Ruifeng Li, Xiaofang Bai, Juan Zhou, Yue Wu, Jianqing She , and Zuyi Yuan 
Research Article (10 pages), Article ID 6689056, Volume 2021 (2021)




Exploring the Relationship of Bone Turnover Markers and Bone Mineral Density in Community-Dwelling Postmenopausal Women

Xu Wei , Yili Zhang , Xinghua Xiang, Menghua Sun, Kai Sun, Tao Han, Baoyu Qi, Yanming Xie, Ranxing Zhang , and Liguozhu 
Research Article (10 pages), Article ID 6690095, Volume 2021 (2021)



The Value of a Seven-Autoantibody Panel Combined with the Mayo Model in the Differential Diagnosis of Pulmonary Nodules

Zhougui Ling , Jifei Chen , Zhongwei Wen, Xiaomou Wei, Rui Su, Zhenming Tang, and Zhuojun Hu 
Research Article (12 pages), Article ID 6677823, Volume 2021 (2021)




Myokines and Heart Failure: Challenging Role in Adverse Cardiac Remodeling, Myopathy, and Clinical Outcomes

Alexander E. Berezin , Alexander A. Berezin , and Michael Lichtenauer 
Review Article (17 pages), Article ID 6644631, Volume 2021 (2021)

Association between Cardiac Autonomic Neuropathy and Coronary Artery Lesions in Patients with Type 2 Diabetes

Lei Liu , Qiansheng Wu, Hong Yan, Baoxian Chen, Xilong Zheng, and Qiang Zhou 
Research Article (6 pages), Article ID 6659166, Volume 2020 (2020)

The Role of Circulating RBP4 in the Type 2 Diabetes Patients with Kidney Diseases: A Systematic Review and Meta-Analysis


Li Zhang , Yan-Li Cheng, Shuai Xue , and Zhong-Gao Xu 
Review Article (12 pages), Article ID 8830471, Volume 2020 (2020)

Evaluation of Altered Glutamatergic Activity in a Piglet Model of Hypoxic-Ischemic Brain Damage Using ¹H-MRS

Yuxue Dang  and Xiaoming Wang 
Research Article (13 pages), Article ID 8850816, Volume 2020 (2020)

Research Article

HDL-C/apoA-I Ratio Is Associated with the Severity of Coronary Artery Stenosis in Diabetic Patients with Acute Coronary Syndrome

Lizhe Sun,¹ Manyun Guo,¹ Chenbo Xu,¹ Xiangrui Qiao,¹ Yiming Hua,¹ Gulinigaer Tuerhongjiang,¹ Bowen Lou,¹ Ruifeng Li,¹ Xiaofang Bai,² Juan Zhou,^{1,3,4} Yue Wu,¹ Jianqing She ¹ and Zuyi Yuan ^{1,3,4}

¹Department of Cardiovascular Medicine, The First Affiliated Hospital, Xi'an Jiaotong University, Xi'an, Shaanxi, China

²Department of Ultrasound Imaging, First Affiliated Hospital of Medical College, Xi'an Jiaotong University, Xi'an, Shaanxi, China

³Key Laboratory of Environment and Genes Related to Diseases, Xi'an Jiaotong University, Ministry of Education, Xi'an, Shaanxi, China

⁴Key Laboratory of Molecular Cardiology of Shaanxi Province, Xi'an, Shaanxi, China

Correspondence should be addressed to Jianqing She; jianqingshe@xjtu.edu.cn and Zuyi Yuan; zuyiyuan@mail.xjtu.edu.cn

Received 13 November 2020; Revised 30 March 2021; Accepted 15 April 2021; Published 18 May 2021

Academic Editor: Alexander Berezin

Copyright © 2021 Lizhe Sun et al. This is an open access article distributed under the Creative Commons Attribution License, which permits unrestricted use, distribution, and reproduction in any medium, provided the original work is properly cited.

Background. Emerging evidence demonstrates that the lipid metabolism in acute coronary syndrome (ACS) patients with type 2 diabetes mellitus (T2DM) differs from nondiabetic patients. However, the distinct lipid profiles and their relationships with the severity of coronary artery stenosis and prognosis in patients with T2DM remain elusive. **Method and Result.** This single-center, prospective cohort study enrolled 468 patients diagnosed with ACS undergoing coronary angiography, consisting of 314 non-DM and 154 DM patients. The HDL-C/apoA-I ratio was significantly higher in DM patients with a multivessel (≥ 3 affected vessels) lesion than a single-vessel (1-2 affected vessels) lesion. Regression analyses showed that the HDL-C/apoA-I ratio was positively correlated to the number of stenotic coronary arteries in DM patients but not non-DM patients. However, Kaplan-Meier survival analysis revealed no significant difference in the major adverse cardiovascular event rate regarding different HDL-C/apoA-I levels in DM or non-DM ACS patients at the end of the 2-year follow-up. **Conclusion.** A higher HDL-C/apoA-I ratio is associated with increased severity of coronary artery stenosis in DM patients with ACS but not with the rate of major adverse cardiovascular events at the end of the 2-year follow-up.

1. Introduction

Acute coronary syndrome (ACS) is one of the major public health problems worldwide, which describes the range of acute myocardial ischemic states, including unstable angina (UA), non-ST elevated myocardial infarction (NSTEMI), and ST elevated myocardial infarction (STEMI) [1]. Hyperglycemia and dyslipidemia are risk factors for ACS [2]. Numerous studies have revealed that type 2 diabetes mellitus (T2DM) patients with ACS suffer from worse outcomes compared to their nondiabetic peers [3–6]. Our previous study demonstrated that hemoglobin

A1c (HbA1c) was positively correlated with the severity of coronary artery stenosis in both diabetic and nondiabetic patients with ACS [7]; however, the underlying pathophysiological mechanism and clinical manifestations remain to be elucidated.

High-density lipoprotein cholesterol (HDL-C) was ascribed as “good” cholesterol and negatively correlated to the risk of cardiovascular diseases, as proven by several clinical and animal studies [8, 9]. The mechanisms of the antiatherogenic effects of HDL-C have been proved to be related to its involvement in the pathways of reverse cholesterol transport, as well as antioxidation, anti-

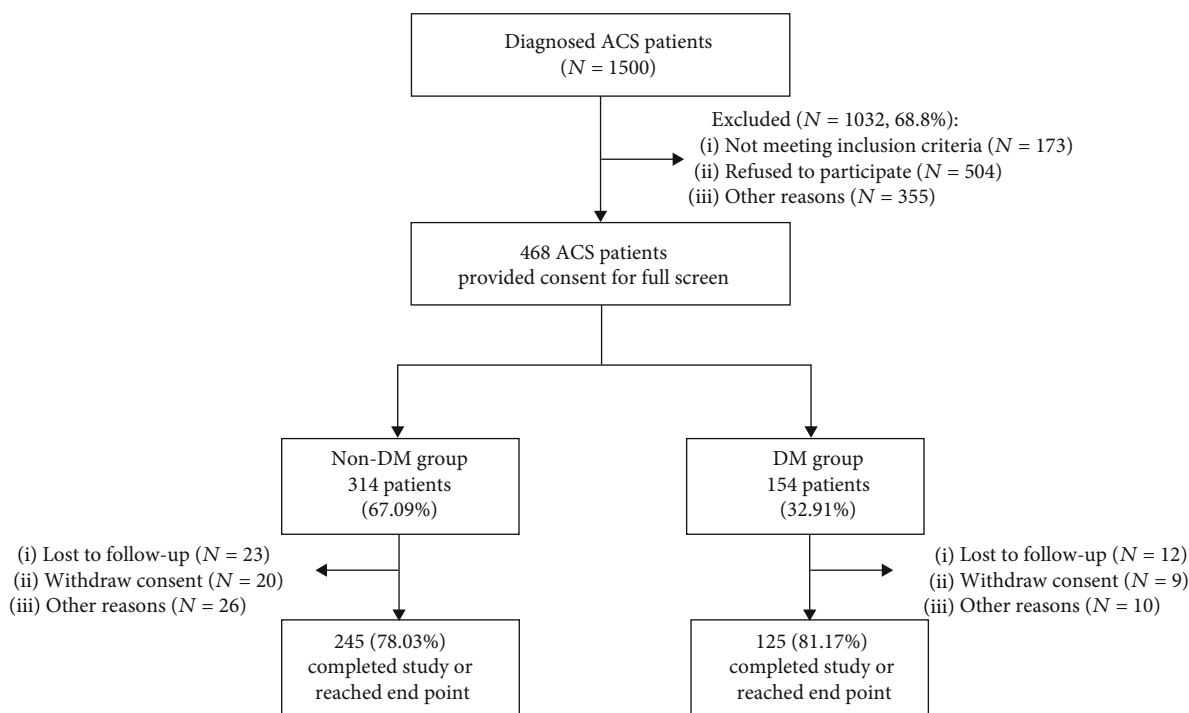


FIGURE 1: Study flowchart.

inflammation, and endothelial protection [8, 10]. However, HDL from T2DM patients showed impaired endothelial-protective capacities due to reduced endothelial progenitor cell-mediated endothelial repair [11]. A systemic review of 14 studies has also revealed that the anti-inflammatory effect of HDL was diminished in individuals with T2DM, although the underlying mechanisms remain to be elucidated [12]. These indicate that HDL may undergo functional remodeling during the progression of chronic inflammatory and metabolic diseases.

Apolipoprotein A-I (apoA-I) is the primary functional apolipoprotein component of HDL participating in cholesterol traffic via multiple mechanisms [13]. For instance, apoA-I plays pivotal roles in the reverse cholesterol transport pathway by modulating HDL-C formation and stabilization, binding to hepatic scavenger receptors, and activating lecithin-cholesterol acyltransferase [14]. Overexpression of the human apoA-I gene on apoE^{-/-} and LDLr^{-/-} mice provided long-term protection on diet-induced atherosclerosis [15, 16]. A previous study indicated that the HDL-C/apoA-I ratio is a more effective marker for coronary artery disease than HDL-C alone [17]. However, it is unknown whether the HDL-C/apoA-I ratio correlates to the severity of coronary artery stenosis and prognosis of diabetic ACS patients.

In this present single-center, prospective study, by analyzing the circulating lipid profile and the major adverse cardiovascular events (MACEs) among ACS patients with or without DM, we aimed to evaluate the relationship between the HDL-C/apoA-I ratio and the severity of coronary artery stenosis and also to explore the short-term prognostic value of the HDL-C/apoA-I ratio in ACS patients.

2. Research Design and Methods

2.1. Study Design and Participants. This is a single-center, prospective cohort study in which 468 ACS patients were recruited, consisting of 229 UA, 71 NSTEMI, and 168 STEMI patients consecutively admitted to the First Affiliated Hospital of Xi'an Jiaotong University from January to December 2016. This study excluded patients who had severe noncardiac disease with an expected survival of less than 1 year, severe renal disease (plasma creatinine $\geq 130 \mu\text{mol/L}$), and chronic liver disease (alanine aminotransferase (ALT) ≥ 2 times the upper limit of normal) or over the age of 80 years. Written informed consent was obtained from all study participants with ethical committee approval from the First Affiliated Hospital of Xi'an Jiaotong University.

2.2. Data Collection and Laboratory Measurement. Baseline characteristics and clinical data were recorded from patients' standard medical records. Blood HbA1c levels of all patients were measured within 3 h of admission using a Siemens DCA analyzer for quantitative assay. Both the concentrations of specific HbA1c and total hemoglobin were measured. The ratio was reported as percent HbA1c.

Venous blood samples were collected in the morning following an overnight fast for other baseline laboratory measurements. TC was detected using a detection kit from FUJIFILM™ via the HMMPs method; HDL-C, LDL-C, and VLDL-C were detected using a detection kit via the direct measurement method from FUJIFILM™; apoA, apoB, and apoE were measured using a detection kit from SEKISUI™ by turbidimetric inhibition immunoassay. All laboratory assays were performed in duplicate, and the results were averaged.

TABLE 1: Baseline characteristics for non-DM and DM ACS patients.

Characteristics	Whole (<i>n</i> = 468)	Non-DM (<i>n</i> = 314)	DM (<i>n</i> = 154)	<i>p</i> value
Age	60.97 ± 9.57	60.59 ± 9.85	61.73 ± 8.94	ns
Male, <i>n</i> (%)	365 (78.00)	249 (79.30)	116 (75.32)	ns
BMI (kg/m ²)	24.95 ± 3.35	24.75 ± 3.35	25.34 ± 3.31	ns
Current smoker, <i>n</i> (%)	135 (28.8)	93 (29.62)	42 (27.27)	ns
Family history of CAD, <i>n</i> (%)	183 (39.10)	129 (41.08)	54 (35.06)	ns
Hypertension, <i>n</i> (%)	255 (54.5)	166 (52.87)	89 (57.79)	ns
Heart rate (bpm)	71.16 ± 16.36	71.10 ± 17.73	71.29 ± 13.20	ns
Systolic BP (mmHg)	126.2 ± 19.03	125.80 ± 18.53	127.02 ± 20.04	ns
Diastolic BP (mmHg)	78.06 ± 11.78	77.59 ± 11.85	79.01 ± 11.62	ns
LVEF (%)	58.27 ± 12.46	58.94 ± 12.36	56.87 ± 12.59	ns
Affected vessels	2.45 ± 0.89	2.39 ± 0.89	2.57 ± 0.87	<0.05
BUN	4.93 ± 1.48	4.84 ± 1.47	5.13 ± 1.50	ns
Creatine (μmol/L)	69.74 ± 20.99	69.10 ± 15.99	71.05 ± 28.61	ns
hsCRP (mg/dL)	2.38 ± 2.33	2.43 ± 2.41	2.28 ± 2.15	ns
HDL-C (mmol/L)	0.91 ± 0.22	0.93 ± 0.23	0.89 ± 0.21	ns
LDL-C (mmol/L)	2.22 ± 0.8	2.26 ± 0.83	2.13 ± 0.74	ns
Triglyceride (mmol/L)	1.68 ± 1.15	1.66 ± 1.21	1.70 ± 1.02	ns
Lipoprotein A (mg/L)	247.74 ± 217.59	255.00 ± 217.61	232.94 ± 217.52	ns
apoA-I (g/L)	1.07 ± 0.19	1.07 ± 0.18	1.08 ± 0.19	ns
HbA1c (%)	6.4 ± 1.31	5.74 ± 0.35	7.75 ± 1.50	<0.001
HDL-C/apoA-I (mmol/g)	0.85 ± 0.12	0.86 ± 0.12	0.82 ± 0.10	<0.01
Medication at discharge				
Aspirin, <i>n</i> (%)	462 (98.7)	309 (98.4)	153 (99.4)	ns
Clopidogrel, <i>n</i> (%)	448 (95.7)	300 (95.5)	148 (96.1)	ns
Statin, <i>n</i> (%)	459 (98.1)	309 (98.4)	150 (97.4)	ns
ACEI/ARB, <i>n</i> (%)	417 (89.1)	278 (88.5)	139 (90.3)	ns
Beta-blockers, <i>n</i> (%)	410 (87.6)	276 (87.9)	134 (87.0)	ns
CCB, <i>n</i> (%)	102 (21.8)	68 (21.7)	34 (22.1)	ns
Main diagnosis				
UA	229 (48.9)	150 (47.77)	79 (51.30)	ns
NSTEMI	71 (15.2)	50 (15.92)	21 (13.64)	ns
STEMI	168 (35.9)	114 (36.31)	54 (35.06)	ns

Data are mean ± SD and number (%). ACS: acute coronary syndrome; ACEI: angiotensin-converting enzyme inhibitor; apoA-I: apolipoprotein A-I; ARB: angiotensin receptor blocker; BMI: body mass index; BP: blood pressure; BUN: blood urea nitrogen; CAD: coronary artery disease; CCB: calcium channel blocker; CKMB: creatine kinase MB; DM: diabetes mellitus; HbA1c: hemoglobin A1c; HDL-C: high-density lipoprotein cholesterol; hsCRP: high-sensitivity C-reactive protein; LDL-C: low-density lipoprotein cholesterol; LVEF: left ventricular ejection fraction; NSTEMI: non-ST elevated myocardial infarction; STEMI: ST elevated myocardial infarction; UA: unstable angina.

2.3. Assessment of Coronary Artery Stenosis. Selective coronary angiography was performed in multiple views by experienced clinicians. The severity of ACS was characterized by the number of coronary vessels with stenosis (>50% of the lumen diameter). A single-vessel lesion was defined as 1-2 affected vessels, and a multivessel lesion was defined as at least 3 affected vessels.

2.4. Outcome and Follow-Up. Follow-up information was obtained via telephone questionnaires or interviews in the hospital by the general practitioner. All-cause death, heart

failure, nonfatal MI, and symptom-driven revascularization were defined as MACEs.

2.5. Statistical Analysis. All statistical analyses were performed using SPSS 18.0. Data were presented as frequencies and percentages for categorical variables and mean ± SD for continuous variables unless otherwise indicated. Differences between two independent groups were compared using the chi-squared test for categorical data, *t*-test for normally distributed data, and nonparametric test for nonnormally distributed data. One-way ANOVA was used to compare

TABLE 2: Baseline characteristics for different ACS patients with single-vessel (1-2 affected vessels) or multivessel (≥ 3 affected vessels) lesions.

Characteristics	Affected vessels		<i>p</i> value
	1-2	≥ 3	
All			
Patient number, <i>n</i> (%)	213 (45.5)	255 (54.5)	
Age	60.28 \pm 9.36	61.22 \pm 9.65	ns
Male, <i>n</i> (%)	154 (75.9)	196 (80.7)	ns
BMI (kg/m ²)	24.94 \pm 3.43	24.94 \pm 3.28	ns
Heart rate (bpm)	70.56 \pm 13.74	72.01 \pm 18.62	ns
Systolic BP (mmHg)	124.81 \pm 17.11	126.76 \pm 19.86	ns
Diastolic BP (mmHg)	77.75 \pm 11.01	78.35 \pm 12.38	ns
LVEF (%)	59.65 \pm 11.46	57.26 \pm 13.18	ns
Creatine (μ mol/L)	69.42 \pm 24.51	70.3 \pm 17.91	ns
HDL-C (mmol/L)	0.92 \pm 0.22	0.9 \pm 0.21	ns
LDL-C (mmol/L)	2.18 \pm 0.8	2.24 \pm 0.77	ns
Triglyceride (mmol/L)	1.69 \pm 1.15	1.66 \pm 1.14	ns
Lipoprotein A (mg/L)	224.96 \pm 191.36	265.6 \pm 233.81	ns
apoA-I (g/L)	1.09 \pm 0.17	1.05 \pm 0.18	<0.05
HbA1c (%)	6.24 \pm 1.14	6.57 \pm 1.45	<0.05
HDL-C/apoA-I (mmol/g)	0.84 \pm 0.11	0.85 \pm 0.11	ns
Non-DM			
Patient number, <i>n</i> (%)	149 (47.5)	165 (52.5)	
Age	59.3 \pm 9.71	61.2 \pm 9.85	ns
Male, <i>n</i> (%)	107 (77.0)	130 (83.3)	ns
BMI (kg/m ²)	24.71 \pm 3.37	24.77 \pm 3.34	ns
HR (bpm)	70.69 \pm 13.88	71.85 \pm 21.14	ns
Systolic BP (mmHg)	124.36 \pm 16.1	126.03 \pm 19.44	ns
Diastolic BP (mmHg)	77.21 \pm 11.21	77.9 \pm 12.4	ns
LVEF (%)	60.34 \pm 11.13	57.8 \pm 13.49	ns
Creatine (μ mol/L)	67.56 \pm 15.56	70.84 \pm 15.96	ns
HDL-C (mmol/L)	0.95 \pm 0.22	0.9 \pm 0.21	ns
LDL-C (mmol/L)	2.18 \pm 0.84	2.31 \pm 0.77	ns
Triglyceride (mmol/L)	1.69 \pm 1.28	1.62 \pm 1.12	ns
Lipoprotein A (mg/L)	231.18 \pm 198.69	277.15 \pm 226.46	ns
apoA-I (g/L)	1.1 \pm 0.17	1.05 \pm 0.18	<0.05
HbA1c (%)	5.7 \pm 0.34	5.76 \pm 0.35	ns
HDL-C/apoA-I (mmol/g)	0.86 \pm 0.12	0.86 \pm 0.1	ns
DM			

TABLE 2: Continued.

Characteristics	Affected vessels		<i>p</i> value
	1-2	≥ 3	
Patient number, <i>n</i> (%)	64 (41.6)	90 (58.4)	
Age	62.39 \pm 8.24	61.25 \pm 9.33	ns
Male, <i>n</i> (%)	47 (73.4)	66 (75.9)	ns
BMI (kg/m ²)	25.52 \pm 3.55	25.22 \pm 3.18	ns
HR (bpm)	70.28 \pm 13.54	72.29 \pm 13.06	ns
Systolic BP (mmHg)	125.76 \pm 19.21	128.06 \pm 20.65	ns
Diastolic BP (mmHg)	78.92 \pm 10.54	79.16 \pm 12.37	ns
LVEF (%)	58.19 \pm 12.08	56.25 \pm 12.59	ns
Creatine (μ mol/L)	73.44 \pm 37.03	69.33 \pm 21.03	ns
HDL-C (mmol/L)	0.87 \pm 0.21	0.9 \pm 0.2	ns
LDL-C (mmol/L)	2.18 \pm 0.73	2.11 \pm 0.75	ns
Triglyceride (mmol/L)	1.69 \pm 0.76	1.72 \pm 1.18	ns
Lipoprotein A (mg/L)	211.45 \pm 175.11	244.89 \pm 246.42	ns
apoA-I (g/L)	1.08 \pm 0.18	1.07 \pm 0.18	ns
HbA1c (%)	7.41 \pm 1.38	8.03 \pm 1.54	<0.05
HDL-C/apoA-I (mmol/g)	0.79 \pm 0.08	0.84 \pm 0.11	<0.05

Data are mean \pm SD and number (%). ACS: acute coronary syndrome; apoA-I: apolipoprotein A-I; BMI: body mass index; BP: blood pressure; DM: diabetes mellitus; HbA1c: hemoglobin A1c; HDL-C: high-density lipoprotein cholesterol; LDL-C: low-density lipoprotein cholesterol; LVEF: left ventricular ejection fraction.

continuous variables among multiple groups. Univariate linear regression analysis was used for calculating the correlation between the HbA1c, the HDL-C/apoA-I ratio, and the severity of coronary artery stenosis. Multivariate regression analysis was conducted to assess the independent contribution of different factors to coronary artery stenosis. DM and non-DM patients were divided into three groups based on tertiles of the HDL-C/apoA-I level. Kaplan-Meier survival curve analysis was conducted to represent the proportional risk of MACE for the HDL-C/apoA-I ratio in patients with or without DM. All probability values were two-tailed. $p < 0.05$ was considered statistically significant.

3. Results

3.1. Study Population and Baseline Characteristics. A total of 1500 patients with a diagnosis of ACS were screened, of which 173 patients did not meet the inclusion criteria, 504 refused to participate, and 355 were not included in this study due to other reasons. 468 ACS patients were enrolled in the observational study, consisting of 314 non-DM (67.09%) and 154 DM (32.91%) patients. At the end of this study, 245 of 314 non-DM patients (78.03%) and 125 of 154 DM patients (81.71%) completed the 2-year follow-up survival analysis or reached endpoints (Figure 1).

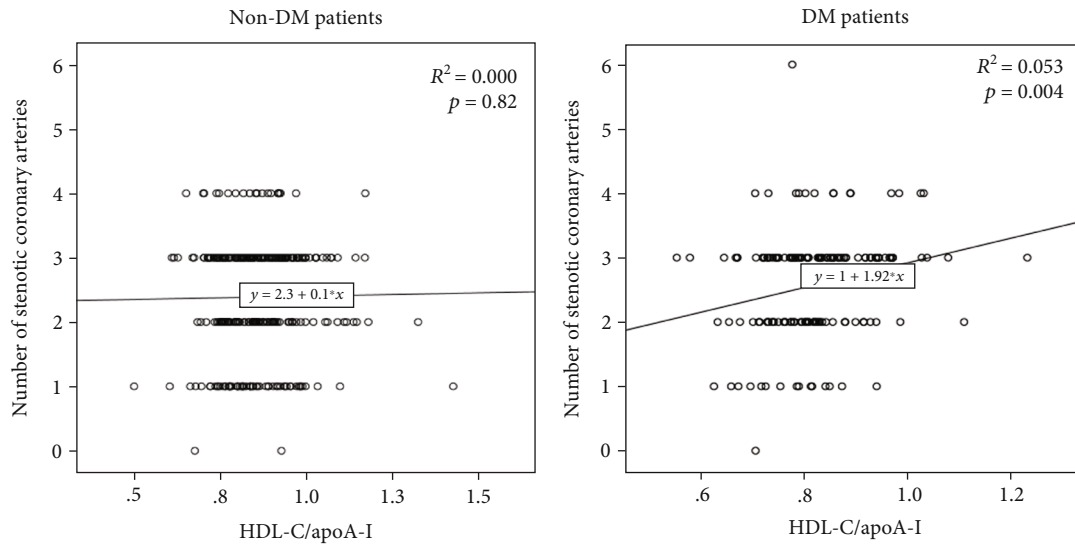


FIGURE 2: Linear regression analysis between the HDL-C/apoA-I ratio and the number of stenotic coronary arteries in non-DM and DM ACS patients.

TABLE 3: Multiregression analysis of the severity of coronary artery stenosis in non-DM and DM ACS patients.

Variable	Coefficient	95% CI	p value
Non-DM			
Age	0.012	-0.002 to 0.025	ns
BMI (kg/m ²)	0.006	-0.033 to 0.045	ns
HDL-C/apoA-I (mmol/g)	-0.091	-1.263 to 1.080	ns
apoA-I (g/L)	-0.299	-0.986 to 0.387	ns
HbA1c (%)	0.178	-0.166 to 0.521	ns
DM			
Age	-0.019	-0.038 to 0.000	ns
BMI (kg/m ²)	0.005	-0.044 to 0.054	ns
HDL-C/apoA-I (mmol/g)	1.801	0.235 to 3.368	<0.05
apoA-I (g/L)	-0.317	-1.252 to 0.618	ns
HbA1c (%)	0.052	-0.057 to 0.162	ns

Data are the mean ± SD and number (%). apoA-I: apolipoprotein A-I; BMI: body mass index; BP: blood pressure; DM: diabetes mellitus; HbA1c: hemoglobin A1c; HDL-C: high-density lipoprotein cholesterol.

Baseline characteristics of all patients and patients in the non-DM/DM subgroups are shown in Table 1. The 468 ACS patients had a mean age of 60.97 ± 9.57 years with a mean HbA1c of 6.4% ± 1.31 and a mean HDL-C/apoA-I ratio of 0.85 ± 0.12 mmol/g. The mean number of affected vessels indicated by coronary angiography was 2.57 ± 0.87 in DM patients, significantly higher than that in non-DM patients (2.39 ± 0.89, *p* < 0.05). Additionally, the HbA1c level was also higher in DM patients compared to non-DM ACS patients (7.75 ± 1.50 vs. 5.74 ± 0.35, *p* < 0.001). Although no differences were found in low-density lipoprotein cholesteryl (LDL-C), HDL-C, and apoA-I, the HDL-C/apoA-I ratio was lower in diabetic ACS patients than in non-DM patients (0.82 ± 0.10 vs. 0.86 ± 0.12, *p* < 0.01). No differences in other risk factors were found between the non-DM and DM ACS patients, such as age, gender, family history of coronary artery disease, history of hyper-

tension, heart rate (HR), creatine, blood urea nitrogen (BUN), and medication at discharge.

3.2. Baseline Characteristics of Patients with Single- and Multivessel Lesions. Baseline characteristics of ACS patients with single-vessel (1-2 affected vessels) and multivessel (≥3 affected vessels) lesions are shown in Table 2. No differences were found in risk factors, including age, gender, BMI, heart rate, systolic/diastolic blood pressure (BP), creatine, left ventricular ejection fraction (LVEF), HDL-C, and LDL-C, between the single- and multivessel lesion groups in either all, non-DM, or DM ACS patients.

In the whole population, 213 patients had multivessel lesions, while 255 patients had a single-vessel lesion. HbA1c was higher in patients with multivessel lesions (6.57 ± 1.45 vs. 6.24 ± 1.14, *p* < 0.05). However, apoA-I is lower in patients with multivessel lesions than a single-vessel lesion (1.05 ± 0.18 vs. 1.09 ± 0.17, *p* < 0.05).

In the non-DM subgroup, 165 and 149 patients had multi- and single-vessel lesions, respectively. HbA1c was unaltered between patients with different numbers of affected vessels, whereas apoA-I was decreased in patients with multivessel lesions compared to those with a single-vessel lesion (1.05 ± 0.18 vs. 1.1 ± 0.17, *p* < 0.05).

In the DM subgroup, 90 and 64 patients had multi- and single-vessel lesions, respectively. HbA1c was 8.03 ± 1.54 in patients with multiple-vessel lesions, which is significantly higher than that in patients with a single-vessel lesion (7.41 ± 1.38, *p* < 0.05). Moreover, the HDL-C/apoA-I ratio was higher in multivessel lesion DM patients than in single-vessel lesion DM patients (0.84 ± 0.11 vs. 0.79 ± 0.08, *p* < 0.05).

3.3. Association between HDL-C/apoA-I and Severity of Coronary Artery Stenosis. The severity of coronary artery stenosis was evaluated by the number of affected vessels suffering from coronary artery stenosis as described.

TABLE 4: Baseline characteristics for ACS patients with or without DM in HDL/apoA tertiles.

Characteristics	<0.77	HDL/apoA 0.77-0.89	>0.89	<i>p</i> value
All				
Patient number	152	161	155	
Age	58.57 ± 8.49	60.64 ± 9.95	63.65 ± 9.52	<0.001
Male, <i>n</i> (%)	121 (79.6)	125 (77.6)	119 (76.8)	ns
BMI (kg/m ²)	25.78 ± 3.42*	24.93 ± 3.14	24.05 ± 3.27	<0.01
HR (bpm)	69.98 ± 19.05	70.95 ± 12.87	72.52 ± 16.74	ns
Systolic BP (mmHg)	125 ± 18.58	127.33 ± 17.88	126.2 ± 20.58	ns
Diastolic BP (mmHg)	78.3 ± 11.39	78.83 ± 11.16	77 ± 12.73	ns
LVEF (%)	59.06 ± 12.57	58.83 ± 11.74	56.93 ± 13	ns
Creatine (μmol/L)	69.2 ± 16.94	70.69 ± 26.76	69.27 ± 17.56	ns
HDL-C (mmol/L)	0.75 ± 0.11	0.9 ± 0.15	1.08 ± 0.23	<0.001
LDL-C (mmol/L)	2.03 ± 0.62	2.26 ± 0.78	2.35 ± 0.93	<0.01
Triglyceride (mmol/L)	2.34 ± 1.48	1.54 ± 0.72	1.15 ± 0.73	<0.001
Lipoprotein A (mg/L)	197.66 ± 192.03	251.75 ± 204.74	292.67 ± 243.59	<0.05
apoA-I (g/L)	1.03 ± 0.14	1.07 ± 0.17	1.11 ± 0.22	<0.01
HbA1c (%)	6.45 ± 1.27	6.52 ± 1.52	6.22 ± 1.06	<0.01
HDL-C/apoA-I (mmol/g)	0.73 ± 0.05*	0.83 ± 0.02*	0.97 ± 0.08*	<0.001
Affected vessels	2.38 ± 0.94	2.43 ± 0.84	2.54 ± 0.88	ns
Non-DM				
Patient number	92	103	110	
Age	58.35 ± 8.68	59.26 ± 10.21	63.48 ± 9.76	<0.001
Male, <i>n</i> (%)	75 (81.5)	84 (81.6)	90 (75.6)	ns
BMI (kg/m ²)	25.93 ± 3.18	24.74 ± 3.09	23.73 ± 3.42	<0.001
HR (bpm)	70.08 ± 22.96	70.45 ± 12.74	72.46 ± 16.86	ns
Systolic BP (mmHg)	124.97 ± 17.14	125.95 ± 16.35	126.3 ± 21.26	ns
Diastolic BP (mmHg)	78.58 ± 11.72	78.24 ± 11.03	76.27 ± 12.58	ns
LVEF (%)	59.55 ± 12.56	60.12 ± 11.11	57.5 ± 13.14	ns
Creatine (μmol/L)	69.59 ± 15.69	68.81 ± 15.04	68.96 ± 17.1	ns
HDL-C (mmol/L)	0.75 ± 0.13	0.9 ± 0.14	1.08 ± 0.24	<0.001
LDL-C (mmol/L)	2.09 ± 0.67	2.3 ± 0.81	2.37 ± 0.94	ns
Triglyceride (mmol/L)	2.44 ± 1.7	1.53 ± 0.57	1.18 ± 0.81	<0.001
Lipoprotein A (mg/L)	194.42 ± 162.65	251.64 ± 204.09	304.74 ± 252.65	<0.01
apoA-I (g/L)	1.03 ± 0.15	1.07 ± 0.16	1.11 ± 0.22	<0.05
HbA1c (%)	5.75 ± 0.37	5.72 ± 0.38	5.76 ± 0.32	ns
HDL-C/apoA-I (mmol/g)	0.73 ± 0.05	0.84 ± 0.03	0.98 ± 0.09	<0.001
Affected vessels	2.34 ± 0.93	2.38 ± 0.86	2.43 ± 0.90	ns
DM				
Patient number	60	58	36	
Age	58.92 ± 8.27	63.1 ± 9.05	64.22 ± 8.79	<0.05
Male, <i>n</i> (%)	46 (76.7)	41 (70.7)	29 (80.6)	ns
BMI (kg/m ²)	25.54 ± 3.8	25.26 ± 3.24	25.1 ± 2.55	ns
HR (bpm)	69.85 ± 10.8	71.86 ± 13.17	72.75 ± 16.61	ns
Systolic BP (mmHg)	125.05 ± 20.77	129.76 ± 20.25	125.89 ± 18.44	ns
Diastolic BP (mmHg)	77.9 ± 10.98	79.9 ± 11.41	79.44 ± 13.09	ns

TABLE 4: Continued.

Characteristics	<0.77	HDL/apoA 0.77-0.89	>0.89	p value
LVEF (%)	58.3 ± 12.68	56.53 ± 12.6	55.09 ± 12.54	ns
Creatine (μmol/L)	68.6 ± 18.83	74.03 ± 39.85	70.33 ± 19.22	ns
HDL-C (mmol/L)	0.76 ± 0.11	0.9 ± 0.17	1.08 ± 0.24	<0.001
LDL-C (mmol/L)	1.96 ± 0.55	2.21 ± 0.75	2.3 ± 0.94	ns
Triglyceride (mmol/L)	2.21 ± 1.1	1.57 ± 0.94	1.07 ± 0.41	<0.001
Lipoprotein A (mg/L)	202.64 ± 231.38	251.94 ± 207.69	252.82 ± 209.19	ns
apoA-I (g/L)	1.05 ± 0.12	1.08 ± 0.19	1.12 ± 0.25	ns
HbA1c (%)	7.54 ± 1.41	7.97 ± 1.72	7.76 ± 1.22	ns
HDL-C/apoA-I (mmol/g)	0.73 ± 0.05	0.83 ± 0.03	0.97 ± 0.07	<0.05
Affected vessels	2.43 ± 0.96	2.52 ± 0.80	2.91 ± 0.71	<0.05

Data are mean ± SD and number (%). ACS: acute coronary syndrome; apoA-I: apolipoprotein A-I; BMI: body mass index; BP: blood pressure; DM: diabetes mellitus; HbA1c: hemoglobin A1c; HDL-C: high-density lipoprotein cholesterol; LDL-C: low-density lipoprotein cholesterol; LVEF: left ventricular ejection fraction.

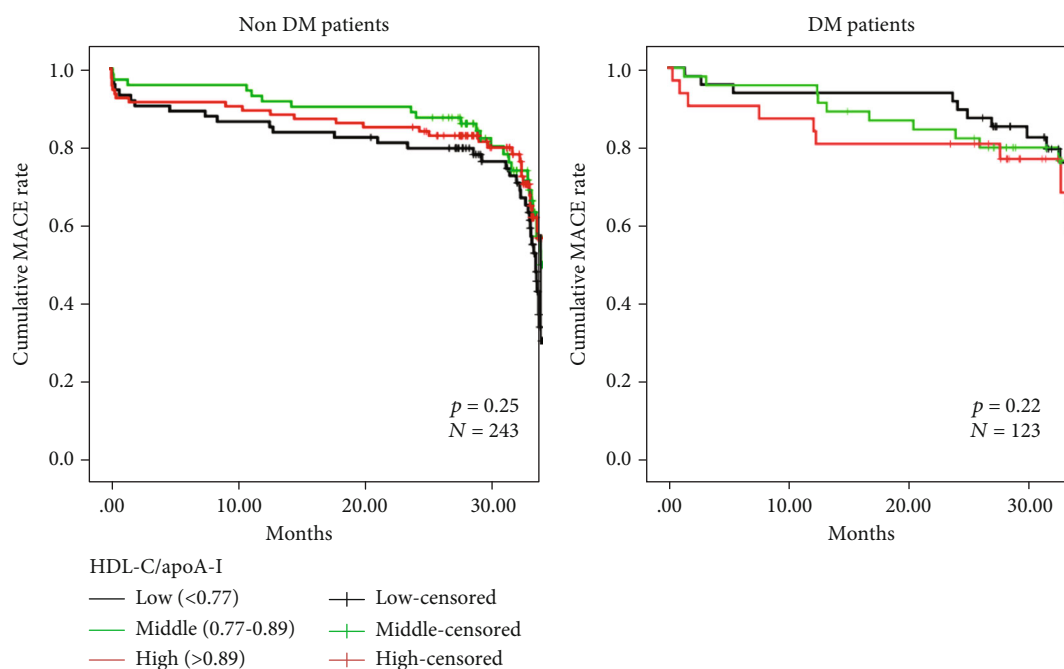


FIGURE 3: Kaplan-Meier survival curves for freedom from MACE in non-DM and DM patients.

Simple linear regression analysis demonstrated that the HDL-C/apoA-I ratio was positively correlated with the severity of coronary artery stenosis in DM ACS patients ($R^2 = 0.053$, $p = 0.004$). However, the HDL-C/apoA-I ratio was not associated with the severity of coronary artery stenosis in non-DM ACS patients (Figure 2).

Multiregression analysis was then performed to further determine the risk factors regarding the severity of coronary artery stenosis (Table 3). Consistently, the HDL-C/apoA-I ratio was only found to be significantly positively correlated to the severity of coronary artery stenosis in diabetic ACS patients (95% CI 0.235 to 3.368, $p < 0.05$).

3.4. Comparison of Characteristics between Patients with Different HDL-C/apoA-I Levels. Patients were divided into 3 groups based on HDL-C/apoA-I tertiles, and the comparison of various characteristics is shown in Table 4. In the whole population, age, HDL-C, LDL-C, and apoA-I were significantly increased in uprising HDL-C/apoA-I levels ($p < 0.05$). On the contrary, BMI was stepwise decreased based on HDL-C/apoA-I levels ($p < 0.001$). Patients with the middle level of HDL-C/apoA-I had the highest level of HbA1c compared to those with low and high levels of HDL-C/apoA-I (6.52 ± 1.52 vs. 6.45 ± 1.27 vs. 6.22 ± 1.06 , $p < 0.01$). No difference in gender, HR, BP, LVEF, and the number of stenotic

coronary arteries was found in this comparison. Similar trends of all these characteristics were found in the non-DM ACS patients.

In the DM ACS patient group, age and HDL-C were also increased as HDL-C/apoA-I levels rise (58.92 ± 8.27 vs. 63.1 ± 9.05 vs. 64.22 ± 8.79 , $p < 0.05$; 0.76 ± 0.11 vs. 0.9 ± 0.17 vs. 1.08 ± 0.24 , $p < 0.001$). Interestingly, the severity of coronary artery stenosis was more obvious in patients with lower HDL-C/apoA-I levels (2.91 ± 0.71 vs. 2.52 ± 0.80 vs. 2.43 ± 0.96 , $p < 0.05$).

3.5. Effect of the HDL-C/apoA-I Level on MACE Occurrence. Kaplan-Meier survival analysis was utilized to evaluate the survival curve in different HDL-C/apoA-I level groups in non-DM and DM ACS patients, as shown in Figure 3. However, the analysis showed no difference in MACE in both groups.

4. Discussion

The HDL-C/apoA-I ratio has been proposed as a novel surrogate marker for the increased risk of CVD-related, cancer-related, and all-cause death [17]. However, the discriminative value of the HDL-C/apoA-I ratio in predicting the risk and severity of CVD in diabetic and nondiabetic patients has not been studied yet. In this study, we found that the HDL-C/apoA-I ratio was positively correlated with the number of stenotic coronary arteries among diabetic ACS patients but not nondiabetic patients, indicating that the HDL-C/apoA-I ratio may be a valuable marker for predicting the severity of coronary artery stenosis in DM patients. However, the HDL-C/apoA-I ratio exhibited no effect on the 2-year MACE rate in both the diabetic and nondiabetic ACS patients.

The plasma HDL-C level is known to be inversely correlated with the risk of CVD [18, 19]. However, cholesteryl ester transfer protein inhibitors, such as torcetrapib and dalcetrapib, which can increase HDL-C levels by 30-70%, were proven to be ineffective in reducing recurrent cardiovascular events in ACS patients in phase 3 clinical trials [20, 21]. Moreover, increasing evidence demonstrates that not all HDL are functionally equivalent, and HDL dysfunction and remodeling are associated with reduced protective functions [22, 23]. For example, HDL isolated from T2DM and coronary artery disease patients exhibited impaired anti-inflammatory and antioxidative capacities compared to healthy controls [11, 24]. Dysfunctional HDL with elevated proinflammatory but impaired efflux capacities was also associated with an increased incidence of ACS [25]. In the present study, no difference was found in the HDL-C level between the DM and non-DM patients, although the number of stenotic coronary arteries was significantly higher in DM patients. Besides, the HDL-C level was also unchanged in patients with multivessel lesions compared to those with a single-vessel lesion, implying that HDL-C function is likely to be a better target for predicting and decreasing the risk of CVD than HDL-C quantity.

apoA-I is the major protein component of HDL, which plays critical roles in modulating the formation and function

of HDL [8]. The HDL-apoA-I exchange (HAE) rate is one of the important approaches to assess the function of HDL, in light of its ability to remodel and release lipid-poor apoA-I [26]. The HAE rate was decreased in T1DM young adults [27] and metabolic syndrome patients [28] compared with healthy control subjects. The HAE rate has also been reported to be inversely associated with the atherosclerotic burden and cardiovascular outcomes in T2DM [29]. Judging from the above studies, it is rational to investigate the value of the HDL-C/apoA-I ratio for cardiovascular outcomes.

Recently, growing evidence has proven that the HDL-C/apoA-I ratio may be an easier approach for estimating HDL function and provide additional insight as a risk marker for CVD. A cross-sectional study of 12,031 men found that the HDL-C level became positively correlated with preclinical atherosclerosis after adjusting for the apoA-I level [30]. The highest HDL-C/apoA-I ratio quartile has been shown to be associated with the increased risk for CVD- and cancer-related deaths [31]. However, a retrospective analysis of 2566 statin-treated coronary artery disease patients reported a controversial result that the increasing level of the HDL-C/apoA-I ratio was associated with less progression of coronary atherosclerosis as evaluated by intravascular ultrasound [32]. In our case, the HDL-C/apoA-I ratio was only increased in DM patients with multivessel lesions and positively correlated with the number of stenotic coronary arteries in DM patients, but not associated with MACEs in diabetic and nondiabetic patients. More well-designed and long-term follow-up studies are still necessary to further investigate the value of HDL-C/apoA-I in the prognosis of ACS patients with and without DM.

5. Limitations

Subjects enrolled in this study are limited to patients admitted to the cardiology department of the First Affiliated Hospital of Xi'an Jiaotong University, and the sample size is relatively small. Therefore, the conclusion should be drawn cautiously. A larger cohort study is needed to verify these findings and investigate the role of HDL-C/apoA-I in predicting long-term major adverse cardiac events in diabetic and nondiabetic ACS patients. Moreover, to evaluate the severity of coronary lesions, functional assessment, such as intravascular ultrasound and fractional flow reserve index, should be considered in future studies. Importantly, a complex and systemic score, i.e., SYNTAX score and TIMI score, could be further recorded to predict the severity of coronary artery stenosis more accurately.

6. Conclusions

A higher HDL-C/apoA-I ratio is associated with increased severity of coronary artery stenosis in DM patients with ACS. Further studies are needed to clarify the role of the HDL-C/apoA-I ratio in predicting short- and long-term CVD events in these patients.

Abbreviations

ACS:	Acute coronary syndrome
apoA-I:	Apolipoprotein A-I
BP:	Blood pressure
BUN:	Blood urea nitrogen
HbA1c:	Hemoglobin A1c
HDL-C:	High-density lipoprotein cholesterol
HR:	Heart rate
LDL-C:	Low-density lipoprotein cholesterol
LVEF:	Left ventricular ejection fraction
MACE:	Major adverse cardiac event
NSTEMI:	Non-ST elevated myocardial infarction
STEMI:	ST elevated myocardial infarction
T2DM:	Type 2 diabetes mellitus
UA:	Unstable angina.

Data Availability

Data supporting the conclusions of this article are included within the article and available from the corresponding authors on reasonable request.

Ethical Approval

This study received ethical committee approval at the First Affiliated Hospital of Xi'an Jiaotong University (ethical approval number: XJTU-1AF2012LSK-312).

Consent

Written informed consent was obtained from all study participants.

Conflicts of Interest

There is no conflict of interest regarding the publication of this article.

Authors' Contributions

ZY and JS designed this study. LS wrote the draft of the manuscript. YW and JZ revised the manuscript. MG, XQ, YH, TG, BL, CX, XB, and RL collected the written informed consent and patient data. LS, MG, and CX performed the statistical analysis. All authors read and approved the final manuscript.

Acknowledgments

This work was supported by the National Natural Science Foundation of China (81800390), the Clinical Research Award of the First Affiliated Hospital of Xi'an Jiaotong University, China (Nos. XJTU1AF-CRF-2018-025 and XJTU1AF-CRF-2016-004), the National Key R&D Program of China (2018YFC1311505), and the Key Project of Research and Development Plan (2017ZDCXL-SF-02-04-01).

References

- [1] A. Eisen, R. P. Giugliano, and E. Braunwald, "Updates on acute coronary syndrome," *JAMA Cardiology*, vol. 1, no. 6, pp. 718–730, 2016.
- [2] A. Timmis, "Acute coronary syndromes," *BMJ*, vol. 351, article h5153, 2015.
- [3] R. Piccolo, A. Franzone, K. C. Koskinas et al., "Effect of diabetes mellitus on frequency of adverse events in patients with acute coronary syndromes undergoing percutaneous coronary intervention," *The American Journal of Cardiology*, vol. 118, no. 3, pp. 345–352, 2016.
- [4] V. Fuster and M. E. Farkouh, "Acute coronary syndromes and diabetes mellitus: a winning ticket for prasugrel," *Circulation*, vol. 118, no. 16, pp. 1607–1608, 2008.
- [5] M. Zhou, J. Liu, Y. Hao et al., "Prevalence and in-hospital outcomes of diabetes among patients with acute coronary syndrome in China: findings from the Improving Care for Cardiovascular Disease in China-Acute Coronary Syndrome Project," *Cardiovascular Diabetology*, vol. 17, no. 1, p. 147, 2018.
- [6] P. Winzap, A. Davies, R. Klingenberg et al., "Diabetes and baseline glucose are associated with inflammation, left ventricular function and short- and long-term outcome in acute coronary syndromes: role of the novel biomarker Cyr 61," *Cardiovascular Diabetology*, vol. 18, no. 1, p. 142, 2019.
- [7] J. She, Y. Deng, Y. Wu et al., "Hemoglobin A1c is associated with severity of coronary artery stenosis but not with long term clinical outcomes in diabetic and nondiabetic patients with acute myocardial infarction undergoing primary angioplasty," *Cardiovascular Diabetology*, vol. 16, no. 1, p. 97, 2017.
- [8] M. Ouimet, T. J. Barrett, and E. A. Fisher, "HDL and reverse cholesterol transport," *Circulation Research*, vol. 124, no. 10, pp. 1505–1518, 2019.
- [9] E. M. Tsompanidi, M. S. Brinkmeier, E. H. Fotiadou, S. M. Giakoumi, and K. E. Kypreos, "HDL biogenesis and functions: role of HDL quality and quantity in atherosclerosis," *Atherosclerosis*, vol. 208, no. 1, pp. 3–9, 2010.
- [10] I. S. Yuhanna, Y. Zhu, B. E. Cox et al., "High-density lipoprotein binding to scavenger receptor-BI activates endothelial nitric oxide synthase," *Nature Medicine*, vol. 7, no. 7, pp. 853–857, 2001.
- [11] S. A. Sorrentino, C. Besler, L. Rohrer et al., "Endothelial-vasoprotective effects of high-density lipoprotein are impaired in patients with type 2 diabetes mellitus but are improved after extended-release niacin therapy," *Circulation*, vol. 121, no. 1, pp. 110–122, 2010.
- [12] R. F. H. Lemmers, M. van Hoek, A. G. Lieveise, A. J. M. Verhoeven, E. J. G. Sijbrands, and M. T. Mulder, "The anti-inflammatory function of high-density lipoprotein in type II diabetes: a systematic review," *Journal of Clinical Lipidology*, vol. 11, no. 3, pp. 712–724.e5, 2017.
- [13] J. D. Smith, "Apolipoprotein A-I and its mimetics for the treatment of atherosclerosis," *Current Opinion in Investigational Drugs*, vol. 11, no. 9, pp. 989–996, 2010.
- [14] R. S. Rosenson, H. B. Brewer Jr., W. S. Davidson et al., "Cholesterol efflux and atheroprotection: advancing the concept of reverse cholesterol transport," *Circulation*, vol. 125, no. 15, pp. 1905–1919, 2012.
- [15] D. T. Valenta, J. J. Bulgrien, C. L. Banka, and L. K. Curtiss, "Overexpression of human ApoAI transgene provides long-

- term atheroprotection in LDL receptor-deficient mice," *Atherosclerosis*, vol. 189, no. 2, pp. 255–263, 2006.
- [16] C. Paszty, N. Maeda, J. Verstuyft, and E. M. Rubin, "Apolipoprotein AI transgene corrects apolipoprotein E deficiency-induced atherosclerosis in mice," *The Journal of Clinical Investigation*, vol. 94, no. 2, pp. 899–903, 1994.
- [17] E. J. Rhee, C. D. Byrne, and K. C. Sung, "The HDL cholesterol/apolipoprotein A-I ratio," *Current Opinion in Endocrinology, Diabetes, and Obesity*, vol. 24, no. 2, pp. 148–153, 2017.
- [18] A. G. Olsson, G. G. Schwartz, M. Szarek et al., "High-density lipoprotein, but not low-density lipoprotein cholesterol levels influence short-term prognosis after acute coronary syndrome: results from the MIRACL trial," *European Heart Journal*, vol. 26, no. 9, pp. 890–896, 2005.
- [19] P. P. Toth, P. J. Barter, R. S. Rosenson et al., "High-density lipoproteins: a consensus statement from the National Lipid Association," *Journal of Clinical Lipidology*, vol. 7, no. 5, pp. 484–525, 2013.
- [20] G. G. Schwartz, A. G. Olsson, M. Abt et al., "Effects of dalcetrapib in patients with a recent acute coronary syndrome," *The New England Journal of Medicine*, vol. 367, no. 22, pp. 2089–2099, 2012.
- [21] P. J. Barter, M. Caulfield, M. Eriksson et al., "Effects of torcetrapib in patients at high risk for coronary events," *The New England Journal of Medicine*, vol. 357, no. 21, pp. 2109–2122, 2007.
- [22] G. E. Ronsein and T. Vaisar, "Inflammation, remodeling, and other factors affecting HDL cholesterol efflux," *Current Opinion in Lipidology*, vol. 28, no. 1, pp. 52–59, 2017.
- [23] R. S. Rosenson, H. B. Brewer Jr., B. J. Ansell et al., "Dysfunctional HDL and atherosclerotic cardiovascular disease," *Nature Reviews. Cardiology*, vol. 13, no. 1, pp. 48–60, 2016.
- [24] C. Besler, K. Heinrich, L. Rohrer et al., "Mechanisms underlying adverse effects of HDL on eNOS-activating pathways in patients with coronary artery disease," *The Journal of Clinical Investigation*, vol. 121, no. 7, pp. 2693–2708, 2011.
- [25] M. T. Soria-Florido, O. Castaner, C. Lassale et al., "Dysfunctional high-density lipoproteins are associated with a greater incidence of acute coronary syndrome in a population at high cardiovascular risk: a nested case-control study," *Circulation*, vol. 141, no. 6, pp. 444–453, 2020.
- [26] M. S. Borja, L. Zhao, B. Hammerson et al., "HDL-apoA-I exchange: rapid detection and association with atherosclerosis," *PLoS One*, vol. 8, no. 8, article e71541, 2013.
- [27] M. Heier, M. S. Borja, C. Brunborg et al., "Reduced HDL function in children and young adults with type 1 diabetes," *Cardiovascular Diabetology*, vol. 16, no. 1, p. 85, 2017.
- [28] M. S. Borja, B. Hammerson, C. Tang, O. V. Savinova, G. C. Shearer, and M. N. Oda, "Apolipoprotein A-I exchange is impaired in metabolic syndrome patients asymptomatic for diabetes and cardiovascular disease," *PLoS One*, vol. 12, no. 8, article e0182217, 2017.
- [29] M. Heier, A. P. Ofstad, M. S. Borja et al., "High-density lipoprotein function is associated with atherosclerotic burden and cardiovascular outcomes in type 2 diabetes," *Atherosclerosis*, vol. 282, pp. 183–187, 2019.
- [30] K. C. Sung, S. H. Wild, and C. D. Byrne, "Controlling for apolipoprotein A-I concentrations changes the inverse direction of the relationship between high HDL-C concentration and a measure of pre-clinical atherosclerosis," *Atherosclerosis*, vol. 231, no. 2, pp. 181–186, 2013.
- [31] K. C. Sung, S. Ryu, S. H. Wild, and C. D. Byrne, "An increased high-density lipoprotein cholesterol/apolipoprotein A-I ratio is associated with increased cardiovascular and all-cause mortality," *Heart*, vol. 101, no. 7, pp. 553–558, 2015.
- [32] P. Mani, K. Uno, J. St. John, E. M. Tuzcu, S. E. Nissen, and S. J. Nicholls, "Relation of high-density lipoprotein cholesterol:apolipoprotein A-I ratio to progression of coronary atherosclerosis in statin-treated patients," *The American Journal of Cardiology*, vol. 114, no. 5, pp. 681–685, 2014.

Research Article

Exploring the Relationship of Bone Turnover Markers and Bone Mineral Density in Community-Dwelling Postmenopausal Women

Xu Wei ^{1,2}, Yili Zhang ^{1,3}, Xinghua Xiang⁴, Menghua Sun,⁵ Kai Sun,¹ Tao Han,¹ Baoyu Qi,¹ Yanming Xie,⁵ Ranxing Zhang ⁶, and Liguozhu ^{1,2}

¹Wangjing Hospital, China Academy of Chinese Medical Sciences, Beijing, China

²Institute of Orthopaedics of Beijing Integrative Medicine, Beijing, China

³Beijing University of Chinese Medicine, Beijing, China

⁴Hunan University of Science and Technology, Xiangtan, China

⁵Institute of Basic Research in Clinical Medicine, China Academy of Chinese Medical Sciences, Beijing, China

⁶Department of Clinical Laboratory, Eye Hospital, China Academy of Chinese Medical Sciences, Beijing, China

Correspondence should be addressed to Ranxing Zhang; bjzrx@sina.com and Liguozhu; tcmspine@163.com

Received 23 December 2020; Revised 15 March 2021; Accepted 30 March 2021; Published 22 April 2021

Academic Editor: Alexander Berezin

Copyright © 2021 Xu Wei et al. This is an open access article distributed under the Creative Commons Attribution License, which permits unrestricted use, distribution, and reproduction in any medium, provided the original work is properly cited.

Aims. To explore the relationships of procollagen type 1 N-terminal propeptide (P1NP) and β cross-linked C-telopeptide of type 1 collagen (β -CTX) with bone mineral density (BMD) in postmenopausal women. **Methods.** All postmenopausal women were selected from a community-based case-control study. The anteroposterior L1-L4 and left proximal femur BMD were measured. P1NP and β -CTX were also collected and tested. The main correlation analysis was applied to explore the relationships of BMD, P1NP, and β -CTX. **Results.** The total 1055 postmenopausal women were enrolled. The BMD at all sites kept a decrease continually with age ($P < 0.01$). In addition, the level of β -CTX increased significantly from 45 to 50 years old and remained at a high level in the later stage, while the level of P1NP changed little or even decreased with age. Logistic regression model showed that β -CTX has better ability to predict BMD than P1NP, as demonstrated by an area under the curve (AUC) of 0.63. **Conclusion.** P1NP and β -CTX are important markers to monitor bone metabolism. This trial is registered with ChiCTR-SOC-17013090. The date of registration is Oct. 23, 2017.

1. Introduction

The most frequently used tool to diagnose osteoporosis (OP), the efficacy evaluation, and predict fracture risk is bone mineral density (BMD) in different sites according to the criteria of the World Health Organization [1]. However, the changes in BMD values are very small within six months and very difficult to detect acute changes in bone turnover [2, 3]. On the contrary, bone turnover markers (BTMs) could identify changes in bone remodeling within a relatively short-time interval before changes in BMD can be detected [4, 5]. The values of BTMs are often used to assess the treatment options and efficiency of antiresorptive anabolic therapies or combination therapies [6]. In postmenopausal osteoporosis

(PMOP), levels of bone resorption markers above the upper limit of the premenopausal range are associated with an increased risk of fracture [7]. Moreover, skeletal turnover is easily and noninvasively evaluated by the measurement of serum or urinary biochemical BTMs [8].

In all serum bone formation and resorption indices, two specific markers are the most recognized in the OP research: procollagen type 1 N-terminal propeptide (P1NP) and β cross-linked C-telopeptide of type 1 collagen (β -CTX) [9]. P1NP is a serum biomarker of bone formation, while β -CTX is a biomarker of bone resorption [10]. The International Osteoporosis Foundation and the International Federation of Clinical Chemistry and Laboratory Medicine recommended that P1NP and β -CTX were used as the

predictor of fracture risk and monitoring of OP treatment as early as 2011 [11, 12]. Based on the background, the research on P1NP and β -CTX in the diagnosis and treatment of OP has attracted more attention than ever. Biochemical bone turnover markers have been already recommended in the national OP clinical practice guideline or consensus documents [13, 14].

Several studies were conducted to explore BTMs in Chinese populations, especially the P1NP and β -CTX levels. A community-based population study was designed to evaluate reference ranges of P1NP and β -CTX in healthy Beijing postmenopausal women [15]. In 2013, the levels of P1NP and β -CTX were measured in a healthy Shanghai population covering premenopausal and postmenopausal women [16]. Another Chinese study analyzed 1436 healthy volunteers in 5 Chinese cities, and the relation of BMD and BTMs was evaluated in a large healthy Chinese population [17]. A high incidence of OP and osteoporotic fractures was demonstrated in the community-dwelling middle-aged and aged people [18, 19]. Nevertheless, there is little information on the levels of P1NP and β -CTX and their relationship with BMD in community-dwelling postmenopausal women in Beijing, China. Accordingly, the case-control study exploring the relation between biochemical indicators and bone mass state in postmenopausal women is required.

2. Methods

2.1. Study Design. This is a case-control study as a part of BEYOND study (BEijing communitY-based Osteoporosis and osteoporotic fracture screening: a cross-sectional and prospective study), starting in November, 2017 [20]. The study protocol was registered in the Chinese Clinical Trial Registry center (registration number: ChiCTR-SOC-17013090). A total of 1642 community residents who lived in Chaoyang and Dongcheng Districts of Beijing City were contacted via community health centers and recruited by clustered sampling in the baseline survey. It was conducted in November 2017 to July 2018 from local communities. In the present study, all postmenopausal women were selected from the surveyed population.

2.2. Ethical Statement. The authors stated that this study was approved by the medical ethics committee, Wangjing Hospital, China Academy of Chinese Medical Sciences (approval number: WJEC-KT-2017-020-P001) and followed the principles outlined in the Declaration of Helsinki for all human. In addition, for the investigations involving human subjects, a written informed consent has been obtained from the participants involved.

2.3. Study Participants. Figure 1 depicts a flowchart for participant selection in our study. All the subjects underwent careful past medical history inquiry and physical examination. The inclusion criteria in our study were as follows: (1) postmenopausal women aged from 45 to 79 years; (2) the subjects lived locally lasting for more than five years; (3) the population accepted the study plan and the laboratory examination including BMD and bone turnover markers (P1NP

and β -CTX); and (4) informed consents were obtained from all the subjects, in writing, before inclusion in the study. The participants in the total population who had incomplete information were excluded from the study. Eventually, 1055 postmenopausal women were eligible and enrolled in the present analysis.

2.4. Interviews. All the participants were interviewed via a standardized questionnaire to collect information and completed a face-to-face paper version of questionnaire. The content mainly contained age, weight, height, and time since menopause, history of previous illness, lifestyles, and so on. The comorbidity including cerebral infarction, coronary heart disease, dyslipidemia, hypertension, and diabetes mellitus was mainly reported by the subjects based on the currently prescribed medications. In addition, the lifestyles consisting of current smoking, habitual drinking, regular exercise, milk intake, and coffee intake were also investigated.

2.5. Bone Mineral Density Measurement. Dual-energy X-ray absorptiometry device (Hologic, WI, USA) was used to assess the value of BMD (g/cm^2). The anteroposterior L1-L4 and left proximal femur including the femoral neck and the total hip BMD were detected, and the T and Z values of each site were also recorded. According to the WHO diagnosis criteria, T -score > -1 was defined as normal bone mass, T -score ≤ -1 and > -2.5 was defined as osteopenia; whereas, T -score ≤ -2.5 was defined as OP based on bone densitometry [21]. After using the instrument daily, a professional staff was responsible for measuring the accuracy and debugging problems. The DXA scanner was calibrated every day, and the coefficient of variability values of the instrument was set at around 1%.

2.6. Bone Turnover Markers Testing. Fasting blood samples of the participants were collected between 8 a.m. and 9 a.m. in the sitting position. And the venipuncture was done in the antecubital region with minimal venostasis for the testing of P1NP and β -CTX. The measurements were conducted through automated electrochemiluminescence immunoassay system (Roche, Cobas E601, Germany), conforming to laboratory quality control procedures in the clinical practice guidelines of bone metabolic biomarkers (WS/T 357-2011) issued by National Health Commission of the People's Republic of China [22]. In addition, the serum segregated for detection was stored at -80 centigrade freezer. As a professional third-party testing organization, Guangzhou Kingmed Diagnostics Limited Liability Company was responsible for collecting and testing blood samples.

2.7. Statistical Analysis. The continuous variables which satisfied normal distribution were presented as the means \pm standard deviations. Data that did not show a normal distribution were expressed as the median [interquartile range (IQR)]. Categorical variables were represented by frequency and percentage (%). The comparison for each examined index between the confirmed OP and non-OP (osteopenia and normal) population used Student's t -test or one-way analysis of variance (ANOVA). The best-fitting mathematical model was applied to analyze the relationships between

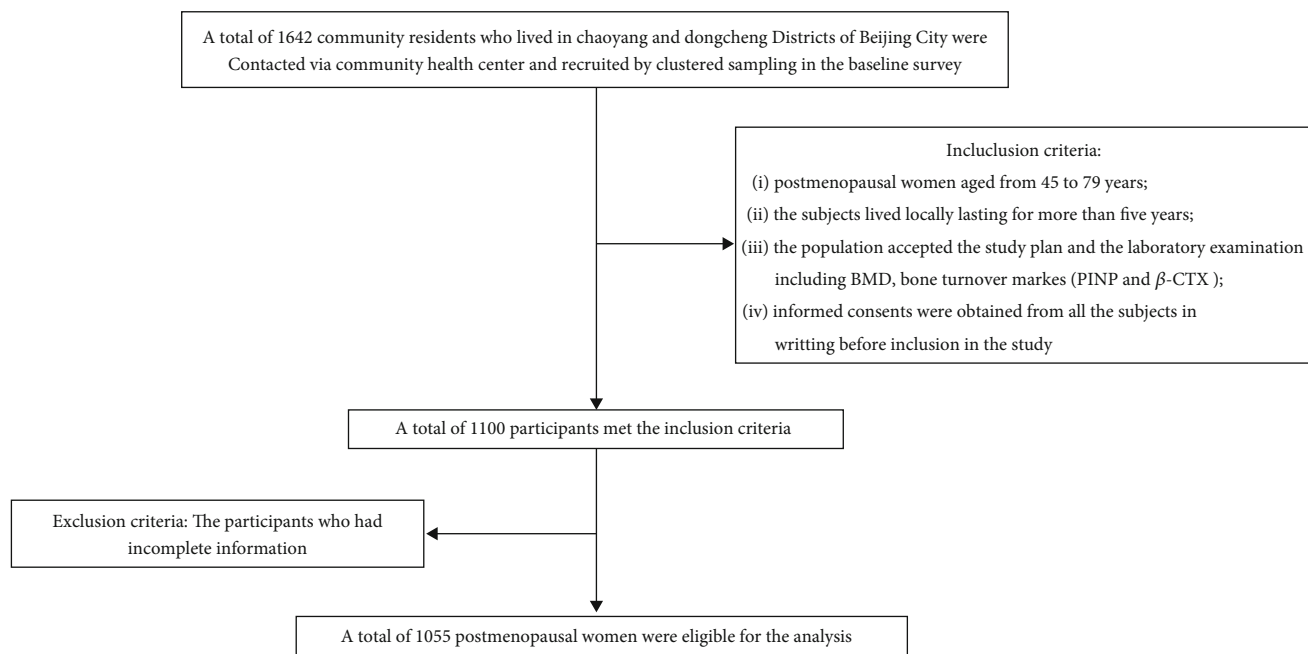


FIGURE 1: Flowchart of the subject selection process. BMD: bone mineral density; PINP: procollagen type 1 N-terminal propeptide; β -CTX: β cross-linked C-telopeptide of type 1 collagen.

BMD and BTMs. Univariate and multivariate logistic regression analyses were used to evaluate the predictive value of bone resorption (β -CTX) and formation (PINP) for BMD. Furthermore, the ability of β -CTX and PINP to identify BMD was assessed through receiver operating characteristic (ROC) curve analysis. All statistical results were analyzed by SPSS 23.0 software (SPSS Inc., Chicago, IL, USA), and P values ≤ 0.05 were considered as statistically significant.

3. Results

3.1. Subject Characteristics. Table 1 presents the characteristics of participants in the study. The basic anthropometry, BMD, BTMs, history or comorbidity, and lifestyle factors were described. The study population was composed of four parts: total population, confirmed OP population, osteopenia population, and normal population. In our study, 432 subjects were diagnosed OP, and the confirmed OP population became the older age group and had a lower body mineral index and longer menopausal duration ($P < 0.01$). The level of PINP and β -CTX in the nonosteoporosis group (osteopenia group and normal group) was significantly lower than that of the confirmed OP group ($P < 0.01$). In addition, the confirmed OP group also occupied a higher proportion in the history of cerebral infarction ($P = 0.01$).

3.2. BMD, PINP, and β -CTX Values in Different Age Groups. Table 2 shows the BMD, PINP, and β -CTX values at lumbar spine, femoral neck, and the total hip in different age groups. The BMD at all sites kept a decrease continually with age ($P < 0.01$). In addition, the level of β -CTX increased significantly from 45 to 50 years old and remained at a high level

in the later stage, while the level of PINP changed little or even decreased with age (Figure 2). The results from the aged 45 to 79 groups confirmed that a relative BMD decrease of 17%, 25%, and 21% was found at lumbar spine, femoral neck, and the total hip, respectively. The results from the aged 45 to 79 groups confirmed that a relative BTM increase of 8% and 35% was found at PINP and β -CTX, respectively.

3.3. Correlations between PINP, β -CTX, and BMD. Table 3 depicts the correlations between the BMD and BTMs, which found that β -CTX was negatively correlated with lumbar spine BMD in the normal group and negatively correlated with total hip BMD in the confirmed OP group ($P < 0.05$). Moreover, Spearman analysis also showed that PINP had a significantly negative correlation with lumbar spine BMD ($P < 0.01$) in OP population. In addition, Figures 3 and 4 depict the correlations of bone turnover markers and BMD at all sites in different population under the cubic model.

3.4. Predictive Value of BTMs (PINP and β -CTX) for BMD. Logistic regression was used to investigate the value of the biomarkers of bone resorption and formation in the prediction of BMD (Table 4). In the univariate analysis, PINP and β -CTX were significant predictors of BMD. Subsequently, these two indicators value with $P < 0.05$ were included in the multivariate logistic regression (forward) analysis, which revealed that only β -CTX was a significant independent predictor of BMD (odds ratio = 39.56, 95% CI: 3.7-422.94; $P = 0.002$). ROC curve analysis was then performed to evaluate the independent predictors of BMD (Figure 5). β -CTX was the best predictor for BMD, as demonstrated by an area under the curve (AUC) of 0.63.

TABLE 1: Characteristics of subjects in the study.

Variables	All participants (N = 1055)	Confirmed OP (N = 432)	Osteopenia (N = 481)	Normal (N = 142)	P value for difference	
					Unadjusted ^a	Adjusted ^b
Age (years)	63.14 (6.72)	65.06 (6.62)	62.33 (6.41)	60.06 (6.35)	<0.001	
BMI (kg/m ²)	25.32 (3.35)	24.41 (3.30)	25.65 (3.20)	26.97 (3.13)	<0.001	
Time since menopause	13.36 (7.71)	15.76 (7.70)	12.51 (7.24)	9.69 (6.73)	<0.001	
Lumbar spine BMD (g/cm ²)	0.84 (0.14)	0.73 (0.09)	0.88 (0.08)	1.05 (0.09)	<0.001	<0.001
Femoral neck BMD (g/cm ²)	0.69 (0.12)	0.61 (0.09)	0.71 (0.08)	0.85 (0.08)	<0.001	<0.001
Total hip BMD (g/cm ²)	0.79 (0.13)	0.70 (0.10)	0.82 (0.08)	0.96 (0.08)	<0.001	<0.001
P1NP (ng/mL)	52.73 (41.02, 68.95)	56.98 (45.41, 74.72)	50.75 (39.70, 66.28)	45.20 (34.64, 55.15)	<0.001	<0.001
β -CTX (ng/mL)	0.27 (0.20, 0.35)	0.29 (0.23, 0.39)	0.25 (0.20, 0.33)	0.22 (0.18, 0.30)	<0.001	<0.001
History or comorbidity (%)						
Cerebral infarction	81 (7.68%)	45 (10.42%)	32 (6.70%)	4 (2.80%)	0.01	
Coronary heart disease	126 (11.94%)	57 (13.19%)	56 (11.70%)	13 (9.20%)	0.42	
Dyslipidemia	267 (25.31%)	110 (25.46%)	119 (24.90%)	38 (26.80%)	0.90	
Hypertension	450 (42.65%)	178 (41.20%)	213 (44.60%)	59 (41.5%)	0.58	
Diabetes (type I)	3 (0.30%)	3 (0.70%)	0 (0.00%)	0 (0.00%)	0.12	
Diabetes (type II)	193 (18.40%)	77 (17.90%)	86 (18.00%)	30 (21.10%)	0.66	
Lifestyle factors (%)						
Current smoking	50 (4.74%)	20 (4.63%)	27 (5.60%)	3 (2.10%)	0.45	
Habitual drinking (\geq once/week)	55 (5.21%)	18 (4.17%)	29 (6.00%)	8 (5.60%)	0.31	
Regular exercise (\geq 3 times/week)	40 (3.79%)	17 (3.94%)	17 (3.70%)	6 (4.60%)	0.62	
Milk intake (\geq 3 times/week)	731 (69.29%)	285 (65.97%)	350 (72.80%)	96 (67.60%)	0.07	
Coffee intake (\geq 3 times/week)	33 (3.13%)	7 (1.62%)	20 (4.20%)	6 (4.20%)	0.25	

N: number of subjects; OP: osteoporosis; BMI: body mass index; BMD: bone mineral density; P1NP: procollagen type 1 N-terminal propeptide; β -CTX: β cross-linked C-telopeptide of type 1 collagen. Values are presented as the mean (standard deviation) or prevalence (%). ^aP values were obtained by Student's *t*-test, Kruskal-Wallis test, or chi-square test. ^bP values were obtained by analysis of covariance.

TABLE 2: BMD at all sites, P1NP, and β -CTX values in different age groups.

Age group (years)	Lumbar spine BMD	Femoral neck BMD	Total hip BMD	P1NP	β -CTX
45-49 (N = 12)	0.964 (0.164)	0.802 (0.104)	0.880 (0.122)	45.40 (41.40, 51.71)	0.20 (0.16, 0.22)
50-54 (N = 102)	0.885 (0.143)	0.747 (0.110)	0.849 (0.122)	55.12 (41.85, 76.14)	0.29 (0.20, 0.36)
55-59 (N = 205)	0.875 (0.132)	0.733 (0.107)	0.842 (0.115)	55.53 (44.83, 70.60)	0.26 (0.21, 0.34)
60-64 (N = 290)	0.831 (0.132)	0.692 (0.105)	0.793 (0.111)	52.68 (39.72, 67.97)	0.26 (0.20, 0.34)
65-69 (N = 251)	0.817 (0.134)	0.659 (0.101)	0.761 (0.113)	52.11 (40.87, 69.16)	0.28 (0.20, 0.36)
70-74 (N = 135)	0.828 (0.163)	0.658 (0.135)	0.760 (0.148)	51.56 (38.61, 64.37)	0.28 (0.22, 0.36)
75-79 (N = 60)	0.799 (0.135)	0.605 (0.114)	0.696 (0.119)	49.17 (36.07, 64.34)	0.27 (0.21, 0.34)
Statistics	8.05	23.19	21.90	8.58	11.80
P	<0.001 ^a	<0.001 ^a	<0.001 ^a	0.20 ^b	0.07 ^b

N: number of subjects; BMD: bone mineral density; P1NP: procollagen type 1 N-terminal propeptide; β -CTX: β cross-linked C-telopeptide of type 1 collagen. ^aP values were obtained by one-way ANOVA. ^bP values were obtained by the Kruskal-Wallis test.

4. Discussion

The association between BTMs and BMD is controversial, due primarily to discrepancy in findings. Moreover, most previous studies were conducted in Caucasian populations [23], with very few studies being done on Asian populations [24]. Thus, the novelty of this study was that we wanted to

evaluate the association between BTMs (P1NP and β -CTX) and BMD in a sample of Chinese women with wide-age groups and explored the contribution of these markers to the variation in BMD.

This case-control study showed that the level of BMD in postmenopausal women was lower than that in premenopausal women. From the viewpoint of different age group,

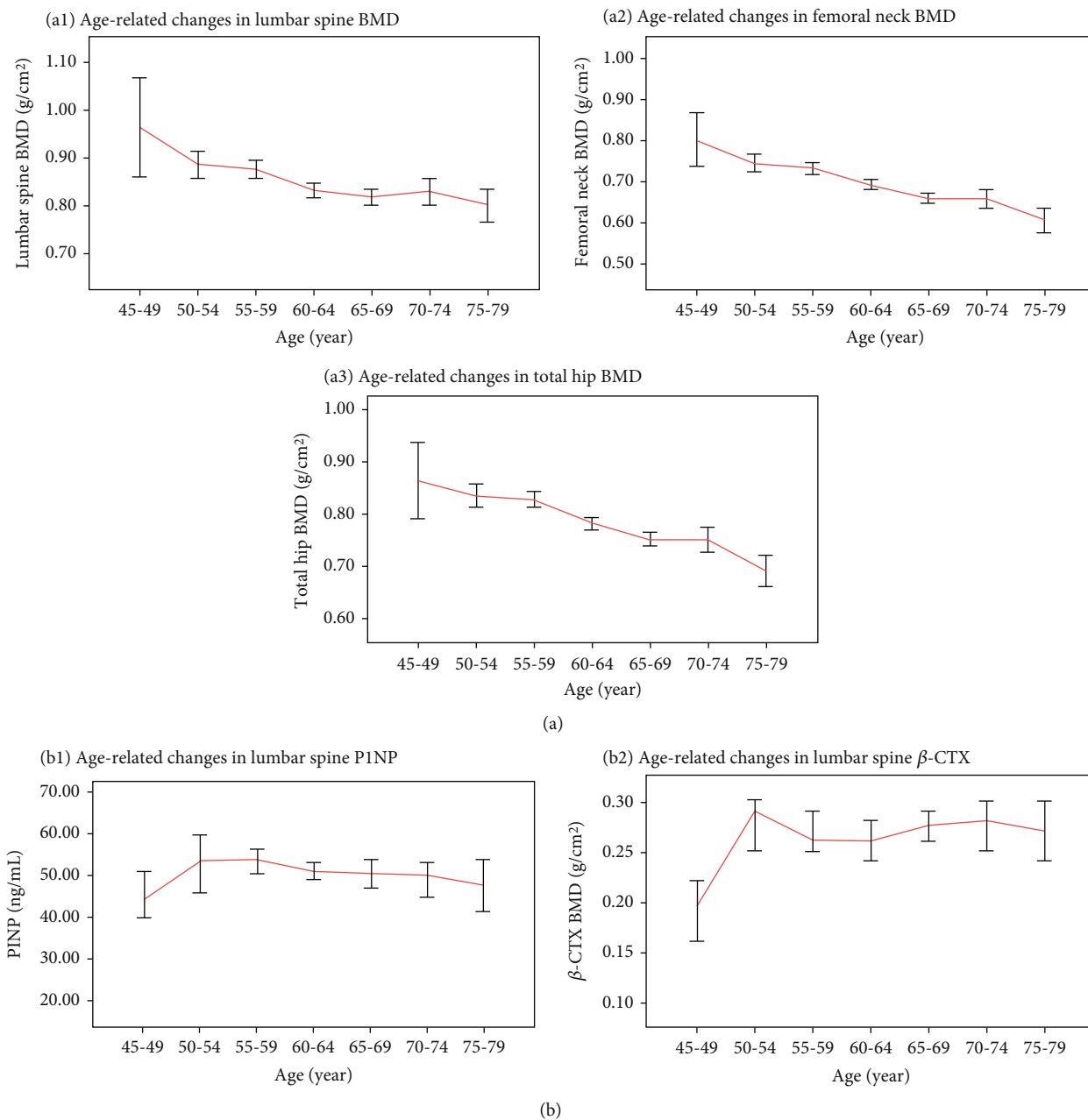


FIGURE 2: Age-related changes in BMD, P1NP, and β -CTX. BMD: bone mineral density; P1NP: procollagen type 1 N-terminal propeptide; β -CTX: β cross-linked C-telopeptide of type 1 collagen.

TABLE 3: Correlations between BMD, P1NP, and CTX.

	Variables	Lumbar spine BMD		Femoral neck BMD		Total hip BMD	
		<i>r</i>	<i>P</i>	<i>r</i>	<i>P</i>	<i>r</i>	<i>P</i>
Normal (<i>N</i> = 142)	P1NP	-0.09	0.31	-0.02	0.80	0.03	0.69
	β -CTX	-0.20	0.02	-0.04	0.60	-0.11	0.20
Confirmed OP (<i>N</i> = 432)	P1NP	-0.15	0.002	-0.07	0.14	-0.04	0.40
	β -CTX	-0.08	0.09	-0.05	0.27	-0.14	0.004

BMD: bone mineral density; P1NP: procollagen type 1 N-terminal propeptide; β -CTX: β cross-linked C-telopeptide of type 1 collagen; *r*: correlation coefficient. *P* values were obtained by Spearman correlation analysis.

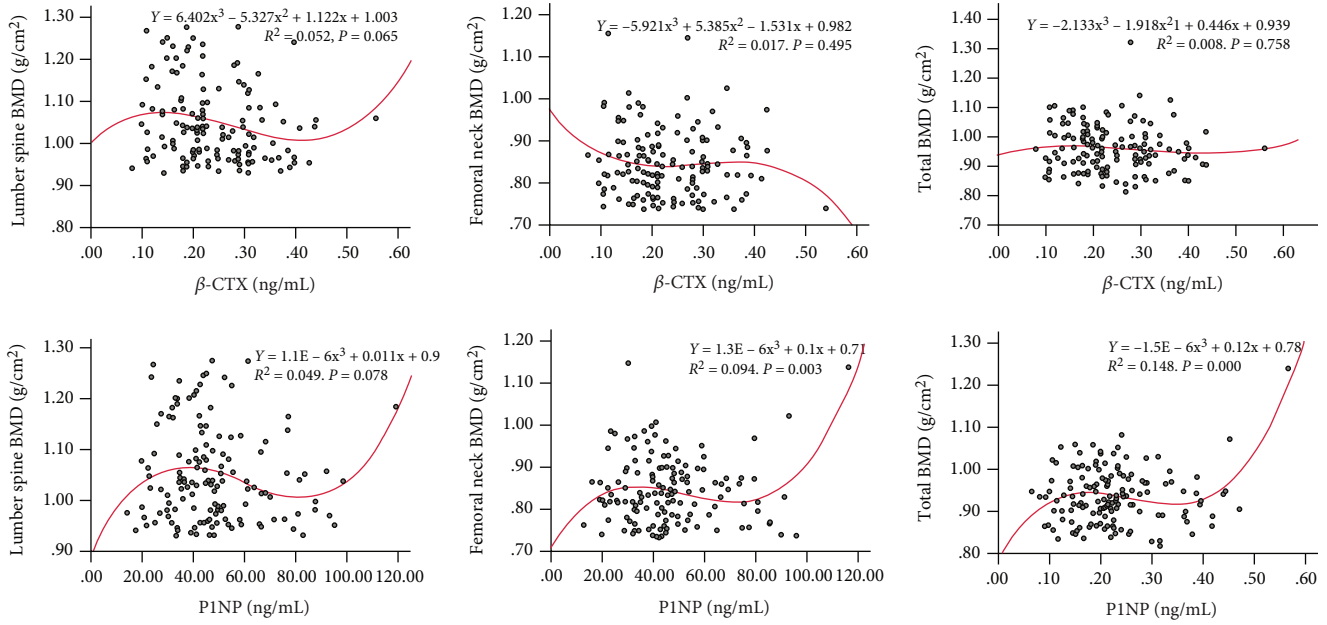


FIGURE 3: Correlations of bone turnover markers and BMD at all sites in normal group under the cubic model. BMD: bone mineral density; P1NP: procollagen type 1 N-terminal propeptide; β -CTX: β cross-linked C-telopeptide of type 1 collagen.

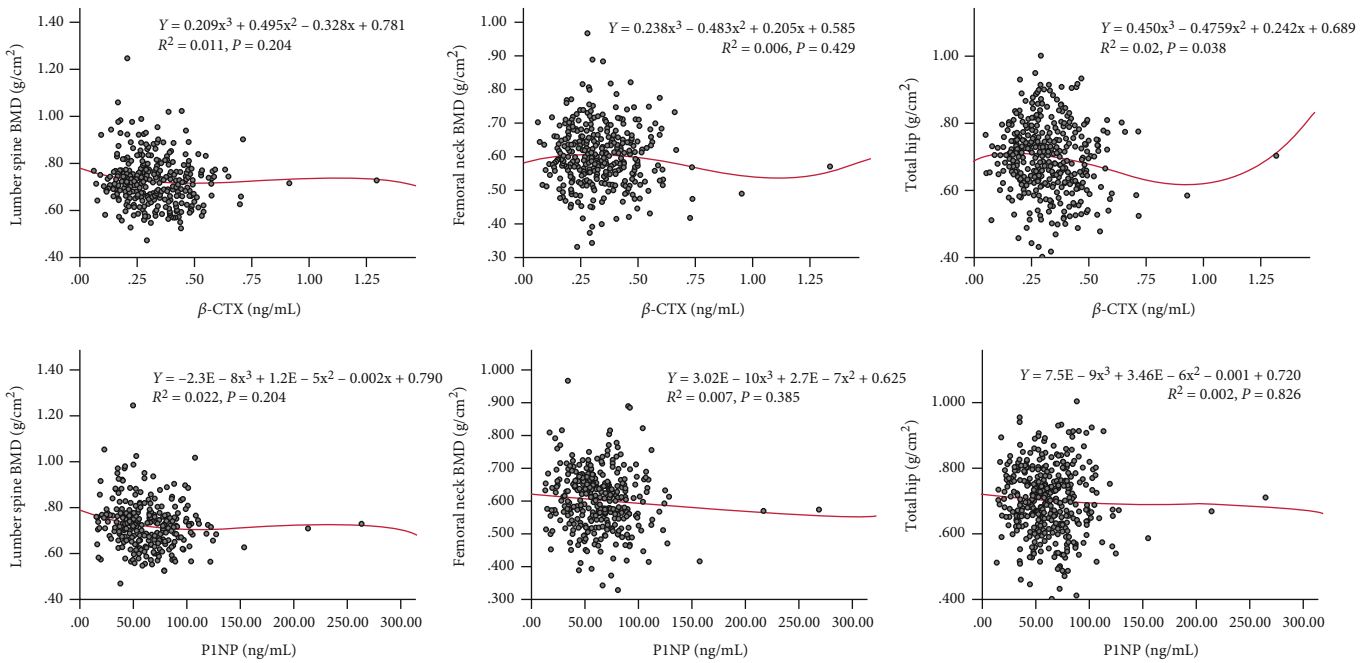


FIGURE 4: Correlations of bone turnover markers and BMD at all sites in confirmed osteoporosis group under the cubic model. BMD: bone mineral density; P1NP: procollagen type 1 N-terminal propeptide; β -CTX: β cross-linked C-telopeptide of type 1 collagen.

TABLE 4: Univariate and multivariate logistic regression analyses of P1NP and β -CTX for predicting BMD.

BTMs	Univariate logistic			Multivariate logistic (enter)		
	OR	95% CI	P value	OR	95% CI	P value
P1NP	1.02	(1.01, 1.03)	<0.001			
β -CTX	158.24	(22.99, 1089.33)	<0.001	39.56	(3.70, 422.94)	0.002

Data was presented by P value, OR, and 95% CI. The value of BTMs to predict BMD was tested using a univariate and multivariate logistic regression model. P value < 0.05 was considered statistically significant. BMD: bone mineral density; P1NP: procollagen type 1 N-terminal propeptide; β -CTX: β cross-linked C-telopeptide of type 1 collagen; CI: confidence interval.

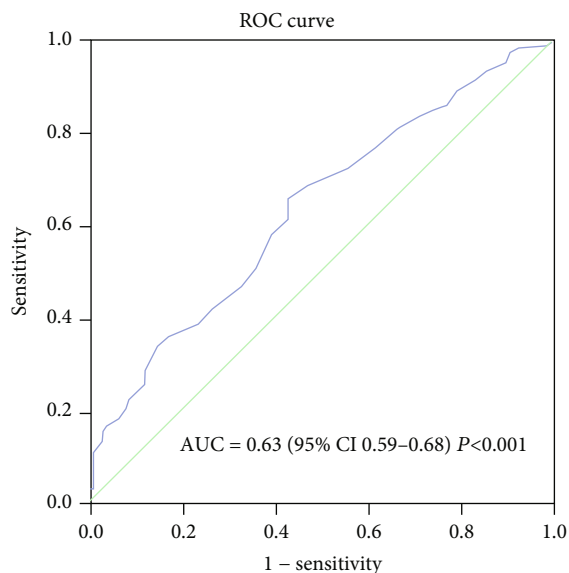


FIGURE 5: Receiver operating characteristic curves displaying the predictive performance of β -CTX in OP patients. ROC: receiver operating characteristic; AUC: area under the ROC curve; CI: confidence interval.

the BMD value at all sites kept a decrease continually with age (Table 2). Previous study has been indicated that the organic components of bones are mainly composed of type I collagen (about 90%), bone-binding proteins (about 10%), and other trace proteins [25]. Bone development stops after puberty, but cellular activity (bone remodeling) continues to maintain a dynamic balance between bone formation and bone resorption. However, menopause and certain pathological processes may upset this balance and lead to OP. Our study showed that P1NP and β -CTX have a relative increasing trend in the early postmenopausal period (Figure 2), which concurred with the results of Vasikaran et al. [26] and Lou et al. [27].

In the organic components of bone matrix, type I collagen is synthesized by osteoblasts, and its N-terminus is P1NP. The increased activity of osteocytes could drive the synthesis of procollagen and increase the blood concentration of P1NP. Hence, the concentration of P1NP in blood can be used as a marker to reflect the ability of osteoblasts to synthesize collagen, which is also the basis for evaluating osteoblast activity and bone formation [28, 29]. β -CTX, the degradation product of C-terminal peptide of type I collagen, is one of the most valuable markers to evaluate osteoclast activity and bone resorption [30, 31], and its increase could reflect the degree of bone resorption. In our study, we found that the level of β -CTX increased significantly from 45 to 50 years old and remained at a high level in the later stage, while the level of P1NP changed little or even decreased with age, which indicated that the degree of bone resorption was greater than bone formation. Similar study confirmed that it was not only consistent with the development trend of BMD but also may explain the reason for the decrease of bone mass [32].

Estrogen research has provided landmark research on understanding the relationship between osteoporosis and

BTMs [33]. Declining circulating estradiol levels, particularly during the menopausal transition, gives rise to increased bone turnover, causing an imbalance between bone resorption and formation [34, 35]. With the extension of time since menopause, the positive correlation of estrogen with BMD and BTMs was found in our study. Moreover, during the aged 45 to 59, the fluctuation of BTMs was more obvious, reflecting that estrogen concentration was one of the most important factors determining BTMs.

Estrogen loss promotes osteoclast formation and bone resorption while inhibiting osteoclast apoptosis through a variety of mechanisms. In the case of withdrawal of estrogen after menopause, the expression of RANKL (a molecule essential for osteoclast formation) in osteoblast lineage including mesenchymal stem cells [36], osteocytes [37], and bone lining cells [38] increased, while OPG production decreased. The increased RANKL could bind to RANK and induce the recruitment of TNF receptor-associated factor 6 (TRAF6), and further activate the downstream NF- κ B and MAPK pathways; both of which drive the activation of NFATc1 and stimulate osteoclast formation [39]. Estrogen deficiency also inhibits osteoclast apoptosis by inhibiting Fas/FasL system [40]. In contrast to postmenopausal bone resorption, bone formation decreased relatively. In its physiological state, estrogen could protect osteoblasts from apoptosis and enhance their proliferation, maturation, and mineralization to maintain bone formation through various signaling pathways [41, 42]. However, these osteoprotective effects are counteracted by estrogen deprivation. Furthermore, previous study revealed that ovariectomy-induced estrogen deficiency stimulated the activation of NF- κ B in differentiated osteoblasts, thus weakening the function of osteoblasts [43].

It is worth noting that previous studies have confirmed that both types of BTMs (resorption and formation) are more increased in early postmenopausal period due to accelerated bone resorption [14, 44]. BTMs still increase in elderly patients, which is usually explained by other mechanisms (vitamin D deficiency, intestinal malabsorption of calcium, and secondary hyperparathyroidism) [45]. In addition, previous studies have confirmed that BTM is correlated with BMD value in different skeleton sites [46, 47]. However, we did not observe the negative correlation of BTMs and BMD value at all sites (Table 3 and Figures 3 and 4) in the present study. However, given the limitations of sample size and study period, the negative correlation between BMD and BTMs has not been observed in this study, which may need to be confirmed by further follow-up studies.

5. Strengths and Novelty

Our study has the following novelty and strengths: (1) as far as we know, this study was the first time to analyze the correlation between BTMs and BMD in Beijing area, which may further deepen and expand the existing evidence [16]; (2) the sample size was large enough and the study participants with a wide age-range were recruited from the urban and suburb, thereby avoiding sample error and being representative of the Chinese population; (3) this study utilized current recommendations and gold standards to evaluate BMD along

with prevalence of osteopenia and osteoporosis; and (4) we well described and screened the participants' characteristics, and have the detailed inclusion and exclusion criteria to ensure a more precise sample population.

6. Limitations

This study did, however, have some limitations. The main limitation of this study was the observational study design with group comparisons, which did not enable causal interpretations. Moreover, BTMs were also affected by dietary and circadian rhythms [48], and the limited number of BTMs analyzed showed an incomplete process of bone metabolism. Therefore, we will continue to expand the sample size for follow-up study to explore the deeper relationship between BTMs and BMD in a larger population.

7. Conclusion

The low bone mass state was significantly associated with the increased levels of BTMs in the development of osteoporosis. For the community-dwelling postmenopausal women with different age, PINP and β -CTX were important markers to monitor bone metabolism. Considering the findings in this study, more future extensive studies are necessary to clarify potential molecular mechanisms to help develop more effective therapeutic interventions that may slow the progression of postmenopausal osteoporosis.

Data Availability

All data used to support the findings of this study are included within the article.

Conflicts of Interest

The authors declare that they have no conflict of interest.

Authors' Contributions

Xu Wei, Yili Zhang, and Xinghua Xiang contributed equally to this paper and they are co-first authors.

Acknowledgments

This work was funded by the Clinical Research Project of State Administration of Traditional Chinese Medicine (Grant number: JDZX2015076), the Foundation for Young Talents Training of China Association of Chinese Medicine (Grant number: CACM-2017-QNRC2-A03), and the Fundamental Research Funds for the Central Public Welfare Research Institutes (Grant number: ZZ13-YQ-039).

References

- [1] World Health Organization, "Assessment of fracture risk and its application to screening for postmenopausal osteoporosis. Report of a WHO Study Group," *World Health Organization Technical Report Series*, vol. 843, pp. 1–129, 1994.
- [2] Y. Nishizawa, M. Miura, S. Ichimura et al., "Executive summary of the Japan Osteoporosis Society Guide for the Use of Bone Turnover Markers in the Diagnosis and Treatment of Osteoporosis (2018 edition)," *Clinica Chimica Acta*, vol. 498, pp. 101–107, 2019.
- [3] J. Lee and S. Vasikaran, "Current recommendations for laboratory testing and use of bone turnover markers in management of osteoporosis," *Annals of Laboratory Medicine*, vol. 32, no. 2, pp. 105–112, 2012.
- [4] J. J. Kelly, "Bone turnover markers in osteoporosis," *Journal of the American Medical Association*, vol. 322, no. 23, p. 2344, 2019.
- [5] S. Botella, P. Restituto, I. Monreal, I. Colina, A. Calleja, and N. Varo, "Traditional and novel bone remodeling markers in premenopausal and postmenopausal women," *The Journal of Clinical Endocrinology and Metabolism*, vol. 98, no. 11, pp. E1740–E1748, 2013.
- [6] S. Y. Park, S. H. Ahn, J. I. Yoo et al., "Position statement on the use of bone turnover markers for osteoporosis treatment," *Journal of bone metabolism*, vol. 26, no. 4, pp. 213–224, 2019.
- [7] T. Vilaca, F. Gossiel, and R. Eastell, "Bone turnover markers: use in fracture prediction," *Journal of Clinical Densitometry*, vol. 20, no. 3, pp. 346–352, 2017.
- [8] E. Biver, F. Chopin, G. Coiffier et al., "Bone turnover markers for osteoporotic status assessment? A systematic review of their diagnosis value at baseline in osteoporosis," *Joint, Bone, Spine*, vol. 79, no. 1, pp. 20–25, 2012.
- [9] D. Bauer, J. Krege, N. Lane et al., "National Bone Health Alliance Bone Turnover Marker Project: current practices and the need for US harmonization, standardization, and common reference ranges," *Osteoporosis International*, vol. 23, no. 10, pp. 2425–2433, 2012.
- [10] M. Samoszuk, M. Leuther, and N. Hoyle, "Role of serum P1NP measurement for monitoring treatment response in osteoporosis," *Biomarkers in Medicine*, vol. 2, no. 5, pp. 495–508, 2008.
- [11] S. Vasikaran, C. Cooper, R. Eastell et al., "International Osteoporosis Foundation and International Federation of Clinical Chemistry and Laboratory Medicine position on bone marker standards in osteoporosis," *Clinical Chemistry and Laboratory Medicine*, vol. 49, no. 8, pp. 1271–1274, 2011.
- [12] for the IOF-IFCC Bone Marker Standards Working Group, S. Vasikaran, R. Eastell et al., "Markers of bone turnover for the prediction of fracture risk and monitoring of osteoporosis treatment: a need for international reference standards," *Osteoporosis International*, vol. 22, no. 2, article 1501, pp. 391–420, 2011.
- [13] Y. Nishizawa, H. Ohta, M. Miura et al., "Guidelines for the use of bone metabolic markers in the diagnosis and treatment of osteoporosis (2012 edition)," *Journal of Bone and Mineral Metabolism*, vol. 31, no. 1, pp. 1–15, 2013.
- [14] E. Cavalier, P. Bergmann, O. Bruyère et al., "The role of biochemical of bone turnover markers in osteoporosis and metabolic bone disease: a consensus paper of the Belgian Bone Club," *Osteoporosis International*, vol. 27, no. 7, pp. 2181–2195, 2016.
- [15] J. Zhao, W. Xia, M. Nie et al., "The levels of bone turnover markers in Chinese postmenopausal women: Peking Vertebral Fracture study," *Menopause*, vol. 18, no. 11, pp. 1237–1243, 2011.
- [16] W. W. Hu, Z. Zhang, J. W. He et al., "Establishing reference intervals for bone turnover markers in the healthy Shanghai

- population and the relationship with bone mineral density in postmenopausal women,” *International Journal of Endocrinology*, vol. 2013, Article ID 513925, 7 pages, 2013.
- [17] M. Li, F. Lv, Z. Zhang et al., “Establishment of a normal reference value of parathyroid hormone in a large healthy Chinese population and evaluation of its relation to bone turnover and bone mineral density,” *Osteoporosis International*, vol. 27, no. 5, pp. 1907–1916, 2016.
- [18] G. Yan, Y. Huang, H. Cao, J. Wu, N. Jiang, and X. Cao, “Association of breastfeeding and postmenopausal osteoporosis in Chinese women: a community-based retrospective study,” *BMC Womens Health*, vol. 19, no. 1, p. 110, 2019.
- [19] C. Gao, Y. Xu, L. Li et al., “Prevalence of osteoporotic vertebral fracture among community-dwelling elderly in Shanghai,” *Chinese Medical Journal*, vol. 132, no. 14, pp. 1749–1751, 2019.
- [20] M. Sun, Y. Zhang, H. Shen et al., “Prevalence of and risk factors for community-based osteoporosis and associated fractures in Beijing: study protocol for a cross-sectional and prospective study,” *Frontiers in Medicine*, vol. 7, p. 544697, 2020.
- [21] J. A. Kanis, L. J. Melton 3rd, C. Christiansen, C. C. Johnston, and N. Khaltaev, “The diagnosis of osteoporosis,” *Journal of Bone and Mineral Research*, vol. 9, no. 8, pp. 1137–1141, 1994.
- [22] National Health Commission of the People’s Republic of China, “Clinical practice guidelines of bone metabolic biomarkers,” <http://www.nhc.gov.cn/wjw/s9492/201112/53784.shtml>.
- [23] S. Adami, G. Bianchi, M. L. Brandi et al., “Determinants of bone turnover markers in healthy premenopausal women,” *Calcified Tissue International*, vol. 82, no. 5, pp. 341–347, 2008.
- [24] A. Makker, M. M. Singh, G. Mishra, B. P. Singh, G. K. Jain, and S. Jadhav, “Relationship between bone turnover biomarkers, mandibular bone mineral density, and systemic skeletal bone mineral density in premenopausal and postmenopausal Indian women,” *Menopause*, vol. 19, no. 6, pp. 642–649, 2012.
- [25] Z. Tan, H. Ren, R. Bai, and X. Wang, “Osteoporosis and biochemical indicators of bone metabolism,” *Chinese Journal of Osteoporosis*, vol. 12, no. 1, pp. 89–93, 2006.
- [26] S. D. Vasikaran, S. A. P. Chubb, P. R. Ebeling et al., “Harmonised Australian reference intervals for serum P1NP and CTX in adults,” *Clinical Biochemist Reviews*, vol. 35, no. 4, pp. 237–242, 2014.
- [27] H. Lou, C. Peng, and Q. Chen, “Clinical value of serum total P1NP, β -CTX and 25(OH)D3 detection in evaluating risks of fragile hip fracture in elderly patients with osteoporosis,” *Nan Fang Yi Ke Da Xue Xue Bao*, vol. 32, no. 9, pp. 1346–1349, 2012.
- [28] Q. Xie, D. Ye, H. Wen, and X. Li, “Relationship between the changes of biochemical markers of bone turnover and osteoporosis in male patients with type 2 diabetes,” *Zhonghua Lin Chuang Shi Yan Shi Guan Li Dian Zi Za Zhi*, vol. 2, no. 1, pp. 51–54, 2014.
- [29] M. K. Koivula, L. Risteli, and J. Risteli, “Measurement of aminoterminal propeptide of type I procollagen (PINP) in serum,” *Clinical Biochemistry*, vol. 45, no. 12, pp. 920–927, 2012.
- [30] R. Eastell and P. Szulc, “Use of bone turnover markers in postmenopausal osteoporosis,” *The Lancet Diabetes and Endocrinology*, vol. 5, no. 11, pp. 908–923, 2017.
- [31] R. S. Filip and J. Zagórski, “Age- and BMD-related differences in biochemical markers of bone metabolism in rural and urban women from Lublin Region, Poland,” *Annals of Agricultural and Environmental Medicine*, vol. 11, no. 2, pp. 255–259, 2004.
- [32] F. Gossiel, H. Altaher, D. M. Reid et al., “Bone turnover markers after the menopause: T-score approach,” *Bone*, vol. 111, pp. 44–48, 2018.
- [33] K. Henriksen, C. Christiansen, and M. A. Karsdal, “Role of biochemical markers in the management of osteoporosis,” *Climacteric*, vol. 18, supplement 2, pp. 10–18, 2015.
- [34] H. Awasthi, D. Mani, D. Singh, and A. Gupta, “The underlying pathophysiology and therapeutic approaches for osteoporosis,” *Medicinal Research Reviews*, vol. 38, no. 6, pp. 2024–2057, 2018.
- [35] E. A. Marques, V. Gudnason, T. Lang et al., “Association of bone turnover markers with volumetric bone loss, periosteal apposition, and fracture risk in older men and women: the AGES-Reykjavik longitudinal study,” *Osteoporosis International*, vol. 27, no. 12, pp. 3485–3494, 2016.
- [36] Q. Cong, H. Jia, S. Biswas et al., “p38 α MAPK regulates lineage commitment and OPG synthesis of bone marrow stromal cells to prevent bone loss under physiological and pathological conditions,” *Stem Cell Reports*, vol. 6, no. 4, pp. 566–578, 2016.
- [37] Y. Fujiwara, M. Piemontese, Y. Liu, J. D. Thostenson, J. Xiong, and C. A. O’Brien, “RANKL (receptor activator of NF κ B ligand) produced by osteocytes is required for the increase in B cells and bone loss caused by estrogen deficiency in mice,” *The Journal of Biological Chemistry*, vol. 291, no. 48, pp. 24838–24850, 2016.
- [38] C. Streicher, A. Heyny, O. Andrukhova et al., “Estrogen regulates bone turnover by targeting RANKL expression in bone lining cells,” *Scientific Reports*, vol. 7, no. 1, p. 6460, 2017.
- [39] T. Ono and T. Nakashima, “Recent advances in osteoclast biology,” *Histochemistry and Cell Biology*, vol. 149, no. 4, pp. 325–341, 2018.
- [40] T. Nakamura, Y. Imai, T. Matsumoto et al., “Estrogen prevents bone loss via estrogen receptor alpha and induction of Fas ligand in osteoclasts,” *Cell*, vol. 130, no. 5, pp. 811–823, 2007.
- [41] X. Sun, X. Yang, Y. Zhao, Y. Li, and L. Guo, “Effects of 17 β -estradiol on mitophagy in the murine MC3T3-E1 osteoblast cell line is mediated via G protein-coupled estrogen receptor and the ERK1/2 signaling pathway,” *Medical Science Monitor*, vol. 24, pp. 903–911, 2018.
- [42] P. I. Lin, Y. T. Tai, W. P. Chan, Y. L. Lin, M. H. Liao, and R. M. Chen, “Estrogen/ER α signaling axis participates in osteoblast maturation via upregulating chromosomal and mitochondrial complex gene expressions,” *Oncotarget*, vol. 9, no. 1, article 23453, pp. 1169–1186, 2018.
- [43] J. Chang, Z. Wang, E. Tang et al., “Inhibition of osteoblastic bone formation by nuclear factor-kappaB,” *Nature Medicine*, vol. 15, no. 6, pp. 682–689, 2009.
- [44] J. Lenora, K. K. Ivaska, K. J. Obrant, and P. Gerdhem, “Prediction of bone loss using biochemical markers of bone turnover,” *Osteoporosis International*, vol. 18, no. 9, pp. 1297–1305, 2007.
- [45] M. J. Seibel, “Biochemical markers of bone turnover: part I: biochemistry and variability,” *Clinical Biochemist Reviews*, vol. 26, no. 4, pp. 97–122, 2005.
- [46] D. C. Bauer, P. M. Sklarin, K. L. Stone et al., “Biochemical markers of bone turnover and prediction of hip bone loss in older women: the study of osteoporotic fractures,” *Journal of Bone and Mineral Research*, vol. 14, no. 8, pp. 1404–1410, 1999.

- [47] L. J. Melton 3rd, S. Khosla, E. J. Atkinson, W. M. O'Fallon, and B. L. Riggs, "Relationship of bone turnover to bone density and fractures," *Journal of Bone and Mineral Research*, vol. 12, no. 7, pp. 1083–1091, 1997.
- [48] for the National Bone Health Alliance Bone Turnover Marker Project, P. Szulc, K. Naylor, N. R. Hoyle, R. Eastell, and E. T. Leary, "Use of CTX-I and PINP as bone turnover markers: National Bone Health Alliance recommendations to standardize sample handling and patient preparation to reduce pre-analytical variability," *Osteoporosis International*, vol. 28, no. 9, pp. 2541–2556, 2017.

Research Article

The Value of a Seven-Autoantibody Panel Combined with the Mayo Model in the Differential Diagnosis of Pulmonary Nodules

Zhougui Ling ¹, Jifei Chen ², Zhongwei Wen,¹ Xiaomou Wei,² Rui Su,¹ Zhenming Tang,¹ and Zhuojun Hu ¹

¹Department of Pulmonary and Critical Care Medicine, The Fourth Affiliated Hospital of Guangxi Medical University, No. 1, Liushi Road, Liuzhou 545005, China

²Clinical Laboratory, The Fourth Affiliated Hospital of Guangxi Medical University, No. 1, Liushi Road, Liuzhou 545005, China

Correspondence should be addressed to Zhuojun Hu; huzhuojun1964@163.com

Received 2 November 2020; Revised 26 January 2021; Accepted 10 February 2021; Published 20 February 2021

Academic Editor: Alexander Berezin

Copyright © 2021 Zhougui Ling et al. This is an open access article distributed under the Creative Commons Attribution License, which permits unrestricted use, distribution, and reproduction in any medium, provided the original work is properly cited.

Background. Identifying malignant pulmonary nodules and detecting early-stage lung cancer (LC) could reduce mortality. This study investigated the clinical value of a seven-autoantibody (7-AAB) panel in combination with the Mayo model for the early detection of LC and distinguishing benign from malignant pulmonary nodules (MPNs). **Methods.** The concentrations of the elements of a 7-AAB panel were quantitated by enzyme-linked immunosorbent assay (ELISA) in 806 participants. The probability of MPNs was calculated using the Mayo predictive model. The performances of the 7-AAB panel and the Mayo model were analyzed by receiver operating characteristic (ROC) analyses, and the difference between groups was evaluated by chi-square tests (χ^2). **Results.** The combined area under the ROC curve (AUC) for all 7 AABs was higher than that of a single one. The sensitivities of the 7-AAB panel were 67.5% in the stage I-II LC patients and 60.3% in the stage III-IV patients, with a specificity of 89.6% for the healthy controls and 83.1% for benign lung disease patients. The detection rate of the 7-AAB panel in the early-stage LC patients was higher than that of traditional tumor markers. The AUC of the 7-AAB panel in combination with the Mayo model was higher than that of the 7-AAB panel alone or the Mayo model alone in distinguishing MPN from benign nodules. For early-stage MPN, the sensitivity and specificity of the combination were 93.5% and 58.0%, respectively. For advanced-stage MPN, the sensitivity and specificity of the combination were 91.4% and 72.8%, respectively. The combination of the 7-AAB panel with the Mayo model significantly improved the detection rate of MPN, but the positive predictive value (PPV) and the specificity were not improved when compared with either the 7-AAB panel alone or the Mayo model alone. **Conclusion.** Our study confirmed the clinical value of the 7-AAB panel for the early detection of lung cancer and in combination with the Mayo model could be used to distinguish benign from malignant pulmonary nodules.

1. Introduction

Lung cancer (LC) remains the highest cause of cancer-related death for both sexes in the United States and worldwide [1, 2]. Early detection of LC and timely resection could reduce the mortality rate associated with this disease. Compared to chest radiography, annual low dose computed tomography (LDCT) screening is associated with a 20% reduction in LC mortality in high-risk individuals [3]. With the movement toward screening for LC at an early stage by LDCT or the widespread use of multidetector CT technology, an increasing number of pulmonary nodules (PNs) are being detected

[4, 5, 6]. However, the drawbacks of LDCT screening, including with high rate of false-positive rate results (96.4%) to distinguish benign nodules from early-stage malignant cancer, not only lead to unnecessary follow-up toxic radiation scans and invasive follow-up procedures [3, 7] but also bring no benefit to the outcomes of small cell lung cancer (SCLC) patients [8]. Due to the small lesion volume and the lack of specific CT imaging features for distinguishing between benign and malignant nodules, it has long been challenging for clinicians to identify malignant pulmonary nodules (MPNs) from benign pulmonary nodules (BPNs). Most clinicians diagnose PNs mainly based on their personal clinical

experience or specific CT imaging features, which may be subjective. A mathematical predictive model is an objective evaluation method based on statistics; therefore, one could be expected to help physicians distinguish benign from malignant nodules, avoiding subjective and one-sided judgments [9]. The Mayo Clinic model, published in 1997, is the first and still widely used model focusing on solitary pulmonary nodules (SPNs). It includes six variables (age, smoking history, cancer history, nodule diameter, location of the nodule, and speculation), with an area under curve (AUC) of 0.832 for predicting malignancy [10]. However, the Mayo model may underestimate the probability of malignancy in low-risk patients or have poor calibration in patients referred for surgical evaluation [11, 12]. Therefore, another adjunctive test is extremely essential to improve differentiating benign from malignant nodules and reduce the false-positive rate.

Tumor-associated autoantibodies (AABs), formulated from tumor-associated antigens (TAAs) captured by the humoral immune system, may be used to identify individuals with early lung cancer or distinguish MPNs from BPNs [13]. AABs can be detected before the disease becomes symptomatic and may even be found up to 5 years before CT is able to identify the tumor [14]. For the heterogeneity of single antigen expression, many studies have focused on panels of autoantibodies as blood biomarkers to diagnose early LC or to distinguish benign from malignant nodules, but the diagnostic accuracy has been inconsistent [13, 15–20]. Our previous meta-analysis showed that the sensitivities of two panels, one using 7 AABs and the other 6 AABs, were 40% and 29.7% in the early detection of LC, while their specificities were 91% and 87%, respectively. [21] Recently, a seven-AAB panel (p53, PGP9.5, SOX2, GAGE7, GBU4-5, CAGE, and MAGEA1) was developed and commoditized in China, which is mainly used as a new biomarker in the early diagnosis of lung cancer, with a sensitivity range from 56.5% to 62% and a specificity range from 90% to 91.6% in the detection of early-stage LC. When combined with CT, the diagnostic yield could be improved in patients presenting with ground-glass nodules (GGNs) and/or solid nodules [13, 22, 23]. However, none of the current panels showed enough sensitivity to make them ideal serum biomarkers for the early detection of LC. In the present study, we not only validated the clinical value of the 7-AAB panel in the early detection of LC but also evaluated the value of the utility of the 7-AAB panel in combination with the Mayo model to distinguish between benign and malignant nodules.

2. Materials and Methods

2.1. Patients and Blood Samples. This study was a diagnostic cohort test (registration number: ChiCTR-DDD-17010378) approved by the ethics committee of the Fourth Affiliated Hospital of Guangxi Medical University (number KY2016208). Blood samples were collected from 806 participants (Tables 1 and 2), which included patients with histopathologically confirmed LC, benign pulmonary disease (BLD) and pulmonary nodules (PNs) as well as healthy controls, in our hospital from January 2017 to May 2019.

Informed written consent was obtained from each participant. LC or MPN was defined based on CT scans and verified by histopathology according to the World Health Organization Classification of Tumors [24]. The diagnosis of BLD was established by clinical data and CT scans. Pulmonary nodules were diagnosed by CT scans, and follow-up was performed strictly according to the Clinical Practice Consensus Guidelines [25]. The patients' blood samples were collected at initial diagnosis. None of the LC patients had received preoperative chemotherapy or radiotherapy. The healthy controls were recruited during health examinations, and none showed evidence of malignancy. A PN is diagnosed clinically as a benign etiology if it accords with one of the following: (1) definitive pathologic diagnosis, (2) radiographic resolution, or (3) no evidence of growth according to CT scan for 1 year [26]. Supernatants were obtained from blood samples through centrifugation at 3,000 g for 15 minutes at 4°C and were immediately subpackaged and then stored at -80°C until analyzed.

2.2. Quantitation of AABs or TAAs in Serum Samples. The serum concentrations of the 7-AAB panel (p53, GAGE7, PGP9.5, CAGE, MAGEA1, SOX2, and GBU4-5) were quantitated by an enzyme-linked immunosorbent assay (ELISA), and a commercial AABs assay (Cancer Probe Biological Technology Co., Ltd, Hangzhou, China) was conducted according to the manufacturer's recommendations and measured as previously described [13, 23]. Briefly, the samples and kit components were equilibrated to room temperature and diluted with phosphate-buffered saline (PBS) [1:109]. Then, 50 μ L of diluted serum samples and standards was added to appropriate wells and incubated for 1 h. After washing the plate 3 times, 50 μ L of diluted secondary antibody anti-human IgG HRP was added to each well to bind the autoantibodies. The plate was washed 3 times and incubated for half an hour. The substrate was added, and the color development reaction was terminated after 15 min with 50 μ L of stop solution. The OD at 450 nm was read using a spectrophotometer within 30 min. Each sample was tested in duplicate. We applied preset commercial cutoff values that had the maximum sensitivity with a fixed specificity of 90% using a Monte Carlo direct search method [27].

The serum concentrations of traditional TAA markers (CYFR21, CEA, NSE, and SCC) were quantitated by an electrochemiluminescent immunoassay. All assays were performed according to instrument and reagent specifications, and cutoff values were set according to the manufacturers' recommendations. The laboratory technicians were blinded to the patient's identity, and the results were analyzed blindly by another investigator.

2.3. Mayo Model for Predicting Malignancy. The probability of malignancy of the PNs was calculated using the Mayo predictive model, which is defined by the following equations: probability (P) = $e^x / (1 + e^x)$, $x = -6.8272 + (0.0391 \times \text{age}) + (0.7917 \times \text{smoking history}) + (1.3388 \times \text{cancer history}) + (0.1274 \times \text{diameter}) + (1.0407 \times \text{speculation}) + (0.7838 \times \text{upper lobe})$, where e is the base of the natural logarithm, and

TABLE 1: Clinical characteristics of the LC patients and controls.

Parameters	LC (<i>n</i> = 193)	BLD (<i>n</i> = 118)	HC (<i>n</i> = 135)	<i>P</i> value
Age (year)				
Range	28-82	35-87	28-87	
Mean (SD)	58.8 (9.9)	57.9 (10.6)	52.3 (11.2)	0.364
Gender				
Male	141 (73.1)	84 (71.2)	97 (71.9)	0.933
Female	52 (26.9)	34 (28.8)	38 (28.1)	
Smoking, <i>n</i> (%)				
Ever/current	128 (66.3)	72 (61.0)	73 (54.1)	0.081
Never	65 (33.7)	46 (39.0)	62 (45.9)	
7-AABs, <i>n</i> (%)				
Positive	122 (63.2)	20 (16.9) [‡]	14 (10.4)	<0.0001
Negative	71 (36.8)	98 (83.1) [‡]	121 (89.6)	
Cancer stage, <i>n</i> (%)		Diseases (<i>n</i>)		
I	32 (16.6)	Bronchitis (26)		
II	45 (23.3)	CAP (55)		
III	47 (24.4)	COPD (8)		
IV	69 (35.7)	Bronchiectasis (12)		
Cancer subtype, <i>n</i> (%)		Pulmonary tuberculosis (6)		
Adenocarcinoma	112 (58.0)	Parapneumonic effusion (4)		
Squamous cell carcinoma	39 (20.3)	OSAS (4)		
Large cell lung carcinoma	2 (1.0)	CVA (3)		
SCLC	40 (20.7)			

HC = health controls; LC = lung cancer; BLD = benign lung diseases; SD = standard deviation; SCLC = small cell lung cancer; COPD = chronic obstructive pulmonary disease; CAP = community-acquired pneumonia; CVA = cough-variant asthma; OSAHS = obstructive sleep apnea syndrome. Compared to HC, [‡]>0.05.

TABLE 2: Baseline characteristics and performances of the patients with PN.

Parameters	Advanced stage MPN (<i>n</i> = 116)	Early-stage MPN (<i>n</i> = 77)	BPN (<i>n</i> = 162)	<i>P</i> value
Age, median (range)	61.4 (40.0-82.0)*	54.2 [‡] (28.0-77.0)	51.1 (29.0-75.0)	<0.01
Sex, <i>n</i> (%)				
Male	94 (81.0)***	47 (61.0) [‡]	86 (53.1)	<0.0001
Female	22 (19.0)	30 (39.0)	76 (46.9)	
Smoking, <i>n</i> (%)				
Ever/current	86 (74.1)***	42 (54.5)***	49 (30.2)	<0.0001
Never	30 (25.9)	35 (45.5)	113 (69.8)	
Nodule size, <i>n</i> (%)				
≤8 mm	10 (8.6)***	31(40.3)***	134 (83.8)	<0.0001
9 mm-30 mm	28 (24.2)*	45 (58.4)***	20 (12.3)	<0.0001
>30 mm	78 (67.2)***	1 (1.3) [‡]	8 (4.9)	<0.0001
7-AABs, <i>n</i> (%)				
Positive	70 (60.3)***	52 (67.5)***	42 (25.9)	<0.0001
Negative	46 (39.7)	25 (32.5)	120 (74.1)	
Mayo model, <i>n</i> (%)				
<5%	4 (3.4)***	28 (36.4)***	100 (61.7)	<0.0001
5-65%	32 (27.6) [‡]	42 (54.5)**	56 (34.6)	0.001
>65%	80 (69.0)***	7 (9.1) [‡]	6 (3.7)	<0.0001

PN = pulmonary nodule; MPN = malignant pulmonary nodule; BPN = benign pulmonary nodule. Compared to BPN, *<0.05, **<0.001, ***<0.0001, and [‡]>0.05.

the smoking history, cancer history, spiculation, and upper lobe variables can be either 1 for yes or 0 for no. Diameter indicates the largest nodule measurement (in mm) reported on initial chest radiograph or CT scan [28]. According to the American College of Chest Physicians (ACCP) guidelines, when the P is $<5\%$, watchful waiting is preferred. When the P is 5% to 65%, needle biopsy is preferred. When the P is $>65\%$, surgery is preferred [29].

2.4. Statistical Analysis. The data were described as the means \pm standard deviations (SDs) for continuous variables and frequency and percentage for categorical variables. The differences of the seven AABs in the serum levels among the groups were compared using nonparametric tests (Mann–Whitney U -test). Sensitivity and specificity were calculated according to the cutoff value. To confirm the sensitivity and specificity results, receiver operating characteristic (ROC) curves were constructed, and the area under the ROC curve (AUC) was calculated. Chi-square tests (χ^2) were used to evaluate the difference between 2 groups. A 2-sided P value < 0.05 indicated statistical significance. All statistical analyses were carried out using the SPSS 22.0 (SPSS Inc., Chicago, IL, USA), and GraphPad Prism 5.0 software (GraphPad Software Inc., San Diego, CA, USA) was used for image editing.

3. Results

3.1. Patients' Characteristics. A total of 806 participants (193 + 135 + 118 + 360) were included in the study. A total of 193 LC patients with different disease stages (153 with non-small-cell lung cancer (NSCLC) and 40 with SCLC), 118 patients with benign lung diseases, and 135 healthy controls were included. There were more LC patients in the advanced-stage (III-IV) (60.1%) than in the early stage (I-II) (39.9%). The etiologic diagnoses of the BLD group included bronchitis, community-acquired pneumonia (CAP), chronic obstructive pulmonary disease (COPD), obstructive sleep apnea syndrome (OSAS), cough-variant asthma (CVA), bronchiectasis, parapneumonic effusion, and pulmonary tuberculosis. The clinical characteristics of the study population are summarized in Table 1.

After screening with LDCT in the high-risk population with a history of heavy tobacco usage, 360 PN patients (including 162 patients with BPN and 198 with undetermined nodules) were included to test the utility of the 7-AAB panel and the Mayo model in the differential diagnosis of PNs. The major clinical characteristics of this population are summarized in Table 2.

3.2. The Reactivity Performance of the 7 AABs in Lung Cancer Patients and Healthy Controls. To determine the reactivity of the panel of 7 AABs, we measured the concentrations of the 7 AABs in 193 LC patients and 135 healthy controls. The results showed that the serum AAB concentrations of p53, PGP9.5, SOX2, GBU4-5, MAGEA1, and CAGE in the LC patients were markedly higher than those in the healthy controls ($P = 0.042$, $P < 0.001$, $P = 0.046$, $P < 0.001$, $P < 0.001$, and $P < 0.001$, respectively), but the expression level of

GAGE7 in the LC group was similar to that of the healthy group ($P = 0.844$) (Figures 1(a)–1(g)). Although most of the AABs except PGP9.5 demonstrated good discriminative ability between lung cancer and healthy controls, the AUCs of the single AAB showed poor diagnostic efficacy (all $P < 0.7$). However, the combined AUC for all 7 AABs improved to 0.727, which indicated good diagnostic efficacy (Figures 1(h) and 1(i)).

3.3. The Diagnostic Value of the 7-AAB Panel for Lung Cancer. Using the commercial assay cutoffs, positivity is defined as having an elevated AAB assay signal to any one of the antigens in the 7-AAB panel. The predictive power of this 7-AAB panel for the diagnosis of whole-stage lung cancer revealed a sensitivity of 63.2% (122/193), with a specificity of 89.6% (121/135) in the healthy controls and 83.1% (98/118) in the BLD group (Table 1, Figures 2(a) and 2(b)).

We also conducted subgroup analyses to investigate the diagnostic value of the 7-AAB panel in patients with different disease stages and histological types. The sensitivities were 67.5% (52/77) in stages I-II of the disease, 60.3% (70/116) in stages III-IV of the disease, 55.0% (22/40) in SCLS, 63.4% (71/112) in adenocarcinoma, and 58.9% (23/39) in squamous cell carcinoma (Figure 2(a)).

Moreover, we simultaneously measured the serum 7-AAB panel and the combination of traditional tumor markers (CYFR21, CEA, NSE, and SCC) in the same patient. The results showed the sensitivity values of the 7-AAB panel in the early-stage LC patients were higher than those of the traditional tumor markers (67.5% vs. 37.5%, $P < 0.01$) but were lower than those in the late-stage LC patients (60.3% vs. 94.0%, $P < 0.001$) (Figure 2(c)).

3.4. The Performance of the 7-AAB Panel in Combination with the Mayo Model in Distinguishing Benign from Early-Stage MPN. The 7-AAB test and the Mayo prediction model were assessed for the presence of PNs. After excluding 198 participants with undetermined nodules, 355 PN patients were included in the analysis. Among them, 116 patients were pathologically diagnosed with advanced stage (III-IV) MPNs, 77 with early-stage (I-II) MPNs, and 162 with benign pulmonary nodules (BPNs).

First, we evaluated the diagnostic value of the 7-AAB panel and the Mayo model to distinguish early-stage (I-II) MPN patients from the BPN controls. The rates of nodule sizes < 8 mm and Mayo malignancy probability $< 5\%$ in the patients with BPN were greater than those of the early-stage MPN patients ($P < 0.0001$), but the rates of nodule sizes > 8 mm and Mayo malignancy probability $> 5\%$ were greater in the MPN patients than in the BPN controls. The positive rates of early-stage malignant nodules were higher than those of benign nodules for both the 7-AAB panel (67.5% vs. 25.9%; $P < 0.0001$) and the Mayo model with probabilities between 5 and 65% (54.5% vs. 34.6%; $P < 0.001$) (Table 2). The AUCs (95% CI) for the 7-AAB panel, the Mayo model, and the 7-AAB panel+the Mayo model between the two groups were as follows: 0.742 (0.674-0.801), 0.670 (0.605-0.730), and 0.795 (0.738-0.845), respectively; the 7-AAB panel+the Mayo model showed improved

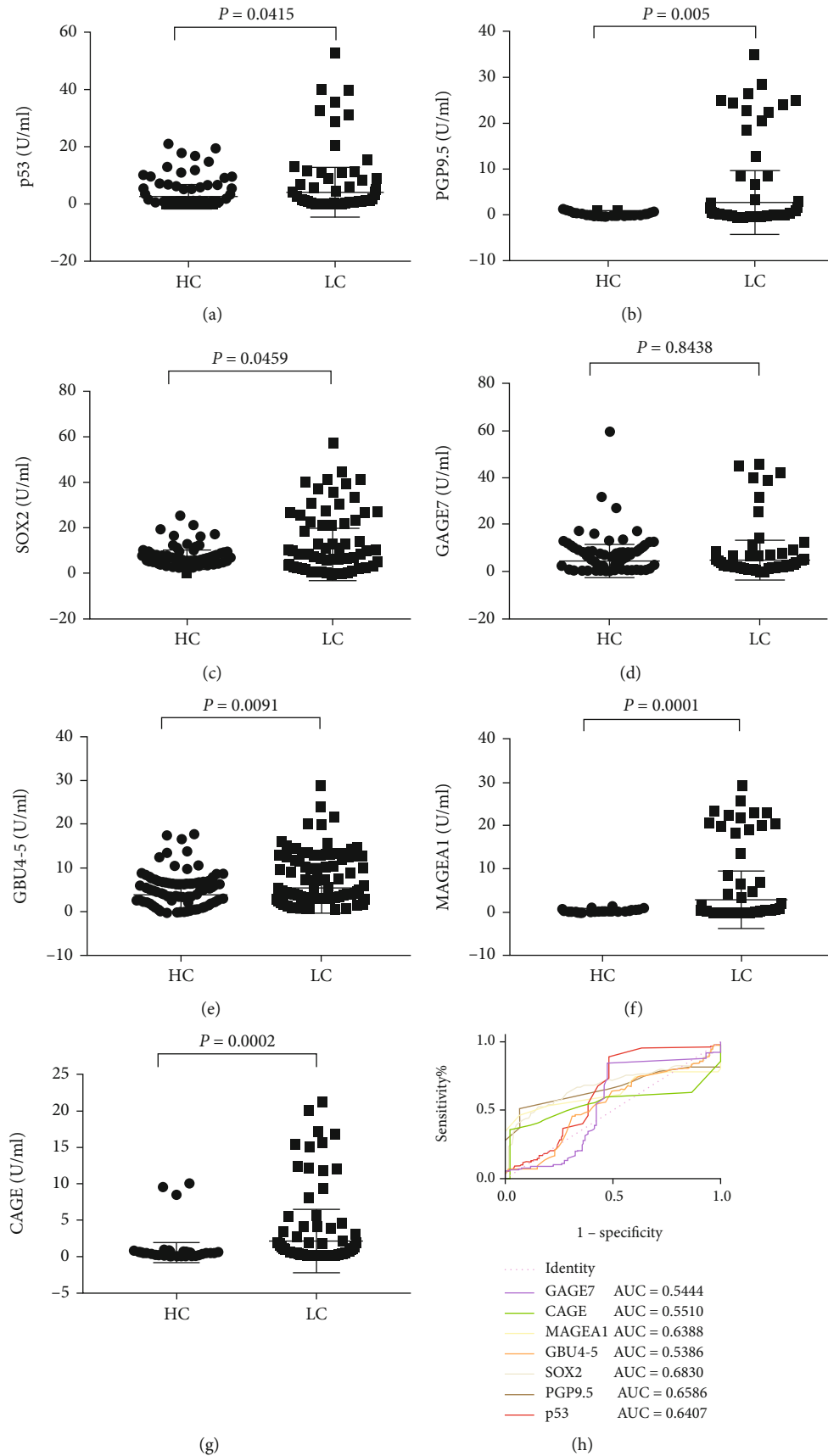


FIGURE 1: Continued.

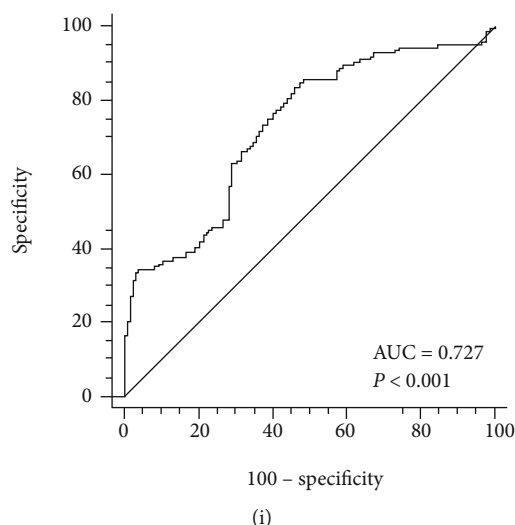


FIGURE 1: Concentration and the area under the curve (AUC) of each autoantibody between lung cancer (LC) cases and health controls (HC). (a) p53; (b) PGP9.5; (c) SOX2; (d) GAGE7; (e) GBU4-5; (f) MAGEA1; (g) CAGE; (h) AUCs for each autoantibody; (i) combined AUC for the 7-AAB panel.

diagnostic accuracy (Figures 3(a)–3(c)). When the cutoff value of malignancy probability was set at $>5\%$, the detection rate was 63.6%. The 7-AAB panel in combination with the Mayo model significantly improved the sensitivity when compared with the AAB panel alone (93.5% vs. 67.5%; $P < 0.0001$) or with the Mayo model alone (93.5% vs. 63.6%; $P < 0.0001$) (Figure 3(d)); however, this combination could not improve the positive predictive values (PPVs) and the specificity when compared with either the panel alone or the model alone (Figures 3(e) and 3(f)).

3.5. The Performance of the 7-AAB Panel in combination with the Mayo Model in Distinguishing Benign from Advanced-Stage MPN. Next, we also evaluated the performance of the 7-AAB panel and the Mayo model in distinguishing advanced-stage (III-IV) MPN patients from the BPN controls. The 7-AAB panels of 116 advanced-stage MPN patients were measured, and their malignancy probabilities were calculated by the Mayo model. Advanced-stage MPN showed more patients with a nodule size > 8 mm and a malignancy probability $> 65\%$ compared to BPN. The AUCs (95% CI) for each model were as follows (Figures 4(a)–4(c)): the 7-AAB panel, 0.602 (0.536-0.665); the Mayo model, 0.933 (0.889-0.964); and the 7-AAB panel+the Mayo model, 0.950 (0.909-0.976). The diagnostic efficacy of the 7-AAB panel in combination with the Mayo model was better than that of the 7-AAB panel alone or the Mayo model alone. When the cutoff value of malignancy probability was set at 65%, the detection rate for advanced-stage MPN was 69.0%. The 7-AAB panel in combination with the Mayo model also significantly improved the sensitivity when compared with the 7-AAB panel alone (91.4% vs. 60.3%; $P < 0.0001$) or with the Mayo model alone (91.4% vs. 69.0%; $P < 0.0001$) (Figure 4(d)). However, this combination decreased the PPV and the specificity when compared with the Mayo model alone (69.0% vs. 93.0%, $P < 0.0001$; 72.8% vs. 96.3%, $P < 0.0001$, respectively) (Figures 4(e) and 4(f)).

4. Discussion

Identifying MPN is crucial in the early detection of LC. In this study, we incorporated a 7-AAB panel with the Mayo prediction model in the differential diagnosis of pulmonary nodules and early detection of lung cancer. Our results confirmed the clinical value of this 7-AAB panel in aiding the diagnosis of early-stage lung cancer, as the detection rate was superior to that of traditional tumor biomarkers. We also validated that the 7-AAB panel in combination with the Mayo model significantly increased the sensitivity, but the PPV and specificity could not be improved in comparison with the 7-AAB panel alone or the Mayo model alone in the differential diagnosis of MPN from BPN, whether MPN was at an early or advanced stage. Based on these findings, we suggest that the 7-AAB panel can be used as a biomarker for the early detection of lung cancer and that it can be incorporated with the Mayo model to determine the probability of malignancy of pulmonary nodules.

Novel biomarkers have been discovered and developed for use in early-stage LC screening, such as autoantibody panels, circulating microRNAs—especially small noncoding RNAs (ncRNAs), circulating tumor DNA, DNA methylation, complement fragments, blood protein profiles, or plasma lipid markers from lipidomics [30, 31, 32]. Among these, the autoantibody panel EarlyCDT-Lung has been reported and validated as an aid for the early detection of lung cancer [18, 19]. Many studies have investigated the diagnostic value of joint detection with AABs. Our review previously meta-analyzed four studies that measured the EarlyCDT-Lung Test 7-AAB panel (p53, CAGE, NYESO-1, GBU4-5, SOX2, MAGE A4, and Hu-D), showing a sensitivity of 47% (95% CI 0.34–0.60) with a high specificity of 90% (95% CI 0.87–0.93) in the early detection of lung cancer [19, 21, 33, 34, 35]. In the present study, we investigated a different 7-AAB panel (p53, GAGE7, PGP9.5, CAGE, MAGEA1, SOX2, and GBU4-5), which identified 67.5% of

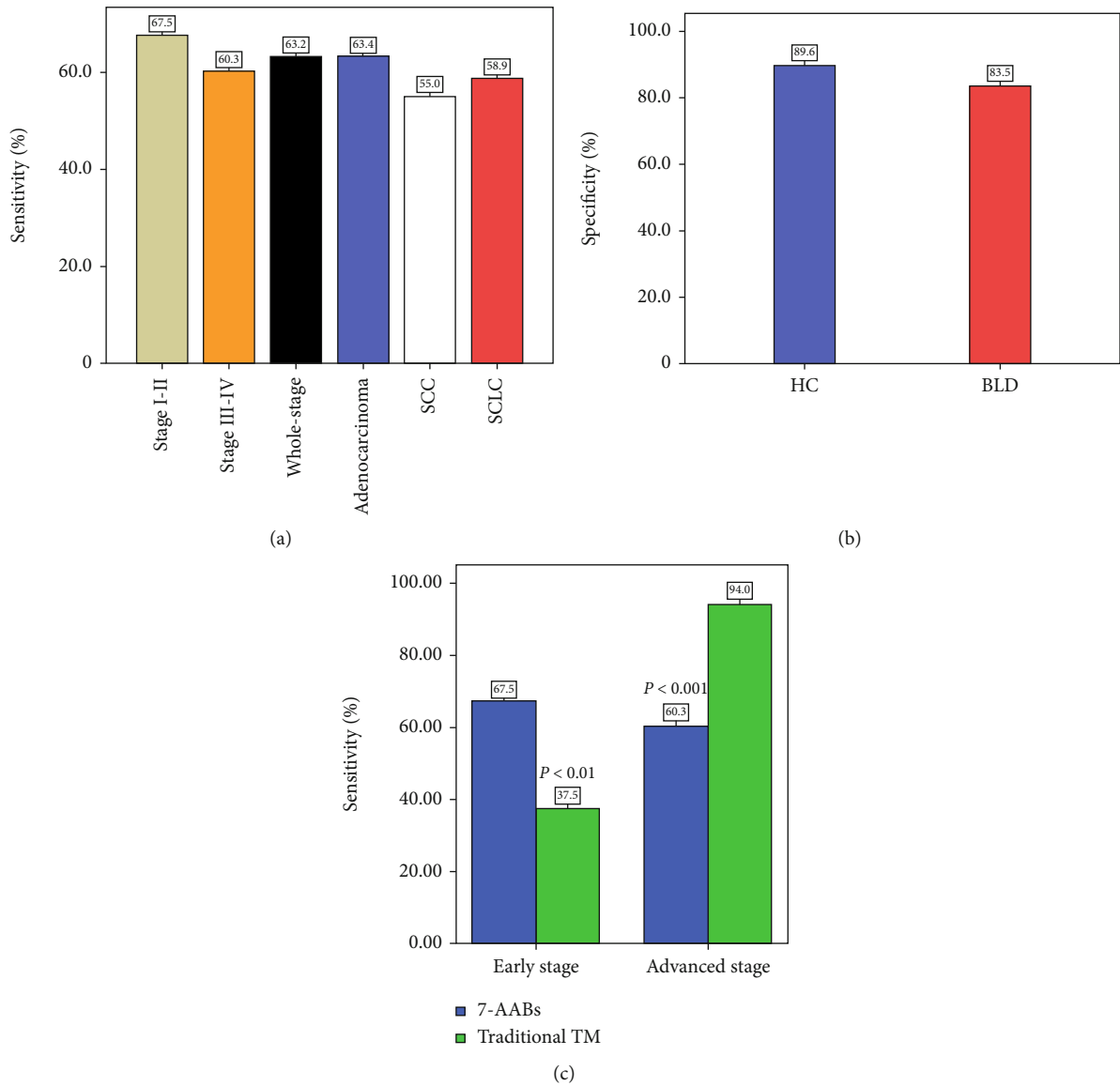


FIGURE 2: Diagnostic performance of the 7-AAB panel in lung cancer (LC) patients. SCC: squamous cell carcinoma; SCLC: small-cell lung cancer; TM: tumor markers; HC: healthy controls; BLD: benign pulmonary disease. (a) Sensitivities of the 7-AAB panel in different disease stages and histological types; (b) specificities of the 7-AAB panel in HC and BLD patients; (c) comparison of the 7-AAB panel and traditional tumor markers in LC patients.

early-stage LC with a specificity of 89.6%. Although these 7-AAB panels possess high specificity as serum diagnostic markers in the diagnosis of early-stage lung cancer, the low sensitivity limits the application of the AAB panels in clinical practice. Thus, there is an urgent need to find approaches that can improve the sensitivity of the detection efficacy of early-stage LC. As noted previously, one recent study [13] evaluated the combination of a 7-AAB panel and low-dose computed tomography (CT) scanning and significantly improved the diagnostic yield in early-stage MPN patients, with the PPV significantly improving to 95.0% when compared with the AAB panel alone (95.0% vs. 85.2%; $P < 0.001$) or with CT scanning alone (95.0% vs. 69.0%; $P < 0.001$). Another study also found that this 7-AAB panel

could distinguish malignant lesions from benign lesions and control cases, with a sensitivity of 56.53% and a specificity of 91.60%, but the specificity could be further increased to 95.80% when combined with CT [22]. To overcome the drawbacks of CT's high false-positive rate and radiologist subjectivity, in the present study, we combined a 7-AAB panel with the Mayo prediction model in the differential diagnosis of pulmonary nodules. The 7-AAB panel showed a sensitivity of 67.5% in the detection of early-stage MPN. However, the 7-AAB panel combined with the Mayo model had a significantly improved detection efficacy when compared with the AAB panel alone or the Mayo model alone, with sensitivities of 93.5% and 91.4% in distinguishing early- and advanced-stage malignant nodules, respectively, from

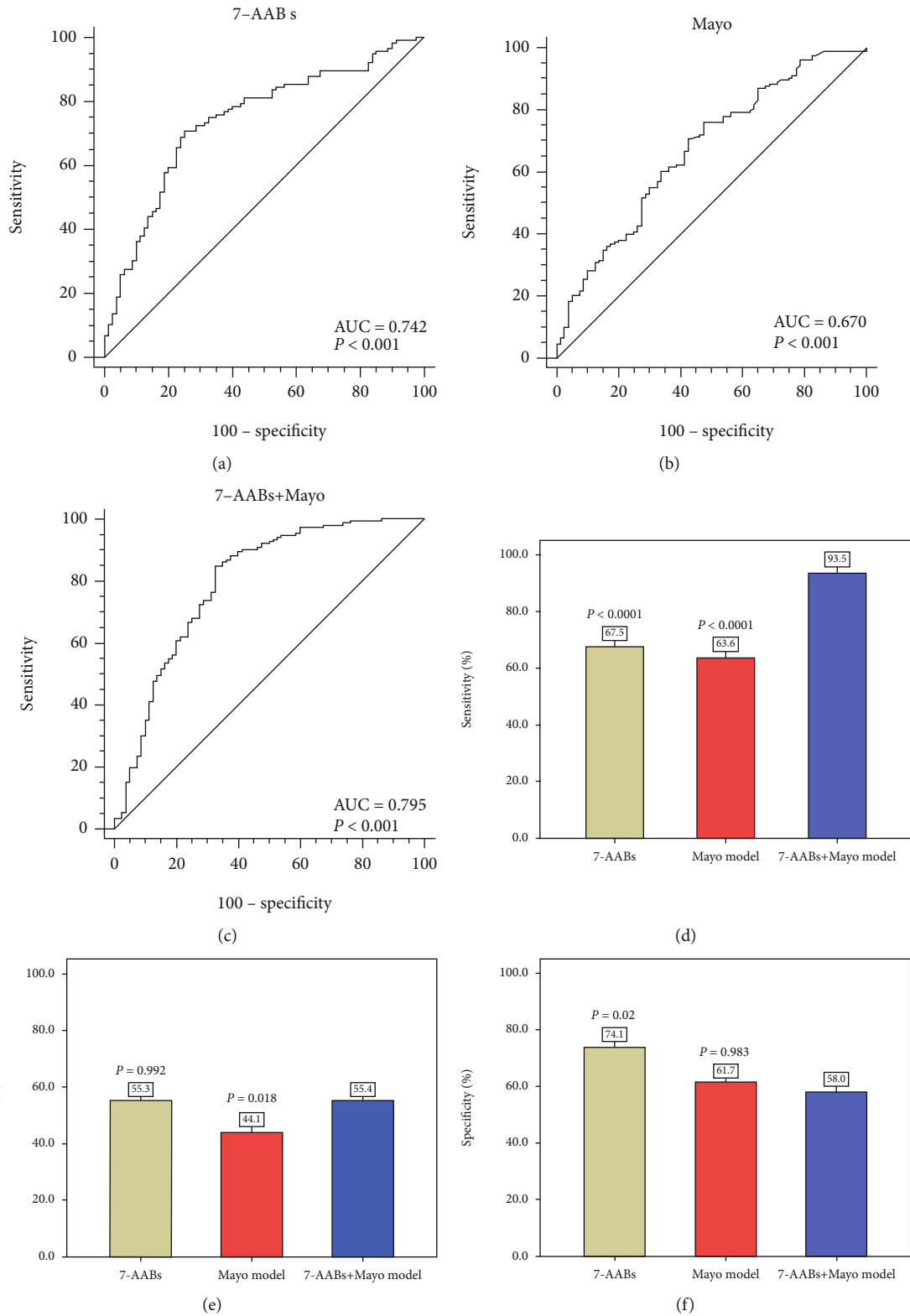


FIGURE 3: Diagnostic performance of the 7-AAB panel and the Mayo model between benign pulmonary nodules (BPN) and malignant pulmonary nodules (MPN) with early-stage. (a) The AUC of the 7-AAB panel; (b) the AUC of the Mayo model; (c) the AUC of the 7-AAB panel combination with the Mayo model; (d) sensitivity in MPN patients with early stage; (e) positive predictive values (PPVs) in MPN patients with early stage; (f) specificity in BPN patients.

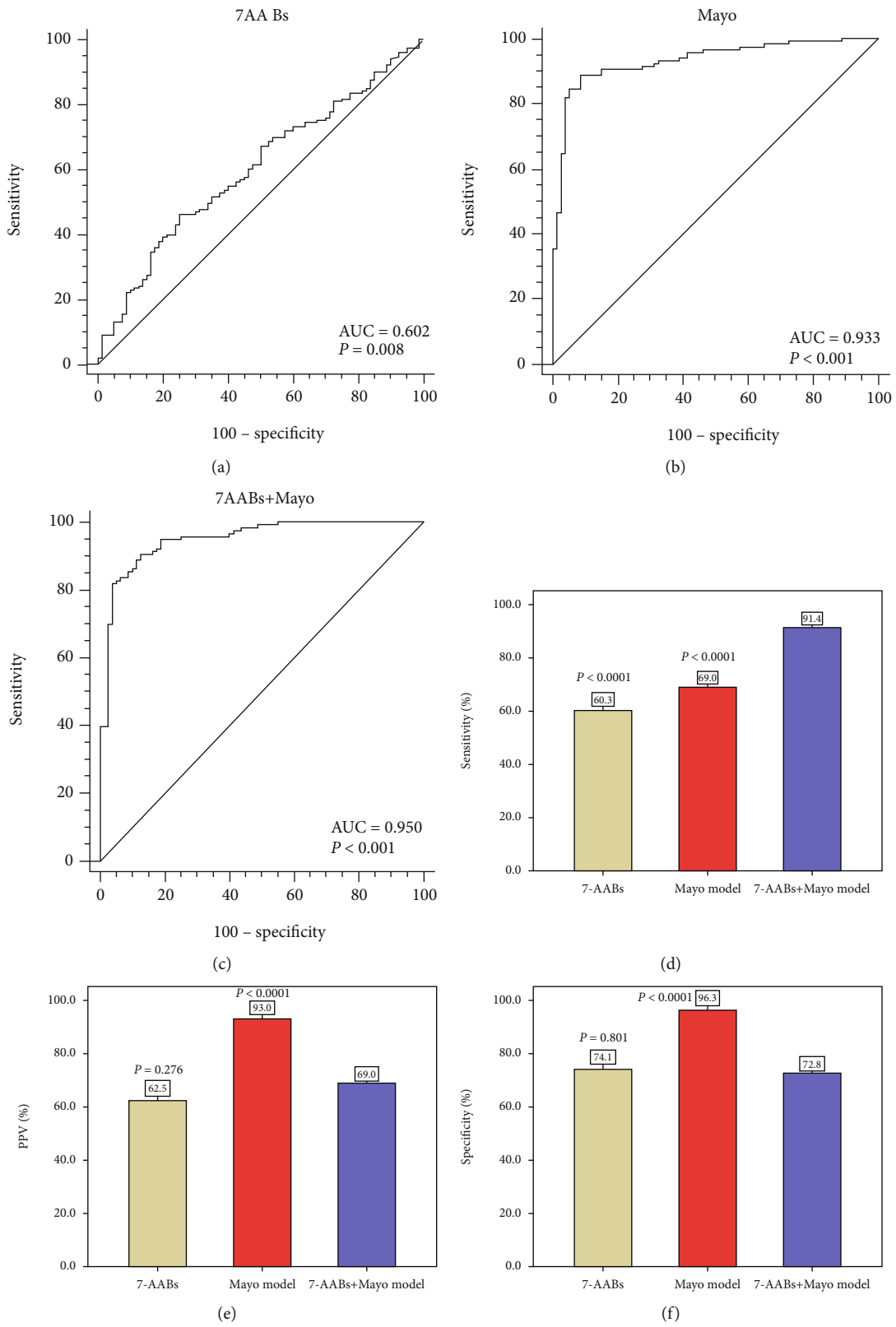


FIGURE 4: Diagnostic performance of the 7-AAB panel and the Mayo model between benign pulmonary nodules (BPN) and malignant pulmonary nodules (MPN) with advanced stage. (a) The AUC of the 7-AAB panel; (b) the AUC of the Mayo model; (c) the AUC of the 7-AAB panel combination with the Mayo model; (d) sensitivity in MPN patients with advanced stage; (e) positive predictive values (PPVs) in MPN patients with advanced stage; (f) specificity in BPN patients.

benign nodules, but the PPV and specificity did not improve correspondingly. The results were not consistent with two previous studies that combined this 7-AAB panel with CT scans. [13, 22] We hypothesize that this could be related to the high false-positive rate of and subjective diagnosis from CT. For improving sensitivity, we view the 7-AAB panel and the Mayo model as complementary rather than competitive, and the combination of the two methods may be beneficial in distinguishing benign from malignant lesions, particularly early-stage MPN, which is potentially curable when detected early.

Recently, several prediction models including clinical and radiological values have been developed that can help physicians distinguish between benign and malignant nodules [9]. A study found that the Mayo, Veterans Association (VA), and Brock models showed similar predictive performance for malignant nodules (AUC: 0.6145, 0.6042, and 0.6820, respectively) and outperform the Herder model (AUC: 0.5567), which includes the [18]FDG uptake value [36]. Another study evaluated three prediction models, the Mayo, VA, and Peking University (PU) models. The area under the ROC curve of the PU model [0.800; 95% confidence interval (CI): 0.708-0.891] was higher than that of the Mayo model (0.753; 95% CI: 0.650-0.857) and of the VA model (0.728; 95% CI: 0.6230-0.833); however, these findings were not statistically significant. This means that these mathematical prediction models have similar accuracy for the prediction of SPN malignancy [11]. Therefore, we selected the most extensively validated Mayo model to aid in distinguishing between benign and malignant nodules. Moreover, our study applied the Mayo model to separately investigate early- or advanced-stage MPN patients, and the results showed that the model's AUC was 0.670 (95% CI: 0.605-0.730) for early-stage MPN and 0.933 (95% CI: 0.889-0.964) for advanced-stage MPN, which is in line with the recently reported literature [11, 36]. It seems that the Mayo model has greater accuracy for predicting malignant PNs at the advanced stage than at the early stage. We assume that this may be related to the larger nodule size and higher malignancy probability (>65%) in late-stage MPN. However, when the Mayo model was combined with the 7-AAB panel, the AUCs were significantly improved for both early-stage and advanced-stage MPN (0.795 and 0.950, respectively).

Because traditional TAA markers, such as cytokeratin 19 fragment antigen (CYFRA21-1), neuron-specific enolase (NSE), carcinoembryonic antigen (CEA), and squamous cell carcinoma antigen (SCC), remain widely used as reference diagnostics for lung cancer [37], we compared the 7-AAB panel with the combination of these traditional TAAs in the diagnosis of LC. We found that the 7-AAB panel was good in the early stages of lung cancer, while the traditional tumor markers showed a higher sensitivity with late-stage LC. This suggests that the 7-AAB panel is not suited for use as a biomarker for late-stage LC patients, whereas the traditional antigen biomarkers such as CEA, NSE, SCC, and CYFRA 21-1 should not be used to diagnose early-stage LC patients.

Identifying malignant pulmonary nodules and achieving the early detection of lung cancer significantly improve the survival rate and decrease mortality associated with this disease. Currently, the EarlyCDT-Lung test is being evaluated in a large-scale screening study in individuals at high risk of lung cancer worldwide. In addition to validating the clinical efficacy of the 7-AAB panel for the early detection of lung cancer, we also found that the combination of the 7-AAB panel with the Mayo model could significantly improve the sensitivity for distinguishing benign from malignant lesions at both early and late stages. As the ELISA of AABs is relatively low cost, noninvasive, and easy-to-perform, and the Mayo model is defined by equations, a combination based on the 7-AAB panel illustrated here and the Mayo model holds promise for the early detection of MPN, and it can be applied in some undeveloped areas or hospitals without high-resolution CT scans. Early detection of malignancy and timely resection are important while the nodule is still relatively small, as this could lead to decreased mortality.

Inevitably, there are some limitations in our research. First, the number of stage I-II MPN cases may not be sufficient. The BPN group was not matched well with the MPN groups for age, gender, or smoking status. Additionally, the study included no other cancer control group aside from lung cancer that could have had some or all AABs in common with those of the panel. Additionally, although the Mayo model was designed for pulmonary nodules, we did not investigate the AAB panel and the Mayo model with different sizes of PNs or subtypes of MPN to further evaluate their validity. Furthermore, we only analyzed the diagnostic efficacy of the AAB panel and the Mayo model in a Chinese population, and a future work is ongoing to validate the sensitivity and specificity of the combination in other ethnicities.

In conclusion, our study confirmed the clinical value of the 7-AAB panel for the early detection of lung cancer, which achieved a sensitivity of 67.5% and a specificity of 89.6%. This 7-AAB panel proved to be better than traditional tumor markers, such as CEA, NSE, SCC, and CYFRA 21-1, in aiding with early diagnosis. The combination of the 7-AAB panel with the Mayo model can improve the sensitivity for distinguishing benign PNs from malignant nodules, but the combination could not improve the PPV or the specificity. Taken together, this study illustrates the robust potential of the 7-AAB panel for the early diagnosis of lung cancer and in combination with the Mayo model could be used to distinguish the probability of malignancy of pulmonary nodules in clinical practice.

Abbreviations

LC:	Lung cancer
MPN:	Malignant pulmonary nodule
ELISA:	Enzyme-linked immunosorbent assay
BPN:	Benign pulmonary nodule
PN:	Pulmonary nodule
SPN:	Solitary pulmonary nodule
AAB:	Autoantibody
GGN:	Ground-glass nodule

BLD: Benign lung diseases
 NSCL: Non-small-cell lung cancer
 SCLC: Small-cell lung cancer
 ROC: Receiver operating characteristic
 AUC: Area under the curve
 CT: Computed tomography
 LDCT: Low dose computed tomography
 TAA: Tumor-associated antigen
 TM: Tumor marker
 SD: Standard deviation
 PPV: Positive predictive value
 CAP: Community-acquired pneumonia
 COPD: Chronic obstructive pulmonary disease
 CVA: Cough-variant asthma
 OSAS: Obstructive sleep apnea syndrome.

Data Availability

Data is available on request. Due to China's new laws and regulations on biosafety data control, the original data protecting patient information is under control. If you need raw data, you can apply with the corresponding author (huzhuojun1964@163.com).

Conflicts of Interest

The authors declare that they have no conflicts of interest.

Authors' Contributions

ZL and ZH conceived and designed the experiments. ZL and XW performed the experiments. ZL and JC analyzed the data. JC and RS contributed reagents/materials/analysis tools. ZL and ZW contributed to the writing of the manuscript. ZW critically revised the manuscript. ZH is responsible for the final approval of the version to be submitted. Zhougui Ling and Jifei Chen contributed equally to this work.

Acknowledgments

This work was supported in part by funding from the Key Research and Development Program of Guangxi Zhuang Autonomous Region (No. AB16380152), in part from the Key Research and Development Program of Liuzhou (2018BJ10509), and in part from "139" Incubation Program for High-Level Medical Talents in Guangxi.

References

- [1] R. L. Siegel, K. D. Miller, and A. Jemal, "Cancer statistics, 2019," *CA: a Cancer Journal for Clinicians*, vol. 69, pp. 7–34, 2018.
- [2] A. A. Adjei, "Lung cancer worldwide," *Journal of Thoracic Oncology*, vol. 14, no. 6, p. 956, 2019.
- [3] National Lung Screening Trial Research Team, D. R. Aberle, A. M. Adams et al., "Reduced lung-cancer mortality with low-dose computed tomographic screening," *New England Journal of Medicine*, vol. 365, no. 5, pp. 395–409, 2011.
- [4] F. L. Jacobson, "Multidetector-row CT of lung cancer screening," *Seminars in Roentgenology*, vol. 38, no. 2, pp. 168–175, 2003.
- [5] S. Perandini, G. A. Soardi, A. R. Larici et al., "Multicenter external validation of two malignancy risk prediction models in patients undergoing 18F-FDG-PET for solitary pulmonary nodule evaluation," *European Radiology*, vol. 27, no. 5, pp. 2042–2046, 2017.
- [6] M. T. Truong, J. P. Ko, S. E. Rossi et al., "Update in the evaluation of the solitary pulmonary nodule," *Radiographics*, vol. 34, no. 6, pp. 1658–1679, 2014.
- [7] P. M. Boiselle, "Computed tomography screening for lung cancer," *Journal of the American Medical Association*, vol. 309, no. 11, pp. 1163–1170, 2013.
- [8] A. Thomas, P. Pattanayak, E. Szabo, and P. Pinsky, "Characteristics and outcomes of small cell lung cancer detected by CT screening," *Chest*, vol. 154, no. 6, pp. 1284–1290, 2018.
- [9] A. al-Ameri, P. Malhotra, H. Thygesen et al., "Risk of malignancy in pulmonary nodules: a validation study of four prediction models," *Lung Cancer*, vol. 89, no. 1, pp. 27–30, 2015.
- [10] S. J. Swensen, M. D. Silverstein, D. M. Ilstrup, C. D. Schleck, and E. S. Edell, "The probability of malignancy in solitary pulmonary nodules. Application to small radiologically indeterminate nodules," *Archives of Internal Medicine*, vol. 157, no. 8, pp. 849–855, 1997.
- [11] X. Zhang, H. H. Yan, J. T. Lin et al., "Comparison of three mathematical prediction models in patients with a solitary pulmonary nodule," *Chinese Journal of Cancer Research*, vol. 26, no. 6, pp. 647–652, 2014.
- [12] J. M. Isbell, S. Deppen, J. B. Putnam Jr. et al., "Existing general population models inaccurately predict lung cancer risk in patients referred for surgical evaluation," *The Annals of Thoracic Surgery*, vol. 91, no. 1, pp. 227–233, 2011, discussion 233.
- [13] S. Ren, S. Zhang, T. Jiang et al., "Early detection of lung cancer by using an autoantibody panel in Chinese population," *Oncoimmunology*, vol. 7, no. 2, p. ???, 2017.
- [14] L. Zhong, S. P. Coe, A. J. Stromberg, N. H. Khattar, J. R. Jett, and E. A. Hirschowitz, "Profiling tumor-associated antibodies for early detection of non-small cell lung cancer," *Journal of Thoracic Oncology*, vol. 1, no. 6, pp. 513–519, 2006.
- [15] G. Veronesi, F. Bianchi, M. Infante, and M. Alloisio, "The challenge of small lung nodules identified in CT screening: can biomarkers assist diagnosis?," *Biomarkers in Medicine*, vol. 10, no. 2, pp. 137–143, 2016.
- [16] J. C. Tsay, C. DeCotiis, A. K. Greenberg, and W. N. Rom, "Current readings: blood-based biomarkers for lung cancer," *Seminars in Thoracic and Cardiovascular Surgery*, vol. 25, no. 4, pp. 328–334, 2013.
- [17] C. J. Chapman, A. Murray, J. E. McElveen et al., "Autoantibodies in lung cancer: possibilities for early detection and subsequent cure," *Thorax*, vol. 63, no. 3, pp. 228–233, 2008.
- [18] S. Lam, P. Boyle, G. F. Healey et al., "EarlyCDT-lung: an immunobiomarker test as an aid to early detection of lung cancer," *Cancer Prevention Research (Philadelphia, Pa.)*, vol. 4, no. 7, pp. 1126–1134, 2011.
- [19] C. J. Chapman, G. F. Healey, A. Murray et al., "EarlyCDT®-Lung test: improved clinical utility through additional autoantibody assays," *Tumour Biology*, vol. 33, no. 5, pp. 1319–1326, 2012.
- [20] V. Doseeva, T. Colpitts, G. Gao, J. Woodcock, and V. Knezevic, "Performance of a multiplexed dual analyte

- immunoassay for the early detection of non-small cell lung cancer,” *Journal of Translational Medicine*, vol. 13, no. 1, p. 55, 2015.
- [21] Z. M. Tang, Z. G. Ling, C. M. Wang, Y. B. Wu, and J. L. Kong, “Serum tumor-associated autoantibodies as diagnostic biomarkers for lung cancer: a systematic review and meta-analysis,” *PLoS One*, vol. 12, no. 7, p. e0182117, 2017.
- [22] Q. du, R. Yu, H. Wang et al., “Significance of tumor-associated autoantibodies in the early diagnosis of lung cancer,” *The Clinical Respiratory Journal*, vol. 12, no. 6, pp. 2020–2028, 2018.
- [23] R. Zhang, L. Ma, W. Li, S. Zhou, and S. Xu, “Diagnostic value of multiple tumor-associated autoantibodies in lung cancer,” *Oncotargets and Therapy*, vol. 12, pp. 457–469, 2019.
- [24] W. D. Travis, E. Brambilla, A. G. Nicholson et al., “The 2015 World Health Organization Classification of Lung Tumors: impact of genetic, clinical and radiologic advances since the 2004 classification,” *Journal of Thoracic Oncology*, vol. 10, no. 9, pp. 1243–1260, 2015.
- [25] C. Bai, C. M. Choi, C. M. Chu et al., “Evaluation of pulmonary nodules: clinical practice consensus guidelines for Asia,” *Chest*, vol. 150, no. 4, pp. 877–893, 2016.
- [26] G. A. Silvestri, N. T. Tanner, P. Kearney et al., “Assessment of plasma proteomics biomarker’s ability to distinguish benign from malignant lung nodules: results of the PANOPTIC (pulmonary nodule plasma proteomic classifier) trial,” *Chest*, vol. 154, no. 3, pp. 491–500, 2018.
- [27] P. Boyle, C. J. Chapman, S. Holdenrieder et al., “Clinical validation of an autoantibody test for lung cancer,” *Annals of oncology : official journal of the European Society for Medical Oncology*, vol. 22, no. 2, pp. 383–389, 2011.
- [28] M. K. Gould, L. Ananth, P. G. Barnett, and S. C. S. G. Veterans Affairs, “A clinical model to estimate the pretest probability of lung cancer in patients with solitary pulmonary nodules,” *Chest*, vol. 131, no. 2, pp. 383–388, 2007.
- [29] M. K. Gould, J. Donington, W. R. Lynch et al., “Evaluation of individuals with pulmonary nodules: when is it lung cancer? Diagnosis and management of lung cancer, 3rd ed: American College of Chest Physicians evidence-based clinical practice guidelines,” *Chest*, vol. 143, no. 5, pp. e93S–e120S, 2013.
- [30] L. M. Seijo, N. Peled, D. Ajona et al., “Biomarkers in lung cancer screening: achievements, promises, and challenges,” *Journal of Thoracic Oncology*, vol. 14, no. 3, pp. 343–357, 2019.
- [31] Y. Dou, Y. Zhu, J. Ai et al., “Plasma small ncRNA pair panels as novel biomarkers for early-stage lung adenocarcinoma screening,” *BMC Genomics*, vol. 19, no. 1, p. 545, 2018.
- [32] Z. Yu, H. Chen, J. Ai et al., “Global lipidomics identified plasma lipids as novel biomarkers for early detection of lung cancer,” *Oncotarget*, vol. 8, no. 64, pp. 107899–107906, 2017.
- [33] G. F. Healey, S. Lam, P. Boyle, G. Hamilton-Fairley, L. J. Peek, and J. F. Robertson, “Signal stratification of autoantibody levels in serum samples and its application to the early detection of lung cancer,” *Journal of Thoracic Disease*, vol. 5, no. 5, pp. 618–625, 2013.
- [34] J. R. Jett, L. J. Peek, L. Fredericks, W. Jewell, W. W. Pingleton, and J. F. Robertson, “Audit of the autoantibody test, EarlyCDT[®]-Lung, in 1600 patients: an evaluation of its performance in routine clinical practice,” *Lung Cancer*, vol. 83, no. 1, pp. 51–55, 2014.
- [35] P. P. Massion, G. F. Healey, L. J. Peek et al., “Autoantibody signature enhances the positive predictive power of computed tomography and nodule-based risk models for detection of lung cancer,” *Journal of Thoracic Oncology*, vol. 12, no. 3, pp. 578–584, 2017.
- [36] B. Yang, B. W. Jhun, S. H. Shin et al., “Comparison of four models predicting the malignancy of pulmonary nodules: a single-center study of Korean adults,” *PLoS One*, vol. 13, no. 7, p. e0201242, 2018.
- [37] Z. Q. Chen, L. S. Huang, and B. Zhu, “Assessment of seven clinical tumor markers in diagnosis of non-small-cell lung cancer,” *Disease Markers*, vol. 2018, Article ID 9845123, 7 pages, 2018.

Review Article

Myokines and Heart Failure: Challenging Role in Adverse Cardiac Remodeling, Myopathy, and Clinical Outcomes

Alexander E. Berezin ¹, Alexander A. Berezin ², and Michael Lichtenauer ³

¹Internal Medicine Department, State Medical University, Ministry of Health of Ukraine, Zaporozhye 69035, Ukraine

²Internal Medicine Department, Medical Academy of Post-Graduate Education, Ministry of Health of Ukraine, Zaporozhye 69096, Ukraine

³Department of Internal Medicine II, Division of Cardiology, Paracelsus Medical University Salzburg, 5020 Salzburg, Austria

Correspondence should be addressed to Alexander E. Berezin; lunik.mender@gmail.com

Received 23 October 2020; Revised 8 December 2020; Accepted 6 January 2021; Published 14 January 2021

Academic Editor: Robert Pichler

Copyright © 2021 Alexander E. Berezin et al. This is an open access article distributed under the Creative Commons Attribution License, which permits unrestricted use, distribution, and reproduction in any medium, provided the original work is properly cited.

Heart failure (HF) is a global medical problem that characterizes poor prognosis and high economic burden for the health system and family of the HF patients. Although modern treatment approaches have significantly decreased a risk of the occurrence of HF among patients having predominant coronary artery disease, hypertension, and myocarditis, the mortality of known HF continues to be unacceptably high. One of the most important symptoms of HF that negatively influences tolerance to physical exercise, well-being, social adaptation, and quality of life is deep fatigue due to HF-related myopathy. Myopathy in HF is associated with weakness of the skeletal muscles, loss of myofibers, and the development of fibrosis due to microvascular inflammation, metabolic disorders, and mitochondrial dysfunction. The pivotal role in the regulation of myocardial and skeletal muscle rejuvenation, attenuation of muscle metabolic homeostasis, and protection against ischemia injury and apoptosis belongs to myokines. Myokines are defined as a wide spectrum of active molecules that are directly synthesized and released by both cardiac and skeletal muscle myocytes and regulate energy homeostasis in autocrine/paracrine manner. In addition, myokines have a large spectrum of pleiotropic capabilities that are involved in the pathogenesis of HF including cardiac remodeling, muscle atrophy, and cardiac cachexia. The aim of the narrative review is to summarize the knowledge with respect to the role of myokines in adverse cardiac remodeling, myopathy, and clinical outcomes among HF patients. Some myokines, such as myostatin, irisin, brain-derived neurotrophic factor, interleukin-15, fibroblast growth factor-21, and growth differential factor-11, being engaged in the regulation of the pathogenesis of HF-related myopathy, can be detected in peripheral blood, and the evaluation of their circulating levels can provide new insights to the course of HF and stratify patients at higher risk of poor outcomes prior to sarcopenic stage.

1. Introduction

Heart failure (HF) remains a global public health problem with rapidly increasing prevalence that affects 37 million individuals and more worldwide [1]. Despite the significant achievements in the management of cardiovascular (CV) risk factors and novel therapies of HF with reduced ejection fraction (HFrEF) and stabilized incidence of new cases of predominant HF with preserved ejection fraction (HFpEF) in many countries, morbidity and mortality in patients with both phenotypes of HF continue to be unacceptably high [2, 3]. Being associated with a high risk of hospitalization,

HF yields a substantial economic burden for health system and patients' families [4, 5].

Current data for the prognosis of the patients having HFrEF and HFpEF show that the proportion of CV deaths is higher in HFrEF than HFpEF, but the number of non-CV death is higher in HFpEF when compared to HFrEF [6]. These findings are a result of an influence of age, CV risk factors, and several comorbid conditions, such as diabetes mellitus, abdominal obesity, hypertension, chronic kidney disease, and coronary artery disease [7]. Although comorbidity is common in both phenotypes of HF, but it is slightly more severe and occurs more frequently in HFpEF than in

HFrEF [8, 9]. There is the assumption that the comorbidities, such as overweight, abdominal obesity, and diabetes mellitus, may alter myocardial structure and impair cardiomyocyte function through several intramyocardial signaling pathways (hypophosphorylation of titin and irisin, cyclic guanosine monophosphate/protein kinase G activity, activation of Janus 1/2 kinases and nuclear factor Kappa B, and suppression of phosphatidylinositol 3-kinase (PI3) kinase/mitogen-activated protein (MAP) kinase/mTOR), which are result of systemic inflammation and thereby cause coronary microvascular endothelial inflammation and oxidative stress [10]. Consequently, substantial reduction of nitric oxide bioavailability and low activity of protein kinase G favors the development of cardiac hypertrophy and increases stiffness of the myocardium due to accumulation of extracellular matrix [11]. Finally, both cardiac hypertrophy and interstitial fibrosis contribute to diastolic abnormalities and the development of HFpEF [12]. In contrast, HFrEF is directly related to sufficient loss of the cardiac myocytes due to necrosis resulting of ischemia, inflammation, and apoptosis that are associated with adverse cardiac remodeling, systemic neurohormonal activation, peripheral vascular effects, skeletal muscle dysfunction, and metabolic abnormalities [13, 14]. However, the impaired physical activity due to muscle weakness, skeletal myopathy, muscle atrophy, and finally cachexia is the attributive factor for HF progression and it is closely associated with increased CV mortality, HF hospitalization, and decrease in the quality of life [15].

The underlying pathophysiological mechanisms of impaired physical activity in HF are abnormal energy metabolism of skeletal muscles, adiposity-related proinflammatory cytokine production, skeletal muscle mitochondrial dysfunction, the transition of myofibers from type I to type II in skeletal muscle, reduction in muscular strength, myocyte apoptosis, and loss of the number of myocytes with shaping of muscle atrophy [16]. Myokines are defined as cytokines that are produced by skeletal muscle myocytes and cardiac myocytes and regulate the crosstalk between skeletal muscle, adipose, and bone tissue [17]. Normally, myokines ensure the molecular adaptations of skeletal muscles to physical exercise and hemodynamic supply acting as regulator of exercise intolerance. The altered myokines' profile is also responsible for metabolic or hormonal derangements in skeletal muscles in HF patients even at early stage of the disease and probably could be a target for the therapy of the disease [18]. The aim of the narrative review is to summarize the knowledge with respect to the role of myokines in adverse cardiac remodeling, myopathy, and clinical outcomes among HF patients.

2. Methodology

The bibliographic database of life science and biomedical information MEDLINE, EMBASE, Medline (PubMed), the Web of Science, and the Cochrane Central were searched for English publications satisfying the key words of this study. We used the following key words [heart failure], [cardiac dysfunction], [adverse cardiac remodeling], [cardiac remodeling], [myokines], [myopathy], [cardiac cachexia], [cardiovascular risk], [cardiovascular risk factors], [cardiac

biomarkers], [circulating biomarkers], [prognosis], and [clinical outcomes]. All authors independently evaluated each other the quality of the articles, correspondence to the main idea of the study, and constructed the final list of the references. Consequently, strengths and weaknesses of each paper that was selected, as well as unblinded list of the references, were deeply considered by all authors. Final version of references, data for evaluation, and completed proof of the narrative review were approved by all authors.

3. Skeletal Muscle Myopathy and HF: The Conventional View

Skeletal muscle myopathy with or without weight loss appears to have a more pronounced significance when compared with weight loss alone with regard to functional capacity, decreased endurance, and quality of life among HF patients [19]. To note, fatigue and muscle weakness can be occurred prior to established diagnosis of skeletal muscle myopathy and even sarcopenic stage of HF, and the altered profile of myokines is deeply discussed as one of the earliest pathophysiological changes of energy metabolism that undoubtedly play a pivotal role in adaptation of skeletal muscles to impair diastolic and pump functions and consequently reduce skeletal muscle perfusion.

The pathogenesis of the skeletal muscle myopathy in HF is reported Figure 1. In fact, HF-related skeletal myopathy is characterized by decreased muscle strength, atrophy of fiber I and IIa subtypes, ongoing microvascular inflammation, oxidative stress and damage under metabolic homeostasis, and impaired repair after muscle injury [20]. Indeed, low perfusion of the skeletal muscles in HF leads to muscle injury that includes ischemia-induced metabolomics (shifted metabolic substrate utilization, altered mRNA expression of insulin-like growth factor (IGF) 1, type 1 receptor (IGF-1R), binding protein 3, lactate accumulation, and acidosis) and mitochondrial (impaired mitochondrial electron transport chain activity, increased formation of reactive oxygen species, and impaired ion homeostasis) abnormalities, which increased expression of the proinflammatory cytokine genes, as well as necrosis and apoptosis of myocytes [21]. Finally, that is associated with myosin heavy chain subtypes switch-off, decreased capillary/fiber ratio, the number of type I fibers, the development of fibrosis, and the loss of the skeletal muscle mass [22]. In addition, systemic inflammation and neurohumoral activation (increased activity of the renin-angiotensin-aldosterone system, sympathetic system, and endothelin-1) lead to decreased bioavailability of nitric oxide and other regulators of vasodilation and angiogenesis, such as bradykinins and vascular endothelial growth factor, and aggravate endothelial dysfunction, muscle perfusion, and muscle metabolism [17, 23]. Moreover, coexisting adipocyte dysfunction supports systemic inflammation through overproduction of inflammatory cytokines (interleukin- (IL-) 6, tumor necrosis factor- (TNF-) alpha) and induces catabolic state and impairs viability and differential capability of various progenitor cells including endothelial and muscle cell precursors [24]. Yet, impaired baroreceptor sensitivity, vagal withdrawal, and uncoupling of the subunits of beta-

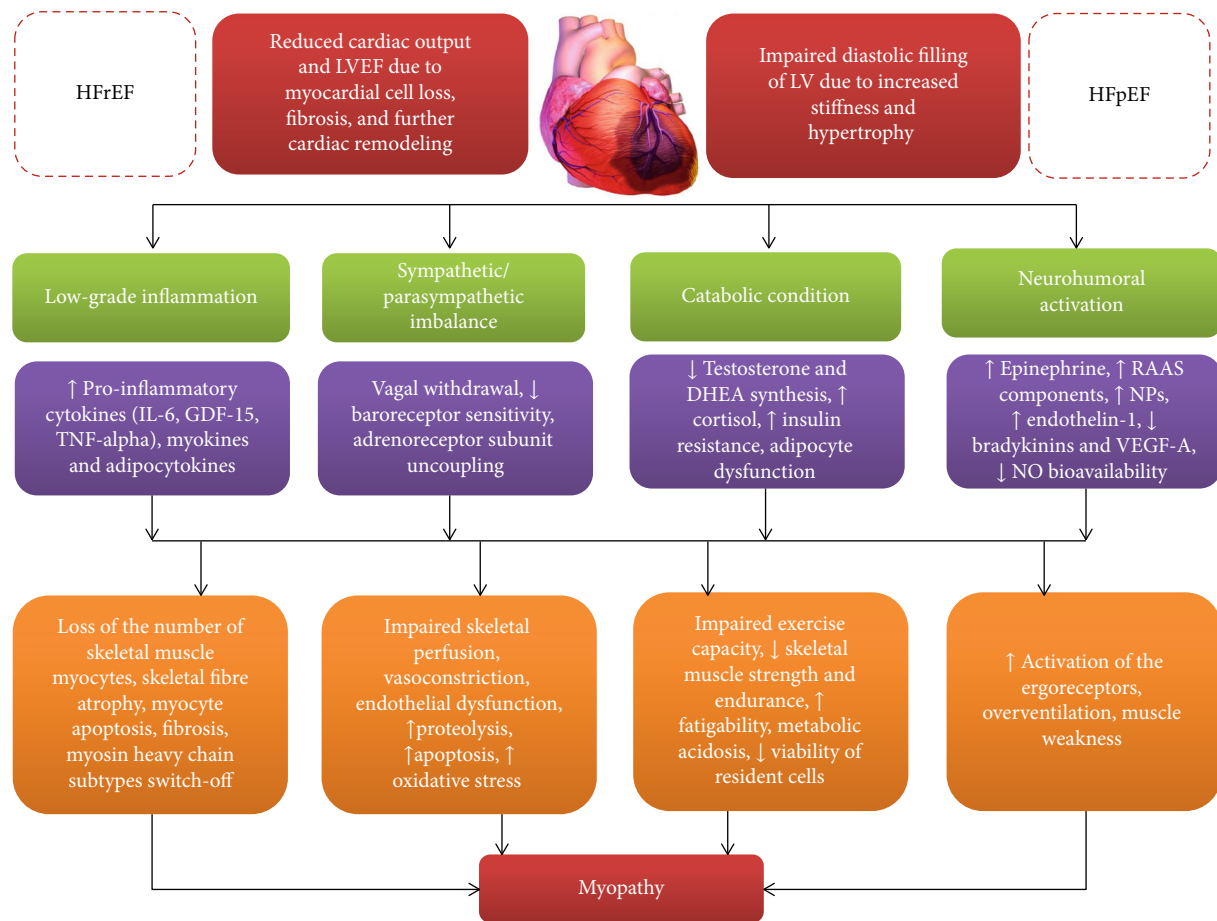


FIGURE 1: The pathogenesis of the skeletal muscle myopathy in HF. RAAS: renin-angiotensin-aldosterone system; NO: nitric oxide; NP: natriuretic peptides; IL: interleukin; GDF: growth differential factor; TNF: tumor necrosis factor; HFrEF: heart failure with reduced ejection fraction; DHEA: dehydroepiandrosterone; HFpEF: heart failure with preserved ejection fraction.

adrenoreceptors maintain vasoconstriction and hypoperfusion of the skeletal muscles tailoring the vicious circle in the pathogenesis of the HF-related myopathy.

Because physical endurance, several anthropomorphic features, body mass, and CV risk factors including abdominal obesity and diabetes occurred in male and female in different ways, there is a suggestion that myokine profiles can distinguish in both sexes [25]. Perhaps, expression pattern and signature of circulating myokines would partially explain the complicated crosstalk between skeletal muscle and other tissues, such as WAT, in different genders and muscle phenotypes [26]. Indeed, metabolic signature in Duchenne muscular dystrophy is related to gender and depended on expression of genes, which were widely involved in the pathogenesis of the disease, i.e., matrix metalloproteinase (MMP-) 9, brain-derived neurotrophic factor (BDNF), adiponectin, persephin, osteomodulin, protooncogene tyrosine-protein kinase receptor Ret, complement decay-accelerating factor, growth differentiation factor 11 (GDF-11), gelsolin, and tumor necrosis factor receptor superfamily member 19L [27, 28]. Although primary causes are significantly different for HF-induced myopathy and Duchenne muscular dystrophy, myokines are engaged in the pathogenesis of cardiac abnormalities for both diseases [28].

4. Myokines in HF Myopathy

The skeletal muscles enable to release a wide range of the biological active molecules with variable potencies called myokines; the profile of which was found to be altered in HF patients [29]. Although HF-related myopathy has been considered as secondary muscle injury that was associated with low capillary perfusion [30], myokines ensure adaptive metabolic autoregulation of structure and function of skeletal muscles at the early stage of the disease and consequently altered profile of the myokines corresponded to progression of HF and occurrence of sarcopenia and cachexia [31]. Moreover, the periods of acute HF exacerbation and hospitalization are associated with substantial low physical activity. Consequently, impaired synthesis and releasing of myokines lead to the protein metabolic derangements in both the skeletal muscles and myocardium aggravating muscle weakness, physical intolerance, and cardiac dysfunction. In addition, several comorbidities, such as abdominal obesity and diabetes mellitus, coexisting with HF can also alter the profile of myokines including irisin, myostatin, brain-derived neurotrophic factor (BDNF), and growth differentiation factor-11 (GDF-11) and lead to muscle weakness [32–34]. Interestingly, there was no strong correlation of HF-induced

myopathy with left ventricular (LV) ejection fraction (EF) in HFpEF/HFrEF patients, whereas global longitudinal strain was positively associated with the occurrence of the myopathy due to HF regardless of LVEF [35]. Probably, *in situ* cardiac dysfunction is not the only factor contributed to advance of HF-induced myopathy and circulating regulators of energy homeostasis can be promising indicator of HF progression. In this context, primary impairment of the skeletal muscle homeostasis has been speculated as a crucial mechanism in the occurrence and the development of the HF in patients with metabolic diseases predominantly diabetes mellitus and abdominal obesity [36, 37]. In fact, there is vicious circle that corresponds to aberrant skeletal muscle impairments and pathophysiological mechanisms of HF development (Figure 2).

There is evidence for the fact that the wide spectrum of myokines provides controversial actions on skeletal muscle cells and mediates pleiotropic effects. Most of myokines are controlled by muscle contractility function, myogenesis, muscle hypertrophy, and reparation and consequently closely regulate exercise tolerance via intracellular signal pathways including the Janus 1 and 2 kinases/3 and 5 signal transducer and activator of transcription proteins/nuclear factor kappa B, PI3 kinase, and MAP kinase pathways [38]. It is interesting that some potential proinflammatory myokines, such as IL-15 and IL-6, simultaneously provide angiopoietic effects and support proapoptotic impact on myoblasts. It has been found interrelationship between NO-mediated cellular signaling and production of the myokines in skeletal muscle cells [39]. However, hyperemia in skeletal muscle over physical exercise was strongly associated with myokine release [40]. In addition, occurrence of cardiac cachexia in HF is accompanied by crossover changes in the spectrum of the myokines; for instance, there were elevated serum concentrations of myostatin and IL-6 found, whereas irisin, fibroblast growth factor- (FGF-) 21, and myonectin demonstrated a significant decrease in their circulating levels. The serum levels of decorin, BDNF, and GDF-11 were variable and exhibited strong relation to age of the HF patients rather than severity of contractility dysfunction and sarcopenia [41–44]. Finally, myokines influence not just skeletal muscles but also the myocardium and adipose tissue and ensure their autocrine metabolic regulation of energy homeostasis, hypertrophy, reparation, and adaptation of skeletal muscles to physical exercise.

The biological effects and HF-related actions of several myokines are reported Table 1.

4.1. Decorin. Decorin is a proteoglycan that is produced by skeletal muscles in a result of stretching and constitutively suppresses the extracellular matrix (ECM) accumulation, particularly type I fibrillar collagen, stimulates angiogenesis and reparation, and negatively regulates inflammation, oxidative stress, and apoptosis [41, 44].

Development of HF was associated with downregulation of decorin expression in the myocardium and consequently increases in activity of matrix metalloproteinase- (MMP-) 2 that corresponded to adverse cardiac remodeling [45]. There is evidence regarding the fact of that decorin interfered with

cardiac myocytes and switched off their transcriptome to suppress synthesis of MMP tissue inhibitors and substantially upregulate cardiac fibrosis-associated transcripts including collagen I and III, elastin, lumican, and periostin [46, 47]. In addition, decorin was potentially encouraged in adverse cardiac remodeling by directly inhibiting the transforming growth factor-beta (TGF-beta) pathway and increasing collagen mRNA transcription in the myocardium [48]. As a result of these actions, cardiac myocytes face increased matrix rigidity that led to diastolic filling abnormality [49]. To sum up, decorin being a natural antagonist of TGF-beta enables to prevent cardiac fibrosis and hypertrophy and improve cardiac function.

4.2. Irisin. Irisin is a multifunctional hormone-like active peptide that is produced in abundance by the myocardium and skeletal muscle in response to ischemia, volume overload, inflammation, and physical exercise [50].

Irisin is synthesized as a result of proteolytic cleavage of specific precursor (fibronectin type III domain-containing protein-5—FNDC5) that is expressed on the surface of myocytes. Having numerous autocrine skeletal muscle effects (attenuation of energy expenditure through enhancement of glucose uptake, improvement of oxidative metabolism, and increase in myoblast differentiation), which are ensured by upregulation of the expression of FNDC5, irisin enables to cooperate with white adipose tissue (WAT) to induce its browning by increasing the expression of mitochondrial uncoupling protein 1 (UCP 1) and subsequently activates nonshivering thermogenesis, supports glucose homeostasis, and reduces endothelial function abnormality, insulin resistance, and adipose tissue inflammation [51–53]. Therefore, irisin protects the myocardium against ischemia and reperfusion injury and attenuates the proliferation of the endothelial precursors acting through the AMPK-Akt-eNOS-NO pathway [54, 55]. There is evidence for reduction of cardiomyocyte apoptosis and alleviation of myocardial hypertrophy caused by pressure overload with irisin [56]. Irisin also plays a pivotal role in the control of bone mass with positive effects on cortical mineral density and bone geometry through an interaction with $\alpha V/\beta 5$ integrin [57, 58]. In addition, irisin is involved in the process of neurogenesis in the central and peripheral nervous system [59, 60].

Serum levels of irisin were independently associated with Framingham risk profile [61]. The circulating levels of irisin were significantly higher in the normoglycemic patients with metabolic syndrome, but not those who had prediabetes or diabetes mellitus in comparison with healthy volunteers [62]. There is evidence for lower levels of irisin in patients with stable coronary artery disease (CAD) or acute coronary syndrome/myocardial infarction [63–65]. Moreover, decreased serum levels of irisin were noticed to be associated with the presence, severity, and higher SYNTAX score of stable CAD [66, 67]. Interestingly, serum levels of irisin among myocardial infarction patients having HF were reduced when compared with healthy volunteers, but did not differ from those who had no HF [64]. However, there were found positive associations between serum levels of irisin and LVEF [64]. Silvestrini et al. (2019) [68] reported that circulating

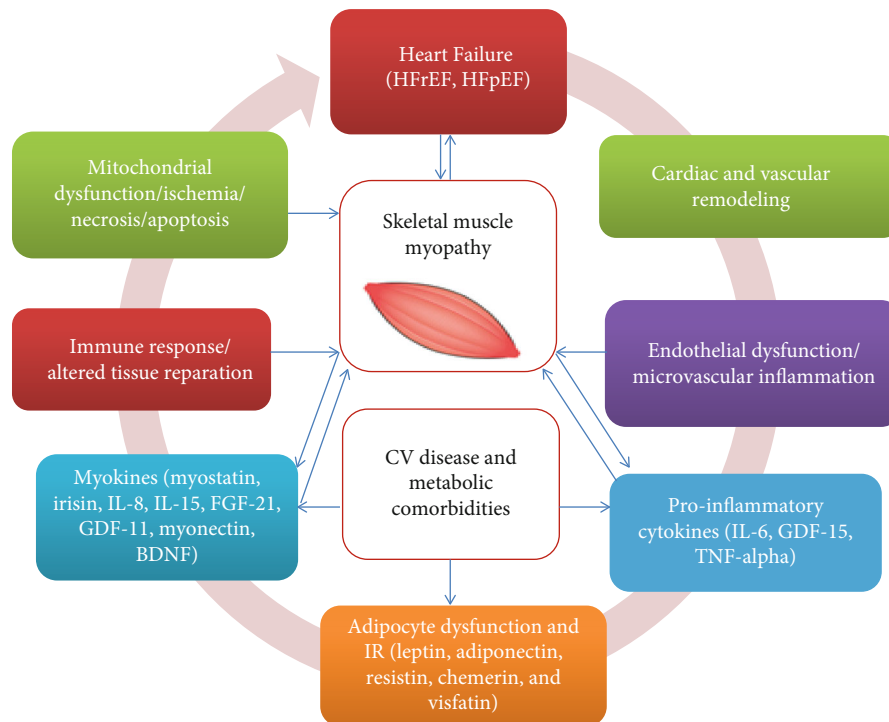


FIGURE 2: The role of skeletal muscle dysfunction in the pathogenesis of HF. HFpEF: HF with preserved ejection fraction; HFrEF: HF with reduced ejection fraction.

levels of irisin were significantly higher in HFpEF than in HFrEF patients and did not correlate with homeostasis model assessment of insulin resistance (HOMA-IR) index in both patient cohorts. Irisin levels demonstrated positive correlation with brain natriuretic peptide (BNP) levels and New York Heart Association (NYHA) class of HF and inverse correlation with body mass index (BMI) and catabolic state including cachexia in HFrEF [69]. Yet, FNDC5 expression in skeletal muscles is related to aerobic performance in patients with HFrHF [70, 71]. Thus, irisin plays a protective role in myocardial ischemia, cardiac myocyte apoptosis, and skeletal myopathy preserving energy homeostasis, attenuating mitochondrial function, and regulating muscle atrophy.

4.3. Myonectin. Myonectin (also known as erythroferrone) is a myokine, which belongs to the C1q/tumor necrosis factor-(TNF-) related protein (CTRP) family and is upregulated in skeletal muscles by physical exercise and is determined in peripheral blood in elevated concentrations [72]. Circulating levels of myonectin were also strongly regulated by the metabolic state (feeding, obesity, diabetes mellitus, and cachexia), and thereby, myonectin is a conductor between skeletal muscle with lipid homeostasis in liver and WAT [73]. Typically, patients with abdominal obesity, metabolic syndrome, and type 2 diabetes mellitus demonstrate higher circulating levels of myonectin than healthy volunteers [73]. In addition, among patients having prediabetes and diabetes mellitus, serum levels of myonectin correlated positively with waist/hip ratio, percentage of body fat, fasting blood glucose, 2-hour blood glucose after glucose overload, fasting insulin, tri-

glyceride, hemoglobin A1c, and HOMA-IR [74]. Although the primary biological role of myonectin is an increase of free fatty acid uptake by skeletal muscles and contributing to lipid and glucose metabolism in adipose tissue, it has several pleiotropic effects, such as suppression of inflammatory response, protection of ischemia-reperfusion injury, and improvement of endothelial function that are mediated through the S1P/cAMP/Akt-dependent signaling pathway [75, 76]. The development of HF is associated with downregulation in myonectin expression due to inflammatory response, but the pathogenetic role of this myokine in the disease is not fully understood [77].

Thus, myonectin acts as an endurance exercise-induced myokine ameliorating compensatory mechanism against insulin resistance and attenuating acute myocardial ischemic injury by inhibition of apoptosis and suppression of inflammation in the myocardium.

4.4. Fibroblast Growth Factor 21. Fibroblast growth factor (FGF-21) is a multifactor protein, which is produced by several organs and engaged in the autocrine/paracrine regulation of fatty acid oxidation, energy expenditure, glucose homeostasis, and the functions of somatotrophic axis and hypothalamic-pituitary-adrenal pathway [78, 79]. This peptide is highly expressed in the myocardium, pancreas, WAT, liver, brain, and kidney, but not constitutively in the skeletal muscles [80]. In addition, FGF-21 is induced in situations of muscle stress, particularly mitochondrial dysfunction. The beneficial effects of FGF21 include weight loss, improvement of glycemia and lipotoxicity, browning WAT, suppression of inflammation and oxidative stress,

TABLE 1: Biological effects and HF-related actions of myokines.

Name of myokine	Affiliation	Origin of myokines	Biological action	HF-related actions	References
Decorin	Proteoglycan	Skeletal muscles, fibroblasts, vascular endothelial cells, cardiac myocytes, and smooth muscle cells	↓ Accumulation of ECM, ↑ cell differentiation, ↑ proliferation, and ↓ apoptosis	<i>Downregulated in HF</i> ↓ Cardiac hypertrophy, ↑ cardiac fibrosis	[41–49]
Irisin	Muscle tissue-secreted peptide FNDC5	Skeletal muscles, myocardium	↑ Expenditure, ↑ oxidative metabolism, ↑ myoblast differentiation, ↑ glucose uptake	<i>Downregulated in HF</i> ↓ Tolerance to physical exercise, ↑ skeletal muscle hypotrophy	[50–71]
Myonectin	CTRP15	Skeletal muscles, adipose tissue	↑ Oxidation of free fatty acid, ↑ oxidative metabolism, ↑ myoblast differentiation, ↑ glucose uptake	<i>Downregulated in HF</i> ↑ Skeletal muscle hypotrophy	[72–77]
FGF-21	FGF super family	Cardiac myocytes, pancreas, adipose tissue, liver, brain, and kidney	↑ Glucose uptake and protein synthesis in skeletal muscle, ↓ lipolysis in WAT, ↑ browning of WAT	<i>Downregulated in HF</i> ↑ Skeletal muscle mass, ↓ IR, ↑ exercise tolerance	[78–94]
Myostatin	TGF- β superfamily	Cardiac myocytes, skeletal muscles	↑ Skeletal muscle fiber-type switches, ↓ fast myosin heavy-chain expression, ↓ differentiation of myoblasts, ↑ ubiquitin-proteasomal activity in myocytes and ILGF-PKB pathway	<i>Upregulated in HF</i> ↑ Skeletal muscle hypotrophy, ↑ IR, ↑ autophagy, ↑ muscle weakness, ↓ exercise tolerance	[95–111, 203]
BDNF	Neurotrophin family	Cardiac myocytes, skeletal muscles, smooth muscle cells, endothelial cells, astrocytes	↑ Myoblast proliferation, ↑ neurogenesis, ↑ angiogenesis, ↑ vascular reparation	<i>Downregulated in HF</i> ↑ Tolerance to physical exercise	[112–134]
IL-8	Cysteine-X-cysteine family of chemokines	Mononuclears, phagocytes, adipocytes, epithelial cells, endothelial cells, and mesenchymal cells	↓ Glucose disposal, ↑ IR	<i>Upregulated in HF</i> ↓ Skeletal muscle energy metabolism	[135–147]
IL-15	Pleiotropic cytokine with structural similarity with IL-2	Cardiac myocytes, mononuclear phagocytes	Anabolic effect, ↓ oxidative stress	<i>Downregulated in HF</i> ↑ Tolerance to physical exercise, ↑ skeletal muscle mass, ↓ WAT, ↓ apoptosis of cardiac myocytes and myoblasts	[149–168]
GDF-11	TGF- β super family	Skeletal muscle, neural stem cells, and cardiac myocytes	↓ Differentiation of myoblasts, angiogenesis, and neovascularization	<i>Downregulated in HF</i> ↓ Physical endurance, ↑ skeletal muscle hypotrophy and weakness	[169–178]
Osteonectin	SPARC protein	Cardiac myocytes, skeletal muscles, adipose tissue, bones, mucosa, vasculature, kidney, liver	Potential mediator of collagen deposition and extracellular matrix remodeling	<i>Upregulated in HF</i> Predictor of poor HF outcomes, ↑ cardiac contractility and reparation at early stage, ↓ cardiac myocyte survival and vascular integrity at late stage	[179–196]

FGF-21: fibroblast growth factor-21; TGF- β : transforming growth factor-beta; IR: insulin resistance; ILGF-PKB: insulin-like growth factor-protein kinase B; WAT: white adipose tissue; GDF-11: growth differentiation factor-11; ECM: extracellular matrix; SPARC: secreted protein acidic and rich in cysteine.

counteracting water intake, and blood pressure elevation [81–84]. FGF-21 induced the expression of genes, which encode proteins involved in antioxidative pathways, such as mitochondrial uncoupling proteins (Ucp2 and Ucp3) and superoxide dismutase-2 (Sod2) and reduced ROS production [85, 86]. In addition, FGF-21 prevented the development of cardiac hypertrophy by activating MAPK signaling through

the activation of FGF-R1c with β -klotho as a coreceptor [87, 88].

In a failing heart, FGF-21 exerts protective effects, preventing the development of cardiac hypertrophy and ischemic injury via the Sirt1 (sirtuin-1) pathway [85, 89]. Patients with multivessel CAD and type 2 diabetes mellitus have revealed decreased expression of FGF-21 in the

myocardium [90]. Among patients with HFrEF and HFpEF, serum levels of FGF-21 were positively associated with echocardiographic parameters of diastolic function, LV end-diastolic pressure, and NT-pro-BNP levels [88–90], as well as with IL-6 levels and lower skeletal muscle mass [91]. Conflicting results in the presence of the strong correlation between serum levels of FGF-21 and NT-pro-BNP are explained by adjustment of the data for cardiac cachexia [91, 92]. There was strong correlation between circulating levels of FGF-21 and NT-pro-BNP in HFrEF patients without cardiac cachexia, but no correlation between these biomarkers was noticed in those who had HFrEF with cardiac cachexia [93]. Probably, some cardioprotective effects of sodium-glucose cotransporter 2 inhibitors (SGLT2i) may be related to their ability to induce the FGF-21/SIRT1 pathway and thereby stimulate endogenous reparation [94, 95].

4.5. Myostatin. Myostatin is established as a negative regulator of skeletal muscle mass that is upregulated in the myocardium of HF [96, 97]. Myostatin belongs to the transforming growth factor- β (TGF- β) family and its main biological function comes down to the inhibition of skeletal muscle growth and prevention of insulin resistance [98]. In the physiological condition, myostatin is predominantly expressed in skeletal muscle, while small basal expression was also noticed in the myocardium and WAT.

The development of the HF is associated with increased expression of myostatin in the myocardium, skeletal muscles, and WAT, and elevated levels of the peptide were discovered in the peripheral blood [99]. Myostatin interacts tightly with insulin-like growth factor I (IGF-I) and enables to stimulate the expression of regulator of G-protein signaling 2, a GTPase-activating protein, which restricts the G α q and G α s signaling pathway and thereby protects against ischemic/reperfusion injury and HF development [100]. Muscle myopathy and sarcopenia are related to overexpression of myostatin that acts as powerful activator of the Smad2/3 pathway and thereby stimulates the proteasomal and the autophagolysosomal capabilities [99–101]. On the other hand, overexpression of myostatin in the myocardium caused interstitial fibrosis and myocyte loss via activation of the TAK-1-MKK3/6-p38 signaling pathway, and thereby, these findings did not support the idea about protective abilities of myostatin [102]. Yet, myostatin has demonstrated an ability to modulate myosin heavy chain isoform (I MyHC isoform) shift in skeletal muscle [103]. However, being a strong predictor of frailty, disability, and mortality sarcopenia occurs in patients with HFrEF in results of abundant molecular mechanisms including Smad2/3 signaling [101, 104]. Probably, these controversies in the protective ability of myostatin relate to etiology (ischemic or nonischemic) of HF [105, 106].

Serum levels of myostatin were found to be higher in chronic HF patients than in healthy volunteers which positively correlated with biomarkers related to HF severity [107–109]. In addition, there is evidence for significant decreasing of serum levels in HF patients [110]. However, the results regarding the association between myostatin levels, HF severity, and other HF biomarkers such as NT-proBNP/BNP are conflicting. Chen et al. (2019) [107] found

strong associations between myostatin and severity of adverse cardiac remodeling, NYHA classes of HFrEF and LVEF, while Zamora et al. (2010) did not notice these relations in HFrEF patients [111]. Thus, myostatin is involved in adverse cardiac remodeling and the evaluation of its circulating levels appears to be promised to predict the course of HF and also to guide a risk stratification of HF patients [110].

4.6. Brain-Derived Neurotrophic Factor. Brain-derived neurotrophic factor (BDNF) is a neuronal growth factor that plays a pivotal role in the maintenance of the nervous system, the development of depression and behavior disorders, cardiac reparation, and skeletal muscle energy metabolism [112, 113]. BDNF is produced by a wide spectrum of the cells including cardiac myocytes, skeletal muscles, smooth muscle cells, and mature and progenitor endothelial cells [112, 114]. Typically, BDNF is considered as multifunctional protein with organ protective capabilities, which is the synthesis in the result of tissue damage (ischemia, hypoxia) and an impact of proinflammatory cytokines (IL-1 β , IL-6, and TNF- α) and acts through the c-Jun N-terminal kinase pathway [114–116]. It has been suggested that physical exercise and strength exercise are able to ensure an effective cardiometabolic protection through increasing BDNF serum levels [117]. There is evidence for the fact that BDNF was found to be a powerful metabolic regulator of myoblast activity, and thereby, this protein is engaged in the endogenous reparation of the skeletal muscle and myocardium [116, 117]. In addition, BDNF is involved in the regulation of glucose and lipid metabolism [118].

There is Val66Met polymorphism (rs6265) of BDNF gene, which has been associated with altered circulating levels of BDNF and corresponds to several neuropsychiatric disorders, regional structural brain changes, and cardiac and vascular protection against hypoxia and ischemia [119–121]. In fact, obesity, metabolic syndrome, type 2 diabetes mellitus, and CV diseases including HF were associated with decreased serum levels of BDNF [122–124]. In contrast, patients having acute coronary syndrome (ACS) and ST segment elevation myocardial infarction had higher circulating levels of BDNF than healthy volunteers and strongly predicted acute HF development [125], while there is evidence regarding that BDNF levels can be reduced in patients having ACS [126]. Moreover, in animal model of HF and among patients with HFrEF, low levels of BDNF were associated with reduced physical activity and a risk of HF-related myopathy [127–131]. In addition, low levels of BDNF predicted a risk of cognitive dysfunction among HFrEF patients [132] and poor clinical outcomes [124, 125, 131, 133]. The serum BDNF levels may be a useful surrogate biomarker of increased CV risk, the HF-related myopathy, and adverse prognosis in patients having HF [134].

4.7. Interleukin-8. IL-8 (also known as chemokine CXCL8) belongs to the CXC chemokine family [135]. It is produced by mononuclears, phagocytes, adipocytes, epithelial cells, endothelial cells, and mesenchymal cells exposed to various inflammatory stimuli [136]. IL-8 acts as paracrine trigger of macrophage migration, neutrophil chemotaxis, and

differentiation and proliferation of profibrogenic mesenchymal progenitor cells [137, 138]. Interestingly, skeletal muscle fibers express IL-8 mRNA, which is regulated by muscle contraction [139]. Thus, IL-8 can partially be considered as a myokine.

Although IL-8 have shown to be predictive for CV events in several studies, its role as clinical biomarkers for HF is unclear [140–142]. Elevated levels of IL-8 were noticed in the patients with ACS and acute HF [143, 144]. There was strong correlation between serum levels of circulating IL-8 and adverse clinical outcome and cardiac remodeling after STEMI [142]. However, there are conflicting reports regarding the role of IL-8 in inducing cardiac dysfunction in HF [145–147]. Indeed, delayed expression of IL-8 in the myocardium after revascularization in STEMI was associated with a high risk of cardiac dysfunction and the development of chronic HF regardless of the presence of traditional CV risk factors [146]. On the other hand, several comorbidities including type 2 diabetes mellitus and abdominal obesity were able to aggravate adverse cardiac remodeling after completed reperfusion through microvascular inflammation [147]. In addition, there were no favorable effects on CV events observed in the large clinical trials of rheumatoid arthritis patients treated with anticytokine therapy (IL-1 β inhibition, IL-1 receptor antagonists, IL-6 receptor antagonists, or TNF inhibition) [148]. Finally, the role of IL-8 in HF development and progression remains uncertain.

4.8. Interleukin-15. IL-15 is pleiotropic proinflammatory cytokine with structural similarity with IL-2, which predominantly exerts anabolic and tissue protective effects by decreasing cardiac myocyte apoptosis, mobilization of endothelial and mesenchymal progenitor cells, reduction of oxidative stress, and improvement of myocardial function [149]. On hypoxia condition, cardiac myocytes express appropriate IL-15 receptor, by which IL-15 protects the myocardium against injury [149]. IL-15 activates signaling by the β and common γ (γ c) chain heterodimer of the IL-2 receptor and thereby supports survival and proliferation of natural killer cells and suppresses oxidative stress [150]. On the other hand, IL-15 maintains chemotaxis of the natural killer cells and their adhesion on endothelium [151]. In contrast to IL-8, IL-15 is a growth factor that is highly expressed in skeletal muscle and exerts muscle hypertrophy through specific receptor (IL-15R) [152, 153]. Despite IL-15 has been revealed as having sufficient anabolic impact on skeletal muscle both *in vitro* and *in vivo*, it plays a crucial role in reducing mass of WAT [139].

IL-15 is upregulated in some CV diseases, such as myocardial infarction, HF and atherosclerosis [154]. In addition, IL-15 was found a regulator of fractalkine (FKN)-CX3CR1 chemokine signaling system, which is involved in the acceleration of atherosclerosis and promoting smooth muscle cell proliferation [155]. There is evidence of the fact that IL-15 has direct cytotoxic impact on endothelial cells and their precursors and thereby induces endothelial dysfunction and microvascular inflammation. Indeed, IL-15 activates antigen-presenting cells (APCs), such as dendritic cells, macrophages, and CD8(+) T cells and acts as a trigger of apopto-

sis of endothelial cells via caspase activation and loss of mitochondrial membrane potential [156, 157]. Thus, IL-15 is able to support inflammatory infiltration of the myocardium and directly induce myocardial injury. Additionally, IL-15 exerts specific endocrine effects on WAT, stimulates synthesis of adipocytokines, and consequently maintains adipocyte tissue oxidation and inflammation [158]. Finally, acting through the regulation of adipocytokine synthesis, IL-15 indirectly modifies IR of skeletal muscles and attenuates HF-related myopathy [159, 160].

Low circulating levels of IL-15 were found in younger and older people with sarcopenia without known HF [161, 162]. A clinical study has shown that IL-15 gene polymorphisms were susceptible biomarkers for development of subclinical atherosclerosis and CAD [163]. Patients with HF have demonstrated altered profile of several cytokines including IL-15; the levels of which were noticed to be dramatically increased [164]. However, circulating levels of IL-15 were not associated with ischemia-induced adverse cardiac remodeling and poor clinical outcomes [164], but in nonischemic HF, patients there found a correlation between IL-15 myocardial expression and a risk of sudden death and HF-related events [165].

To sum up, the results of preclinical and clinical studies for the integral role of IL-15 as a trigger of adverse cardiac remodeling and HF-related myopathy have been noticed inconclusive. Although the natural killer cell receptor/IL-15 signaling pathway contributes to progressive inflammatory muscle destruction and myopathy [166], whether this molecular mechanism is essential for regulation of HF-related myopathy is not fully clear. Thus, muscle-derived IL-15 appears to have important roles in metabolism of both the myocardium and skeletal muscles, and exercise plays a role in the interplay between WAT modification and inflammation, but its value in HF-related myopathy remains to be poorly understood [167, 168].

4.9. Growth Differential Factor-11. GDF-11 belongs to the superfamily of transforming growth factor-beta and is widely expressed in several tissues including the myocardium and skeletal muscles [169]. GDF-11 reverses age-related cardiac hypertrophy, improves muscle regeneration and angiogenesis, maintains differentiation of progenitor cells, and protects against myocardial ischemia and reperfusion injury by activation of Smad2/3 signaling [170–172]. Nevertheless, in animal model of HF, GDF-11 stimulated oxidative stress, potentiated apoptosis, and induced tissue injury by upregulating Nox4 in H9C2 cells (cardiomyoblast cell line derived from embryonic rat heart tissue) and the production of reactive oxygen species in a result of modulation of NADPH oxidases [173].

GDF-11 is upregulated in the myocardium and skeletal muscles in patients with CAD and HF [174, 175] and acts on skeletal muscles inducing low physical tolerance and muscle weakness [176]. It has been suggested that GDF-11 induces specific genes called astrogens, which induce the ubiquitin-proteasome system, leading to protein degradation in skeletal muscles and mitochondrial dysfunction [176]. Finally, GDF-11 is discussed as a factor that contributes to

disease progression and loss of skeletal muscle mass [177]. In contrast, there is a suggestion that elevation of GDF-11 is associated with cardioprotection, because patients having stable CAD and elevated levels of GDF-11 levels were associated with lower risk of CV events and death [178]. Thus, GDF-11 had cardioprotective activities and probably plays a pivotal role in prevention of HF-related myopathy and sarcopenia.

Overall, the development of HF is associated with upregulation of myostatin and IL-8 and downregulation of irisin, myonectin, FGF-21, BDNF, and IL-15.

4.10. SPARC. SPARC (secreted protein acidic and rich in cysteine), also called osteonectin, is an extracellular collagen-binding matrix protein responsible for cell function as well as cell-matrix interactions [179]. In numerous studies, SPARC was shown to act as a potential mediator of collagen deposition and collagen assembly [180]. Moreover, it was also reported to be involved in cell migration and proliferation as well as tissue repair [181]. The secretion of SPARC is known to be induced through physical exercise, stress, and tissue damage and can be found throughout all body tissues [181, 182]. In mouse models with an inhibited SPARC expression, a reduction in organ fibrosis in the lung, heart, skin, liver, and eye was reported in response to fibrotic stimuli [183]. Similarly, reduced levels of SPARC are associated with osteogenesis imperfecta [184]. Moreover, SPARC is also involved in different malignancies [185, 186]. In the heart, SPARC is expressed by endothelial cells and fibroblasts and by cardiac myocytes to some extent [187]. It is not only upregulated in response to cardiac injury and in areas of cardiac remodeling but also in response to pressure overload [188]. In a mouse model of pressure overload, SPARC was observed to play a pivotal role in the deposition of insoluble collagen deposition, thus contributing to myocardial stiffness [189]. In the same study, macrophages were identified as possible source for increased SPARC levels in response to pressure overload [190]. Apart from cardiac injury and pressure overload, SPARC was also reported to be connected to the age-dependent increase in left ventricular stiffness [179, 190]. Contrary, SPARC was shown to be increased after acute MI while a temporal relation to scar formation was evident [191, 192]. Similarly, SPARC inactivation leads to an increase in cardiac rupture and dysfunction after acute myocardial infarction in a mouse model [193]. Vice versa, overexpression of SPARC after myocardial infarction showed a cardiac and vascular protective effect [194]. In this regard, an increase in Smad2 phosphorylation was suggested [195]. Moreover, studies have proposed a positive inotropic effect of SPARC in the heart [196]. Thus, given its role in collagen deposition and assembly, the role of SPARC in the heart might have to be interpreted in clinical context. While it may have a positive effect with regard to acute tissue damage, chronically elevated levels of SPARC seem to have a negative effect especially with regard to cardiac remodeling and endothelial integrity. However, further studies on SPARC are warranted to clarify its role in cardiac injury and remodeling to further extent.

5. Myokines and Heart Failure-Related Clinical Outcomes

There is a large body of conflicted evidence for predictive values of several myokines for adverse clinical outcomes predominantly in HFrEF [197]. Serum irisin levels were found to be higher in acute HF patients deceased in 1-year follow-up [198]. In addition, there was a close positive correlation between elevated levels of irisin and CV clinical outcomes after myocardial infarction regardless of HF presence [199]. Moreover, irisin has demonstrated better prediction for MACEs to NT-proBNP [199]. Collectively, elevated serum levels of irisin were powerful predictive biomarker for 1-year all-cause and CV mortality in acute and chronic HF patients. Higher circulating levels of FGF-21 were also associated with a high mortality rate, but not CV events in patient with ESRD at a risk of HF [200]. Myostatin was found to be an independent predictor of mortality in HF patients and rehospitalization due to HF progression [107]. Decreased serum levels of BDNF were significantly associated with adverse outcomes in HF patients [124, 125]. There is a large body of evidence regarding the fact that elevated levels of some SPARC proteins, such as osteonectin and osteopontin, have demonstrated a strong association with poor long-term HF-related outcomes including death, and a risk for recurrent hospitalization due to HF among patients with normal body mass, overweight, and obesity [201, 202]. However, there was no finding that osteonectin predicted cardiac cachexia and poor clinical events in patients with HF-related myopathy. The discovery of exact molecular pathways that correspond to the link between myokines and HF outcomes remains uncertain and requires being clearly elucidated in the future [18]. However, the idea regarding that the myokines could be new biological target to point-of-care therapy in HF with various phenotypes is promising especially among HF patients with metabolic comorbidities.

6. Perspectives in the Future

Myokines are predictive biological markers that are independently associated with an increased risk of HF-related myopathy and cachexia, while their role in the prediction of adverse cardiac remodeling and risk stratification of clinical outcomes requires thorough investigation in the large clinical trials. Another direction for studies in the future is a modification of myokines' profile in a result of aerobic and interval isometric physical exercise. Because HF-related myopathy is an established predictor of poor clinical prognosis and physical exercise has been determined to be predictably valued, the monitoring of serum levels of myokines could be attractive to stratify HF patients at higher risk of the progression of the myopathy. In addition, myokines can be useful to determine whether the physical exercises are adequate. Therefore, myokines can be targets for the personalized therapy of HFrEF and HFpEF to prevent HF-related myopathy and cardiac cachexia. In this context, new anti-cytokine drugs, such as anti-IL-17 anti-IL-23, could be investigated with this purpose.

7. Conclusion

Altered circulating signature of myokines is noticed at the early stage of HF occurrence and was associated with the adverse cardiac remodeling, diastolic filling abnormalities, reduced systolic function and progression of skeletal muscle myopathy. Myokines are not only involved in the pathogenesis of skeletal muscle myopathy but also they could provide new insights to the course of HF and stratify patients at higher risk of poor outcomes prior to sarcopenic stage. Although changes in peripheral blood concentrations of several myokines reflect altered metabolic homeostasis in connection with advance in HF, there is limiting strong evidence regarding independent predictive ability of myokines' signature for mortality and HF-related outcomes and superiority these novel biomarkers to traditional circulating cardiac biomarkers during face-to-face comparisons. Irisin, BDNF, FGF-21, and probably osteonectin are the most promising biomarkers of HF-related myopathy and cachexia, while their role in the prediction of adverse cardiac remodeling and poor outcomes requires to be elucidated in the future.

Abbreviations

BDNF:	Brain-derived neurotrophic factor
CV:	Cardiovascular
ECM:	Extracellular matrix
EF:	Ejection fraction
FGF-21:	Fibroblast growth factor-21
GDF-11:	Growth/differential factor-11
HF:	Heart failure
HFpEF:	Heart failure with preserved ejection fraction
HOMA-IR:	Homeostasis model assessment of insulin resistance
HFrEF:	Heart failure with reduced ejection fraction
IGF:	Insulin-like growth factor
IL:	Interleukin
LV:	Left ventricle
MAPK:	Mitogen-activated protein kinase
NO:	Nitric oxide
NPs:	Natriuretic peptides
RAAS:	Renin-angiotensin-aldosterone system
TNF:	Tumor necrosis factor.

Data Availability

The manuscript is narrative review and dataset was not generated.

Conflicts of Interest

All authors declare that there are no conflicts of interest regarding the publication of this paper.

References

- [1] B. Ziaiean and G. C. Fonarow, "Epidemiology and aetiology of heart failure," *Nature Reviews Cardiology*, vol. 13, no. 6, pp. 368–378, 2016.
- [2] S. P. Chaudhry and G. C. Stewart, "Advanced heart failure: prevalence, natural history, and prognosis," *Heart Failure Clinics*, vol. 12, no. 3, pp. 323–333, 2016.
- [3] E. J. Benjamin, S. S. Virani, C. W. Callaway et al., "Heart Disease and Stroke Statistics-2018 update: a report from the American Heart Association," *Circulation*, vol. 137, no. 12, pp. e67–492, 2018.
- [4] E. E. S. van Riet, A. W. Hoes, K. P. Wagenaar, A. Limburg, M. A. J. Landman, and F. H. Rutten, "Epidemiology of heart failure: the prevalence of heart failure and ventricular dysfunction in older adults over time. A systematic review," *European Journal of Heart Failure*, vol. 18, no. 3, pp. 242–252, 2016.
- [5] H. E. Carter, D. Schofield, and R. Shrestha, "Productivity costs of cardiovascular disease mortality across disease types and socioeconomic groups," *Open Heart*, vol. 6, no. 1, article e000939, 2019.
- [6] S. M. Dunlay, V. L. Roger, and M. M. Redfield, "Epidemiology of heart failure with preserved ejection fraction," *Nature Reviews Cardiology*, vol. 14, no. 10, pp. 591–602, 2017.
- [7] M. Lehrke and N. Marx, "Diabetes mellitus and heart failure," *The American Journal of Cardiology*, vol. 120, no. 1, pp. S37–S47, 2017.
- [8] M. T. Maeder, M. Buser, R. Brenner, and H. Rickli, "Herzinsuffizienz mit erhaltener linksventrikulärer Auswurfraction (HFpEF) [Heart failure with preserved ejection fraction (HFpEF)]," *Therapeutische Umschau*, vol. 75, no. 3, pp. 161–169, 2018.
- [9] J. Yap, S. Y. Chia, F. Y. Lim et al., "The Singapore Heart Failure Risk Score: prediction of survival in Southeast Asian patients," *Annals Academy of Medicine Singapore*, vol. 48, no. 3, pp. 86–94, 2019.
- [10] W. J. Paulus and C. Tschöpe, "A novel paradigm for heart failure with preserved ejection fraction: comorbidities drive myocardial dysfunction and remodeling through coronary microvascular endothelial inflammation," *Journal of the American College of Cardiology*, vol. 62, no. 4, pp. 263–271, 2013.
- [11] J. Slivnick and B. C. Lampert, "Hypertension and heart failure," *Heart Failure Clinics*, vol. 15, no. 4, pp. 531–541, 2019.
- [12] B. A. Borlaug, "The pathophysiology of heart failure with preserved ejection fraction," *Nature Reviews Cardiology*, vol. 11, no. 9, pp. 507–515, 2014.
- [13] A. J. Kriegel, M. Gartz, M. Z. Afzal, W. J. de Lange, J. C. Ralphe, and J. L. Strande, "Molecular approaches in HFpEF: microRNAs and iPSC-derived cardiomyocytes," *Journal of Cardiovascular Translational Research*, vol. 10, no. 3, pp. 295–304, 2017.
- [14] Z. Ge, A. Li, J. McNamara, C. Dos Remedios, and S. Lal, "Pathogenesis and pathophysiology of heart failure with reduced ejection fraction: translation to human studies," *Heart Failure Reviews*, vol. 24, no. 5, pp. 743–758, 2019.
- [15] D. Jewiss, C. Ostman, and N. A. Smart, "The effect of resistance training on clinical outcomes in heart failure: a systematic review and meta-analysis," *International journal of cardiology*, vol. 221, pp. 674–681, 2016.
- [16] A. Philippou, D. Xanthis, C. Chryssanthopoulos, M. Maridaki, and M. Koutsilieris, "Heart failure-induced skeletal muscle wasting," *Current Heart Failure Reports*, vol. 17, no. 5, pp. 299–308, 2020.
- [17] F. Li, Y. Li, Y. Duan, C. A. Hu, Y. Tang, and Y. Yin, "Myokines and adipokines: involvement in the crosstalk between

- skeletal muscle and adipose tissue,” *Cytokine & Growth Factor Reviews*, vol. 33, pp. 73–82, 2017.
- [18] S. Takada, H. Sabe, and S. Kinugawa, “Abnormalities of skeletal muscle, adipocyte tissue, and lipid metabolism in heart failure: practical therapeutic targets,” *Frontiers in Cardiovascular Medicine*, vol. 7, p. 79, 2020.
- [19] A. Emami, M. Saitoh, M. Valentova et al., “Comparison of sarcopenia and cachexia in men with chronic heart failure: results from the Studies Investigating Co-morbidities Aggravating Heart Failure (SICA-HF),” *European Journal of Heart Failure*, vol. 20, no. 11, pp. 1580–1587, 2018.
- [20] T. Song, P. Manoharan, D. P. Millay et al., “Dilated cardiomyopathy-mediated heart failure induces a unique skeletal muscle myopathy with inflammation,” *Skelet Muscle*, vol. 9, no. 1, p. 4, 2019.
- [21] D. A. Brown, J. B. Perry, M. E. Allen et al., “Mitochondrial function as a therapeutic target in heart failure,” *Nature Reviews Cardiology*, vol. 14, no. 4, pp. 238–250, 2017.
- [22] W. J. Evans, “Skeletal muscle loss: cachexia, sarcopenia, and inactivity,” *The American Journal of Clinical Nutrition*, vol. 91, pp. 1123S–1127S, 2010.
- [23] C. Planella-Farrugia, F. Comas, M. Sabater-Masdeu et al., “Circulating irisin and myostatin as markers of muscle strength and physical condition in elderly subjects,” *Frontiers in Physiology*, vol. 10, p. 871, 2019.
- [24] H. S. Chung and K. M. Choi, “Adipokines and myokines: a pivotal role in metabolic and cardiovascular disorders,” *Current Medicinal Chemistry*, vol. 25, no. 20, pp. 2401–2415, 2018.
- [25] W. H. Jia, N. Q. Wang, L. Yin et al., “Effect of skeletal muscle phenotype and gender on fasting-induced myokine expression in mice,” *Biochemical and Biophysical Research Communications*, vol. 514, no. 2, pp. 407–414, 2019.
- [26] S. Kim, J. Y. Choi, S. Moon, D. H. Park, H. B. Kwak, and J. H. Kang, “Roles of myokines in exercise-induced improvement of neuropsychiatric function,” *Pflügers Archiv-European Journal of Physiology*, vol. 471, no. 3, pp. 491–505, 2019.
- [27] Y. Hathout, R. L. Marathi, S. Rayavarapu et al., “Discovery of serum protein biomarkers in the mdx mouse model and cross-species comparison to Duchenne muscular dystrophy patients,” *Human Molecular Genetics*, vol. 23, no. 24, pp. 6458–6469, 2014.
- [28] A. Aartsma-Rus and P. Spitali, “Circulating biomarkers for Duchenne muscular dystrophy,” *Journal of Neuromuscular Diseases*, vol. 2, no. s2, pp. S49–S58, 2015.
- [29] D. Di Raimondo, A. Tuttolomondo, G. Musiari, C. Schimmenti, A. D’Angelo, and A. Pinto, “Are the myokines the mediators of physical activity-induced health benefits?,” *Current Pharmaceutical Design*, vol. 22, no. 24, pp. 3622–3647, 2016.
- [30] K. J. Lavine and O. L. Sierra, “Skeletal muscle inflammation and atrophy in heart failure,” *Heart Failure Reviews*, vol. 22, no. 2, pp. 179–189, 2017.
- [31] S. Aydin, “Three new players in energy regulation: preptin, adropin and irisin,” *Peptides*, vol. 56, pp. 94–110, 2014.
- [32] A. E. Berezin, “Cardiac biomarkers in diabetes mellitus: new dawn for risk stratification?,” *Diabetes & Metabolic Syndrome: Clinical Research & Reviews*, vol. 11, Suppl 1, pp. S201–S208, 2017.
- [33] I. Nakano, S. Kinugawa, H. Hori et al., “Serum brain-derived neurotrophic factor levels are associated with skeletal muscle function but not with muscle mass in patients with heart failure,” *International Heart Journal*, vol. 61, no. 1, pp. 96–102, 2020.
- [34] D. C. Poole, D. M. Hirai, S. W. Copp, and T. I. Musch, “Muscle oxygen transport and utilization in heart failure: implications for exercise (in)tolerance,” *American Journal of Physiology. Heart and Circulatory Physiology*, vol. 302, no. 5, pp. H1050–H1063, 2012.
- [35] M. Paneroni, E. Pasini, L. Comini et al., “Skeletal muscle myopathy in heart failure: the role of ejection fraction,” *Current Cardiology Reports*, vol. 20, no. 11, p. 116, 2018.
- [36] L. P. Carvalho, R. P. Basso-Vanelli, L. di Thommazo-Luporini et al., “Myostatin and adipokines: the role of the metabolically unhealthy obese phenotype in muscle function and aerobic capacity in young adults,” *Cytokine*, vol. 107, pp. 118–124, 2018.
- [37] S. Fulster, M. Tacke, A. Sandek et al., “Muscle wasting in patients with chronic heart failure: results from the studies investigating co-morbidities aggravating heart failure (SICA-HF),” *European Heart Journal*, vol. 34, no. 7, pp. 512–519, 2013.
- [38] P. C. Brum, A. V. Bacurau, T. F. Cunha, L. R. Bechara, and J. B. Moreira, “Skeletal myopathy in heart failure: effects of aerobic exercise training,” *Experimental Physiology*, vol. 99, no. 4, pp. 616–620, 2014.
- [39] G. Tzanis, A. Philippou, E. Karatzanos et al., “Effects of high-intensity interval exercise training on skeletal myopathy of chronic heart failure,” *Journal of Cardiac Failure*, vol. 23, no. 1, pp. 36–46, 2017.
- [40] M. J. Joyner and D. P. Casey, “Regulation of increased blood flow (hyperemia) to muscles during exercise: a hierarchy of competing physiological needs,” *Physiological Reviews*, vol. 95, no. 2, pp. 549–601, 2015.
- [41] T. T. Vu, J. Marquez, L. T. Le, A. T. T. Nguyen, H. K. Kim, and J. Han, “The role of decorin in cardiovascular diseases: more than just a decoration,” *Free Radical Research*, vol. 52, no. 11–12, pp. 1210–1219, 2018.
- [42] A. Shibata, A. Hanatani, Y. Izumi, R. Kitada, S. Iwata, and M. Yoshiyama, “Serum brain-derived neurotrophic factor level and exercise tolerance complement each other in predicting the prognosis of patients with heart failure,” *Heart Vessels*, vol. 33, no. 11, pp. 1325–1333, 2018.
- [43] J. D. Roh, R. Hobson, V. Chaudhari et al., “Activin type II receptor signaling in cardiac aging and heart failure,” *Science Translational Medicine*, vol. 11, no. 482, article eaau8680, 2019.
- [44] V. S. Mujumdar, L. M. Smiley, and S. C. Tyagi, “Activation of matrix metalloproteinase dilates and decreases cardiac tensile strength,” *International Journal of Cardiology*, vol. 79, no. 2–3, pp. 277–286, 2001.
- [45] V. S. Mujumdar and S. C. Tyagi, “Temporal regulation of extracellular matrix components in transition from compensatory hypertrophy to decompensatory heart failure,” *Journal of Hypertension*, vol. 17, no. 2, pp. 261–270, 1999.
- [46] C. O. Heras-Bautista, N. Mikhael, J. Lam et al., “Cardiomyocytes facing fibrotic conditions re-express extracellular matrix transcripts,” *Acta Biomaterialia*, vol. 89, pp. 180–192, 2019.
- [47] J. J. Hwang, P. D. Allen, G. C. Tseng et al., “Microarray gene expression profiles in dilated and hypertrophic cardiomyopathic end-stage heart failure,” *Physiological Genomics*, vol. 10, no. 1, pp. 31–44, 2002.

- [48] J. Jahanyar, D. L. Joyce, R. E. Southard et al., “Decorin-mediated Transforming Growth Factor- β Inhibition Ameliorates Adverse Cardiac Remodeling,” *The Journal of Heart and Lung Transplantation*, vol. 26, no. 1, pp. 34–40, 2007.
- [49] Y. Y. Li, C. F. McTiernan, and A. M. Feldman, “Interplay of matrix metalloproteinases, tissue inhibitors of metalloproteinases and their regulators in cardiac matrix remodeling,” *Cardiovascular Research*, vol. 46, no. 2, pp. 214–224, 2000.
- [50] G. Colaianni, S. Cinti, S. Colucci, and M. Grano, “Irisin and musculoskeletal health,” *Annals of the New York Academy of Sciences*, vol. 1402, no. 1, pp. 5–9, 2017.
- [51] S. A. Polyzos, A. D. Anastasilakis, Z. A. Efstathiadou et al., “Irisin in metabolic diseases,” *Endocrine*, vol. 59, no. 2, pp. 260–274, 2018.
- [52] N. Perakakis, G. A. Triantafyllou, J. M. Fernández-Real et al., “Physiology and role of irisin in glucose homeostasis,” *Nature Reviews Endocrinology*, vol. 13, no. 6, pp. 324–337, 2017.
- [53] M. O. Mahgoub, C. D’Souza, R. S. M. H. Al Darmaki, M. M. Y. H. Baniyas, and E. Adegate, “An update on the role of irisin in the regulation of endocrine and metabolic functions,” *Peptides*, vol. 104, pp. 15–23, 2018.
- [54] H. Wang, Y. T. Zhao, S. Zhang et al., “Irisin plays a pivotal role to protect the heart against ischemia and reperfusion injury,” *Journal of Cellular Physiology*, vol. 232, no. 12, pp. 3775–3785, 2017.
- [55] Y. Zhang, H. Song, Y. Zhang et al., “Irisin inhibits atherosclerosis by promoting endothelial proliferation through micro-RNA126-5p,” *Journal of the American Heart Association*, vol. 5, no. 9, 2016.
- [56] R. Li, X. Wang, S. Wu et al., “Irisin ameliorates angiotensin II-induced cardiomyocyte apoptosis through autophagy,” *Journal of Cellular Physiology*, vol. 234, no. 10, pp. 17578–17588, 2019.
- [57] S. I. Briganti, G. Gaspa, G. Tabacco et al., “Irisin as a regulator of bone and glucose metabolism,” *Minerva Endocrinologica*, vol. 43, no. 4, pp. 489–500, 2018.
- [58] H. Kim, C. D. Wrann, M. Jedrychowski et al., “Irisin mediates effects on bone and fat via α V integrin receptors,” *Cell*, vol. 175, no. 7, pp. 1756–1768.e17, 2018.
- [59] O. Y. Kim and J. Song, “The role of irisin in Alzheimer’s disease,” *Journal of Clinical Medicine*, vol. 7, no. 11, p. 407, 2018.
- [60] B. Grygiel-Górniak and M. Puszczewicz, “A review on irisin, a new protagonist that mediates muscle-adipose-bone-neuron connectivity,” *European Review for Medical and Pharmacological Sciences*, vol. 21, no. 20, pp. 4687–4693, 2017.
- [61] K. Hee Park, L. Zaichenko, M. Brinkoetter et al., “Circulating irisin in relation to insulin resistance and the metabolic syndrome,” *The Journal of Clinical Endocrinology and Metabolism*, vol. 98, no. 12, pp. 4899–4907, 2013.
- [62] G. Y. Saber, V. Kasabri, M. I. Saleh et al., “Increased irisin versus reduced fibroblast growth factor1 (FGF1) in relation to adiposity, atherogenicity and hematological indices in metabolic syndrome patients with and without prediabetes,” *Hormone Molecular Biology and Clinical Investigation*, vol. 38, no. 1, 2019.
- [63] A. D. Anastasilakis, D. Koulaxis, N. Kefala et al., “Circulating irisin levels are lower in patients with either stable coronary artery disease (CAD) or myocardial infarction (MI) versus healthy controls, whereas follistatin and activin A levels are higher and can discriminate MI from CAD with similar to CK-MB accuracy,” *Metabolism*, vol. 73, pp. 1–8, 2017.
- [64] N. A. Abd El-Mottaleb, H. M. Galal, K. M. El Maghraby, and A. I. Gadallah, “Serum irisin level in myocardial infarction patients with or without heart failure,” *Canadian Journal of Physiology and Pharmacology*, vol. 97, no. 10, pp. 932–938, 2019.
- [65] K. N. Aronis, M. Moreno, S. A. Polyzos et al., “Circulating irisin levels and coronary heart disease: association with future acute coronary syndrome and major adverse cardiovascular events,” *International Journal of Obesity*, vol. 39, no. 1, pp. 156–161, 2015.
- [66] T. H. Efe, B. Açar, A. G. Ertem et al., “Serum irisin level can predict the severity of coronary artery disease in patients with stable angina,” *Korean Circulation Journal*, vol. 47, no. 1, pp. 44–49, 2017.
- [67] W. Deng, “Association of serum irisin concentrations with presence and severity of coronary artery disease,” *Medical Science Monitor*, vol. 22, pp. 4193–4197, 2016.
- [68] A. Silvestrini, C. Bruno, E. Vergani et al., “Circulating irisin levels in heart failure with preserved or reduced ejection fraction: a pilot study,” *PLoS One*, vol. 14, no. 1, article e0210320, 2019.
- [69] A. K. Kalkan, H. A. Cakmak, M. Erturk et al., “Adropin and irisin in patients with cardiac cachexia,” *Arquivos Brasileiros de Cardiologia*, vol. 111, no. 1, pp. 39–47, 2018.
- [70] G. Sobieszek, T. Powrózek, M. Mazurek, A. Skwarek-Dziękowska, and T. Małecka-Massalska, “Electrical and hormonal biomarkers in cachectic elderly women with chronic heart failure,” *Journal of Clinical Medicine*, vol. 9, no. 4, p. 1021, 2020.
- [71] S. H. Lecker, A. Zavin, P. Cao et al., “Expression of the irisin precursor FNDC5 in skeletal muscle correlates with aerobic exercise performance in patients with heart failure,” *Circulation: Heart Failure*, vol. 5, no. 6, pp. 812–818, 2012.
- [72] M. M. Seldin, J. M. Peterson, M. S. Byerly, Z. Wei, and G. W. Wong, “Myonectin (CTRP15), a novel myokine that links skeletal muscle to systemic lipid homeostasis,” *Journal of Biological Chemistry*, vol. 287, no. 15, pp. 11968–11980, 2012.
- [73] K. Li, X. Liao, K. Wang et al., “Myonectin predicts the development of type 2 diabetes,” *The Journal of Clinical Endocrinology & Metabolism*, vol. 103, no. 1, pp. 139–147, 2018.
- [74] H. C. Little, S. Rodriguez, X. Lei et al., “Myonectin deletion promotes adipose fat storage and reduces liver steatosis,” *The FASEB Journal*, vol. 33, no. 7, pp. 8666–8687, 2019.
- [75] N. Otaka, R. Shibata, K. Ohashi et al., “Myonectin is an exercise-induced myokine that protects the heart from ischemia-reperfusion injury,” *Circulation Research*, vol. 123, no. 12, pp. 1326–1338, 2018.
- [76] I. Rabinovich-Nikitin and L. A. Kirshenbaum, “Exercise-induced myonectin protects against ischemia-reperfusion injury,” *Circulation Research*, vol. 123, no. 12, pp. 1264–1266, 2018.
- [77] D. K. Das, Z. A. Graham, and C. P. Cardozo, “Myokines in skeletal muscle physiology and metabolism: recent advances and future perspectives,” *Acta Physiologica*, vol. 228, no. 2, article e13367, 2020.
- [78] F. M. Fisher and E. Maratos-Flier, “Understanding the physiology of FGF21,” *Annual Review of Physiology*, vol. 78, no. 1, pp. 223–241, 2016.
- [79] J. E. Lewis, F. J. P. Ebling, R. J. Samms, and K. Tsintzas, “Going back to the biology of FGF21: new insights,” *Trends in Endocrinology & Metabolism*, vol. 30, no. 8, pp. 491–504, 2019.

- [80] A. Salminen, K. Kaarniranta, and A. Kauppinen, "Regulation of longevity by FGF21: interaction between energy metabolism and stress responses," *Ageing Research Reviews*, vol. 37, pp. 79–93, 2017.
- [81] M. Z. Strowski, "Impact of FGF21 on glycemic control," *Hormone Molecular Biology and Clinical Investigation*, vol. 30, no. 2, 2017.
- [82] T. Olsen, B. Øvrebø, N. Haj-Yasein et al., "Effects of dietary methionine and cysteine restriction on plasma biomarkers, serum fibroblast growth factor 21, and adipose tissue gene expression in women with overweight or obesity: a double-blind randomized controlled pilot study," *Journal of Translational Medicine*, vol. 18, no. 1, p. 122, 2020.
- [83] T. Turner, X. Chen, M. Zahner et al., "FGF21 increases water intake, urine output and blood pressure in rats," *PLoS One*, vol. 13, no. 8, article e0202182, 2018.
- [84] M. Á. Gómez-Sámamo, M. Grajales-Gómez, J. M. Zuarth-Vázquez et al., "Fibroblast growth factor 21 and its novel association with oxidative stress," *Redox Biology*, vol. 11, pp. 335–341, 2017.
- [85] A. Planavila, I. Redondo-Angulo, F. Ribas et al., "Fibroblast growth factor 21 protects the heart from oxidative stress," *Cardiovascular Research*, vol. 106, no. 1, pp. 19–31, 2015.
- [86] F. Di Lisa and N. Itoh, "Cardiac Fgf21 synthesis and release: an autocrine loop for boosting up antioxidant defenses in failing hearts," *Cardiovascular Research*, vol. 106, no. 1, pp. 1–3, 2015.
- [87] N. Itoh and H. Ohta, "Pathophysiological roles of FGF signaling in the heart," *Frontiers in Physiology*, vol. 4, 2013.
- [88] A. E. Berezin and A. A. Berezin, "Impaired function of fibroblast growth factor 23 / Klotho protein axis in prediabetes and diabetes mellitus: Promising predictor of cardiovascular risk," *Diabetes & Metabolic Syndrome: Clinical Research & Reviews*, vol. 13, no. 4, pp. 2549–2556, 2019.
- [89] A. Mancini, E. Vergani, C. Bruno et al., "Oxidative stress as a possible mechanism underlying multi-hormonal deficiency in chronic heart failure," *European Review for Medical and Pharmacological Sciences*, vol. 22, no. 12, pp. 3936–3961, 2018.
- [90] M. Haberka, G. Machnik, A. Kowalówka et al., "Epicardial, paracardial and perivascular fat quantity, genes expression and serum cytokines in coronary artery disease and diabetes," *Polish Archives of Internal Medicine*, vol. 129, no. 11, pp. 738–746, 2019.
- [91] R. H. Chou, P. H. Huang, C. Y. Hsu et al., "Circulating fibroblast growth factor 21 is associated with diastolic dysfunction in heart failure patients with preserved ejection fraction," *Scientific Reports*, vol. 6, no. 1, 2016.
- [92] M. Refsgaard Holm, H. Christensen, J. Rasmussen et al., "Fibroblast growth factor 21 in patients with cardiac cachexia: a possible role of chronic inflammation," *ESC Heart Failure*, vol. 6, no. 5, pp. 983–991, 2019.
- [93] A. Planavila, J. Fernández-Solà, and F. Villarroya, "Cardiokines as modulators of stress-induced cardiac disorders," *Advances in Protein Chemistry and Structural Biology*, vol. 108, pp. 227–256, 2017.
- [94] M. Packer, "Cardioprotective effects of sirtuin-1 and its downstream Effectors," *Circulation: Heart Failure*, vol. 13, no. 9, 2020.
- [95] T. Saito, T. Uchiumi, M. Yagi et al., "Cardiomyocyte-specific loss of mitochondrial p32/C1qbp causes cardiomyopathy and activates stress responses," *Cardiovascular Research*, vol. 113, no. 10, pp. 1173–1185, 2017.
- [96] J. Ishida, M. Konishi, M. Saitoh, M. Anker, S. D. Anker, and J. Springer, "Myostatin signaling is up-regulated in female patients with advanced heart failure," *International Journal of Cardiology*, vol. 238, pp. 37–42, 2017.
- [97] R. L. Damatto, A. R. Lima, P. F. Martinez, M. D. Cezar, K. Okoshi, and M. P. Okoshi, "Myocardial myostatin in spontaneously hypertensive rats with heart failure," *International Journal of Cardiology*, vol. 215, pp. 384–387, 2016.
- [98] A. Breitbart, M. Auger-Messier, J. D. Molkentin, and J. Heineke, "Myostatin from the heart: local and systemic actions in cardiac failure and muscle wasting," *American Journal of Physiology-Heart and Circulatory Physiology*, vol. 300, no. 6, pp. H1973–H1982, 2011.
- [99] S. Schiaffino, K. A. Dyar, S. Ciciliot, B. Blaauw, and M. Sandri, "Mechanisms regulating skeletal muscle growth and atrophy," *FEBS Journal*, vol. 280, no. 17, pp. 4294–4314, 2013.
- [100] P. Bonaldo and M. Sandri, "Cellular and molecular mechanisms of muscle atrophy," *Disease Models & Mechanisms*, vol. 6, no. 1, pp. 25–39, 2013.
- [101] J. Springer, J. I. Springer, and S. D. Anker, "Muscle wasting and sarcopenia in heart failure and beyond: update 2017," *ESC Heart Failure*, vol. 4, no. 4, pp. 492–498, 2017.
- [102] N. Biesemann, L. Mendler, S. Kostin, A. Wietelmann, T. Borchardt, and T. Braun, "Myostatin induces interstitial fibrosis in the heart via TAK1 and p38," *Cell and Tissue Research*, vol. 361, no. 3, pp. 779–787, 2015.
- [103] R. L. Damatto, P. F. Martinez, A. R. Lima et al., "Heart failure-induced skeletal myopathy in spontaneously hypertensive rats," *International Journal of Cardiology*, vol. 167, no. 3, pp. 698–703, 2013.
- [104] T. Suzuki, S. Palus, and J. Springer, "Skeletal muscle wasting in chronic heart failure," *ESC Heart Failure*, vol. 5, no. 6, pp. 1099–1107, 2018.
- [105] J. A. Baán, Z. V. Varga, P. Leszek et al., "Myostatin and IGF-I signaling in end-stage human heart failure: a qRT-PCR study," *Journal of Translational Medicine*, vol. 13, no. 1, p. 1, 2015.
- [106] E. Castillero, H. Akashi, M. Najjar et al., "Activin type II receptor ligand signaling inhibition after experimental ischemic heart failure attenuates cardiac remodeling and prevents fibrosis," *American Journal of Physiology-Heart and Circulatory Physiology*, vol. 318, no. 2, pp. H378–H390, 2020.
- [107] P. Chen, Z. Liu, Y. Luo et al., "Predictive value of serum myostatin for the severity and clinical outcome of heart failure," *European Journal of Internal Medicine*, vol. 64, pp. 33–40, 2019.
- [108] D. Gruson, S. A. Ahn, J. M. Ketelslegers, and M. F. Rousseau, "Increased plasma myostatin in heart failure," *European Journal of Heart Failure*, vol. 13, no. 7, pp. 734–736, 2011.
- [109] I. George, L. T. Bish, G. Kamalakkannan et al., "Myostatin activation in patients with advanced heart failure and after mechanical unloading," *European Journal of Heart Failure*, vol. 12, no. 5, pp. 444–453, 2010.
- [110] S. Goletti and D. Gruson, "Personalized risk assessment of heart failure patients: more perspectives from transforming growth factor super-family members," *Clinica Chimica Acta*, vol. 443, pp. 94–99, 2015.
- [111] E. Zamora, R. Simó, J. Lupón et al., "Niveles sericos de miosatina en insuficiencia cardiaca cronica," *Revista Española de Cardiología (English Edition)*, vol. 63, no. 8, pp. 992–996, 2010.

- [112] D. K. Binder and H. E. Scharfman, "Brain-derived neurotrophic factor," *Growth Factors*, vol. 22, no. 3, pp. 123–131, 2009.
- [113] A. Sonal and V. Raghavan, "Brain derived neurotrophic factor (BDNF) and suicidal behavior: a review of studies from Asian countries," *Asian Journal of Psychiatry*, vol. 33, pp. 128–132, 2018.
- [114] M. Fukumoto, T. Takeuchi, E. Koubayashi et al., "Induction of brain-derived neurotrophic factor in enteric glial cells stimulated by interleukin-1 β via a c-Jun N-terminal kinase pathway," *Journal of Clinical Biochemistry and Nutrition*, vol. 66, no. 2, pp. 103–109, 2020.
- [115] İ. Abidin, S. Aydin-Abidin, A. Bodur, İ. Ince, and A. Alver, "Brain-derived neurotrophic factor (BDNF) heterozygous mice are more susceptible to synaptic protein loss in cerebral cortex during high fat diet," *Archives of Physiology and Biochemistry*, vol. 124, no. 5, pp. 442–447, 2018.
- [116] B. R. McKay, J. P. Nederveen, S. A. Fortino et al., "Brain-derived neurotrophic factor is associated with human muscle satellite cell differentiation in response to muscle-damaging exercise," *Applied Physiology, Nutrition, and Metabolism*, vol. 45, no. 6, pp. 581–590, 2020.
- [117] C. Figueiredo, B. M. Antunes, T. R. Giaccon et al., "Influence of acute and chronic high-intensity intermittent aerobic plus strength exercise on BDNF, lipid and autonomic parameters," *Journal of Sports Science & Medicine*, vol. 18, no. 2, pp. 359–368, 2019.
- [118] H. Jamshed, R. A. Beyl, D. L. Della Manna, E. S. Yang, E. Ravussin, and C. M. Peterson, "Early time-restricted feeding improves 24-hour glucose levels and affects markers of the circadian clock, aging, and autophagy in humans," *Nutrients*, vol. 11, no. 6, p. 1234, 2019.
- [119] C. M. de Araujo, A. Zugman, W. Swardfager et al., "Effects of the brain-derived neurotrophic factor variant *Val66Met* on cortical structure in late childhood and early adolescence," *Journal of Psychiatric Research*, vol. 98, pp. 51–58, 2018.
- [120] P. G. Nestor, H. E. Lapp, S. B. Boodai, K. O'Donovan, V. C. Hasler, and R. Hunter, "The role of brain-derived neurotrophic factor and serotonin polymorphisms in stress-related personality and psychiatric symptoms: implications for cardiovascular health," *Heart and Mind*, vol. 4, pp. 85–91, 2020.
- [121] O. V. Petyunina, M. P. Kopytsya, A. E. Berezin, and O. V. Skrynnyk, "The role of *Val66Met* single nucleotide polymorphism in brain-derived neurotrophic factor gene in prediction of adverse outcomes after ST-segment elevation myocardial infarction," *Heart and Mind*, vol. 3, no. 1, pp. 7–14, 2019.
- [122] J. D. Martínez-Ezquerro, M. E. Rendón-Macías, G. Zamora-Mendoza et al., "Association between the brain-derived neurotrophic factor *Val66Met* polymorphism and overweight/obesity in pediatric population," *Archives of Medical Research*, vol. 48, no. 7, pp. 599–608, 2017.
- [123] K. S. Krabbe, A. R. Nielsen, R. Krogh-Madsen et al., "Brain-derived neurotrophic factor (BDNF) and type 2 diabetes," *Diabetologia*, vol. 50, no. 2, pp. 431–438, 2007.
- [124] A. Fukushima, S. Kinugawa, T. Homma et al., "Serum brain-derived neurotrophic factor level predicts adverse clinical outcomes in patients with heart failure," *Journal of Cardiac Failure*, vol. 21, no. 4, pp. 300–306, 2015.
- [125] H. A. Barman, I. Şahin, A. Atıcı et al., "Prognostic significance of brain-derived neurotrophic factor levels in patients with heart failure and reduced left ventricular ejection fraction," *Anatolian Journal of Cardiology*, vol. 22, no. 6, pp. 309–316, 2019.
- [126] H. Wu, G. Cao, Y. Wang, H. Tian, and R. Du, "Increased serum CA125 and brain-derived neurotrophic factor (BDNF) levels on acute myocardial infarction: a predictor for acute heart failure," *Medical Science Monitor: International Medical Journal of Experimental and Clinical Research*, vol. 25, pp. 913–919, 2019.
- [127] L. Manni, V. Nikolova, D. Vyagova, G. N. Chaldakov, and L. Aloe, "Reduced plasma levels of NGF and BDNF in patients with acute coronary syndromes," *International Journal of Cardiology*, vol. 102, no. 1, pp. 169–171, 2005.
- [128] J. Matsumoto, S. Takada, S. Kinugawa et al., "Brain-derived neurotrophic factor improves limited exercise capacity in mice with heart failure," *Circulation*, vol. 138, no. 18, pp. 2064–2066, 2018.
- [129] H. W. Lee, M. Ahmad, H. W. Wang, and F. H. Leenen, "Effects of exercise training on brain-derived neurotrophic factor in skeletal muscle and heart of rats post myocardial infarction," *Experimental Physiology*, vol. 102, no. 3, pp. 314–328, 2017.
- [130] S. Takashio, S. Sugiyama, M. Yamamuro et al., "Significance of low plasma levels of brain-derived neurotrophic factor in patients with heart failure," *The American Journal of Cardiology*, vol. 116, no. 2, pp. 243–249, 2015.
- [131] H. S. Costa, M. M. O. Lima, P. H. S. Figueiredo et al., "Prognostic value of serum brain-derived neurotrophic factor levels in patients with Chagas cardiomyopathy," *Memórias do Instituto Oswaldo Cruz*, vol. 113, no. 10, Article e180224, 2018.
- [132] H. Suzuki, Y. Matsumoto, H. Ota et al., "Reduced brain-derived neurotrophic factor is associated with cognitive dysfunction in patients with chronic heart failure," *Geriatrics & Gerontology International*, vol. 17, no. 5, pp. 852–854, 2017.
- [133] S. Kadowaki, T. Shishido, Y. Honda et al., "Additive clinical value of serum brain-derived neurotrophic factor for prediction of chronic heart failure outcome," *Heart and Vessels*, vol. 31, no. 4, pp. 535–544, 2016.
- [134] M. Šagud, N. Jakšić, B. Vuksan-Čusa et al., "Cardiovascular disease risk factors in patients with posttraumatic stress disorder (PTSD): a narrative review," *Psychiatria Danubina*, vol. 29, no. 4, pp. 421–430, 2017.
- [135] S. Apostolakis, K. Vogiatzi, V. Amanatidou, and D. A. Spanhidis, "Interleukin 8 and cardiovascular disease," *Cardiovascular Research*, vol. 84, no. 3, pp. 353–360, 2009.
- [136] A. Rot, E. Hub, J. Middleton et al., "Some aspects of IL-8 pathophysiology. III: chemokine interaction with endothelial cells," *Journal of Leukocyte Biology*, vol. 59, no. 1, pp. 39–44, 1996.
- [137] L. Yang, J. Herrera, A. Gilbertsen et al., "IL-8 mediates idiopathic pulmonary fibrosis mesenchymal progenitor cell fibrogenicity," *American Journal of Physiology-Lung Cellular and Molecular Physiology*, vol. 314, no. 1, pp. L127–L136, 2018.
- [138] T. Sasaki, Y. Suzuki, K. Kakisaka et al., "IL-8 induces transdifferentiation of mature hepatocytes toward the cholangiocyte phenotype," *FEBS Open Bio*, vol. 9, no. 12, pp. 2105–2116, 2019.
- [139] A. R. Nielsen and B. K. Pedersen, "The biological roles of exercise-induced cytokines: IL-6, IL-8, and IL-15," *Applied Physiology, Nutrition, and Metabolism*, vol. 32, no. 5, pp. 833–839, 2007.

- [140] P. Aukrust, B. Halvorsen, A. Yndestad et al., "Chemokines and cardiovascular risk," *Arteriosclerosis, Thrombosis, and Vascular Biology*, vol. 28, no. 11, pp. 1909–1919, 2008.
- [141] T. Ueland, L. Gullestad, S. H. Nymo, A. Yndestad, P. Aukrust, and E. T. Askevold, "Inflammatory cytokines as biomarkers in heart failure," *Clinica Chimica Acta*, vol. 443, pp. 71–77, 2015.
- [142] R. J. Zhang, X. D. Li, S. W. Zhang, X. H. Li, and L. Wu, "IL-8-251A/T polymorphism contributes to coronary artery disease susceptibility in a Chinese population," *Genetics and Molecular Research*, vol. 16, no. 1, 2017.
- [143] C. Shetelig, S. Limalanathan, P. Hoffmann et al., "Association of IL-8 with infarct size and clinical outcomes in patients with STEMI," *Journal of the American College of Cardiology*, vol. 72, no. 2, pp. 187–198, 2018.
- [144] O. A. Segiet, A. Piecuch, L. Mielanczyk, M. Michalski, and E. Nowalany-Kozielska, "Role of interleukins in heart failure with reduced ejection fraction," *The Anatolian Journal of Cardiology*, vol. 22, no. 6, pp. 287–299, 2019.
- [145] M. Bartekova, J. Radosinska, M. Jelemsky, and N. S. Dhalla, "Role of cytokines and inflammation in heart function during health and disease," *Heart Failure Reviews*, vol. 23, no. 5, pp. 733–758, 2018.
- [146] C. Moro, M.-G. Jouan, A. Rakotovoao et al., "Delayed expression of cytokines after reperfused myocardial infarction: possible trigger for cardiac dysfunction and ventricular remodeling," *American Journal of Physiology-Heart and Circulatory Physiology*, vol. 293, no. 5, pp. H3014–H3019, 2007.
- [147] P. Ferdinandy, R. Schulz, and G. F. Baxter, "Interaction of cardiovascular risk factors with myocardial ischemia/reperfusion injury, preconditioning, and postconditioning," *Pharmacological Reviews*, vol. 59, no. 4, pp. 418–458, 2007.
- [148] M. H. T. Hartman, H. E. Groot, I. M. Leach, J. C. Karper, and P. van der Harst, "Translational overview of cytokine inhibition in acute myocardial infarction and chronic heart failure," *Trends in Cardiovascular Medicine*, vol. 28, no. 6, pp. 369–379, 2018.
- [149] Y. Yeghiazarians, N. Honbo, I. Imhof et al., "IL-15: a novel prosurvival signaling pathway in cardiomyocytes," *Journal of Cardiovascular Pharmacology*, vol. 63, no. 5, pp. 406–411, 2014.
- [150] O. M. Anton, M. E. Peterson, M. J. Hollander et al., "Trans-endocytosis of intact IL-15R α -IL-15 complex from presenting cells into NK cells favors signaling for proliferation," *Proceedings of the National Academy of Sciences*, vol. 117, no. 1, pp. 522–531, 2020.
- [151] P. Allavena, G. Giardino, G. Bianchi, and A. Mantovani, "IL-15 is chemotactic for natural killer cells and stimulates their adhesion to vascular endothelium," *Journal of Leukocyte Biology*, vol. 61, no. 6, pp. 729–735, 1997.
- [152] V. Budagian, E. Bulanova, R. Paus, and S. Bulfone-Paus, "IL-15/IL-15 receptor biology: a guided tour through an expanding universe," *Cytokine & Growth Factor Reviews*, vol. 17, no. 4, pp. 259–280, 2006.
- [153] E. M. Bugera, T. A. Duhamel, J. D. Peeler, and S. M. Cornish, "The systemic myokine response of decorin, interleukin-6 (IL-6) and interleukin-15 (IL-15) to an acute bout of blood flow restricted exercise," *European Journal of Applied Physiology*, vol. 118, no. 12, pp. 2679–2686, 2018.
- [154] L. Guo, M. F. Liu, J. N. Huang, J. M. Li, J. Jiang, and J. A. Wang, "Role of interleukin-15 in cardiovascular diseases," *Journal of Cellular and Molecular Medicine*, vol. 24, no. 13, pp. 7094–7101, 2020.
- [155] M. Cercek, M. Matsumoto, H. Li et al., "Autocrine role of vascular IL-15 in intimal thickening," *Biochemical and Biophysical Research Communications*, vol. 339, no. 2, pp. 618–623, 2006.
- [156] P. P. Manna, S. K. Hira, A. A. Das, S. Bandyopadhyay, and K. K. Gupta, "IL-15 activated human peripheral blood dendritic cell kill allogeneic and xenogeneic endothelial cells via apoptosis," *Cytokine*, vol. 61, no. 1, pp. 118–126, 2013.
- [157] S. G. Fonseca, M. M. Reis, V. Coelho et al., "Locally produced survival cytokines IL-15 and IL-7 may be associated to the predominance of CD8+ T cells at heart lesions of human chronic Chagas disease cardiomyopathy," *Scandinavian Journal of Immunology*, vol. 66, no. 2-3, pp. 362–371, 2007.
- [158] B. K. Pedersen, "The disease of physical inactivity—and the role of myokines in muscle–fat cross talk," *The Journal of Physiology*, vol. 587, no. 23, pp. 5559–5568, 2009.
- [159] E. Dozio, A. E. Malavazos, E. Vianello et al., "Interleukin-15 and soluble interleukin-15 receptor α in coronary artery disease patients: association with epicardial fat and indices of adipose tissue distribution," *PLoS One*, vol. 9, no. 3, article e90960, 2014.
- [160] B. Pajak, S. Orzechowska, B. Pijet et al., "Crossroads of cytokine signaling—the chase to stop muscle cachexia," *Journal of Physiology and Pharmacology*, vol. 59, Supplement 9, pp. 251–264, 2008.
- [161] A. Yalcin, K. Silay, A. R. Balik, G. Avcioglu, and A. S. Aydin, "The relationship between plasma interleukin-15 levels and sarcopenia in outpatient older people," *Aging Clinical and Experimental Research*, vol. 30, no. 7, pp. 783–790, 2018.
- [162] K. Sakuma and A. Yamaguchi, "Sarcopenic obesity and endocrinal adaptation with age," *International Journal of Endocrinology*, vol. 2013, Article ID 204164, 12 pages, 2013.
- [163] J. Angeles-Martínez, R. Posadas-Sánchez, N. Pérez-Hernández et al., "IL-15 polymorphisms are associated with sub-clinical atherosclerosis and cardiovascular risk factors. The Genetics of Atherosclerosis Disease (GEA) Mexican Study," *Cytokine*, vol. 99, pp. 173–178, 2017.
- [164] G. Novo, C. Bellia, M. Fiore et al., "A risk score derived from the analysis of a cluster of 27 serum inflammatory cytokines to predict long term outcome in patients with acute myocardial infarction: a pilot study," *Annals of Clinical & Laboratory Science*, vol. 45, no. 4, pp. 382–390, 2015.
- [165] C. Pomara, M. Neri, S. Bello, A. Pennella, E. Turillazzi, and V. Fineschi, "C3a, TNF- α and interleukin myocardial expression in a case of fatal sudden cardiac failure during clinic reactivation of systemic lupus erythematosus," *Lupus*, vol. 19, no. 10, pp. 1246–1249, 2010.
- [166] T. Ruck, S. Bittner, A. M. Afzali et al., "The NKG2D-IL-15 signaling pathway contributes to T-cell mediated pathology in inflammatory myopathies," *Oncotarget*, vol. 6, no. 41, pp. 43230–43243, 2015.
- [167] T. Sente, A. M. Van Berendoncks, A. I. Jonckheere et al., "Primary skeletal muscle myoblasts from chronic heart failure patients exhibit loss of anti-inflammatory and proliferative activity," *BMC Cardiovascular Disorders*, vol. 16, p. 107, 2016.
- [168] P. R. Kemp, R. Paul, A. C. Hinken, D. Neil, A. Russell, and M. J. Griffiths, "Metabolic profiling shows pre-existing mitochondrial dysfunction contributes to muscle loss in a model of ICU-acquired weakness," *Journal of Cachexia, Sarcopenia and Muscle*, vol. 11, no. 5, pp. 1321–1335, 2020.
- [169] M. A. Egerman, S. M. Cadena, J. A. Gilbert et al., "GDF11 increases with age and inhibits skeletal muscle regeneration," *Cell Metabolism*, vol. 22, no. 1, pp. 164–174, 2015.

- [170] H. H. Su, J. M. Liao, Y. H. Wang et al., "Exogenous GDF11 attenuates non-canonical TGF- β signaling to protect the heart from acute myocardial ischemia-reperfusion injury," *Basic Research in Cardiology*, vol. 114, no. 3, p. 20, 2019.
- [171] F. S. Loffredo, M. L. Steinhilber, S. M. Jay et al., "Growth Differentiation Factor 11 Is a Circulating Factor that Reverses Age-Related Cardiac Hypertrophy," *Cell*, vol. 153, no. 4, pp. 828–839, 2013.
- [172] G. Q. du, Z. B. Shao, J. Wu et al., "Targeted myocardial delivery of GDF11 gene rejuvenates the aged mouse heart and enhances myocardial regeneration after ischemia-reperfusion injury," *Basic Research in Cardiology*, vol. 112, no. 1, p. 7, 2017.
- [173] X. J. Zhang, H. Tan, Z. F. Shi, N. Li, Y. Jia, and Z. Hao, "Growth differentiation factor 11 is involved in isoproterenol-induced heart failure," *Molecular Medicine Reports*, vol. 19, no. 5, pp. 4109–4118, 2019.
- [174] T. B. Opstad, A. A. Kalstad, A. Å. Pettersen, H. Arnesen, and I. Seljeflot, "Novel biomolecules of ageing, sex differences and potential underlying mechanisms of telomere shortening in coronary artery disease," *Experimental Gerontology*, vol. 119, pp. 53–60, 2019.
- [175] H. Lim and Y. Z. Zhu, "Role of transforming growth factor- β in the progression of heart failure," *Cellular and Molecular Life Sciences*, vol. 63, no. 22, pp. 2584–2596, 2006.
- [176] L. M. Leitner, R. J. Wilson, Z. Yan, and A. Gödecke, "Reactive oxygen species/nitric oxide mediated inter-organ communication in skeletal muscle wasting diseases," *Antioxidants & Redox Signaling*, vol. 26, no. 13, pp. 700–717, 2017.
- [177] P. D. Lopez, P. Nepal, A. Akinlonu et al., "Low skeletal muscle mass independently predicts mortality in patients with chronic heart failure after an acute hospitalization," *Cardiology*, vol. 142, no. 1, pp. 28–36, 2019.
- [178] K. A. Olson, A. L. Beatty, B. Heidecker et al., "Association of growth differentiation factor 11/8, putative anti-ageing factor, with cardiovascular outcomes and overall mortality in humans: analysis of the Heart and Soul and HUNT3 cohorts," *European Heart Journal*, vol. 36, no. 48, pp. 3426–3434, 2015.
- [179] L. E. de Castro Brás, H. Toba, C. F. Baicu et al., "Age and SPARC change the extracellular matrix composition of the left ventricle," *BioMed Research International*, vol. 2014, Article ID 810562, 7 pages, 2014.
- [180] G. Workman and A. D. Bradshaw, "Production and purification of recombinant human SPARC," *Methods in Cell Biology*, vol. 143, pp. 335–345, 2018.
- [181] A. D. Bradshaw, C. F. Baicu, T. J. Rentz et al., "Pressure overload-induced alterations in fibrillar collagen content and myocardial diastolic function: role of secreted protein acidic and rich in cysteine (SPARC) in post-synthetic procollagen processing," *Circulation*, vol. 119, no. 2, pp. 269–280, 2009.
- [182] M. O'Brien, C. F. Baicu, A. O. van Laer et al., "Pressure overload generates a cardiac-specific profile of inflammatory mediators," *American Journal of Physiology-Heart and Circulatory Physiology*, vol. 319, no. 2, pp. H331–H340, 2020.
- [183] G. M. Harris, I. Raitman, and J. E. Schwarzbauer, "Cell-derived decellularized extracellular matrices," *Methods in Cell Biology*, vol. 143, pp. 97–114, 2018.
- [184] A. Ghanemi, M. Yoshioka, and J. St-Amant, "Secreted protein acidic and rich in cysteine: metabolic and homeostatic properties beyond the extracellular matrix structure," *Applied Sciences*, vol. 10, no. 7, p. 2388, 2020.
- [185] K. Khetan, V. Baloda, R. K. Sahoo et al., "SPARC expression in desmoplastic and non desmoplastic pancreatic carcinoma and cholangiocarcinoma," *Pathology-Research and Practice*, vol. 215, no. 12, p. 152685, 2019.
- [186] W. Aoi, Y. Naito, T. Takagi et al., "A novel myokine, secreted protein acidic and rich in cysteine (SPARC), suppresses colon tumorigenesis via regular exercise," *Gut*, vol. 62, no. 6, pp. 882–889, 2013.
- [187] S. Deckx, D. M. Johnson, M. Rienks et al., "Extracellular SPARC increases cardiomyocyte contraction during health and disease," *PLoS ONE*, vol. 14, no. 4, article e0209534, 2019.
- [188] S. McCurdy, C. F. Baicu, S. Heymans, and A. D. Bradshaw, "Cardiac extracellular matrix remodeling: fibrillar collagens and secreted protein acidic and rich in cysteine (SPARC)," *Journal of Molecular and Cellular Cardiology*, vol. 48, no. 3, pp. 544–549, 2010.
- [189] L. T. McDonald, M. R. Zile, Y. Zhang et al., "Increased macrophage-derived SPARC precedes collagen deposition in myocardial fibrosis," *American Journal of Physiology-Heart and Circulatory Physiology*, vol. 315, no. 1, pp. H92–H100, 2018.
- [190] S. Omi, K. Yamanouchi, K. Nakamura, T. Matsuwaki, and M. Nishihara, "Reduced fibrillar collagen accumulation in skeletal muscle of secreted protein acidic and rich in cysteine (SPARC)-null mice," *Journal of Veterinary Medical Science*, vol. 81, no. 11, pp. 1649–1654, 2019.
- [191] M. Dobaczewski, M. Bujak, P. Zymek, G. Ren, M. L. Entman, and N. G. Frangogiannis, "Extracellular matrix remodeling in canine and mouse myocardial infarcts," *Cell and Tissue Research*, vol. 324, no. 3, pp. 475–488, 2006.
- [192] I. Komatsubara, T. Murakami, S. Kusachi et al., "Spatially and temporally different expression of osteonectin and osteopontin in the infarct zone of experimentally induced myocardial infarction in rats," *Cardiovascular Pathology*, vol. 12, no. 4, pp. 186–194, 2003.
- [193] M. W. M. Schellings, D. Vanhoutte, M. Swinnen et al., "Absence of SPARC results in increased cardiac rupture and dysfunction after acute myocardial infarction," *Journal of Experimental Medicine*, vol. 206, no. 1, pp. 113–123, 2009.
- [194] A. D. Bradshaw, "The role of secreted protein acidic and rich in cysteine (SPARC) in cardiac repair and fibrosis: does expression of SPARC by macrophages influence outcomes?," *Journal of Molecular and Cellular Cardiology*, vol. 93, pp. 156–161, 2016.
- [195] N. G. Frangogiannis, "Cardiac fibrosis: cell biological mechanisms, molecular pathways and therapeutic opportunities," *Molecular Aspects of Medicine*, vol. 65, pp. 70–99, 2019.
- [196] N. G. Frangogiannis and J. C. Kovacic, "Extracellular Matrix in Ischemic Heart Disease, Part 4/4," *Journal of the American College of Cardiology*, vol. 75, no. 17, pp. 2219–2235, 2020.
- [197] J. Duan, B. Zhu, Y. Wu, Z. Chen, and L. Yang, "Myokines: an available biomarker to evaluate cardiac functions?," *Cardiology*, vol. 142, no. 4, pp. 211–212, 2019.
- [198] S. Shen, R. Gao, Y. Bei et al., "Serum irisin predicts mortality risk in acute heart failure patients," *Cellular Physiology and Biochemistry*, vol. 42, no. 2, pp. 615–622, 2017.
- [199] I. C. Hsieh, M. Y. Ho, M. S. Wen et al., "Serum irisin levels are associated with adverse cardiovascular outcomes in patients with acute myocardial infarction," *International Journal of Cardiology*, vol. 261, pp. 12–17, 2018.

- [200] M. Kohara, T. Masuda, K. Shiizaki et al., "Association between circulating fibroblast growth factor 21 and mortality in end-stage renal disease," *PLoS One*, vol. 12, no. 6, article e0178971, 2017.
- [201] A. E. Berezin and A. A. Kremzer, "Predictive value of circulating osteonectin in patients with ischemic symptomatic chronic heart failure," *Biomedical Journal*, vol. 38, no. 6, pp. 523–530, 2015.
- [202] A. E. Berezin, A. A. Kremzer, Y. V. Martovitskaya et al., "The utility of biomarker risk prediction score in patients with chronic heart failure," *International Journal of Clinical and Experimental Medicine*, vol. 8, no. 10, pp. 18255–18264, 2015.
- [203] T. Furihata, S. Kinugawa, A. Fukushima et al., "Serum myostatin levels are independently associated with skeletal muscle wasting in patients with heart failure," *International Journal of Cardiology*, vol. 220, pp. 483–487, 2016.

Research Article

Association between Cardiac Autonomic Neuropathy and Coronary Artery Lesions in Patients with Type 2 Diabetes

Lei Liu ¹, Qiansheng Wu,² Hong Yan,¹ Baoxian Chen,¹ Xilong Zheng,³ and Qiang Zhou ¹

¹Division of Cardiology, Department of Internal Medicine, Tongji Hospital, Tongji Medical College, Huazhong University of Science and Technology, Wuhan, China

²Division of Cardiothoracic and Vascular Surgery, Tongji Hospital, Tongji Medical College, Huazhong University of Science and Technology, Wuhan, China

³Department of Biochemistry and Molecular Biology, Cumming School of Medicine, Libin Cardiovascular Institute of Alberta, University of Calgary, Alberta, Canada

Correspondence should be addressed to Qiang Zhou; thisiszhou@163.com

Received 13 October 2020; Revised 22 November 2020; Accepted 19 December 2020; Published 30 December 2020

Academic Editor: Alexander Berezin

Copyright © 2020 Lei Liu et al. This is an open access article distributed under the Creative Commons Attribution License, which permits unrestricted use, distribution, and reproduction in any medium, provided the original work is properly cited.

Objective. Cardiac autonomic neuropathy (CAN) is a common and serious complication of diabetes mellitus with various systemic involvements, such as atherosclerotic cardiovascular disease. We aimed to evaluate the association between CAN and coronary artery lesions in patients with type 2 diabetes. **Research Design and Methods.** We retrospectively reviewed the medical records of 104 patients with type 2 diabetes and coronary artery disease (CAD). We evaluated heart rate variability (HRV) parameters (SDANN, SDNN, and pNN50) to assess cardiac autonomic function. The severity of coronary lesions was assessed by the Gensini scores and the number of affected vessels. Correlation analyses between HRV parameters and the severity of coronary lesions and clinical parameters were performed. **Results.** Spearman's correlation analysis showed a significant negative correlation between SDANN and Gensini scores ($r = -0.22$, $P = 0.03$). Interestingly, this finding remained significant after adjusting for clinical covariates ($r = -0.23$, $P = 0.03$). However, there was no association between HRV parameters and the severity of coronary lesions as assessed by the number of affected vessels. Clinical parameters were not significantly correlated with HRV parameters (all $P > 0.05$). **Conclusions.** Cardiac autonomic neuropathy might be related to the degree of coronary atheromatous burden in patients with type 2 diabetes. Screening for cardiac autonomic neuropathy might potentially be beneficial in the risk stratification of patients with type 2 diabetes.

1. Introduction

Diabetes mellitus has emerged as a major threat on patient survival and quality of life, with huge, socioeconomic, and social challenges [1]. The prevalence of diabetes mellitus is rapidly increasing due to an increased burden of obesity and related risk factors, such as increased consumption of highly processed foods, socioeconomic development, and a decrease in physical activity [2]. Type 2 diabetes accounts for 95% of diagnosed diabetes mellitus and is projected to affect hundreds of millions of people globally in the next few decades. Most patients with diabetes mellitus manifest at least one of its complications. Diabetes mellitus has both

macrovascular and microvascular complications, which become more prevalent with increased disease duration [3].

An increasing body of evidence has shown that type 2 diabetes is a common chronic disease that is associated with substantial morbidity and mortality due to coronary artery disease (CAD), which is a macrovascular complication of diabetes mellitus [4]. Moreover, cardiac autonomic neuropathy (CAN) is a common and serious complication of diabetes mellitus with various systemic involvements, resulting in atherosclerotic cardiovascular disease [5]. Diabetic autonomic neuropathy is implicated in the pathogenesis of vascular damage and subsequent coronary artery disease, which may result in disabling clinical and functional manifestations.

Recently, studies that dysfunction of the cardiac autonomic system may be effective in the development of vascular atherosclerosis have been well documented [6, 7]. There is a lot of evidence that cardiac autonomic neuropathy plays a crucial role in the pathogenesis of progressive vessel atherosclerosis [8, 9]. Furthermore, diabetic autonomic neuropathy is closely associated with subclinical myocardial dysfunction, interstitial myocardial fibrosis, and metabolic changes [10, 11]. Furthermore, CAN also significantly increases the incidence of cardiovascular disease and its related mortality. However, the independent relationship of cardiac autonomic neuropathy with the severity of coronary lesions in type 2 diabetic patients has not been established.

Heart rate variability (HRV), which reflects the status of the cardiac sympathovagal balance, is a noninvasive, practical, and reproducible index used to assess cardiac autonomic function [12, 13]. Recently, more attention has been placed on HRV assessment as a diagnostic tool in the prediction of prognosis in various neurological disorders and in the evaluation of autonomic impairment [14]. Numerous studies have demonstrated changes in HRV patterns are associated with the cardiac autonomic system in subjects with physiological and pathological conditions, particularly in type 2 diabetic patients [15].

There is increasing evidence that reduced HRV may be related to worse cardiovascular outcome among patients with type 2 diabetes [16, 17]. However, little is known regarding the relationship between the severities of coronary artery lesions and CAN in patients with type 2 diabetes. Therefore, we aimed to investigate the association between HRV and the severity of coronary artery lesions in patients with type 2 diabetes and CAD.

2. Methods

2.1. Study Population. We conducted a retrospective study on 104 patients with type 2 diabetes and CAD admitted to the Tongji Hospital in Wuhan (China) from July 2017 to October 2019. All data were extracted and reviewed from the patient medical records. In addition, CAN diagnosis was made based on medical records. We used the guidelines of the CAN Subcommittee of the Toronto Consensus Panel on Diabetic Neuropathy for CAN diagnosis and staging [18]. None of the participants received antiarrhythmic therapy such as beta-blockers or calcium channel blockers prior to 24-hour dynamic electrocardiogram; therefore, their HRV was not affected by the above-mentioned therapy. Patients were diagnosed with type 2 diabetes based on their medical history or according to the American Diabetes Association criteria as previously reported [19]. Detailed diagnostic criteria for CAD have been previously described [20]. Precisely, CAD was defined as the presence of at least one significant coronary artery stenosis with luminal diameter > 50% on coronary angiography. The severity of atherosclerosis was assessed using the Gensini scores and the number of diseased vessels (stenosis > 50%). The Gensini scores were calculated using a method previously described [21]. In each coronary segment, the narrowing of the coronary artery lumen was rated 1, 2, 4, 8, 16, and 32 for 0–25%, 26–50%,

51–75%, 76–90%, 91–99%, and 100% stenosis, respectively. Then, a multiplier was assigned to each segment depending on the prognostic importance of the area supplied by that segment: 5 for the left main coronary artery, 2.5 for the proximal left anterior descending coronary artery (LAD), right coronary artery, and proximal left circumflex branch, 1.5 for the midsegment of LAD, 0.5 for the second diagonal branch and posterolateral branches, and 1 for the other branches. The final Gensini score for each patient was the sum of the total scores for all affected segments.

We excluded patients with comorbidities, such as valvular heart disease, rheumatic diseases, connective tissue disease, severe liver and kidney dysfunction, hyperthyroidism, and infection. Moreover, we excluded patients with chronic obstructive coronary lesions, previous myocardial infarction, or coronary artery bypass grafting.

Ethics committee review was not necessary because this study was a retrospective analysis. Informed consent was waived because this study involved an analysis of existing medical records with neither breach of privacy nor interference with clinical decisions related to patient care. The study was conducted in accordance with the principles of the Declaration of Helsinki.

2.2. Clinical and Paraclinical Evaluation. Demographic factors, including sex, age, height, weight, ethnicity, cigarette smoking, alcohol consumption, and medical history, were obtained by reviewing participants' medical records. Fasting blood samples were obtained for the analysis of lipid profile, glycated hemoglobin A1c (HbA1c), and glucose levels using standard methods at the Department of Clinical Laboratory at Tongji Hospital.

Electrocardiographic recordings were acquired using 24-hour electrocardiogram (ECG) Holter monitoring (DMS 300-4, Holter Reader, Producer DMS, Nevada, USA) in all patients. Parameters from Holter recordings were automatically analyzed by a computer software, which computed all of the basic HRV parameters using the HRV analysis module. The HRV time-domain variables used were as follows: SDNN expressed in milliseconds (ms) represented the standard deviation of all normal-to-normal intervals. SDANN expressed in ms represented the standard deviation of the averages of normal-to-normal intervals in all 5 min segments of the entire recording, and pNN50 represented the ratio of the number of pairs of adjacent normal-to-normal intervals more than 50 ms to the total number of all normal-to-normal intervals.

A standard two-dimensional Doppler echocardiographic examination was performed in all patients according to routine procedures (GE Vingmed Vivid 7 or Vivid 9, Horten, Norway). The following parameters were obtained as previously reported [13]. The left ventricular end-diastolic dimension (LVEDD) was measured using M-mode in the parasternal left ventricular long-axis view. The left ventricular biplane Simpson method was used to measure the ejection fraction (EF) in apical 4- and 2-chamber views. Doppler echocardiography was used to record left ventricular flow velocity and measure LV diastolic function parameters. The peak velocities of early (E-wave velocity) and late

(A-wave velocity) transmitral flow were measured, and the E/A ratio was calculated.

2.3. Statistical Analyses. Descriptive and experimental measures were expressed as means \pm standard deviation or percentages as indicated. The one-sample Kolmogorov-Smirnov test was used to test whether a sample comes from a population with a specific distribution. The Gensini scores showed a markedly skewed distribution toward high values and therefore were presented as medians and quartiles. Correlations between variables were determined using Spearman's correlation or Pearson's correlation coefficient analysis. The analysis of variance test was used for intergroup comparisons of continuous variables. Trends were analyzed with the linear-by-linear association. Two-sided P values were used for all tests, and a P value < 0.05 was applied to identify the results with statistical significance. All statistical analyses were performed using SPSS version 15.0 for Windows.

3. Results

3.1. Baseline Characteristics of the Patients. Table 1 summarizes the baseline characteristics, clinical, and biochemical findings of the study population. We included 104 patients with type 2 diabetes and CAD, including 33 females (31.7%) and 71 males (68.3%), with a mean age of 60.6 ± 8.8 years (range 42–77 years). The proportion of patients that reported smoking and alcohol consumption was 47.1% and 32.7%, respectively. The mean body mass index (BMI) was 24.0 ± 2.8 kg/m². Fifty-six patients (53.8%) had hypertension. The mean glycated hemoglobin A1c (HbA1c) value was $6.8 \pm 0.6\%$, and the median Gensini score was 28 (19, 46). The time-domain measures of HRV parameters were as follows: the means of SDNN, SDANN, and pNN50 were 58 ± 19 ms, 101 ± 32 ms, and $11 \pm 13\%$, respectively.

3.2. Correlation Analysis according to HRV Parameters. We investigated the association between the HRV parameters and clinical characteristics in all 104 patients. As shown in Table 2, there was no statistical linear correlation between the HRV parameters (SDNN, SDANN, and pNN50) and clinical characteristics (all P values > 0.05). Furthermore, we analyzed the correlations between myocardium parameters (E/A ratio, EF, and LVEDD) and HRV parameters (SDNN, SDANN, and pNN50). Results of the linear correlation analysis are also shown in Table 2. However, there were no statistically significant correlations (all P values > 0.05).

We further analyzed the possible correlation between the HRV parameters and the severity of coronary lesions as measured both by Gensini scores and the number of affected vessels. As presented in Table 3, there was a significant negative correlation between SDANN and Gensini scores ($r = -0.22$, $P = 0.03$). Notably, after adjustment for clinical covariates, the relationship remained significant ($r = -0.23$, $P = 0.03$). In contrast, no significant correlation was found between the other HRV parameters and Gensini scores (Table 3). Results of the linear correlation between 1-, 2-, and 3-vessel disease and HRV parameters are shown in Table 4. Similarly,

TABLE 1: Demographic characteristics of CAD patients with type 2 diabetes.

Characteristics	Study subjects ($n = 104$)
Men, n (%)	71 (68.3)
Age (years)	60.6 ± 8.8
BMI (kg/m ²)	24.0 ± 2.8
Current smokers, n (%)	49 (47.1)
Alcohol drinkers, n (%)	34 (32.7)
Hypertension, n (%)	56 (53.8)
HbA1c (%)	6.8 ± 0.6
FBG (mmol/L)	7.1 ± 1.2
UA (μ mol/L)	416 ± 95
TG (mmol/L)	1.9 ± 1.2
TC (mmol/L)	5.0 ± 0.9
LDL (mmol/L)	3.0 ± 0.9
HDL (mmol/L)	1.1 ± 0.3
EF (%)	57 ± 6
E/A ratio	1.1 ± 0.2
LVEDD (mm)	47.9 ± 4.0
SDANN	101 ± 32
SDNN	58 ± 19
pNN50	11 ± 13
Gensini scores	28 (19, 46)

TABLE 2: The correlations between the HRV parameters and clinical variables.

Variables	SDANN		SDNN		pNN50	
	r	P	r	P	r	P
Age	-0.11	0.25	-0.08	0.41	-0.04	0.71
BMI	-0.03	0.78	0.01	0.98	-0.14	0.16
HbA1c	0.02	0.85	0.01	0.96	-0.01	0.91
FBG	-0.04	0.71	-0.04	0.72	0.12	0.20
UA	0.01	0.98	0.04	0.66	-0.04	0.72
TG	0.04	0.69	-0.08	0.39	-0.01	0.97
TC	0.07	0.51	0.07	0.50	0.09	0.36
LDL	0.08	0.45	0.09	0.35	-0.06	0.54
HDL	0.01	0.90	0.02	0.86	-0.01	0.97
EF (%)	0.07	0.47	-0.01	0.90	-0.14	0.17
E/A ratio	0.13	0.20	0.18	0.07	0.07	0.46
LVEDD	-0.05	0.60	0.17	0.09	0.18	0.06

there was no statistical correlation between the number of affected vessels and the HRV parameters (all P values > 0.05).

4. Discussion

In this study, we evaluated the relationship between CAN and the severity of coronary lesions among patients with type 2 diabetes and CAD. CAN is known to be associated with increased cardiovascular morbidity and mortality [22]. The

TABLE 3: Assessment of association between HRV parameters with Gensini scores.

Variables	Crude		Adjust	
	<i>r</i>	<i>P</i>	<i>r</i>	<i>P</i>
SDANN	-0.22	0.03	-0.23	0.03
SDNN	-0.14	0.16	-0.10	0.34
pNN50	-0.04	0.67	-0.06	0.60

Spearman's correlation analysis. Adjusted: age, sex, body mass index, smoking, alcohol, hypertension, triglyceride, total cholesterol, HDL, LDL, uric, myocardial parameters, FBG, and HbA1c.

TABLE 4: Correlation between HRV parameters and number of stenotic branches of coronary arteries.

Variables	1VD (<i>n</i> = 19)	2VD (<i>n</i> = 33)	3VD (<i>n</i> = 52)	<i>P/P</i> for trend
SDANN	101 ± 26	102 ± 26	101 ± 37	0.98/0.97
SDNN	56 ± 18	58 ± 17	58 ± 21	0.91/0.69
pNN50	8 ± 8	8 ± 11	13 ± 16	0.10/0.06

1VD=1-vessel disease; 2VD=2-vessel disease; 3VD=3-vessel disease.

present retrospective study extends these observations by demonstrating that some parameters of HRV were independently associated with the severity of coronary lesions in patients with type 2 diabetes and CAD. These findings suggest that CAN contribute to the development of coronary artery atherosclerosis in patients with type 2 diabetes.

The mechanisms whereby CAN is implicated in the pathogenesis of vascular atherosclerosis are complicated and have not been clarified. Clinical and experimental evidence showed that long-term treatment with antisympathetic drugs resulted in significant reductions of coronary and cerebrovascular complications, thereby reducing mortality and morbidity by the retardation of atherosclerosis development [23]. During the past decade, cardiac autonomic dysfunction has been proposed as a precursor of vascular atherosclerosis development [24]. Autonomic nervous system alterations have been considered as a significant risk factor in the acceleration of atherosclerosis and serve as a trigger for acute coronary and cerebrovascular events. The pathophysiology of CAN is complex and involves the endocrine system with associated inflammatory, hemostatic, and metabolic abnormalities [25]. Although the body of evidence examining the CAN-atherosclerosis association is growing, this association is not fully understood.

It is well known that the diabetes mellitus burden has emerged as an important public health problem of epidemic proportions in the last few decades. In particular, type 2 diabetes mellitus has exponentially grown in the past decades around the world. Clinical studies have demonstrated that type 2 diabetes mellitus can be considered as a CAD risk equivalent with such a strong association and relation with diabetes and CAD development in both men and women [26]. The pathophysiology of type 2 diabetes mellitus in CAD has been attributed to a variety of mechanisms including vascular endothelial injury, atherosclerosis, and CAN.

CAN is one of the most common and often overlooked diabetes-related complications that have a significant influence on CAD in patients with type 2 diabetes mellitus [22]. Improving the understanding of the pathogenesis of CAN and its effect on CAD, therefore, has attracted a great deal of interest as a potential therapeutic target.

However, the independent relationship between cardiac autonomic neuropathy and the severity of coronary lesions has been difficult to clarify due to the similar etiologies of these conditions in type 2 diabetes mellitus. Accordingly, we performed the current retrospective study to investigate this important issue. This study showed that the global association of CAN and coronary lesions might be independent of known factors in the pathogenesis of vascular endothelial injury and atherosclerosis in patients with type 2 diabetes mellitus. These findings suggest endothelial dysfunction and cardiac autonomic nervous dysfunction are related pathophysiologically in type 2 diabetes mellitus [27]. Additionally, we indicated that CAN may reflect the progression of coronary atherosclerosis in patients with type 2 diabetes. Previous studies have consistently reported that reduced HRV indexes depend on the degree of damage on coronary artery lesions in patients with stable angina pectoris [28, 29]. Thus, these findings indicate that CAN may reflect the progression of coronary lesions in patients with type 2 diabetes.

A previous study showed that CAN have an independent negative association with exercise capacity in patients with CAD [30]. Moreover, other studies revealed that CAN was associated with left ventricular dysfunction in patients with type 2 diabetes [31–33]. However, we found no significant correlation between HRV indexes and the echocardiographic assessment of LV function in the current study. The lack of association between HRV indexes and echocardiographic assessment of left ventricular function in the present study is not totally surprising, when we consider the complex pathogenesis of these diseases. The divergent findings may be attributed to the heterogeneity of left ventricular dysfunction in patients with type 2 diabetes and CAD. Our study had a few limitations due to the small sample size and the retrospective nature of the study. Moreover, the study was conducted in a single center; therefore, the results cannot be generalized at this point. Notably, future prospective, multicenter, and large-scale studies are warranted to clarify and consolidate our study findings.

In conclusion, we found an association between CAN and the severity of coronary stenosis among patients with type 2 diabetes mellitus and CAD. The combined assessment of cardiac autonomic nervous function and plaque enhancement may improve CAD risk stratification in patients with type 2 diabetes mellitus. Future prospective studies on a larger scale are needed to confirm our findings.

Data Availability

The data used to support the findings of this study are available from the corresponding author upon request.

Conflicts of Interest

No potential conflicts of interest relevant to this article were reported.

Authors' Contributions

LL researched data and edited the manuscript; QW, YH, and BC researched data and contributed to discussion; XZ reviewed the manuscript; QZ wrote the manuscript and researched data.

Acknowledgments

We would like to thank Editage (<http://www.editage.cn/>) for English language editing. This work was supported by the National Nature Science Foundation of China (81974031). The authors thank the subjects for their participation in this study and the staff of the hospital for their help in collecting and recording the data.

References

- [1] P. Zimmet, Z. Shi, A. El-Osta, and L. Ji, "Epidemic T2DM, early development and epigenetics: implications of the Chinese famine," *Nature Reviews. Endocrinology*, vol. 14, no. 12, pp. 738–746, 2018.
- [2] Y. Zheng, S. H. Ley, and F. B. Hu, "Global aetiology and epidemiology of type 2 diabetes mellitus and its complications," *Nature Reviews. Endocrinology*, vol. 14, no. 2, pp. 88–98, 2018.
- [3] D. Glovaci, W. Fan, and N. D. Wong, "Epidemiology of diabetes mellitus and cardiovascular disease," *Current Cardiology Reports*, vol. 21, no. 4, p. 21, 2019.
- [4] J. D. Newman, A. Z. Schwartzbard, H. S. Weintraub, I. J. Goldberg, and J. S. Berger, "Primary prevention of cardiovascular disease in diabetes mellitus," *Journal of the American College of Cardiology*, vol. 70, no. 7, pp. 883–893, 2017.
- [5] A. Flotats and I. Carrio, "Is cardiac autonomic neuropathy the basis of nonischemic diabetic cardiomyopathy?," *JACC. Cardiovascular Imaging*, vol. 3, no. 12, pp. 1216–1218, 2010.
- [6] J. P. Halcox, W. H. Schenke, G. Zalos et al., "Prognostic value of coronary vascular endothelial dysfunction," *Circulation*, vol. 106, no. 6, pp. 653–658, 2002.
- [7] L. Nattero-Chavez, S. Redondo Lopez, S. Alonso Diaz et al., "Association of cardiovascular autonomic dysfunction with peripheral arterial stiffness in patients with type 1 diabetes," *The Journal of Clinical Endocrinology and Metabolism*, vol. 104, no. 7, pp. 2675–2684, 2019.
- [8] S. Mala, V. Potockova, L. Hoskovcova et al., "Cardiac autonomic neuropathy may play a role in pathogenesis of atherosclerosis in type 1 diabetes mellitus," *Diabetes Research and Clinical Practice*, vol. 134, pp. 139–144, 2017.
- [9] M. S. Shah and M. Brownlee, "Molecular and cellular mechanisms of cardiovascular disorders in diabetes," *Circulation Research*, vol. 118, no. 11, pp. 1808–1829, 2016.
- [10] Y. Shang, X. Zhang, W. Leng et al., "Increased fractal dimension of left ventricular trabeculations is associated with subclinical diastolic dysfunction in patients with type-2 diabetes mellitus," *The International Journal of Cardiovascular Imaging*, vol. 35, no. 4, pp. 665–673, 2019.
- [11] T. P. Didangelos, G. Arsos, T. Karamitsos et al., "Left ventricular systolic and diastolic function in normotensive type 2 diabetic patients with or without autonomic neuropathy: a radionuclide ventriculography study," *Angiology*, vol. 65, no. 10, pp. 877–882, 2014.
- [12] L. Soares-Miranda, J. Sattelmair, P. Chaves et al., "Physical activity and heart rate variability in older adults: the Cardiovascular Health Study," *Circulation*, vol. 129, no. 21, pp. 2100–2110, 2014.
- [13] L. Liu, Q. Wu, H. Yan, X. Zheng, and Q. Zhou, "Plasma homocysteine and autonomic nervous dysfunction: association and clinical relevance in OSAS," *Disease Markers*, vol. 2020, Article ID 4378505, 6 pages, 2020.
- [14] I. Cygankiewicz and W. Zareba, "Heart rate variability," *Handbook of Clinical Neurology*, vol. 117, pp. 379–393, 2013.
- [15] A. S. Shah, L. El Ghormli, M. E. Vajravelu et al., "Heart rate variability and cardiac autonomic dysfunction: prevalence, risk factors, and relationship to arterial stiffness in the treatment options for type 2 diabetes in adolescents and youth (TODAY) study," *Diabetes Care*, vol. 42, no. 11, pp. 2143–2150, 2019.
- [16] A. S. Shah, M. Jaiswal, D. Dabelea et al., "Cardiovascular risk and heart rate variability in young adults with type 2 diabetes and arterial stiffness: the SEARCH for diabetes in youth study," *Journal of Diabetes and its Complications*, vol. 34, no. 10, p. 107676, 2020.
- [17] P. Hammerle, C. Eick, S. Blum et al., "Heart rate variability triangular index as a predictor of cardiovascular mortality in patients with atrial fibrillation," *Journal of the American Heart Association*, vol. 9, no. 15, article e016075, 2020.
- [18] V. Spallone, D. Ziegler, R. Freeman et al., "Cardiovascular autonomic neuropathy in diabetes: clinical impact, assessment, diagnosis, and management," *Diabetes Metabolism Research and Reviews*, vol. 27, no. 7, pp. 639–653, 2011.
- [19] L. Liu, L. Tan, J. Lai, S. Li, and D. W. Wang, "Enhanced Rho-kinase activity: pathophysiological relevance in type 2 diabetes," *Clinica chimica acta; international journal of clinical chemistry*, vol. 462, pp. 107–110, 2016.
- [20] L. Liu, L. You, L. Tan, D. W. Wang, and W. Cui, "Genetic insight into the role of MRAS in coronary artery disease risk," *Gene*, vol. 564, no. 1, pp. 63–66, 2015.
- [21] P. Montorsi, P. M. Ravagnani, S. Galli et al., "Association between erectile dysfunction and coronary artery disease. Role of coronary clinical presentation and extent of coronary vessels involvement: the COBRA trial," *European heart journal*, vol. 27, no. 22, pp. 2632–2639, 2006.
- [22] G. Dimitropoulos, A. A. Tahrani, and M. J. Stevens, "Cardiac autonomic neuropathy in patients with diabetes mellitus," *World Journal of Diabetes*, vol. 5, no. 1, pp. 17–39, 2014.
- [23] B. Ablad, J. A. Bjorkman, D. Gustafsson, G. Hansson, A. M. Ostlund-Lindqvist, and K. Pettersson, "The role of sympathetic activity in atherogenesis: effects of β -blockade," *American Heart Journal*, vol. 116, no. 1, pp. 322–327, 1988.
- [24] D. S. Mendo, S. A. Gonzalez, and H. A. Bonaccorsi, "Association between autonomic disorders and subclinical atherosclerosis," *Hipertension y riesgo vascular*, vol. 37, no. 3, pp. 108–114, 2020.
- [25] K. M. Chinnaiyan, "Role of stress management for cardiovascular disease prevention," *Current Opinion in Cardiology*, vol. 34, no. 5, pp. 531–535, 2019.
- [26] K. Malmberg, S. Yusuf, H. C. Gerstein et al., "Impact of diabetes on long-term prognosis in patients with unstable angina

- and non-Q-wave myocardial infarction: results of the OASIS (Organization to Assess Strategies for Ischemic Syndromes) registry," *Circulation*, vol. 102, no. 9, pp. 1014–1019, 2000.
- [27] P. Bhati, R. Alam, J. A. Moiz, and M. E. Hussain, "Subclinical inflammation and endothelial dysfunction are linked to cardiac autonomic neuropathy in type 2 diabetes," *Journal of Diabetes and Metabolic Disorders*, vol. 18, no. 2, pp. 419–428, 2019.
- [28] J. Feng, A. Wang, C. Gao et al., "Altered heart rate variability depend on the characteristics of coronary lesions in stable angina pectoris," *Anatolian Journal of Cardiology*, vol. 15, no. 16, pp. 496–501, 2015.
- [29] Y. Chen, Y. Yu, W. Zou, M. Zhang, Y. Wang, and Y. Gu, "Association between cardiac autonomic nervous dysfunction and the severity of coronary lesions in patients with stable coronary artery disease," *The Journal of International Medical Research*, vol. 46, no. 9, pp. 3729–3740, 2018.
- [30] J. J. Karjalainen, A. M. Kiviniemi, A. J. Hautala et al., "Determinants and prognostic value of cardiovascular autonomic function in coronary artery disease patients with and without type 2 diabetes," *Diabetes Care*, vol. 37, no. 1, pp. 286–294, 2013.
- [31] W. Dinh, R. Futh, M. Lankisch et al., "Cardiovascular autonomic neuropathy contributes to left ventricular diastolic dysfunction in subjects with type 2 diabetes and impaired glucose tolerance undergoing coronary angiography," *Diabetic medicine : a journal of the British Diabetic Association*, vol. 28, no. 3, pp. 311–318, 2011.
- [32] J. W. Sacre, B. Franjic, C. L. Jellis, C. Jenkins, J. S. Coombes, and T. H. Marwick, "Association of cardiac autonomic neuropathy with subclinical myocardial dysfunction in type 2 diabetes," *JACC. Cardiovascular Imaging*, vol. 3, no. 12, pp. 1207–1215, 2010.
- [33] J. C. Habek, N. Lakusic, P. Kruzliak, J. Sikic, D. Mahovic, and L. Vrbanic, "Left ventricular diastolic function in diabetes mellitus type 2 patients: correlation with heart rate and its variability," *Acta Diabetologica*, vol. 51, no. 6, pp. 999–1005, 2014.

Review Article

The Role of Circulating RBP4 in the Type 2 Diabetes Patients with Kidney Diseases: A Systematic Review and Meta-Analysis

Li Zhang ¹, Yan-Li Cheng,¹ Shuai Xue ,² and Zhong-Gao Xu ¹

¹Department of Nephrology, The 1st hospital of Jilin University, Changchun 130021, China

²Department of Thyroid Surgery, The 1st hospital of Jilin University, Changchun 130021, China

Correspondence should be addressed to Shuai Xue; xueshuai.jlu.edu@hotmail.com
and Zhong-Gao Xu; nephrology_jdyy@hotmail.com

Received 18 July 2020; Revised 20 August 2020; Accepted 26 August 2020; Published 5 October 2020

Academic Editor: Michael Lichtenauer

Copyright © 2020 Li Zhang et al. This is an open access article distributed under the Creative Commons Attribution License, which permits unrestricted use, distribution, and reproduction in any medium, provided the original work is properly cited.

Background. Diabetic nephropathy is a common and serious complication of diabetes mellitus (DM) and is one of the leading causes of end-stage renal disease worldwide. Although there have been many investigations on biomarkers for DN, there is no consistent conclusion about reliable biomarkers. The purpose of this study was to perform a systematic review and meta-analysis of the role of circulating retinol-binding protein 4 (RBP4) in the type 2 diabetes mellitus (T2DM) patients with kidney diseases. **Materials and Methods.** We searched the PubMed, MEDLINE, EMBASE, and Web of Science databases for publications. For the 12 cross-sectional studies that we included in the review, we calculated standard mean differences (SMD) with 95% confidence intervals (CI) for continuous data when the applied scales were different. Risk of bias of included trials was assessed by using the Newcastle-Ottawa Scale. **Results.** RBP4 concentrations in the micro-, macro-, or micro+macroalbuminuria groups were significantly higher than those in the normal albuminuria group of T2DM patients [$P = 0.001$, SMD 1.07, 95% CI (0.41, 1.73)]. The estimated glomerular filtration rate (eGFR) was negatively associated with circulating RBP4 concentrations in patients with T2DM [summary Fisher's $Z = -0.48$, 95% CI (-0.69, -0.26), $P < 0.0001$]. The albumin-to-creatinine ratio (ACR) was positively associated with circulating RBP4 concentrations in patients with T2DM [summary Fisher's $Z = 0.20$, 95% CI (0.08, 0.32), $P = 0.001$]. **Conclusion.** The levels of circulating RBP4 were significantly higher both in T2DM subjects with micro/macroalbuminuria and in T2DM subjects with declined eGFR. The levels of circulating RBP4 were positively correlated with ACR but negatively correlated with eGFR. Circulating RBP4 could be a reliable biomarker for kidney diseases in T2DM.

1. Introduction

Diabetes mellitus (DM) affects more than 463 million people globally, and this number is supposed to increase to 700 million by 2045 [1]. Diabetic nephropathy (DN) is a common and serious complication of DM [2] and is one of the leading causes of end-stage renal disease (ESRD) worldwide [3]. It is also associated with cardiovascular and all-cause mortality [4]. Therefore, accurate identification of DN is critically important to improve clinical prognosis and reduce the economic burden. Although there have been many investigations on biomarkers for DN, there is no consistent conclusion about reliable biomarkers.

Retinol-binding protein 4 (RBP4; formerly called RBP) was identified in 2005 and is mainly synthesized in adipose

tissues and hepatocytes. It is a circulating transport protein of retinol [5] and delivers retinol to tissues as a retinol-RBP complex in circulation [6]. Several studies have revealed that RBP4 increases the synthesis of the gluconeogenic enzyme, phosphoenolpyruvate carboxykinase, and inhibits insulin signaling in the muscle [7]. Moreover, the deletion of the *RBP4* gene can elevate insulin sensitivity [7]. Recent clinical studies in adults have demonstrated that RBP4 levels were associated with metabolic syndrome, obesity, insulin resistance, and type 2 DM (T2DM) [7–10]. Furthermore, there is some evidence that serum or plasma RBP4 levels were increased in patients with advanced renal impairment of T2DM [11, 12]. However, Akbay et al. [13] found that although serum RBP4 concentrations were not significantly higher in DM patients than in non-DM control subjects, they

were significantly higher in the micro-macroalbuminuria group than in the normal albuminuria group of DM patients [13]. Raila et al. [14] also reported that kidney function could be the leading determinant of serum RBP4 levels in T2DM subjects. However, although albuminuria and kidney function appear to be related to serum RBP4 levels, no causal clinical correlations have been established [11].

To our knowledge, a meta-analysis has not yet been performed to explore the role of circulating RBP4 in T2DM subjects with kidney diseases, although many studies of circulating RBP4 and kidney diseases in T2DM patients have been published. Hence, we conducted this study to systematically synthesize available evidence on circulating RBP4 in the patients with DN and investigate the associations between RBP4 concentrations and clinical indices of renal function and albuminuria in patients with T2DM.

2. Materials and Methods

This review was conducted in conformity with the *Cochrane Handbook for Systematic Reviews of Interventions* guidelines [15].

2.1. Literature Search. We searched the PubMed, MEDLINE, EMBASE, and Web of Science databases for publications in all languages until June 12, 2020. We searched these databases by using Medical Subject Headings terms and corresponding keywords including “diabetes,” “diabetic nephropathy,” “diabetic kidney disease,” “Retinol-binding protein,” “RBP-4,” “estimated glomerular filtration rate decline,” “renal function*” OR “kidney disease,” “renal dysfunction,” “renal failure,” “predictor*,” “correlated OR correlation,” and “biomarker*.”

2.2. Study Selection. Inclusion criteria are as follows: (i) patients: adults who had been diagnosed with T2DM according to the 1999 World Health Organization criteria [16]; (ii) intervention and comparator: DM with albuminuria/chronic kidney disease (CKD) and without albuminuria/CKD; in the random spot collection, having an albumin-to-creatinine ratio (ACR) of $<30 \mu\text{g}/\text{mg}$ was regarded as normal albuminuria, whereas $30\text{--}299 \mu\text{g}/\text{mg}$ was evaluated as microalbuminuria and $\geq 300 \mu\text{g}/\text{mg}$ was considered as macroalbuminuria [17]. The estimated glomerular filtration rate (eGFR) was determined by using the Modification of Diet in Renal Disease Formula (MDRD-GFR) [18]; (iii) outcomes: RBP4 concentrations or correlation analysis with RBP4 and eGFR/ACR; and (iv) study designs: randomized, controlled trial or case-control trial or cross-sectional study.

Exclusion criteria are as follows: (i) type 1 DM; (ii) patients with eGFR $< 15 \text{ mL}/\text{min}/1.73 \text{ m}^2$, on regular dialysis, with kidney transplantation, or with kidney disease other than DN; and (iii) patients with active inflammatory disease or a history of chronic disease of the pancreas and liver or other diseases.

2.3. Data Extraction. All of the search results were imported into the EndNote reference management software (Clarivate Analytics). Duplicate records were removed by the software and by manual checking. Two reviewers (L. Z. and S. X.)

independently screened the titles and abstracts of the remaining records for relevance against the protocol criteria and labeled these records as excluded, included, or uncertain. In cases of uncertainty, the full texts were retrieved to check the details. Any disagreements were resolved by consulting a third reviewer (Z.-G. X.). The risk of bias of the included studies was evaluated by using the relevant, validated tool for each study design, and the risk of bias assessment was independently confirmed.

2.4. Risk of Bias. Risk of bias of included trials was assessed using the Newcastle-Ottawa Scale (NOS) [19]. We assessed the publication bias by using Egger’s regression and Begg’s rank correlation analysis with Stata/SE software (version 15.0). A significance set at $P < 0.05$ indicated that there was a possibility of publication bias [15].

2.5. Statistical Analysis. Review Manager (RevMan) 5.3 software (Nordic Cochrane Centre) was used for analysis. We calculated the standardized mean difference (SMD) with 95% confidence intervals (CI) for continuous data when the applied scales were different. We conducted the heterogeneity test across studies using the I^2 statistic; $P < 0.1$ and $I^2 > 50\%$ indicated existing statistical significance. If there was obvious heterogeneity, we used a random-effects model; otherwise, we chose a fixed-effects model [20]. We performed sensitivity analysis by excluding one study at a time to test its influence on the pooled effects. Subgroup analysis was also used to reduce high levels of heterogeneity.

As the correlation coefficient r does not obey normal distribution, when $r > 0.5$, Fisher proposed “Fisher’s Z Transformation” to convert the correlation coefficient r into a normally distributed variable Z [21]. The formulae are as follows:

$$\text{Fisher's } Z = 0.5 * \ln \frac{1+r}{1-r}, \quad (1)$$

$$\text{SE} = \sqrt{\frac{1}{n-3}} \quad (n \text{ is the sample size}), \quad (2)$$

$$\text{Summary } r = \frac{e^{2Z} - 1}{e^{2Z} + 1} \quad (Z \text{ is the summary Fisher's } Z). \quad (3)$$

Data were converted by using Excel 2019 Software. Fisher’s Z value and the standard error (SE) were obtained by using formulae (1) and (2). The summary Fisher’s Z value was obtained by using the inverted variance method in RevMan 5.3 software [22]. Finally, the combined effect value of the correlation coefficient was obtained by using formula (3) to evaluate the strength of the correlation between RBP4 and DN. Generally, the range of absolute values of summary r is used to judge the strength of correlation of two variables: ≥ 0.8 is high correlation, $0.3\text{--}0.8$ is moderate correlation, and ≤ 0.3 is low correlation [21].

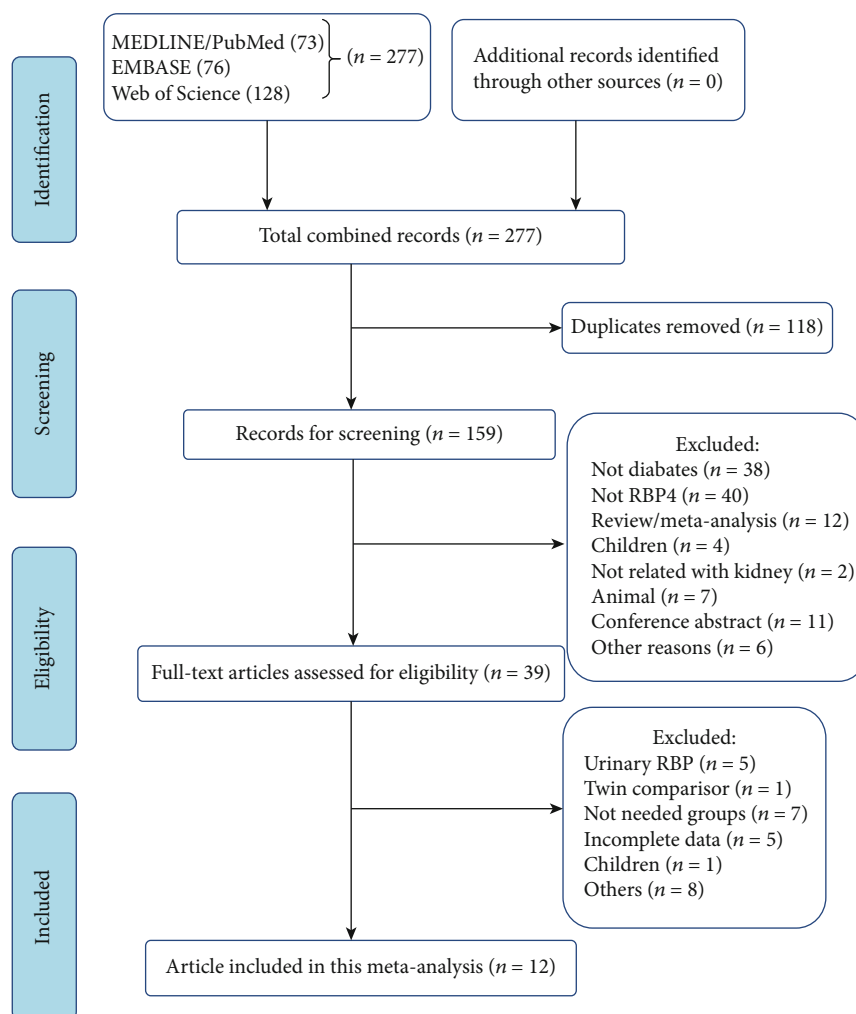


FIGURE 1: Flow chart of the study selection.

3. Results

3.1. Study Selection. We identified 277 articles by searching the PubMed, MEDLINE, EMBASE, and Web of Science databases. After excluding duplicated records and screening the abstracts, we obtained 26 articles. Finally, we included 12 cross-sectional studies in our review (Figure 1).

This meta-analysis included a total of 3847 participants. Two studies were conducted in Taiwan, China ($n = 350$) [23, 24], one in Serbia ($n = 106$) [25], one in Saudi Arabia ($n = 2177$) [26], one in Japan ($n = 58$) [27], one in Germany ($n = 97$) [14], one in the Republic of Korea ($n = 689$) [28], two in Turkey ($n = 170$) [13, 29], and three in Mainland China ($n = 382$) [30–32]. Quality assessment of the included studies was performed using the NOS (Table 1). The scores of all the studies were greater than five, confirming the good quality of the selected studies.

3.2. Albuminuria in DM. Five articles [13, 23, 26, 27, 30] reported normal albuminuria and micro+macro albuminuria in subjects with DM. Because the data of circulating RBP4 concentrations were on different scales, we selected SMD as a summary statistic in our analysis. The RBP4 concentrations

in the micro+macro albuminuria group were significantly higher than those in the normal albuminuria group in DM patients [$P = 0.001$, SMD 1.07, 95% CI (0.41, 1.73)] and showed significant heterogeneity (Figure 2(a)).

Six studies [14, 23, 26, 27, 30, 32], including 533 participants, reported circulating RBP4 concentrations in the microalbuminuria and normal albuminuria groups. The results of the analysis showed that the RBP4 concentrations in the microalbuminuria group were significantly higher than those in the normal albuminuria group of DM patients [$P = 0.005$, SMD 0.73, 95% CI (0.22, 1.25)] (Figure 2(b)). Four studies [23, 26, 27, 30], including 264 participants, reported RBP4 concentrations in the macroalbuminuria and microalbuminuria groups. There was a significant difference between the RBP4 concentrations in the macroalbuminuria and microalbuminuria groups [$P = 0.005$, SMD 0.73, 95% CI (0.22, 1.25)] (Figure 2(c)). Compared with RBP4 concentrations in the normal control group (non-DM), the circulating RBP4 concentrations in the macroalbuminuria and microalbuminuria groups were elevated ($P = 0.005$, $P = 0.04$, respectively). However, there was no significant difference in the RBP4 levels between the normal albuminuria DM group and the non-DM group.

TABLE 1: Characteristics of included studies.

Author	Year	Country/region	Sample size	Sex (female/total)		Age (year, mean \pm SD)		Method	Sample	NOS
				DM	Control	DM	Control			
Akbay	2010	Turkey	83	28/53	21/31	54.8 \pm 8.2	45.6 \pm 12.8	ELISA	Serum	7
Chang	2008	Taiwan, China	111	54/95	11/16	63.5 \pm 11.6	61.3 \pm 5.4	ELISA	Serum	8
Chu	2011	Taiwan, China	239	22/86	63/153	70 \pm 11*	60 \pm 12*	ELISA	Serum	8
Klasic	2020	Serbia	106	24/40	41/66	62.72 \pm 8.31*	63.88 \pm 5.13*	ELISA	Serum	7
Mahfouz	2016	Saudi Arabia	200	91/150	35/50	55 \pm 6.2	45.1 \pm 4.8	ELISA	Serum	7
Masaki	2008	Japan	58	24/48	NA	59.9 \pm 13.3	NA	ELISA	Plasma	7
Ni	2018	Mainland China	192	69/172	13/20	59.3 \pm 13.6	58.0 \pm 12.3	ELISA	Serum	8
Park	2014	Republic of Korea	689	239/471	41/75	63.13 \pm 9.93	40.28 \pm 0.98	ELISA	Serum	8
Raila	2007	Germany	97	32/62	21/35	NA	49 (21-71) [#]	ELISA	Plasma	7
Toruner	2011	Turkey	87	22/39	27/48	57.8 \pm 10.0	56.3 \pm 9.9	ELISA	Serum	7
Wang	2013	Mainland China	190	37/120	NA	61.52 \pm 14.07	NA	ELISA	Plasma	6
Xu	2017	Mainland China	1795	303/524	479/763	62.6 \pm 9.3	61.2 \pm 9.9	ELISA	Serum	8

Abbreviations: DM: diabetes mellitus; NOS: Newcastle-Ottawa Scale; ELISA: enzyme-linked immunosorbent assay; NA: not available. Note: *DM means DM with CKD, control means DM without CKD. [#]Data was expressed as median (range).

3.3. Chronic Kidney Disease. Four trials, including 490 participants, reported the circulating RBP4 concentrations in the DM with CKD and DM without CKD groups [23, 25, 27, 29]. There was a significant difference in the RBP4 concentrations in the DM with CKD group compared with those in the DM without CKD group (Figure 3) [$P = 0.0009$, SMD 2.14, 95% CI (0.88, 3.40)].

3.4. Correlation Analysis between RBP4 and Kidney Disease. To explore the relationship between circulating RBP4 concentration and kidney diseases, we performed a correlation analysis between RBP4 and eGFR/ACR.

3.4.1. RBP4 and eGFR. Seven trials [24–29, 32] had performed correlation analysis between circulating RBP4 concentrations and eGFR. We found that eGFR (total $n = 1254$; Figure 4(a)) was negatively correlated with serum RBP4 concentrations in patients with T2DM [summary Fisher's $Z = -0.48$, 95% CI (-0.69, -0.26), $P < 0.0001$]. The summary r was -0.45, indicating moderate correlation.

3.4.2. RBP4 and ACR. Five trials [24, 26, 28, 29, 31] performed correlation analysis between serum RBP4 concentrations and ACR. It was found that ACR (total $n = 2072$; Figure 4(b)) was positively correlated with circulating RBP4 concentrations in patients with T2DM [summary Fisher's $Z = 0.20$, 95% CI (0.08, 0.32), $P = 0.001$]. The summary r was 0.20, indicating low correlation.

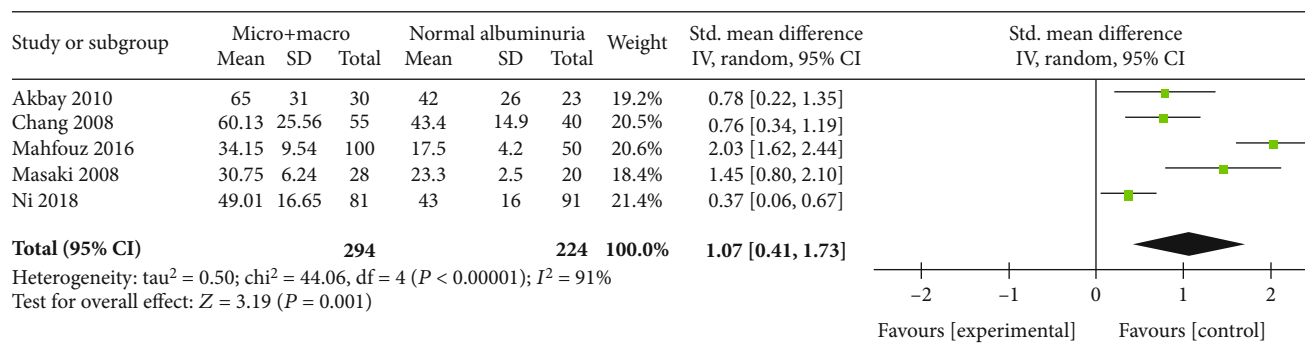
3.5. Publication Bias. Egger's regression and Begg's rank correlation analysis were performed to evaluate publication bias (Table 2). The P values of all factors in the analysis were greater than 0.05, indicating the absence of publication bias.

3.6. Sensitivity Analysis and Subgroup Analysis. There was significant heterogeneity in all factors. We performed leave-one-out sensitivity analysis to find possible reasons for this heterogeneity. The heterogeneity of only two comparisons

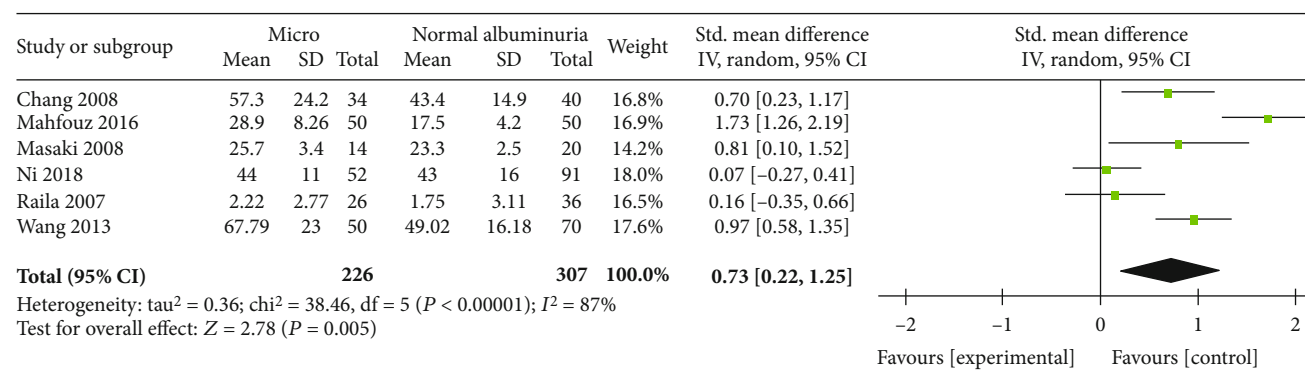
can be obviously reduced when a single study is excluded. After excluding the study by Mahfouz et al. [26], I^2 of heterogeneity was reduced to 29% in the comparison of RBP4 concentrations in the macroalbuminuria and normal control groups (Figure 5(a)) and to 20% in the correlation analysis between RBP4 and ACR (Figure 5(b)). In the correlation analysis of eGFR and RBP4, we performed subgroup analysis according to whether the sample number n was greater than 100 or whether the sample was serum or plasma (Figures 6(a) and 6(b)). However, we did not find the reasons for the observed heterogeneity. This was true even for other comparisons in this meta-analysis (data not shown). However, excluding each study, one by one, did not significantly change the results, indicating that the combined results were stable.

4. Discussion

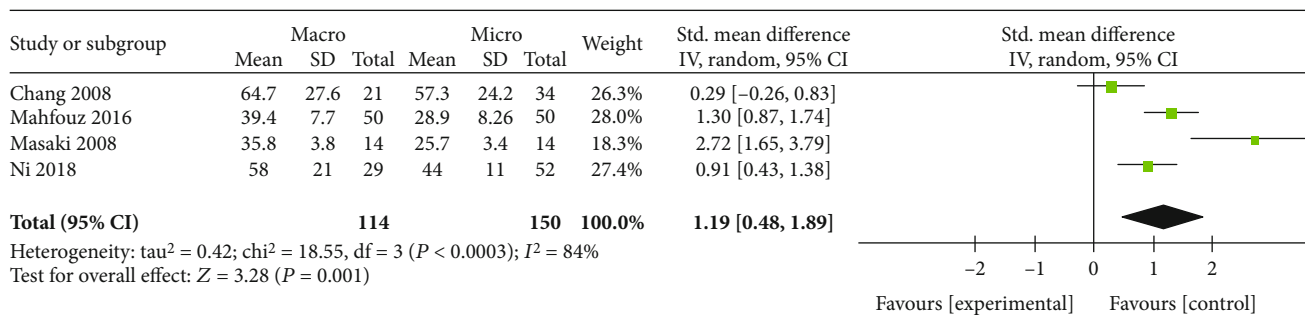
In this meta-analysis, we found that RBP4 levels were significantly elevated in the micro-, macro-, and micro+macro albuminuria groups compared with those in the normal albuminuria group of subjects with T2DM. Compared with the non-DM control, the concentrations of RBP4 were increased in the microalbuminuria and macroalbuminuria DM groups but were similar in the normal albuminuria DM group. This observation was not consistent with the findings of several studies that had demonstrated that RBP4 was associated with early diabetes even with isolated impairment of glucose tolerance [31, 32]. This could be attributed to the fact that the subjects in both the non-DM and DM groups were obese [13]. Graham et al. [33] and Frey et al. [34] had previously reported that the mean circulating RBP4 concentrations were comparable in the non-DM obese and DM obese subjects. In addition, Wang et al. [32] had speculated that the lack of any significant difference between plasma RBP4 levels of T2DM patients and normal control subjects could be because the patients with simple T2DM had been recently diagnosed



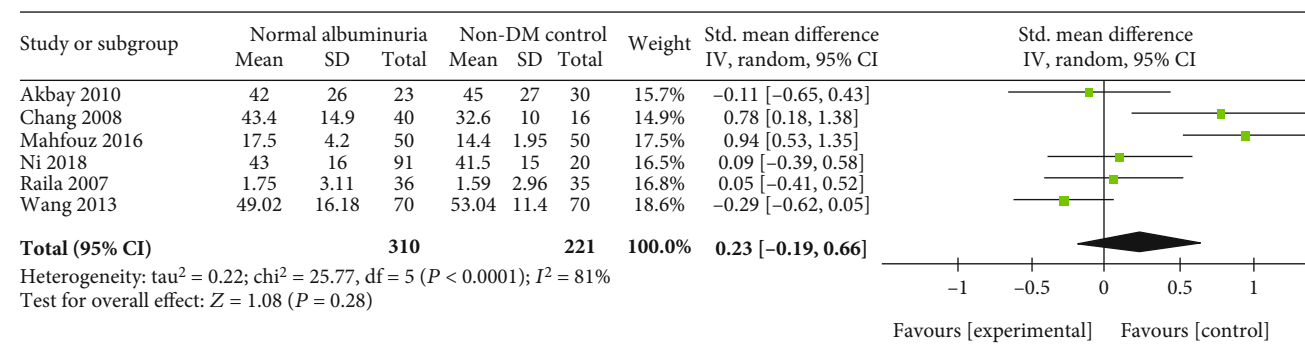
(a) Micro + macro vs normal albuminuria in DM



(b) Micro vs normal albuminuria in DM

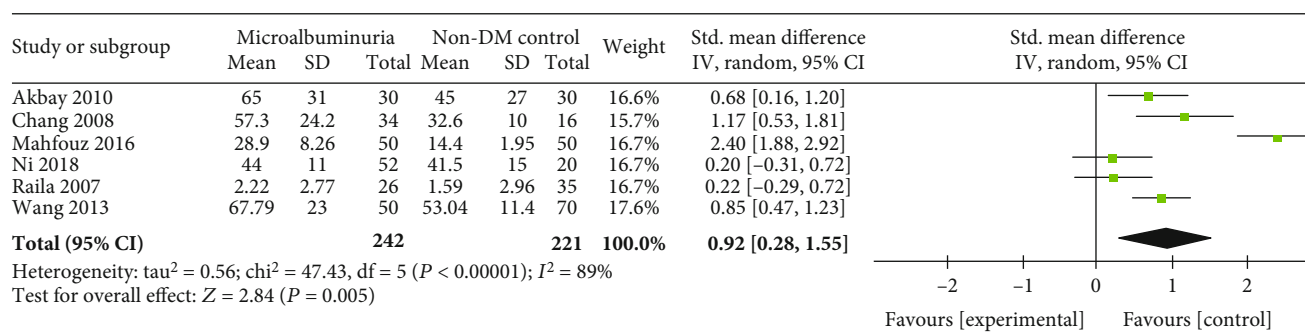


(c) Macro vs micro albuminuria in DM

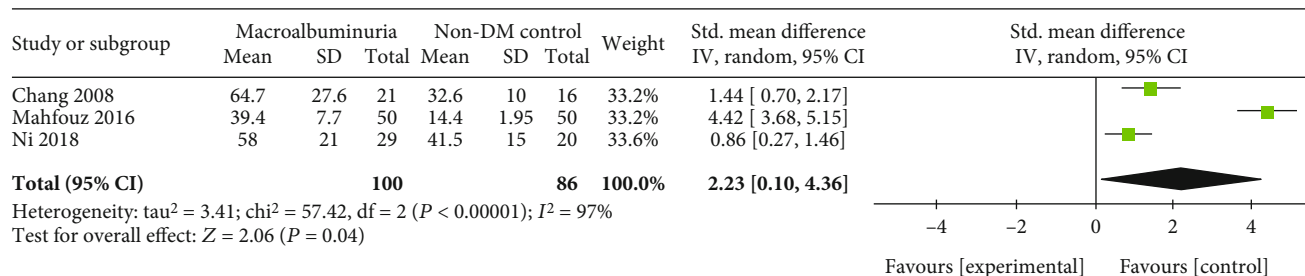


(d) DM with normal albuminuria vs non-DM control

FIGURE 2: Continued.



(e) DM with microalbuminuria vs non-DM control



(f) DM with macroalbuminuria vs non-DM control

FIGURE 2: Meta-analysis forest plot of different albuminuria in DM.

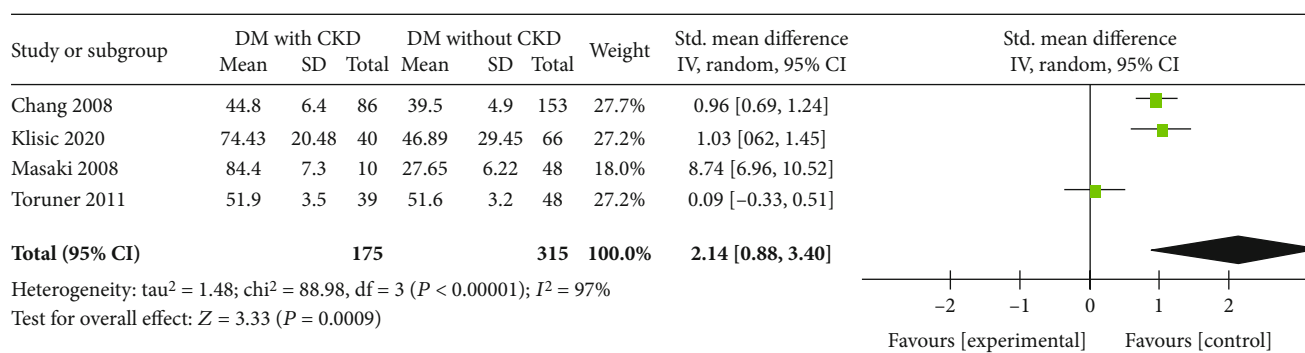


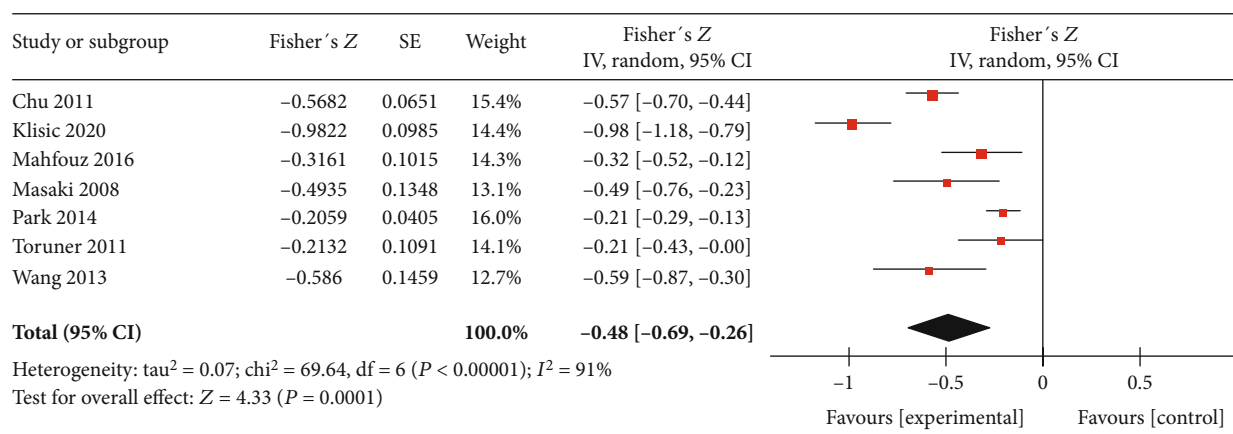
FIGURE 3: Meta-analysis forest plot of the circulating RBP4 concentrations in the DM with CKD and DM without CKD groups.

and might have a relatively short duration of insulin resistance (IR). Thus, the presence of albuminuria was an independent determinant for elevated circulating RBP4 levels in diabetic patients [13].

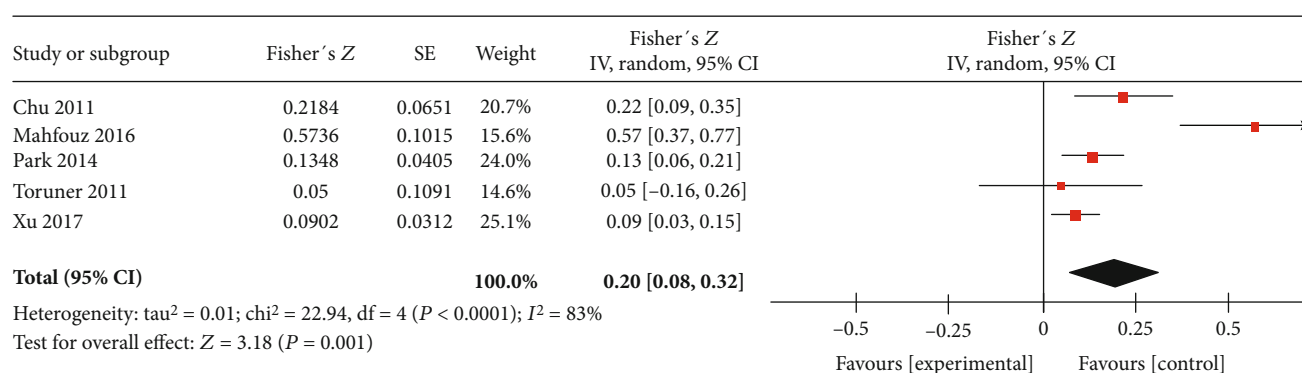
RBP4 levels have been found to be significantly increased in a T2DM group with CKD and low eGFR compared with the non-CKD group of subjects with T2DM in this article. Levels of adipocytokines, such as adiponectin and leptin, were elevated in renal failure [35–37]. Similarly, circulating RBP4 levels in subjects with T2DM and advanced kidney diseases were significantly higher than those in patients without kidney diseases [27]. One explanation is that reduced clearance or catabolism of RBP4 by the kidney may result in the accumulation of RBP4 in circulation [27]. Moreover, multiple stepwise linear regressions in the study by Chang et al. [23] for RBP4 after adjustment for age and gender showed

that eGFR was independently and negatively correlated with serum RBP4 levels in subjects with T2DM ($\beta = -0.003$, $P < 0.001$). Thus, eGFR is another independent determinant for elevated circulating RBP4 levels in diabetic patients.

Furthermore, a strong correlation was reported between eGFR/ACR and circulating RBP4 concentrations in subjects with T2DM in our article. This is consistent with the results of the meta-analysis by Park et al. [38] in which they found two studies that reported that the creatinine clearance rate and eGFR were negatively correlated with RBP4 levels and that creatinine levels were positively correlated with serum RBP4 levels [38]. The summary correlation coefficient for eGFR was -0.39 (95% CI $(-0.44, -0.33)$) in the study by Park et al. [38], which is similar to -0.48 (95% CI $(-0.69, -0.26)$) reported by us. However, Park et al. [38] did not show any correlation between ACR and circulating RBP4 levels. Our



(a) Correlation between RBP4 and eGFR



(b) Correlation between RBP4 and ACR

FIGURE 4: Meta-analysis forest plot of correlation between RBP4 and eGFR (a) and between RBP4 and ACR (b).

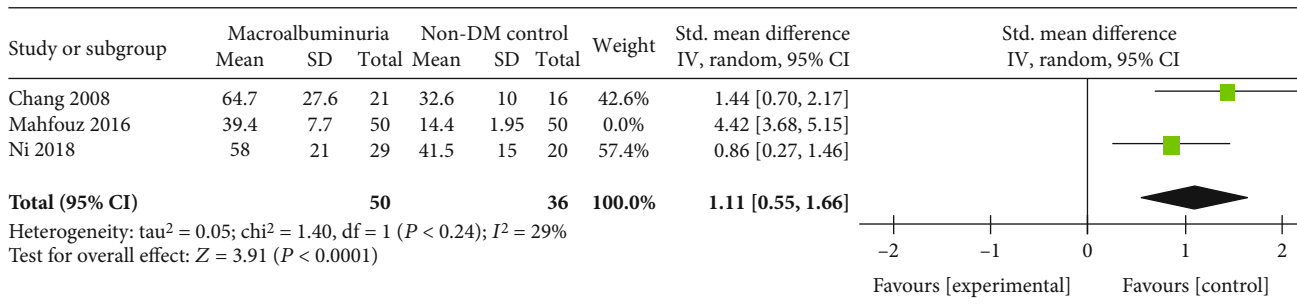
TABLE 2: Egger's test and Begg's test for publication bias.

Factors	<i>t</i>	<i>P</i>	Egger's test		Begg's test <i>P</i> > <i>Z</i>
				95% CI	
Micro- vs. normal albuminuria	0.58	0.593	-12.5805	19.23444	1.00
Micro+macro- vs. normal albuminuria	0.89	0.439	-13.51018	24.01409	0.462
Micro- vs. macroalbuminuria	0.90	0.464	-16.12686	24.6385	1.000
Normal albuminuria vs. control	0.82	0.460	-9.797105	17.95984	0.707
Microalbuminuria vs. control	0.22	0.837	-22.71148	26.60553	0.707
Macroalbuminuria vs. control	0.92	0.526	-375.3805	434.11	0.296
CKD vs. non-CKD	1.68	0.236	-13.13514	29.90505	0.734

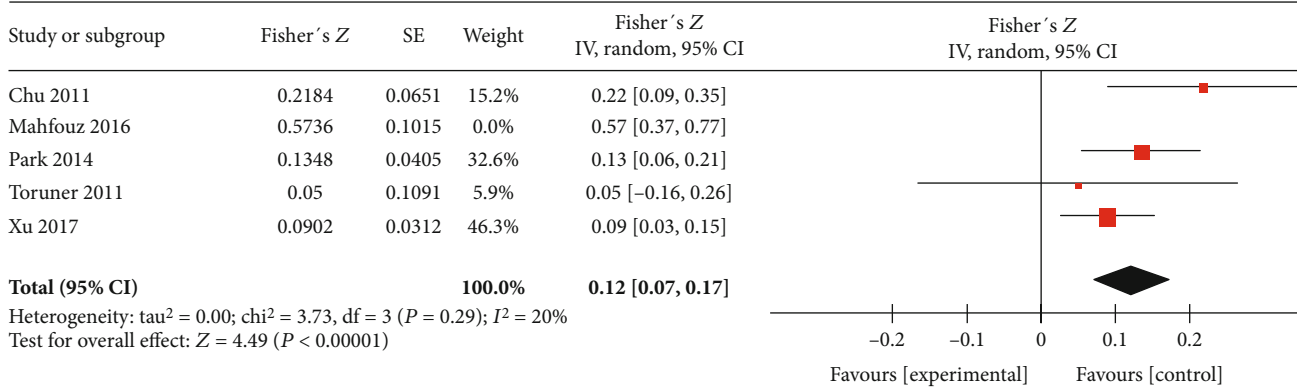
analysis showed a poor correlation between RBP4 concentrations and ACR with a summary correlation coefficient of 0.20. Better correlation was observed between circulating RBP4 levels and eGFR than with ACR.

Albuminuria and renal dysfunction are the most common clinical manifestations of DN in patients with T2DM. Our meta-analysis revealed that circulating RBP4 levels were elevated only in patients with diabetic kidney diseases, rather than in simple diabetes subjects without DN. There may be two reasons to explain these differences in circulating RBP4 levels in diabetic subjects with and without kidney diseases.

First, hepatocytes and adipocytes are important sites of synthesis of RBP4, whereas the kidneys are important sites of catabolism of circulating RBP4 [39]. Maintenance of retinol homeostasis throughout the body is mediated by filtration through the glomeruli and subsequent reabsorption of RBP4 in the proximal tubule tissues. Thus, reduced catabolism resulting from microvascular damage in the kidney leads to a gradual elevation in the plasma RBP4 concentration and hence to higher levels in subjects with DN than in T2DM patients without DN. Second, RBP4 is a novel adipokine whose increased circulating levels are linked to IR in patients



(a) Macro albuminuria and control



(b) Correlation between RBP-4 and ACR

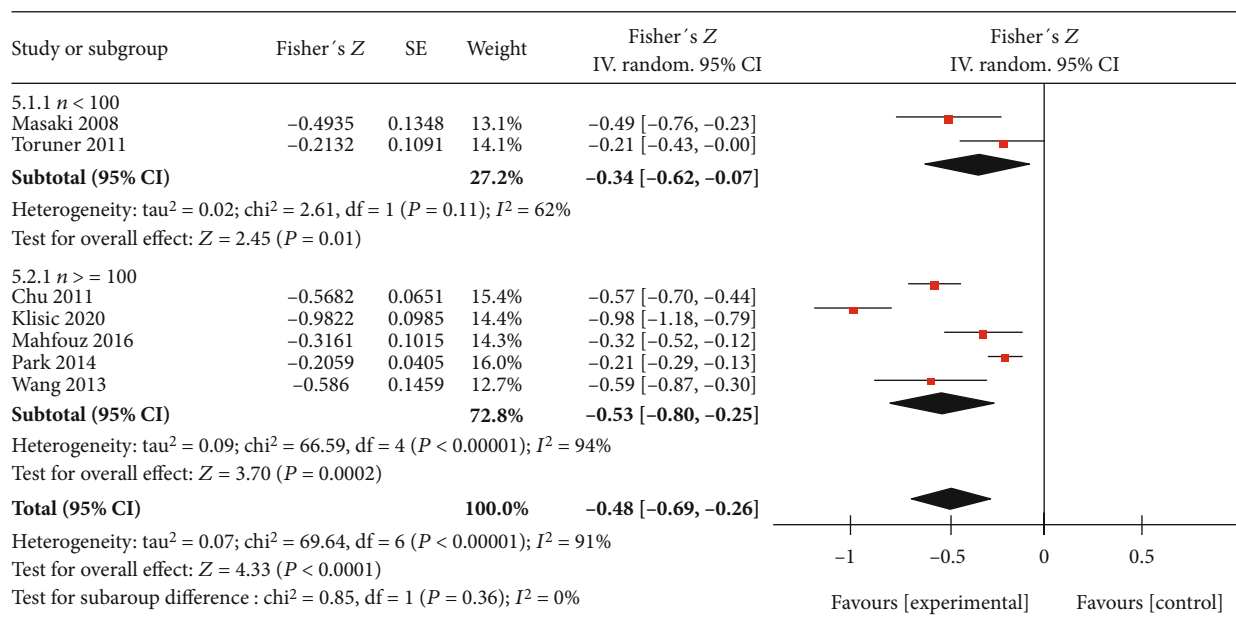
FIGURE 5: Meta-analysis forest plot sensitivity analysis.

with diabetic kidney diseases [33]. This can be attributed to increased synthesis of the gluconeogenic enzyme, phosphoenolpyruvate carboxykinase, and glucose transporter-4, inhibition of insulin signaling, and impairment of glucose uptake in skeletal muscle cells, leading to higher glucose production in the liver [7, 30]. Thus, the development of IR may cause the deterioration of microvascular injury in the kidneys and lead to further decline in renal function [31]. Moreover, in Park et al.'s study, higher circulating RBP4 levels were accompanied by increased urinary RBP4 levels [28] with a correlation coefficient of 0.132 ($P = 0.001$). However, this relationship between serum and urinary RBP4 concentrations needs to be investigated further. The present meta-analysis revealed that circulating RBP4 levels were associated with renal dysfunction related to DM, which should be further investigated experimentally.

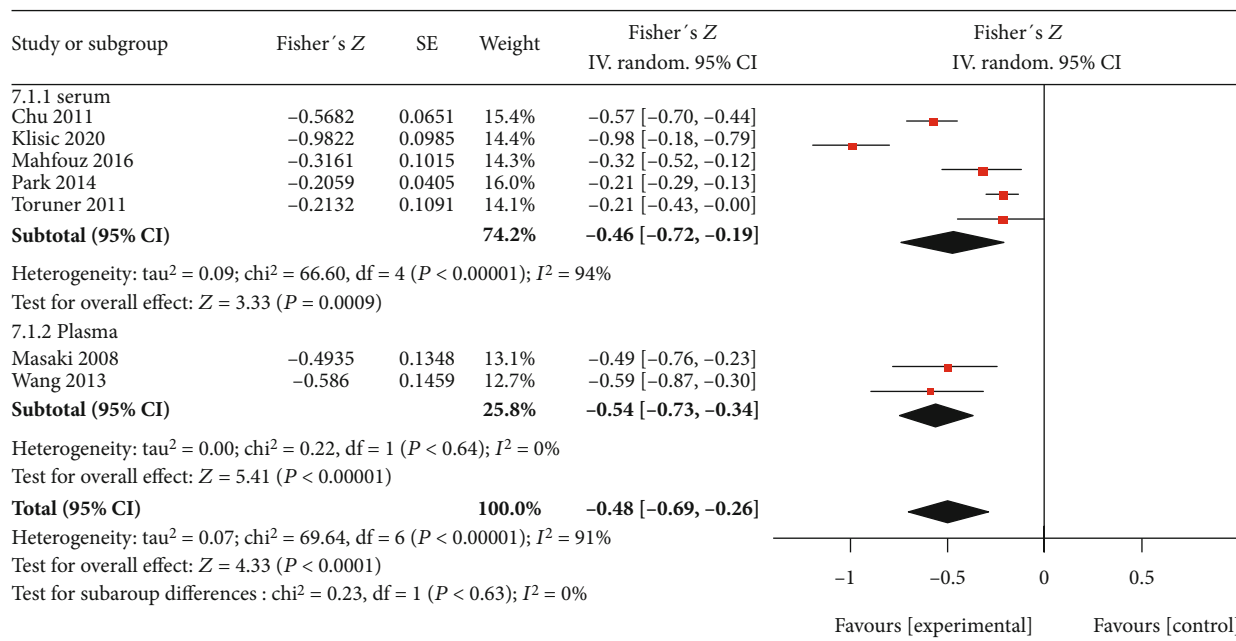
Moreover, many researchers have explored the role of RBP4 in DM and other diseases. Li et al. [40] reported that plasma RBP4 levels were correlated with the incidence of diabetic retinopathy. They deduced that RBP4 may play a role in the pathogenesis of diabetic retinopathy and that lowering RBP4 levels may be a novel treatment strategy for diabetic retinopathy. Li et al. [41] found that childhood RBP4 levels were correlated with the 10-year risk estimates for IR and metabolic syndrome and that RBP4 may be an early biomarker for metabolic syndrome. Fan et al. [42] showed that the relationship between serum RBP4 levels and the risk of incident T2DM in subjects with prediabetes was U-shaped,

with even low RBP4 concentrations being associated with an elevated risk of DM in subjects with prediabetes. Habashy et al. [43] showed that plasma RBP4 levels were not elevated in DM patients, whereas the RBP4-to-retinol ratio was increased. Furthermore, Wessel et al. [44] found that plasma RBP4 levels were correlated with levels of large very low-density lipoprotein cholesterol and small low-density lipoprotein particles, indicating a possible involvement of RBP4 in the proatherogenic plasma lipoprotein profiles in subjects with T2DM and even without T2DM. Wang et al. [45] showed that higher levels of serum RBP4 could be a predictor for poor metabolic control in subjects with T2DM and were related to an increased risk of hypertension and dyslipidemia. Several other studies have shown that RBP4 concentrations were correlated with incident cardiovascular diseases [46–49]. Some studies have reported the correlation between RBP4 and obesity [49–51] as well as nonalcoholic fatty liver disease [52–55]. Thus, RBP4 may play a more important role in a variety of metabolism-related diseases than we thought earlier.

This meta-analysis is the first to present the role of circulating RBP4 in kidney diseases in subjects with T2DM. Most of the trials included in the analysis were of high quality. Moreover, there was no publication bias in any of the comparisons. However, there were some limitations of our study. Firstly, the sample size was small, and some critical data had not been presented in the publications. For example, only one study performed ROC analysis of



(a)



(b)

FIGURE 6: Subgroup analysis.

prediction for eGFR [25] and another one for albuminuria [26]. Hence, we could not perform a pooled analysis for sensitivity and specificity in the diagnosis of eGFR and albuminuria. Secondly, the heterogeneity in this meta-analysis was obvious, although the sensitivity analysis indicated that the results were stable. The serum or plasma RBP4 concentrations had been measured by using different reagent kits, and the diagnostic thresholds of the various studies were not consistent. Additionally, there were some differences in the inclusion criteria of each study. All of these aspects may contribute to the heterogeneity

in our results. Finally, all of the included studies were cross-sectional. To address the effects of RBP4 levels on the development of DN, we need more prospective longitudinal studies.

In summary, the levels of circulating RBP4 were significantly higher both in T2DM subjects with micro/macroalbuminuria and in T2DM subjects with declined eGFR. The levels of circulating RBP4 were positively correlated with ACR but negatively correlated with eGFR. Circulating RBP4 could be a reliable biomarker for kidney diseases in T2DM.

Data Availability

All relevant data are within the manuscript and its supporting information files.

Conflicts of Interest

The authors declare that there is no conflict of interest regarding the publication of this paper.

Authors' Contributions

L. Zhang and S. Xue searched for the articles and assessed the search results. Any disagreement was resolved through discussion or by consulting with Z.-G. Xu. L. Zhang evaluated the risk of bias in each included study. Y.L. Cheng checked the risk of bias in the assessment. L. Zhang and S. Xue wrote the manuscript. S. Xue and Y.L. Cheng were responsible for the intellectual content in the revision of the manuscript. All authors gave their final approval for the submitted version.

Supplementary Materials

Appendix: full search strategy of PubMed/MEDLINE. (*Supplementary Materials*)

References

- [1] G. G. Nair, E. S. Tzanakakis, and M. Hebrok, "Emerging routes to the generation of functional β -cells for diabetes mellitus cell therapy," *Nature Reviews Endocrinology*, vol. 16, no. 9, pp. 506–518, 2020.
- [2] T. Ninomiya, V. Perkovic, B. E. de Galan et al., "Albuminuria and kidney function independently predict cardiovascular and renal outcomes in diabetes," *Journal of the American Society of Nephrology*, vol. 20, no. 8, pp. 1813–1821, 2009.
- [3] S. Vijay, A. Hamide, G. P. Senthilkumar, and V. Mehalingam, "Utility of urinary biomarkers as a diagnostic tool for early diabetic nephropathy in patients with type 2 diabetes mellitus," *Diabetes and Metabolic Syndrome: Clinical Research and Reviews*, vol. 12, no. 5, pp. 649–652, 2018.
- [4] G. Targher, G. Zoppi, M. Chonchol et al., "Glomerular filtration rate, albuminuria and risk of cardiovascular and all-cause mortality in type 2 diabetic individuals," *Nutrition, Metabolism, and Cardiovascular Diseases*, vol. 21, no. 4, pp. 294–301, 2010.
- [5] S. Hu, Q. Liu, X. Huang, and H. Tan, "Serum level and polymorphisms of retinol-binding protein-4 and risk for gestational diabetes mellitus: a meta-analysis," *BMC Pregnancy and Childbirth*, vol. 16, no. 1, p. 52, 2016.
- [6] W. S. Blamer, "Retinol-binding protein: the serum transport protein for vitamin A," *Endocrine Reviews*, vol. 10, p. 3, 1989.
- [7] Q. Yang, T. E. Graham, N. Mody et al., "Serum retinol binding protein 4 contributes to insulin resistance in obesity and type 2 diabetes," *Nature*, vol. 436, no. 7049, pp. 356–362, 2005.
- [8] P. Balagopal, T. E. Graham, B. B. Kahn, A. Altomare, V. Funanage, and D. George, "Reduction of elevated serum retinol binding protein in obese children by lifestyle intervention: association with subclinical inflammation," *The Journal of Clinical Endocrinology and Metabolism*, vol. 92, no. 5, pp. 1971–1974, 2007.
- [9] W. Jia, H. Wu, Y. Bao et al., "Association of serum retinol-binding protein 4 and visceral adiposity in Chinese subjects with and without type 2 diabetes," *The Journal of Clinical Endocrinology and Metabolism*, vol. 92, no. 8, pp. 3224–3229, 2007.
- [10] Q. Qi, Z. Yu, X. Ye et al., "Elevated retinol-binding protein 4 levels are associated with metabolic syndrome in Chinese people," *The Journal of Clinical Endocrinology and Metabolism*, vol. 92, no. 12, pp. 4827–4834, 2007.
- [11] A. Cabré, I. Lázaro, J. Girona et al., "Retinol-binding protein 4 as a plasma biomarker of renal dysfunction and cardiovascular disease in type 2 diabetes," *Journal of Internal Medicine*, vol. 262, no. 4, pp. 496–503, 2007.
- [12] M. Murata, T. Saito, T. Otani et al., "An increase in serum retinol-binding protein 4 in the type 2 diabetic subjects with nephropathy," *Endocrine Journal*, vol. 56, no. 2, pp. 287–294, 2009.
- [13] E. Akbay, N. Muslu, E. Nayir, O. Ozhan, and A. Kiykim, "Serum retinol binding protein 4 level is related with renal functions in type 2 diabetes," *Journal of Endocrinological Investigation*, vol. 33, no. 10, pp. 725–729, 2010.
- [14] J. Raila, A. Henze, J. Spranger, M. Mohlig, A. F. Pfeiffer, and F. J. Schweigert, "Microalbuminuria is a major determinant of elevated plasma retinol-binding protein 4 in type 2 diabetic patients," *Kidney International*, vol. 72, no. 4, pp. 505–511, 2007.
- [15] T. J. Higgins Julian, *Cochrane Handbook for Systematic Reviews of Interventions*, Cochrane Collaboration, 2019, Version 6.
- [16] The ADVANCE Collaborative Group, "Intensive blood glucose control and vascular outcomes in patients with type 2 diabetes," *The New England Journal of Medicine*, vol. 358, pp. 2560–2572, 2008.
- [17] Association AD, "Standards of medical care in diabetes," *Diabetes Care*, vol. 32, pp. S13–S61, 2009.
- [18] S. Andrew, J. P. Bosch, J. B. Lewis et al., "A more accurate method to estimate glomerular filtration rate from serum creatinine: a new prediction equation," *Annals of Internal Medicine*, vol. 130, pp. 461–470, 1999.
- [19] G. S. B. Wells, D. O'Connell, and J. Peterson, *The Newcastle-Ottawa Scale (NOS) for assessing the quality of nonrandomised studies in meta-analyses*, 2018.
- [20] J. P. T. Higgins, S. G. Thompson, J. J. Deeks, and D. G. Altman, "Measuring inconsistency in meta-analyses," *BMJ*, vol. 327, no. 7414, pp. 557–560, 2003.
- [21] M. Borenstein, L. V. Hedges, J. P. Higgins, and H. R. Rothstein, *Introduction to Meta-Analysis*, 2009.
- [22] I. Tsiglianni, J. Kocks, N. Tzanakis, N. Sifakakis, and T. van der Molen, "Factors that influence disease-specific quality of life or health status in patients with COPD: a review and meta-analysis of Pearson correlations," *Primary Care Respiratory Journal*, vol. 20, no. 3, pp. 257–268, 2011.
- [23] Y. H. Chang, K. D. Lin, C. L. Wang, M. C. Hsieh, P. J. Hsiao, and S. J. Shin, "Elevated serum retinol-binding protein 4 concentrations are associated with renal dysfunction and uric acid in type 2 diabetic patients," *Diabetes/Metabolism Research and Reviews*, vol. 24, no. 8, pp. 629–634, 2008.
- [24] C.-H. Chu, H.-C. Lam, J.-K. Lee et al., "Elevated serum retinol-binding protein 4 concentrations are associated with chronic

- kidney disease but not with the higher carotid intima-media thickness in type 2 diabetic subjects," *Endocrine Journal*, vol. 58, no. 10, pp. 841–847, 2011.
- [25] A. Klisic, N. Kavacic, and A. Ninic, "Retinol-binding protein 4 versus albuminuria as predictors of estimated glomerular filtration rate decline in patients with type 2 diabetes," *Journal of Research in Medical Sciences : The Official Journal of Isfahan University of Medical Sciences*, vol. 23, no. 1, p. 44, 2018.
- [26] M. H. Mahfouz, A. M. Assiri, and M. H. Mukhtar, "Assessment of neutrophil gelatinase-associated lipocalin (NGAL) and retinol-binding protein 4 (RBP4) in type 2 diabetic patients with nephropathy," *Biomarker Insights*, vol. 11, pp. 31–40, 2016.
- [27] T. Masaki, F. Anan, T. Tsubone et al., "Retinol binding protein 4 concentrations are influenced by renal function in patients with type 2 diabetes mellitus," *Metabolism*, vol. 57, no. 10, pp. 1340–1344, 2008.
- [28] S. E. Park, N. S. Lee, J. W. Park et al., "Association of urinary RBP4 with insulin resistance, inflammation, and microalbuminuria," *European Journal of Endocrinology*, vol. 171, no. 4, pp. 443–449, 2014.
- [29] F. Toruner, A. E. Altinova, M. Akturk et al., "The relationship between adipocyte fatty acid binding protein-4, retinol binding protein-4 levels and early diabetic nephropathy in patients with type 2 diabetes," *Diabetes Research and Clinical Practice*, vol. 91, no. 2, pp. 203–207, 2011.
- [30] X. Ni, Y. Gu, H. Yu et al., "Serum adipocyte fatty acid-binding protein 4 levels are independently associated with radioisotope glomerular filtration rate in type 2 diabetic patients with early diabetic nephropathy," *BioMed Research International*, vol. 2018, Article ID 4578140, 9 pages, 2018.
- [31] M. Xu, X. Y. Li, J. G. Wang et al., "Retinol-binding protein 4 is associated with impaired glucose regulation and microalbuminuria in a Chinese population," *Diabetologia*, vol. 52, no. 8, pp. 1511–1519, 2009.
- [32] W. Junjun, W. Jia, S. Jiayi et al., "Associations of RBP4 with lipid metabolism and renal function in diabetes mellitus," *European Journal of Lipid Science and Technology*, vol. 115, no. 8, pp. 831–837, 2013.
- [33] T. E. Graham, Q. Yang, M. Blüher et al., "Retinol-binding protein 4 and insulin resistance in lean, obese, and diabetic subjects," *The New England Journal of Medicine*, vol. 354, no. 24, pp. 2552–2563, 2006.
- [34] S. K. Frey, J. Spranger, A. Henze, A. F. Pfeiffer, F. J. Schweigert, and J. Raila, "Factors that influence retinol-binding protein 4-transferrin interaction are not altered in overweight subjects and overweight subjects with type 2 diabetes mellitus," *Metabolism*, vol. 58, no. 10, pp. 1386–1392, 2009.
- [35] T. Shoji, K. Shinohara, S. Hatsuda et al., "Altered relationship between body fat and plasma adiponectin in end-stage renal disease," *Metabolism*, vol. 54, no. 3, pp. 330–334, 2005.
- [36] B. Fruehwald-Schultes, W. Kern, J. Beyer, T. Forst, A. Pfützner, and A. Peters, "Elevated serum leptin concentrations in type 2 diabetic patients with microalbuminuria and macroalbuminuria," *Metabolism*, vol. 48, no. 10, pp. 1290–1293, 1999.
- [37] J. Axelsson, A. Bergsten, A. R. Qureshi et al., "Elevated resistin levels in chronic kidney disease are associated with decreased glomerular filtration rate and inflammation, but not with insulin resistance," *Kidney International*, vol. 69, no. 3, pp. 596–604, 2006.
- [38] H. Park, M. H. Green, and M. L. Shaffer, "Association between serum retinol-binding protein 4 concentrations and clinical indices in subjects with type 2 diabetes: a meta-analysis," *Journal of Human Nutrition and Dietetics*, vol. 25, no. 4, pp. 300–310, 2012.
- [39] M. Marinó, D. Andrews, D. Brown, and R. T. McCluskey, "Transcytosis of retinol-binding protein across renal proximal tubule cells after megalin (gp 330)-mediated endocytosis," *Journal of the American Society of Nephrology*, vol. 12, no. 4, pp. 637–648, 2001.
- [40] J.-Y. Li, X. X. Chen, X. H. Lu, C. B. Zhang, Q. P. Shi, and L. Feng, "Elevated RBP4 plasma levels were associated with diabetic retinopathy in type 2 diabetes," *Bioscience Reports*, vol. 38, no. 5, 2018.
- [41] G. Li, I. C. Esangbedo, L. Xu et al., "Childhood retinol-binding protein 4 (RBP4) levels predicting the 10-year risk of insulin resistance and metabolic syndrome: the BCAMS study," *Cardiovascular Diabetology*, vol. 17, no. 1, p. 69, 2018.
- [42] J. Fan, S. Yin, D. Lin et al., "Association of serum retinol-binding protein 4 levels and the risk of incident type 2 diabetes in subjects with prediabetes," *Diabetes Care*, vol. 42, no. 8, pp. 1574–1581, 2019.
- [43] S. el Habashy, A. Adly, M. Kader, and S. Ali, "Predictors of future microalbuminuria in children and adolescents with type 1 diabetes mellitus in Egypt," *Archives of Medical Science - Atherosclerotic Diseases*, vol. 4, no. 1, pp. 286–297, 2019.
- [44] H. Wessel, A. Saeed, J. Heegsma, M. A. Connelly, K. N. Faber, and R. P. F. Dullaart, "Plasma levels of retinol binding protein 4 relate to large VLDL and small LDL particles in subjects with and without type 2 diabetes," *Journal of Clinical Medicine*, vol. 8, no. 11, p. 1792, 2019.
- [45] M. N. Wang, Y. Han, Q. Li et al., "Higher serum retinol binding protein 4 may be a predictor of weak metabolic control in Chinese patients with type 2 diabetes mellitus," *Journal of International Medical Research*, vol. 40, no. 4, pp. 1317–1324, 2012.
- [46] Z. Mallat, T. Simon, J. Benessiano et al., "Retinol-binding protein 4 and prediction of incident coronary events in healthy men and women," *The Journal of Clinical Endocrinology and Metabolism*, vol. 94, no. 1, pp. 255–260, 2009.
- [47] Q. Sun, U. A. Kiernan, L. Shi et al., "Plasma retinol-binding protein 4 (RBP4) levels and risk of coronary heart disease: a prospective analysis among women in the nurses' health study," *Circulation*, vol. 127, no. 19, pp. 1938–1947, 2013.
- [48] Y. Liu, Y. Zhong, H. Chen et al., "Retinol-binding protein-dependent cholesterol uptake regulates macrophage foam cell formation and promotes atherosclerosis," *Circulation*, vol. 135, no. 14, pp. 1339–1354, 2017.
- [49] T. Olsen and R. Blomhoff, "Retinol, retinoic acid, and retinol-binding protein 4 are differentially associated with cardiovascular disease, type 2 diabetes, and obesity: an overview of human studies," *Advances in Nutrition*, vol. 11, no. 3, pp. 644–666, 2020.
- [50] N. Klötting, T. E. Graham, J. Berndt et al., "Serum retinol-binding protein is more highly expressed in visceral than in subcutaneous adipose tissue and is a marker of intra-abdominal fat mass," *Cell Metabolism*, vol. 6, no. 1, pp. 79–87, 2007.
- [51] M. Hogstrom, A. Nordstrom, and P. Nordstrom, "Retinol, retinol-binding protein 4, abdominal fat mass, peak bone mineral density, and markers of bone metabolism in men: the

- Northern Osteoporosis and Obesity (NO2) study,” *European Journal of Endocrinology*, vol. 158, no. 5, pp. 765–770, 2008.
- [52] H. Wu, W. Jia, Y. Bao et al., “Serum retinol binding protein 4 and nonalcoholic fatty liver disease in patients with type 2 diabetes mellitus,” *Diabetes Research and Clinical Practice*, vol. 79, no. 2, pp. 185–190, 2008.
- [53] V. Nobili, N. Alkhoury, A. Alisi et al., “Retinol-binding protein 4: a promising circulating marker of liver damage in pediatric nonalcoholic fatty liver disease,” *Clinical Gastroenterology and Hepatology*, vol. 7, no. 5, pp. 575–579, 2009.
- [54] C. Cengiz, Y. Ardicoglu, S. Bulut, and S. Boyacioglu, “Serum retinol-binding protein 4 in patients with nonalcoholic fatty liver disease: does it have a significant impact on pathogenesis?,” *European Journal of Gastroenterology & Hepatology*, vol. 22, no. 7, pp. 813–819, 2010.
- [55] N. Alkhoury, R. Lopez, M. Berk, and A. E. Feldstein, “Serum retinol-binding protein 4 levels in patients with nonalcoholic fatty liver disease,” *Journal of Clinical Gastroenterology*, vol. 43, no. 10, pp. 985–989, 2009.

Research Article

Evaluation of Altered Glutamatergic Activity in a Piglet Model of Hypoxic-Ischemic Brain Damage Using ^1H -MRS

Yuxue Dang  and Xiaoming Wang 

Department of Radiology, Shengjing Hospital of China Medical University, Shenyang 110004, China

Correspondence should be addressed to Xiaoming Wang; wangxm024@163.com

Received 30 July 2020; Revised 5 September 2020; Accepted 11 September 2020; Published 24 September 2020

Academic Editor: Alexander Berezin

Copyright © 2020 Yuxue Dang and Xiaoming Wang. This is an open access article distributed under the Creative Commons Attribution License, which permits unrestricted use, distribution, and reproduction in any medium, provided the original work is properly cited.

Background and Objective. The excitotoxicity of glutamate (Glu) is a major risk factor for neonatal hypoxic-ischemic brain damage (HIBD). The role of excitatory amino acid transporter 2 (EAAT2) and the α -amino-3-hydroxy-5-methyl-4-isoxazole-propionic acid receptor (AMPA) subunit GluR2 in mediating the Glu excitotoxicity has always been the hotspot. This study was aimed at investigating the early changes of glutamate metabolism in the basal ganglia following hypoxia-ischemia (HI) in a neonatal piglet model using ^1H -MRS. **Methods.** Twenty-five newborn piglets were selected and then randomly assigned to the control group ($n = 5$) and the model group ($n = 20$) subjected to HI. HI was induced by blocking bilateral carotid blood flow under simultaneous inhalation of a 6% oxygen mixture. ^1H -MRS data were acquired from the basal ganglia at the following time points after HI: 6, 12, 24, and 72 h. Changes in protein levels of EAAT2 and GluR2 were determined by immunohistochemical analysis. Correlations among metabolite concentrations, metabolite ratios, and the protein levels of EAAT2 and GluR2 were investigated. **Results.** The Glu level sharply increased after HI, reached a transient low level of depletion that approached the normal level in the control group, and subsequently increased again. Negative correlations were found between concentrations of Glu and EAAT2 protein levels ($R_s = -0.662$, $P < 0.001$) and between the Glu/creatinine (Cr) ratio and EAAT2 protein level ($R_s = -0.664$, $P < 0.001$). Moreover, changes in GluR2 protein level were significantly and negatively correlated with those in Glu level (the absolute Glu concentration, $R_s = -0.797$, $P < 0.001$; Glu/Cr, $R_s = -0.567$, $P = 0.003$). **Conclusions.** Changes in Glu level measured by ^1H -MRS were inversely correlated with those in EAAT2 and GluR2 protein levels following HI, and the results demonstrated that ^1H -MRS can reflect the early changes of glutamatergic activity in vivo.

1. Introduction

The excitatory amino acid glutamate (Glu) is a major excitatory neurotransmitter in the central nervous system of mammals and has a crucial role in maintaining normal brain function. Under normal physiological conditions, the Glu level in extracellular fluid is only $0.5\text{--}5\ \mu\text{M}$ [1]. Astrocytes maintain a low Glu level in extracellular fluid and prevent Glu excitotoxicity and abnormal synaptic transmission. Glial fibrillary acidic protein (GFAP) is widely recognized as a specific molecular marker of astrocytes, as it is the protein mostly related to astrocytic functions [2, 3]. The excitatory amino acid transporter 2 (EAAT2, also called glutamate transporter 1 (GLT-1) in rodents) on the astrocyte cell membrane is responsible for the majority of Glu transport in the

body [4, 5]. Glu released by presynaptic neurons enters into astrocytes by reuptake and is transformed into the nonexcitatory amino acid glutamine (Gln) by glutamine synthetase, which subsequently undergoes uptake by presynaptic neurons to complete the Glu-Gln cycle [6].

Exposure to hypoxia-ischemia (HI) injury induces substantial Glu release from presynaptic neurons [7] and impairs the activity of Glu reuptake systems. Consequently, excessive Glu accumulate in the synaptic spaces and bind with glutamate receptors located on the postsynaptic neural membranes, which results in excitotoxicity. The main excitatory ionotropic glutamate receptors are the *N*-methyl-D-aspartate acid receptor (NMDAR) [8] and the α -amino-3-hydroxy-5-methyl-4-isoxazole-propionic acid receptor (AMPA) [9]. The NMDAR and AMPAR can be activated by excess Glu,

and they have crucial roles in mediating Glu excitotoxicity [8–10]. Most studies have focused on determining the mechanism of NMDAR mediation of Glu excitotoxicity in hypoxic-ischemic brain damage (HIBD). Subsequent research proposed the “GluR2 hypothesis” [9], which considers that HI-induced structural changes in AMPAR mediate neuronal injury. The GluR2 subunit is an important functional moiety of the AMPAR; GluR2 determines the Ca^{2+} permeability of AMPAR [11–13] and is involved in mediating Glu excitotoxicity.

The occurrence of HIBD in perinatal newborns generally injures specific brain regions. The deep gray matter nuclei are very easily injured by HI [14], and the basal ganglia are highly susceptible to Glu excitotoxicity [15]. The immature brain of infants is more susceptible to Glu excitotoxicity than the mature adult brain [14–16]. HIBD is an important cause of permanent dysfunction and death of perinatal newborns, occurring approximately 2–3 per 1000 term births [17], which affects both the families and society. No therapeutic strategies have been developed to effectively improve the quality of life and the survival of these patients.

The present study was aimed at investigating the glutamate metabolism alterations in the basal ganglia using ^1H -MRS following HI insult in a piglet model and preliminarily exploring the possible mechanisms of Glu excitotoxicity.

2. Materials and Methods

2.1. Experimental Animals. All animal experiments were performed in accordance with the Regulations for the Administration of Affairs Concerning Experimental Animals (<http://www.asianlii.org/cn/legis/cen/laws/rftaoacea704/>). The protocol was approved by the Animal Ethics Committee of Shengjing Hospital of China Medical University, Shenyang, China. Twenty-five newborn male Yorkshire piglets (P3–5, body weight: 1.5–2.0 kg) were selected from the Laboratory Animal Center and then randomly assigned to the control group (sham-operation group, $n = 5$) and the HI model group ($n = 20$). The HI model group was allocated into four subgroups with differing assessment times after HI-induced brain injury: 6, 12, 24, and 72 h ($n = 5$ piglets per group). The experimental animals were maintained with unlimited food and water in a quiet and warm environment.

2.2. Preparation of Animal Models. The newborn piglets in the model group were initially anesthetized with intramuscular injection of 0.6 mL/kg xylazine hydrochloride. After anesthesia, the animals were fixed on the operation bench in a supine position. Heating pads were employed during surgery to maintain body temperature at $37 \pm 0.5^\circ\text{C}$. Tracheal intubation ($\varnothing 2.5$ mm) was performed, and then, each piglet was connected to a TKR-200C small animal ventilator for mechanical ventilation with 100% oxygen and the following ventilator parameters: inspiration/expiration (I/E) = 1 : 1.5 (respiration ratio) and respiration rate = 30/min. The heart rate and oxygen saturation of blood were monitored continuously using a TuffSat handheld pulse oximeter (GE Healthcare, Milwaukee, Wisconsin, USA). The incision site and adjacent skin were disinfected, and the piglets were subjected

to a middle anterior neck incision. Bilateral common carotid arteries were isolated from adjacent internal jugular veins and vagus nerves. After the condition of the animal was stable for 40 min, the bilateral common carotid arteries were occluded using small arterial clamps. Then, a gas mixture containing 6% oxygen and 94% nitrogen was inhaled mechanically for 40 min. After 40 min, the small artery clamps on the bilateral common carotid arteries were removed, and blood flow was recovered. Simultaneously, oxygen (100%) was mechanically inhaled again, and the incision was stitched. After the operation, each piglet was transferred to an incubator (37°C) to maintain normal body temperature during postsurgical recovery. Piglets in the control group (pseudooperation group) underwent the same presurgical preparation as those in the model group but were not subjected to the HI induction procedures.

All operations were conducted under effective analgesia and anesthesia to reduce animal suffering.

2.3. Magnetic Resonance Imaging. The MRI examination was conducted for all animals in both the sham-operation and model groups. The piglets were anesthetized with xylazine hydrochloride. Then, the animals were placed in a supine position with a special foam pad around their heads to keep the head centered. Then, the following scans were performed: conventional fast-field echo (FFE) T1-weighted imaging (T1WI) (repetition time (TR)/echo time (TE), 200/2.3 ms; matrix, 224×162 ; and slice thickness, 5 mm) and turbo spin-echo (TSE) T2-weighted imaging (T2WI) (TR/TE, 5000/80 ms; matrix, 224×162 ; and slice thickness, 5 mm). MRI scans were performed using the Philips Achieva 3.0T MRI system (Best, Netherlands) with 8-channel phase array head coils. The newborn piglets were also carefully wrapped in thick quilts to maintain temperature.

^1H -MRS scans were performed using a point-resolved spectroscopy (PRESS) sequence for single-voxel acquisition (TR, 2000 ms; TE, 37 ms; samples, 1024; bandwidth, 2000 Hz; and NSA, 64). A short TE sequence (TE = 37 ms) was utilized for better demonstration of the Glu peak, which could reduce the impact of relaxation effect, obtaining a better spectrum. Automatic shimming was completed before scanning. The location was determined at the level of the basal ganglia by axial T2WI, and the volume of interest (VOI) of $10 \times 10 \times 10$ mm was placed in the left basal ganglia. Care was taken to avoid noise caused by the surrounding areas, such as cerebrospinal fluid, blood vessels, fat, and air. The saturation band was placed at an area outside the VOI, and field shimming and water-suppressing operations were performed within the VOI, achieving full width at half maximum (FWHM) ≤ 10 Hz and water suppression $> 98\%$ and allowing subsequent collection of spectral data. The basal ganglia were selected as the region of interest (ROI) because they are one of the most susceptible regions to HIBD in newborns.

2.4. ^1H -MRS Postprocessing and Data Analysis. Spectral raw data obtained by ^1H -MRS scanning were quantitatively analyzed using linear combination model software (LCModel, version 6.3-1B, S.W. Provencher) [18]. This popular software

for quantitative analysis of spectral data employs a black box operation that allows automatic averaging of the original spectral images, baseline correction and smoothing, phase correction, metabolite identification, and finally acquisition of data for different metabolites. The absolute quantities of metabolites were obtained, and the Cramér-Rao lower bounds (CRLBs) were calculated; these were used as an index of metabolite quantification to evaluate the reliability of the fitted results. Spectra were fitted with a chemical shift at approximately 0.2-4.0 ppm ($\text{ppm} = 10^{-6}$) using the LCMoDel software. The final simulated spectra included the following 17 metabolites: alanine (Ala), aspartate (Asp), creatine (Cr), phosphocreatine (PCr), γ -aminobutyric acid (GABA), glucose (Glc), Glu, Gln, glycerophosphorylcholine (GPC), phosphorylcholine (PCho), glutathione (GSH), inositol (Ins), lactic acid (Lac), *N*-acetylaspartate (NAA), *N*-acetylaspartylglutamate (NAAG), scyllitol (Src), and taurine (Tau). The baseline setting of the basic set also included macromolecules and lipids. Only the spectrum data with CRLBs < 50% and generally < 25% and signal-to-noise ratio (SNR) ≥ 5 were included in the statistical analysis.

We analyzed the levels of Glu, Gln, Glx (Glu+Gln complex), NAA (NAA+NAAG), choline-containing compounds (Cho) (GPC+PCho), and Cr (Cr+PCr), and the total amounts were used for NAA, Cho, and Cr to guarantee the reliability of data. Glu generates complex signals at approximately 2.04-2.35 ppm and 3.75 ppm with a prominent peak at 2.35 ppm. Neurotoxicity occurs when the Glu content exceeds the physiological demand of Glu for neurotransmission. Gln, which is an intermediate metabolite supporting multiple pathways of energy metabolism and neurological transmission, forms resonance peaks at 2.45, 3.78, and 2.15 ppm. Although the J-coupling effect between Glu and Gln causes their peaks to overlap with each other, we found that the software could correctly separate them to a certain extent. Therefore, qualitative analysis was carried out for Glu and Gln individually. The main NAA peak is at 2.02 ppm, which reflects the mitochondrial functions of neurons [19]. Cho is an important cell membrane phospholipid, and its main peak is at 3.20 ppm. The predominant Cr peaks are at 3.03 and 3.94 ppm; Cr is important for energy metabolism in neurons and the astrocyte cytoplasm.

In this study, the absolute concentrations of Glu, Gln, Glx, NAA, Cho, and Cr in the basal ganglia were analyzed. Additionally, we measured the Glu/Cr, Gln/Cr, Glx/Cr, NAA/Cr, and Cho/Cr concentration ratios (namely, the relative concentration) which were also provided by the LCMoDel software.

2.5. Histological Examination. After the MRI examination was completed at the specified time points, the newborn piglets were immediately sacrificed and their brains were rapidly collected for pathological examination. The brains were fixed in 10% formaldehyde solution for 48 h and then sectioned at a coronal plane. Then, sections containing the basal ganglia were embedded in paraffin and thin-sectioned with 4 μm thickness for conventional hematoxylin-eosin (HE) and immunohistochemical (IHC) staining.

The HE-stained brain sections were evaluated under a light microscope for pathological changes in the basal ganglia. The brain changes were assessed and scored with reference to the brain pathological evaluation standards of Li et al. [20]: a score of 0-6 for nervous pathological injury, with 0-3 for cerebral edema (0, none; 1, mild; 2, moderate; and 3, severe) and 0-3 for nerve cell injury and necrosis (0, none; 1, mild; 2, moderate; and 3, severe). The total score was the sum of individual scores, and a higher total score indicated more severe injury. Brain edema includes cytotoxic edema and vasogenic edema. Cell necrosis includes the death of individual cells, groups of cells, and all cells in a certain region. The evaluation was conducted by an experienced professional physician who was blinded to the experimental grouping, and it was based on the observation of cell morphological changes under the light microscope (400x magnification).

IHC staining procedures were as follows. The paraffin sections were incubated with 3% H_2O_2 at room temperature for 15 min to block endogenous peroxidase activity and then blocked with 5% normal goat serum at room temperature for 30 min. Thereafter, these sections were incubated overnight at 4°C with the following primary antibodies: rabbit anti-GFAP (1: 1000, Abcam), rabbit anti-EAAT2 (1: 200, Abcam), and mouse anti-GluR2 (1: 100, Abcam). Then, the sections were washed, incubated with biotinylated anti-rabbit/mouse immunoglobulin G at 37°C for 1 h, developed with DAB, counterstained with hematoxylin, and mounted with neutral balsam. The prepared sections were observed under light microscopy for staining of the basal ganglia. Phosphate-buffered saline was used instead of primary antibodies for negative controls, and other procedures were the same. After the addition of the secondary antibodies, all procedures were performed while protecting the sections from light. All images were analyzed with the image analysis system. Five fields (400x magnification) were randomly selected to measure the optical density of antibody binding, and the mean optical density (OD) was used as the measured value (arbitrary units) of GFAP, EAAT2, and GluR2 expression.

2.6. Statistical Analysis. The homogeneity of data variance was analyzed by the Levene test. The homogeneity of variance determined via multigroup comparison was analyzed by one-way ANOVA. The heterogeneity of variance was analyzed by Welch's *t*-test. The categorical data was analyzed by the Kruskal-Wallis test. Correlations between spectral data and pathological results were analyzed using the Spearman correlation analysis with R_s as the correlation coefficient. SPSS v. 20.0 statistical software (IBM, NY, USA) was used for all analyses. All statistical tests were two-tailed, with $P < 0.05$ considered statistically significant.

3. Results

3.1. HI-Induced Changes in Neuron and Astrocyte Morphologies in the Basal Ganglia. In the control group, neurons were regularly arranged, with normal cell morphology, rich cytoplasm, and clear nuclei. Astrocytes have low GFAP-positive response, light staining, small cell volume, slender and short protrusions, and sparse distribution.

However, in the HI model group, the number of GFAP-positive cells increased, the staining was deep, the cell body was large, and the protrusions grew thick. The HI-treated neurons and astrocytes displayed the following changes at specific time points: at 6 h after HI, neurons did not display any significant morphological changes; at 12 h, many astrocytes were swollen and displayed a lightly stained cytoplasm and vacuoles; at 24 h, many neurons and astrocytes were swollen; and at 72 h, astrocytes were clearly swollen and degenerated, the neuronal cell membrane was damaged, and nuclei were swollen and lightly stained (Figures 1 and 2). The pathological damage of brain tissues became more severe over time. The pathological scores at various time points are presented in Table 1.

3.2. HI-Induced Changes in GFAP, EAAT2, and GluR2 Expression in the Basal Ganglia. GFAP, as a biomarker protein of astrocytes, changed significantly after HI. The results showed an increase in expression levels of GFAP immunostaining observed after HI in comparison to the control group. And there were statistically significant differences in HI insult 12 h, 24 h, and 72 h subgroups with respect to the control group (both $P < 0.05$) (Figure 2).

In the normal control group, EAAT2 was mainly expressed in the plasma membranes of cells. HI caused significant changes in the expression of EAAT2. The EAAT2 expression level in the basal ganglia was significantly lower in the HI insult 6 h subgroup than in the control group ($P = 0.001$). Then, EAAT2 expression tended to markedly increase in the 12 h subgroup and thereafter decreased again (Figure 3). There was a statistically significant difference between EAAT2 expression in the 12 h subgroup, the 72 h subgroup, and the control group ($P < 0.001$ or $P = 0.033$).

The GluR2 protein level in the basal ganglia decreased significantly over time after HI compared with that in the control, and the differences were statistically significant (both $P < 0.05$) (Figure 4). The results also indicated that the GluR2 protein level was negatively correlated with the severity of pathological lesions ($R_s = -0.876$, $P < 0.001$) and the GluR2 expression was lower when HI-induced brain damage was more severe.

3.3. $^1\text{H-MRS}$ Results. The results in Figure 5 showed the changes of metabolites by $^1\text{H-MRS}$. Compared with the control group, the absolute Glu concentrations markedly changed over time after HI insult (Figure 5(c)). The Glu levels showed a biphasic change. The Glu concentrations clearly increased at 6 h after HI treatment and then reached a transient minimum at 12 h that was approaching the level in the control group and then increased again at 24 h. There were statistically significant differences in Glu concentrations between the various groups ($F = 14.781$, $P < 0.001$). The intergroup analysis indicated that there were significant differences between the control and HI groups at 6, 12, 24, and 72 h after HI injury ($P < 0.001$, $P = 0.017$, $P < 0.001$, and $P < 0.001$, respectively) and between HI groups at 12 h versus 6, 24, and 72 h ($P = 0.008$, $P = 0.001$, and $P = 0.013$), but there were no significant differences between other subgroups. The trend of the absolute concentration of Glx was

similar to that of Glu, which was significantly elevated at 6 h, 24 h, and 72 h after HI when compared with the control group (both $P < 0.05$). The Cho concentrations appeared to increase over time after the HI insult. There were significant differences between the 24 h and 72 h HI subgroups and the control group ($P = 0.006$ and $P = 0.006$, respectively). Moreover, significant correlations were found between Cho concentrations and the pathological scores ($R_s = 0.703$, $P < 0.001$). While there were no differences in the absolute concentrations of Gln, NAA or Cr was observed between the different groups ($F = 0.360$, $P > 0.05$; $F = 1.382$, $P > 0.05$; and $F = 1.965$, $P > 0.05$).

Changes in Glu/Cr and Glx/Cr ratios were similar to the changes in the Glu or Glx concentrations (Figure 5(d)). This study also analyzed the changes in NAA/Cr and Cho/Cr ratios. NAA/Cr gradually declined over time after HI insult, with statistically significant differences observed between the 72 h HI subgroup and the control group ($P = 0.003$). The results also indicated that changes in NAA/Cr were negatively correlated with the severity of pathological lesions in the basal ganglia ($R_s = -0.456$, $P = 0.022$). There was a similar change in Cho/Cr concentration ratios with the absolute Cho concentrations. The increase in Cho/Cr ratios in the 12 h, 24 h, and 72 h HI subgroups was considered to have statistically significant difference as compared with the control group ($P = 0.020$, $P = 0.004$, and $P = 0.010$, respectively). And the Cho/Cr ratio showed a significant correlation with the pathological scores ($R_s = 0.638$, $P = 0.001$).

3.4. Correlations among HI-Induced Changes in GluR2, EAAT2, and Glu Levels in the Basal Ganglia. After HI insult, the changes in Glu concentrations and the dynamic changes in EAAT2 expression were significantly negatively correlated in the basal ganglia ($R_s = -0.662$, $P < 0.001$), and changes in the Glu/Cr ratios were significantly negatively correlated with EAAT2 expression ($R_s = -0.664$, $P < 0.001$) (Figures 6(a) and 6(b)). However, there was no significant correlation between the absolute concentration of Glx, the Glx/Cr ratio, and the expression of EAAT2 ($R_s = -0.346$, $P > 0.05$; $R_s = -0.338$, $P > 0.05$) (Figures 6(c) and 6(d)).

Moreover, the absolute Glu concentrations and GluR2 protein expression level in the basal ganglia were significantly correlated ($R_s = -0.797$, $P < 0.001$), as were the Glu/Cr ratio and GluR2 protein level ($R_s = -0.567$, $P = 0.003$) (Figures 6(e) and 6(f)). Similarly, the absolute concentration of Glx and the Glx/Cr ratio were negatively correlated with GluR2 expression ($R_s = -0.670$, $P < 0.001$; $R_s = -0.476$, $P = 0.016$) (Figures 6(g) and 6(h)).

4. Discussion

This study investigated the metabolic changes in Glu levels using $^1\text{H-MRS}$ in vivo and analyzed the role of EAAT2 and GluR2 in regulating the Glu levels during the acute stage of HIBD. Considerable studies have shown that Glu has an important role in maintaining normal brain functions, and Glu concentration in the extracellular fluid must be kept at a low level ($< 100 \mu\text{M}$) to prevent excitotoxicity. Astrocytes play an important role in maintaining Glu homeostasis.

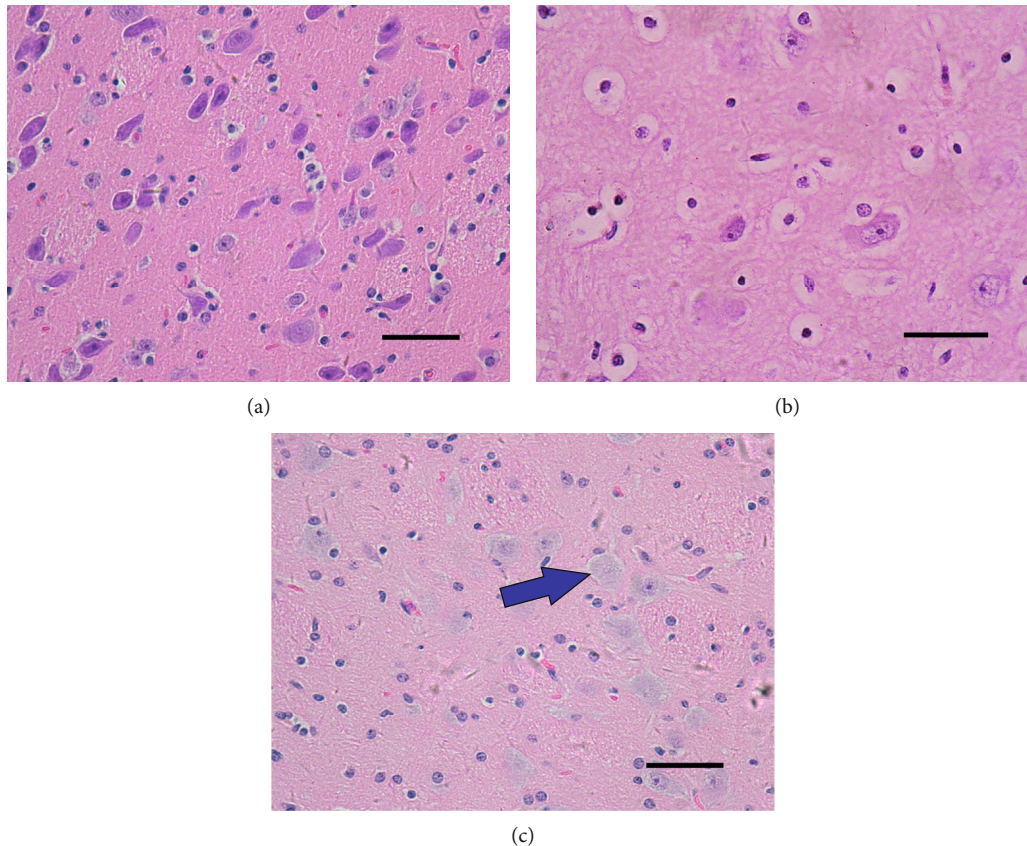


FIGURE 1: Typical images of hematoxylin and eosin staining of the piglet basal ganglia (400x magnification). Scale bar = 50 μm . (a) In the control group, piglet nerve cells were regularly arranged with normal morphology. (b, c) At the later stage following HI, piglet nerve cells were significantly swollen, the cells were slightly stained, the intracellular space was widened, and karyolysis (arrow) was observed.

Accumulated Glu in the extracellular fluid is mainly taken up by cells via sodium-dependent EAATs. Once inside the astrocytes, Glu is transformed by glutamine synthetase into Gln, which is released from astrocytes. Extracellular Gln is taken up by presynaptic neurons, which complete the Glu-Gln cycle between neurons and astrocytes. HI injury disrupts astrocyte Glu uptake. Thus, HI injury induces extracellular Glu accumulation to high levels, and the resultant excitotoxicity can aggravate brain injury in newborns [21]. Our results are consistent with those of the previous study. The Glu metabolism level sharply increased after HI compared with that in the control group (Figure 5). The degree of injury in newborn piglets became more severe over time after HI insult, indicating that increasing Glu accumulation is closely related to brain damage caused by the resulting excitotoxicity [22]. During the early stage of HI injury, Na^+/K^+ pump dysfunction may significantly increase the extracellular K^+ concentration, promote neuronal depolarization, activate the voltage-dependent calcium channel and massive Ca^{2+} influx, and trigger synaptic terminals to release excessive Glu [15]. During the later stage of HI injury (i.e., 24 h after HI in this study), ATP levels are depleted and reperfusion injury causes cell rupture and/or impaired astrocyte reuptake [23], which again lead to Glu release.

EAAT2 is the primary subtype of EAATs present in the corpus striatum, and EAAT2 in the cell membranes of astro-

cytes is thought to be responsible for 90% of Glu transport in humans [24], which is crucial for maintaining homeostasis of the Glu-Gln cycle. Therefore, this study focused on changes of EAAT2 after HI. This study demonstrated that Glu levels were significantly increased after HI injury compared with the control, and changes in Glu levels (including the absolute Glu concentration and Glu/Cr ratio) were inversely correlated with changes in EAAT2 expression. This indicates that EAAT2 may have a key role in HI injury by reducing Glu excitotoxicity. EAAT2 expression decreased during early HI injury and subsequently increased, possibly because early HI promoted massive Glu release but inhibited EAAT2 function on the cell membrane and reduced EAAT2 expression. As the HI time increased, EAAT2 expression was elevated, and some Glu underwent oxidative metabolism to provide energy for efficient EAAT2 transport, and Glu depletion reached its peak, suggesting that EAAT2 began to function to prevent massive Glu accumulation. What is more, the protein levels of GFAP increased at this stage; this reactive astrogliosis may be a self-protection mechanism of astrocytes. During a later stage, the expression level of GFAP was still elevated, and this overexpression may be one of the important mechanisms of potential excitotoxicity of neurons. Some studies have also suggested that this overexpression can lead to the formation of glial scars in brain injury areas, which is an important cause of brain nerve regeneration disorders

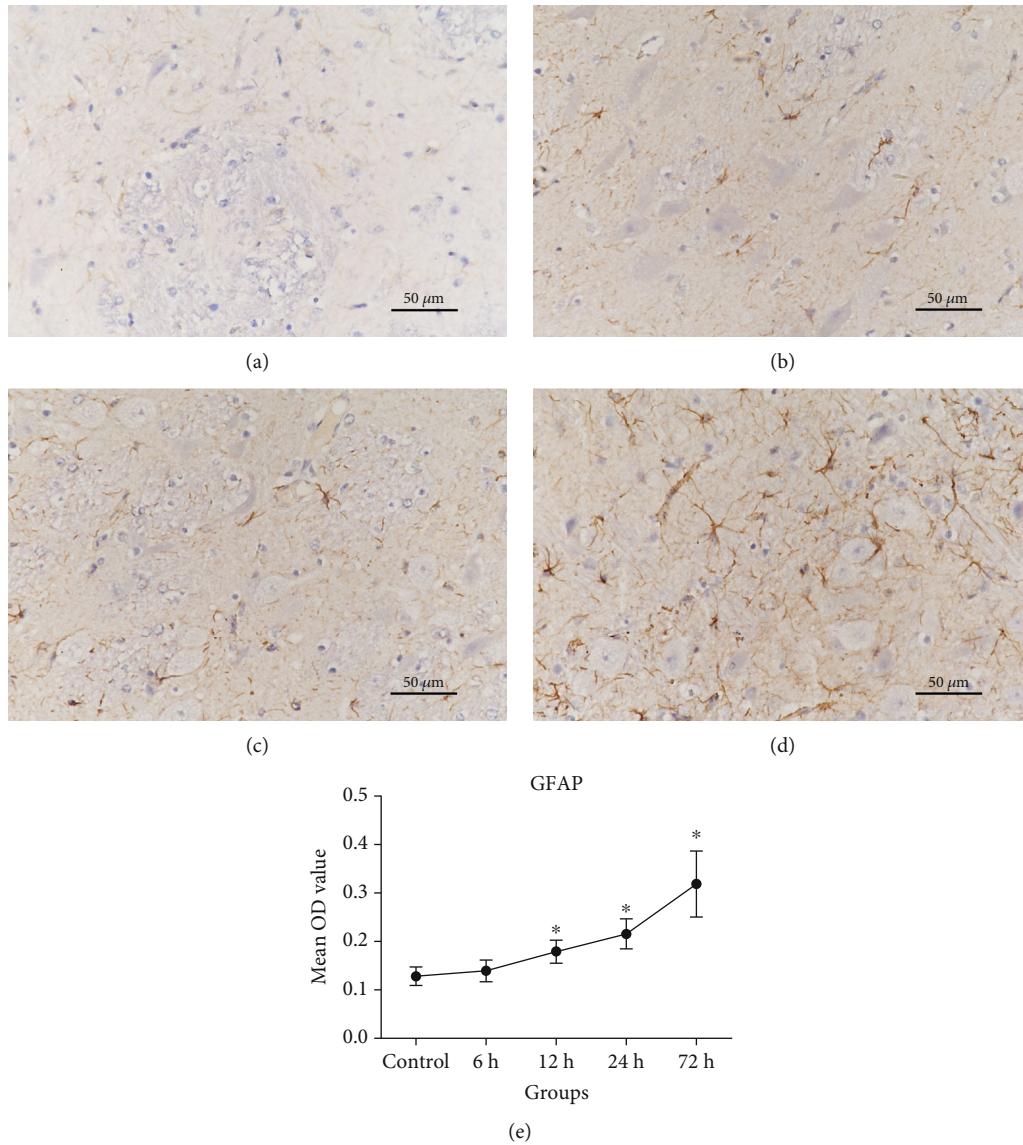


FIGURE 2: Changes in GFAP expression in the basal ganglia of piglets (400x magnification). Scale bar = 50 μm . (a–d) Representative figures of GFAP IHC staining in the control group and HI insult 12 h, 24 h, and 72 h subgroups. (e) Changes in the average OD of GFAP protein level. Compared with the control group, the expression levels of the GFAP were significantly increased in the HI group. GFAP: glial fibrillary acidic protein; IHC: immunohistochemical; OD: optical density. Error bars represent the standard deviation values ($n = 5/\text{group}$). * $P < 0.05$ compared with the control group.

TABLE 1: Pathological scoring of the piglet basal ganglia at different time points after HI treatment.

	Control group ($n = 5$)	HI model group			
		6 h ($n = 5$)	12 h ($n = 5$)	24 h ($n = 5$)	72 h ($n = 5$)
Pathological score	0 (0-0)	1 (1-2)	2 (1.5-2.5)	3 (2.5-3.5)*	4 (3.5-4.5)*

Note: data are displayed as median (25th-75th percentile). * $P < 0.05$ compared with the control group.

[25]. While the EAAT2 protein expression level declined, the Glu level increased, perhaps because it was difficult to maintain Glu homeostasis due to neuronal necrosis and the functional inhibition of EAAT2 on the astrocyte membrane. Our results confirm that EAAT2 has a critical effect on HIBD. Numerous investigators have tried to reduce HI-induced brain damage by regulating EAAT2 expression. Many cur-

rent studies that focus on upregulating EAAT2 expression, increasing Glu uptake, reducing Glu excitotoxicity, and relieving nerve injury with resveratrol [26], sulbactam [27], histamine [28], and ceftriaxone [24] confirmed that cerebral ischemic preconditioning could upregulate GLT-1 expression in astrocytes and thus enhance the effects of cerebral ischemic tolerance. At present, some researchers have found

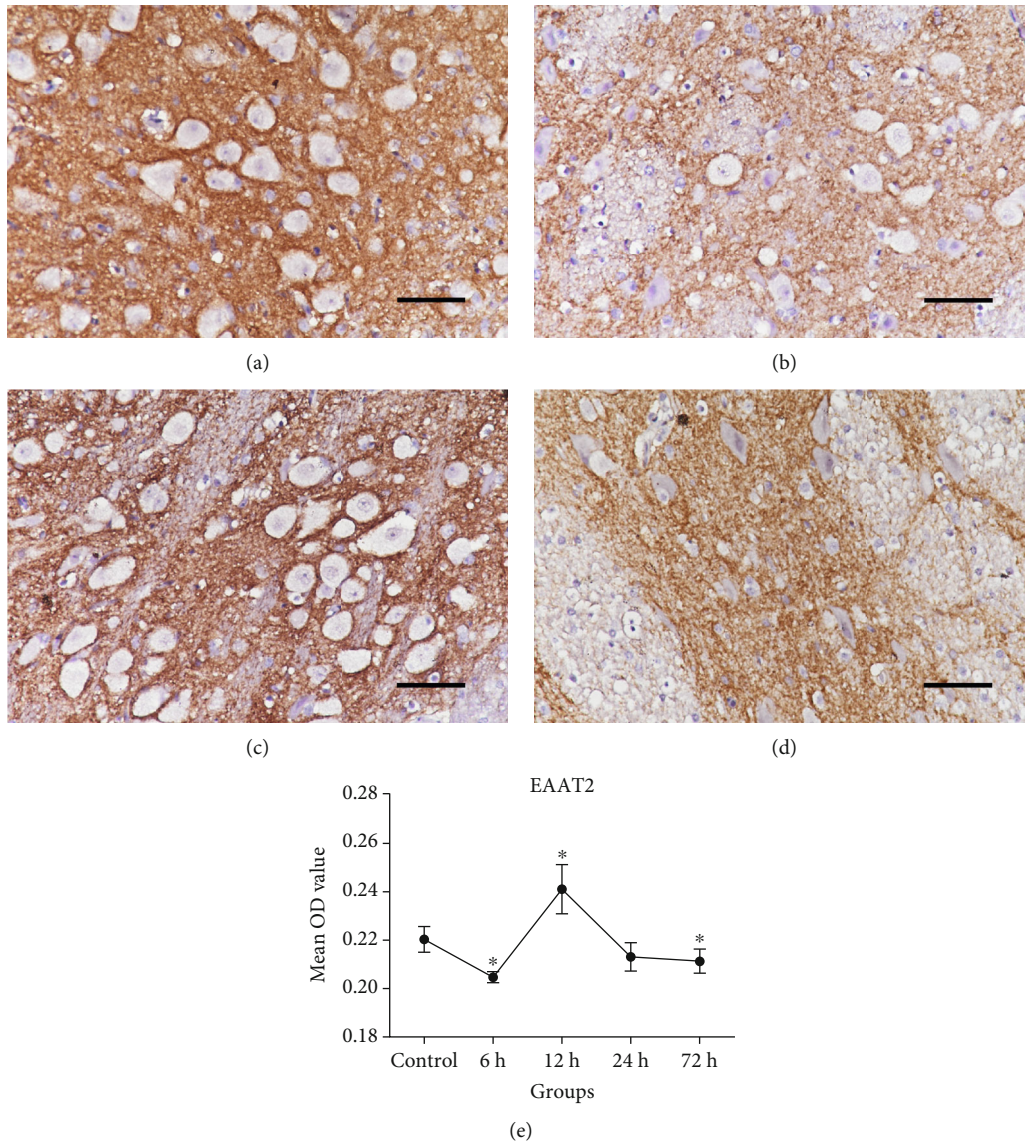


FIGURE 3: EAAT2 protein levels in the basal ganglia before (control) and after HI injury (400x magnification). Scale bar = 50 μm . (a–d) Representative figures of EAAT2 IHC staining in the control group and in 6 h, 12 h, and 72 h HI subgroups. (e) Changes in the average OD of EAAT2 protein. During early HI, EAAT2 protein level slightly decreased compared with the control; subsequently, it tended to increase and then decrease over time after HI injury. EAAT2: excitatory amino acid transporter 2; IHC: immunohistochemical; OD: optical density. Error bars represent the standard deviation values ($n = 5/\text{group}$). * $P < 0.05$ compared with the control group.

that inducing EAAT2 expression in mesenchymal stem cells can significantly reduce glutamate excitotoxicity [29]. Of course, clinical application of these methods requires further validation.

HI-related disruption of the Glu-Gln cycle causes changes in intracellular and extracellular Glu levels. When extracellular Glu reaches a certain level, the activation of related receptors leads to a series of changes, both physiological and pathological. The AMPAR is an important subtype of ionic Glu receptors and is widely expressed in medium spiny neurons of the basal ganglia. AMPAR contains four different subunits, GluR1 to GluR4. GluR2 has been characterized as an important functional moiety of AMPAR. Under normal physiological conditions, GluR2 is highly expressed in AMPAR of most neurons, and it is

not permeable to Ca^{2+} , which depends on editing of the GluR2 pre-mRNA Q/R (Gln/arginine) site. Changes in GluR2 expression can change Ca^{2+} permeability [9, 12, 13] and thereby play a role in HI-mediated injury. This study evaluated the changes in GluR2 protein levels after HI insult and possible mechanisms mediating HI-induced brain damage. We found that the GluR2 protein levels in the basal ganglia showed a decreasing trend with prolonged HI time. The GluR2 protein levels were negatively correlated with the severity of pathological lesions. We also observed that changes in Glu metabolism levels were negatively correlated with GluR2 protein levels. These results suggest that Glu accumulation after HI leads to the activation of AMPAR and then downregulation of GluR2 expression; what is more, GluR2 expression level further declined

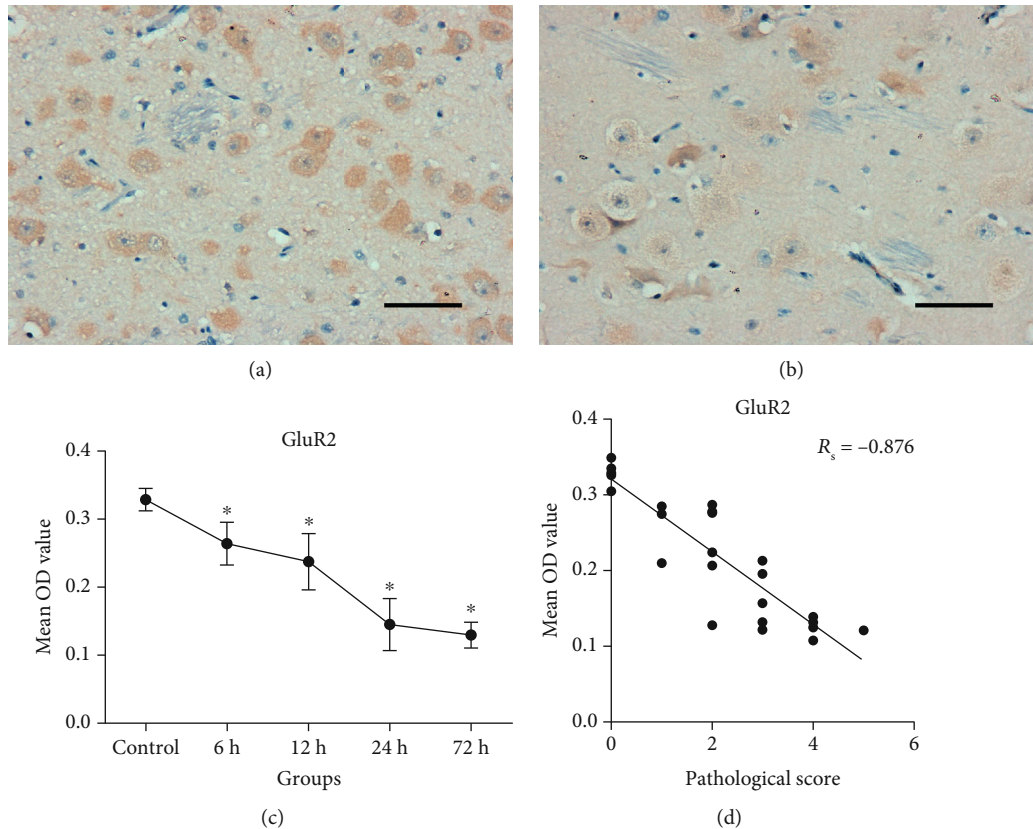


FIGURE 4: AMPAR subunit GluR2 protein levels in the basal ganglia before (control) and after HI injury (400x magnification). Scale bar = 50 μm . (a) High GluR2 protein levels in the basal ganglia in the control group. (b) At 72 h after HI injury, the GluR2 protein level was markedly reduced. (c) Changes in the average OD of GluR2 protein level visualized with IHC staining. GluR2 protein level declined in piglets subjected to HI injury compared with the control. (d) GluR2 protein level was negatively correlated with the severity of pathological lesions; i.e., the more severe the brain injury, the more obvious the downregulation of GluR2 protein level. AMPAR: α -amino-3-hydroxy-5-methyl-4-isoxazole-propionic acid receptor; IHC: immunohistochemical; OD: optical density. Error bars represent the standard deviation values ($n = 5/\text{group}$). * $P < 0.05$ compared with the control group. The Spearman rank correlation coefficient was presented as R_s .

as HI injury worsened. Therefore, GluR2 may be involved in the susceptibility of the basal ganglia.

The mechanism obstructing rapid Ca^{2+} influx is markedly weakened after HI-mediated GluR2 decrease, and Ca^{2+} flows into cells via the activated Ca^{2+} -permeable AMPAR. This causes intracellular Ca^{2+} overload, which enhances Glu toxicity and causes neuronal death. This mechanism may account for secondary damage to HI. Recent studies showed that GluR2 mRNA expression was downregulated after HI and changes in the functional reactivity of AMPA receptors may mediate Ca^{2+} influx [13]. There was a significant reduction in the GluR2 expression level after reperfusion in the global cerebral ischemia rat model [30], which is consistent with our results. Intracerebral injection of antisense oligonucleotide knocked down GluR2 expression in rats [31], and the death of pyramidal neuronal cells in the hippocampal CA1 region enhanced the pathogenicity of transient ischemic attack.

The mechanisms mediating decreased GluR2 expression after HI remain to be clarified, and several questions remain unanswered. For example, how is GluR2 mRNA transcript editing affected by HI, how do other AMPAR subunits change, and how do the electrophysiological characteristics

of AMPAR change? Previous studies suggest that acute downregulation of GluR2 expression can function as a “molecular switch” to form Ca^{2+} -permeable AMPAR [9, 13] and strengthen Glu toxicity during nerve injury. Some investigators successfully mitigated or reversed the downregulation of GluR2 expression by treating cells with 3,5,3'-triiodo-L-thyronine (T3) [32], genistein (4',5,7-trihydroxyisoflavone) [33], or isoflurane [34], thereby protecting neurons from injury induced by Glu excitotoxicity. We used $^1\text{H-MRS}$ to evaluate the NAA and Cho levels. The results suggest that NAA/Cr ratios gradually declined over time after HI injury and were negatively correlated with the severity of damage to basal ganglia ($R_s = -0.456$, $P = 0.022$). Our results were consistent with previous studies [35, 36], which reported that low NAA/Cr indicated poor prognosis after HI. NAA is considered to be a neuronal marker, and NAA levels are closely associated with the number and activity of neurons. The reduction in NAA level after HI is usually irreversible, indicating neuron loss and irreversible brain damage [37]. However, due to the high plasticity of the neonatal brain, differentiation of neuronal stem cells can help to recover damaged neurons in some conditions [38].

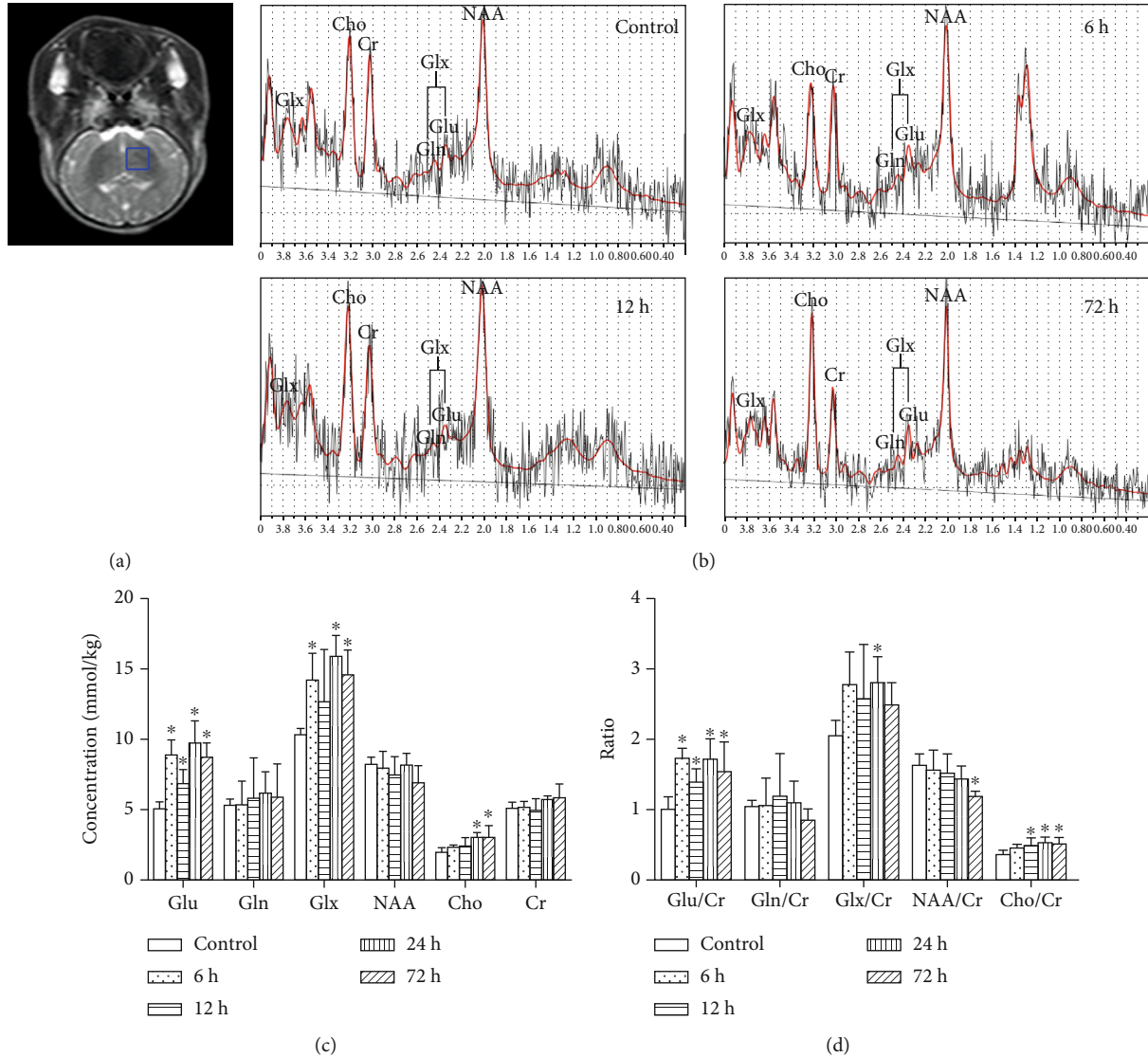


FIGURE 5: Representative ¹H-MRS images of the basal ganglia of piglets at different time points after HI and changes in metabolite absolute concentrations and ratios. (a) Axial T2-weighted MR image obtained from a control piglet; the blue box indicates the voxel location. (b) The following metabolite peaks were observed: Glu, Gln, Glx, NAA, Cho, and Cr. (c, d) Changes in metabolite absolute concentrations and metabolite ratios in the control and HI-induced groups at different time points are shown. Glu: glutamate; Gln: glutamine; Glx: glutamate/glutamine complex; NAA: N-acetylaspartate; Cho: choline; Cr: creatine. Error bars represent the standard deviation values (*n* = 5/group). **P* < 0.05 compared with the control group.

Therefore, NAA is not entirely irreversible. Several studies [39, 40] reported that the NAA level was not significantly lower in patients with mild to moderate HIBD but was permanently depleted in those with severe HIBD. Our results were consistent with these studies. During early HI injury, NAA/Cr did not significantly differ from that in the control group. At 72 h after HI injury, the NAA level was significantly lower than that in the control group. This provided further evidence that a permanent depletion of NAA/Cr could be used as an indicator for poor prognosis in HIBD. An interesting thing to note is that our results, different from the previous studies [35, 39, 41], showed that Cho level increased after HI. It may be interpreted as reflecting astrogliosis [42] or deficient development of the neurons [43].

Furthermore, the Cho level correlated positively with the pathological scores in our study (the absolute Cho concentration, $R_s = 0.703$, $P < 0.001$; Cho/Cr, $R_s = 0.638$, $P = 0.001$). The Cho and Cho/Cr might be used as makers for assessing the degree of brain injury. Future studies with bigger sample sizes need to be conducted to validate this view.

After HI, the immature brain often has a latent period of 8-24 h, which is closely followed by excitotoxicity, inflammation, and oxidative stress response (known as the “deadly triad”) [44, 45]. This can induce secondary energy failure and eventually irreversible neuronal injury. Nerve-protecting strategies must be applied before the occurrence of irreversible injury. The brains of newborn piglets are very similar to those of newborn humans, so newborn piglets were

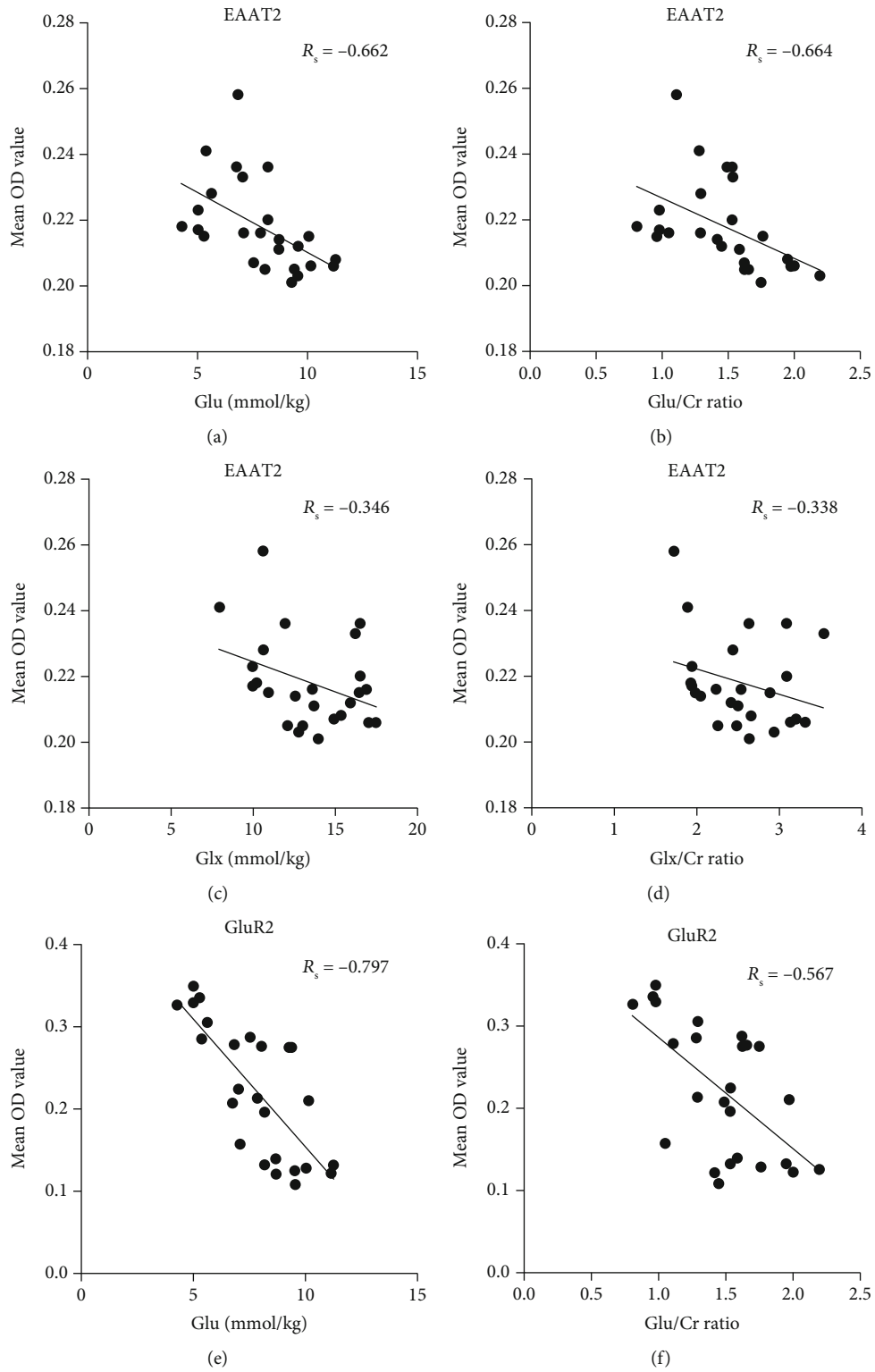


FIGURE 6: Continued.

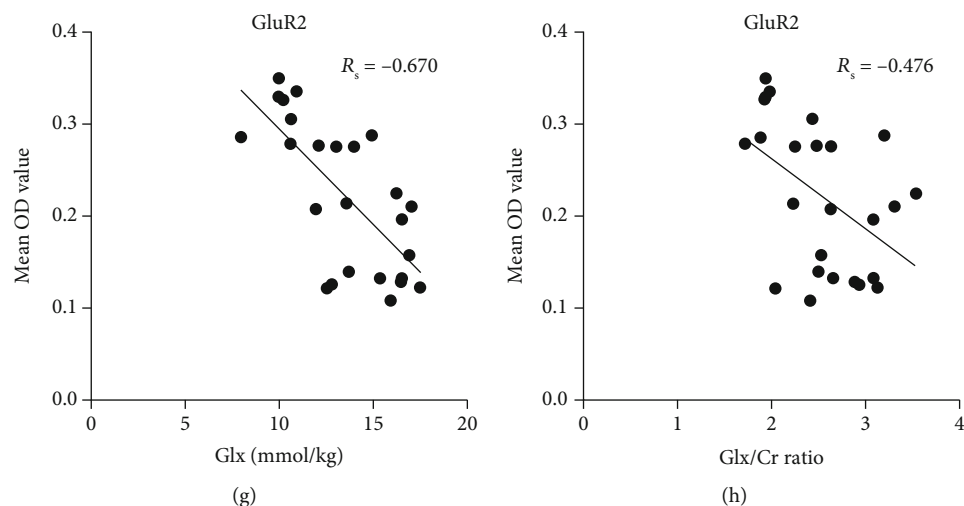


FIGURE 6: Scatter plot of correlations between the expression levels of EAAT2 or AMPAR subunit GluR2 protein levels and the Glu or Glx metabolite levels in the basal ganglia of piglets. EAAT2: excitatory amino acid transporter 2; AMPAR: α -amino-3-hydroxy-5-methyl-4-isoxazole-propionic acid receptor; OD: optical density; Glu: glutamate; Glx: glutamate/glutamine complex. The Spearman rank correlation coefficient was presented as R_s .

selected as experimental animals in this study. The HI newborn piglet model was used to simulate the pathological process of HIBD in human infants. Histological staining revealed that neuronal injury was not obvious at 6 h after HI, neuronal edema was initially observed at 12 h, and a large number of neurons were edematous at 24 h, but the main pathological change was reversible neuronal necrosis. Neuronal edema became more evident at 72 h, and the brain tissues had irreversible, serious pathological changes (including neuronal apoptosis and necrosis). Our results revealed that there was no irreversible injury and the slight recovery of Glu level within 12 h after HI indicated that this time period before the development of secondary energy failure may be the best time for clinical treatment. In this time window, if drugs or other interventions are used to regulate the expression of EAAT2 and GluR2 proteins to reduce the Glu excitotoxicity, it is expected to open up a new path for pediatricians to carry out timely and effective treatment of HIBD. Notably, the determination of this optimal time window still needs further study.

There are some limitations of note. First, due to the complex of etiology and pathogenesis of HIBD, animal HI models established were different from the clinical cases, which may not accurately display the genesis, development, and pathology of neonatal HIBD. Secondly, a small sample size was used in this study and may suffer from a bias. Further thorough studies in a larger sample are needed to confirm the present results.

5. Conclusions

We observed that the Glu levels in the basal ganglia increased after HI and showed a biphasic change. Changes in Glu levels were inversely correlated with changes in EAAT2 and GluR2 expression after HI. The results of this study highlight that $^1\text{H-MRS}$ can be of use in estimating the activation status of EAAT2 and GluR2 in vivo and provide a reliable imaging evi-

dence for the timely and effective treatment of HIBD. Future studies can focus on reducing excitotoxicity-induced brain damage by regulating the levels of EAAT2 and GluR2 proteins. Because of the particularity of the newborn, more work is needed to be conducted to ensure the safety and effectiveness of clinical medication.

Data Availability

All data used to support the findings of this study are included within the article.

Conflicts of Interest

The authors declare that there is no conflict of interest regarding the publication of this paper.

Acknowledgments

The authors would like to thank our colleagues in the Department of Radiology, Shengjing Hospital of China Medical University, for the statistical and technical support. This work was supported by the National Natural Science Foundation of China (grant no. 81871408), the Outstanding Scientific Fund of Shengjing Hospital (item no. 201402), and the 345 Talent Project in Shengjing Hospital of China Medical University.

References

- [1] D. E. Featherstone and S. A. Shippy, "Regulation of synaptic transmission by ambient extracellular glutamate," *The Neuroscientist*, vol. 14, no. 2, pp. 171–181, 2007.
- [2] X. R. Qi, W. Kamphuis, and L. Shan, "Astrocyte changes in the prefrontal cortex from aged non-suicidal depressed patients," *Frontiers in Cellular Neuroscience*, vol. 13, 2019.
- [3] L. F. Eng and R. S. Ghirnikar, "GFAP and astrogliosis," *Brain Pathology*, vol. 4, no. 3, pp. 229–237, 1994.

- [4] S. Pregnotato, E. Chakkarapani, A. R. Isles, and K. Luyt, "Glutamate transport and preterm brain injury," *Frontiers in Physiology*, vol. 10, 2019.
- [5] S. M. Robert and H. Sontheimer, "Glutamate transporters in the biology of malignant gliomas," *Cellular and Molecular Life Sciences*, vol. 71, no. 10, pp. 1839–1854, 2014.
- [6] D. A. Coulter and T. Eid, "Astrocytic regulation of glutamate homeostasis in epilepsy," *Glia*, vol. 60, no. 8, pp. 1215–1226, 2012.
- [7] S. J. Vannucci and H. Hagberg, "Hypoxia-ischemia in the immature brain," *The Journal of Experimental Biology*, vol. 207, no. 18, pp. 3149–3154, 2004.
- [8] L. L. Jantzie, D. M. Talos, M. C. Jackson et al., "Developmental expression of N-methyl-D-aspartate (NMDA) receptor subunits in human white and gray matter: potential mechanism of increased vulnerability in the immature brain," *Cerebral Cortex*, vol. 25, no. 2, pp. 482–495, 2015.
- [9] D. E. Pellegrini-Giampietro, J. A. Gorter, M. V. Bennett, and R. S. Zukin, "The GluR2 (GluR-B) hypothesis: Ca²⁺-permeable AMPA receptors in neurological disorders," *Trends in Neurosciences*, vol. 20, no. 10, pp. 464–470, 1997.
- [10] C. Portera-Cailliau, D. L. Price, and L. J. Martin, "Non-NMDA and NMDA receptor-mediated excitotoxic neuronal deaths in adult brain are morphologically distinct: further evidence for an apoptosis-necrosis continuum," *The Journal of Comparative Neurology*, vol. 378, no. 1, pp. 88–104, 1997.
- [11] A. Rozov, Y. Zilberter, L. P. Wollmuth, and N. Burnashev, "Facilitation of currents through rat Ca²⁺-permeable AMPA receptor channels by activity-dependent relief from polyamine block," *The Journal of Physiology*, vol. 511, no. 2, pp. 361–377, 1998.
- [12] R. Dingledine, K. Borges, D. Bowie, and S. F. Traynelis, "The glutamate receptor ion channels," *Pharmacological Reviews*, vol. 51, no. 1, pp. 7–61, 1999.
- [13] H. Tanaka, S. Y. Grooms, M. V. Bennett, and R. S. Zukin, "The AMPAR subunit GluR2: still front and center-stage," *Brain Research*, vol. 886, no. 1-2, pp. 190–207, 2000.
- [14] D. M. Ferriero, "Neonatal brain injury," *The New England Journal of Medicine*, vol. 351, no. 19, pp. 1985–1995, 2004.
- [15] M. V. Johnston, W. H. Trescher, A. Ishida, W. Nakajima, and A. Zipursky, "The developing nervous system: a series of review articles: neurobiology of hypoxic-ischemic injury in the developing brain," *Pediatric Research*, vol. 49, no. 6, pp. 735–741, 2001.
- [16] J. D. Barks and F. S. Silverstein, "Excitatory amino acids contribute to the pathogenesis of perinatal hypoxic-ischemic brain injury," *Brain Pathology*, vol. 2, no. 3, pp. 235–243, 1992.
- [17] J. S. Wyatt, P. D. Gluckman, P. Y. Liu et al., "Determinants of outcomes after head cooling for neonatal encephalopathy," *Pediatrics*, vol. 119, no. 5, pp. 912–921, 2007.
- [18] S. W. Provencher, "Automatic quantitation of localized *in vivo*¹H spectra with LCMoDel," *NMR in Biomedicine*, vol. 14, no. 4, pp. 260–264, 2001.
- [19] T. E. Bates, M. Strangward, J. Keelan, G. P. Davey, P. M. G. Munro, and J. B. Clark, "Inhibition of N-acetylaspartate production," *Neuroreport*, vol. 7, no. 8, pp. 1397–1400, 1996.
- [20] Y. K. Li, G. R. Liu, X. G. Zhou, and A. Q. Cai, "Experimental hypoxic-ischemic encephalopathy: comparison of apparent diffusion coefficients and proton magnetic resonance spectroscopy," *Magnetic Resonance Imaging*, vol. 28, no. 4, pp. 487–494, 2010.
- [21] C. Portera-Cailliau, D. L. Price, and L. J. Martin, "Excitotoxic neuronal death in the immature brain is an apoptosis-necrosis morphological continuum," *The Journal of Comparative Neurology*, vol. 378, no. 1, pp. 70–87, 1997.
- [22] M. R. Pazos, N. Mohammed, H. Lafuente et al., "Mechanisms of cannabidiol neuroprotection in hypoxic-ischemic newborn pigs: role of 5HT_{1A} and CB2 receptors," *Neuropharmacology*, vol. 71, pp. 282–291, 2013.
- [23] K. Matsumoto, E. H. Lo, A. R. Pierce, E. F. Halpern, and R. Newcomb, "Secondary elevation of extracellular neurotransmitter amino acids in the reperfusion phase following focal cerebral ischemia," *Journal of Cerebral Blood Flow and Metabolism*, vol. 16, no. 1, pp. 114–124, 1996.
- [24] K. Kim, S. G. Lee, T. P. Kegelman et al., "Role of excitatory amino acid transporter-2 (EAAT2) and glutamate in neurodegeneration: opportunities for developing novel therapeutics," *Journal of Cellular Physiology*, vol. 226, no. 10, pp. 2484–2493, 2011.
- [25] K. Shrivastava, M. Chertoff, G. Llovera, M. Recasens, and L. Acarin, "Short and long-term analysis and comparison of neurodegeneration and inflammatory cell response in the ipsilateral and contralateral hemisphere of the neonatal mouse brain after hypoxia/ischemia," *Neurology Research International*, vol. 2012, Article ID 781512, 28 pages, 2012.
- [26] C. Girbovan and H. Plamondon, "Resveratrol downregulates type-1 glutamate transporter expression and microglia activation in the hippocampus following cerebral ischemia reperfusion in rats," *Brain Research*, vol. 1608, pp. 203–214, 2015.
- [27] X. Cui, L. Li, Y. Y. Hu, S. Ren, M. Zhang, and W. B. Li, "Sulbactam plays neuronal protective effect against brain ischemia via upregulating GLT1 in rats," *Molecular Neurobiology*, vol. 51, no. 3, pp. 1322–1333, 2015.
- [28] Q. Fang, W. W. Hu, X. F. Wang et al., "Histamine up-regulates astrocytic glutamate transporter 1 and protects neurons against ischemic injury," *Neuropharmacology*, vol. 77, pp. 156–166, 2014.
- [29] M. Pérez-Mato, R. Iglesias-Rey, A. Vieites-Prado et al., "Blood glutamate EAAT2-cell grabbing therapy in cerebral ischemia," *EBioMedicine*, vol. 39, pp. 118–131, 2019.
- [30] X. J. Han, Z. S. Shi, L. X. Xia et al., "Changes in synaptic plasticity and expression of glutamate receptor subunits in the CA1 and CA3 areas of the hippocampus after transient global ischemia," *Neuroscience*, vol. 327, pp. 64–78, 2016.
- [31] K. Oguro, N. Oguro, T. Kojima et al., "Knockdown of AMPA receptor GluR2 expression causes delayed neurodegeneration and increases damage by sublethal ischemia in hippocampal CA1 and CA3 neurons," *The Journal of Neuroscience*, vol. 19, no. 21, pp. 9218–9227, 1999.
- [32] D. Talhada, J. Feiteiro, A. R. Costa et al., "Triiodothyronine modulates neuronal plasticity mechanisms to enhance functional outcome after stroke," *Acta Neuropathol Commun*, vol. 7, no. 1, p. 216, 2019.
- [33] Y. X. Wang, K. Tian, C. C. He et al., "Genistein inhibits hypoxia, ischemic-induced death, and apoptosis in PC12 cells," *Environmental Toxicology and Pharmacology*, vol. 50, pp. 227–233, 2017.
- [34] Y. Xu, H. Xue, P. Zhao et al., "Isoflurane postconditioning induces concentration- and timing-dependent neuroprotection partly mediated by the GluR2 AMPA receptor in neonatal rats after brain hypoxia-ischemia," *Journal of Anesthesia*, vol. 30, no. 3, pp. 427–436, 2016.

- [35] C. Boichot, P. M. Walker, C. Durand et al., "Term neonate prognoses after perinatal asphyxia: contributions of MR imaging, MR spectroscopy, relaxation times, and apparent diffusion coefficients," *Radiology*, vol. 239, no. 3, pp. 839–848, 2006.
- [36] J. L. Cheong, E. B. Cady, J. Penrice, J. S. Wyatt, I. J. Cox, and N. J. Robertson, "Proton MR spectroscopy in neonates with perinatal cerebral hypoxic-ischemic injury: metabolite peak-area ratios, relaxation times, and absolute concentrations," *American Journal of Neuroradiology*, vol. 27, no. 7, pp. 1546–1554, 2006.
- [37] D. Gano, V. Chau, K. J. Poskitt et al., "Evolution of pattern of injury and quantitative MRI on days 1 and 3 in term newborns with hypoxic-ischemic encephalopathy," *Pediatric Research*, vol. 74, no. 1, pp. 82–87, 2013.
- [38] R. J. Felling, M. J. Snyder, M. J. Romanko et al., "Neural stem/progenitor cells participate in the regenerative response to perinatal hypoxia/ischemia," *The Journal of Neuroscience*, vol. 26, no. 16, pp. 4359–4369, 2006.
- [39] E. B. Cady, "Metabolite concentrations and relaxation in perinatal cerebral hypoxic-ischemic injury," *Neurochemical Research*, vol. 21, no. 9, pp. 1043–1052, 1996.
- [40] S. K. Shu, S. Ashwal, B. A. Holshouser, G. Nystrom, and D. B. Hinshaw Jr., "Prognostic value of 1H-MRS in perinatal CNS insults," *Pediatric Neurology*, vol. 17, no. 4, pp. 309–318, 1997.
- [41] H. Seo, K. H. Lim, J. H. Choi, and S. M. Jeong, "Similar neuroprotective effects of ischemic and hypoxic preconditioning on hypoxia-ischemia in the neonatal rat: a proton MRS study," *International Journal of Developmental Neuroscience*, vol. 31, no. 7, pp. 616–623, 2013.
- [42] J. P. Kim, M. R. Lentz, S. V. Westmoreland et al., "Relationships between astrogliosis and 1H MR spectroscopic measures of brain choline/creatine and myo-inositol/creatine in a primate model," *American Journal of Neuroradiology*, vol. 26, no. 4, pp. 752–759, 2005.
- [43] P. J. van Doormaal, L. C. Meiners, H. J. ter Horst, C. N. van der Veere, and P. E. Sijens, "The prognostic value of multivoxel magnetic resonance spectroscopy determined metabolite levels in white and grey matter brain tissue for adverse outcome in term newborns following perinatal asphyxia," *European Radiology*, vol. 22, no. 4, pp. 772–778, 2012.
- [44] M. T. Martin, B. Holmquist, J. F. Riordan, and B. Holmquist, "An angiotensin converting enzyme inhibitor is a tight-binding slow substrate of carboxypeptidase A," *Journal of Inorganic Biochemistry*, vol. 36, no. 1, pp. 39–50, 1989.
- [45] M. V. Johnston, A. Fatemi, M. A. Wilson, and F. Northington, "Treatment advances in neonatal neuroprotection and neurointensive care," *The Lancet Neurology*, vol. 10, no. 4, pp. 372–382, 2011.